A Flux Atlas for Representativeness and Statistical Extrapolation of the AmeriFlux Network

William W. Hargrove
Environmental Science Division
Oak Ridge National Laboratory
Building 1507, Room 211, M.S. 6407
Oak Ridge, TN 37831–6407
(865) 241–2748
hnw@fire.esd.ornl.gov

Forrest M. Hoffman
Computer Science & Mathematics Division
Oak Ridge National Laboratory
Building 5600, Room B109, M.S. 6008
Oak Ridge, TN 37831–6008
(865) 576-7680
forrest@climate.ornl.gov

April 28, 2004

Contents

List of Figures

List of Tables

Abstract

The ecoregion concept has proven useful as a way to generalize the complex multivariate aspects of environmental conditions for plants and animals. Grouping such complex environmental combinations into a series of relatively homogeneous areas on a map helps ecologists to better understand the complex factors affecting the distribution of organisms across the landscape. Ecoregions have both theoretical and practical uses, and often form the basis for sampling designs and conservation strategies.

Here we borrow the utility of the ecoregion concept and apply it to the problem of sampling and estimating the amount and direction of carbon flux from terrestrial ecosystems. Unlike hand-drawn ecoregions produced by human experts, however, we employ a multivariate clustering procedure using a parallel supercomputer to produce a spectrum of homogeneous carbon flux regions. Each of these flux ecoregions is created statistically on the basis of a number of input maps so that ecosystems within a single flux ecoregion would be expected, from first principles, to have about the same magnitude and direction of carbon flux. We do not try (yet!) to estimate the magnitude or direction of carbon flux for each homogeneous flux ecoregion. Instead, our strategy is to statistically pre-stratify carbon flux environments across the conterminous United States as a way to simplify subsequent carbon flux sampling, measurement, and estimation.

As many as 30 maps were used as input to the multivariate clustering procedure to produce a spectrum of homogeneous carbon flux ecoregions for the conterminous United States. The spectrum represents different combinations of input maps and seasonality. Most input maps were created specifically for this project, and were themselves created of many individual components. Input maps were constructed to minimize cross-correlation with other inputs and to maximize the content of unique information relevant for carbon flux processes. For example, an elevation layer was not used. Instead, we included degree-day heat and cold sums, diurnal temperature differences, and precipitation totals, since the effects of elevation on vegetation are probably mediated through temperature and precipitation.

A number of investigators are trying to scale flux tower measurements from the bottom up to represent larger geographic regions. The flux ecoregion approach, on the other hand, relies on remotely sensed data to scale flux tower measurements to continental scales in a top-down way. It may be easier to obtain continental-scale flux fields to satisfy the goals set by the North American Carbon Program (NACP) and the AmeriFlux Program using top-down approaches, although both strategies will be needed for verification and testing.

If funded, a suite of AmeriFlux-specific results will follow in the second half of the project, based on the statistical foundation provided by this flux atlas. Although we use map colors to help visualize multivariate similarities, our statistical techniques are fully quantitative, and similarities and differences between different carbon flux environments can be expressed numerically. We will use the quantitative similarity of the suite of ecosystem characteristics that are relevant to carbon fluxes to extrapolate from existing flux measurements to estimate fluxes within ecoregions where fluxes are unmeasured. We hope to statistically model the multidimensional relationship of carbon flux with respect to each flux ecoregion characteristic, and then modify the expected flux according to the quantified differences in the flux environments between the unmeasured flux ecoregion and the most similar flux ecoregion containing an AmeriFlux tower. This quantitative ecoregion-based, top-down approach to stratifying carbon flux and

then estimating flux from existing measurements, if successful, may be the fastest way to help fulfill the NACP and AmeriFlux Program goals of seasonally mapping regions of sources and sinks of carbon within the North American continent.

Chapter 1

Introduction

The North American Carbon Program (NACP) Plan for carbon cycle research is focused on measuring and understanding the sources and sinks of CO_2 in North America and adjacent ocean regions, and is an important component of both the interagency U.S. Carbon Cycle Science Program and the new U.S. Climate Change Science Program. Although individual towers in the AmeriFlux network give important information about carbon flux in the immediate area surrounding each tower, there are insufficient numbers of towers to provide the regional and continental scale information on sources and sinks desired by NACP. It is unlikely that enough towers can be added to the network to make the density of measurements adequate for spatially continuous continental resolution within the timeframe required by NACP. A method for extrapolating spatially localized measurements into a continuous field across the continent is needed.

This project will ultimately determine the degree to which the existing network of carbon eddy flux towers within the AmeriFlux network are representative of flux environments across the continental United States (CONUS). Better data quality maximize the chances of success within the CONUS; if successful, the process can be expanded to the North American continent. This representativeness information can be used to determine how many additional towers will be required, and where additional towers should be placed. In addition, the uniqueness of each existing tower to the AmeriFlux network will be calculated. More importantly, this work will provide a statistical basis for quantitatively determining the similarity of flux environments in two different locations. If flux has been measured in one of these environments, it may be possible to "adjust" the tower measurement, using the quantitative differences between the flux environments, to obtain a reasonable estimate of flux in the unmeasured location.

In the first phase of this project, we have statistically created a series of flux-relevant ecoregions which divide the conterminous U.S. into a set of areas within which the carbon flux from terrestrial ecosystems is expected to be relatively uniform and homogeneous. Starting with digital geographic information system (GIS) layers of factors deemed important in regulating carbon fixation and loss from terrestrial ecosystems, we have created a set of multivariate descriptors which characterize the environment in each map cell. Then, we used a k-means clustering procedure to classify each map cell into a particular group whose cells have sufficiently similar environments. The classification procedure is iterative and converges on a final assignment solution when fewer than a specified number of cells change from the last assignment.

Each environmental descriptor is itself a map, and most maps were developed specifically for this project. These maps are at $1km^2$ resolution over the conterminous United States, and consist of nearly eight million cells each. Because there are as many as 30 environmental descriptor maps, each with nearly eight million cells, it is necessary to perform the clustering process on a parallel supercomputer.

Because the process is quantitative, the similarity of a selected flux-ecoregion to every other ecoregion in the map can be calculated. A map can be produced that shows the degree of similarity to the chosen flux-ecoregion as a series of gray shades. By sequentially selecting the regions currently containing an AmeriFlux tower, a map of the geographic area which is represented by that flux tower can be produced.

This project began at the end of FY2003 and represents the first phase of work proposed in a solicited proposal to the U.S. Department of Energy (DOE). This report presents maps of homogeneous flux-relevant ecoregions and describes how we obtained them. Based on the reviews of this report, a decision will be made on the funding requested for the second phase of the proposed research.

The second phase of the project will utilize these flux-relevant ecoregions to determine the overall representativeness of the existing AmeriFlux network, calculate uniqueness values for each tower, and determine the most favorable locations for the next five towers. Additionally, we will utilize the quantified similarities of flux-ecoregions having AmeriFlux towers to those without towers in order to estimate **net ecosystem exchange (NEE)** across the U.S. By using the similarity values as weight coefficients, it may be possible to "adjust" flux measurements within measured flux-ecoregions by how similar their environments are to flux-regions which have no measurements.

Representativeness analyses are being conducted at the ecoregion scale at 1 square kilometer resolution. Results obtained will be with respect to the particular ecosystem characteristics upon which the flux-ecoregions were based. If a characteristic which is overridingly important for carbon flux has not been included, or if a characteristic which is not related to flux has been included, the relevance of the ecoregions which are produced will be decreased. Unusual local site conditions such as managed ecosystems, disturbances, or topographic peaks or bowls may make particular tower locations less representative of the square kilometer within which they sit. However, this resolution is probably a good match with the "fetch" of an individual flux tower when integrated over time.

1.1 The Multivariate Geographic Clustering (MGC) Method

Hargrove and Hoffman have developed a method based on a multivariate statistical approach to divide any map, based on a set of multivariate characteristics, into a set of regions which are relatively homogeneous with respect to those conditions (Hargrove and Hoffman, 2004). The number of regions which are produced is under user control. Once produced, any two regions taken from the map will have roughly equivalent within-region heterogeneity with regard to the combinations of characteristics used as input. The process utilizes information contained within the variance structure of the input data, and creates regions such that the variance is equally divided among all of the resulting regions. Regions that are produced may be spatially disjoint; for example, environments on geographically distant mountaintops, if similar enough, will be classified into the same flux-ecoregion.

Because the number of characteristics considered can be very large, and because the process operates on a cell-by-cell basis on high-resolution maps, a parallel supercomputer is needed to produce such regionalizations (Hargrove et al., 2001). The non-hierarchical algorithm consists of a reversible

transformation between two realms, one in two-dimensional geographic space, and one in multi-dimensional data space. Normalized variable values from each map cell are used as coordinates to plot each map cell in an environmental space with as many axes as there are multivariate environmental dimensions. Because the plotted location of map cells in data space pinpoints the combination of environmental variables within that map cell, two map cells which are plotted close to one another in data space will have similar mixtures of environmental conditions, and are likely to be classified into the same ecoregion cluster. Thus, similarity is coded as the separation distance in this data space. We use an iterative k-means clustering algorithm (Hartigan, 1975), which begins with a user-specified number of ecoregion clusters, k, into which the map cells are to be grouped. All map cells are examined sequentially to find the most widely separated set of cells which will provide k initial "seed" **centroids**, one for each of the desired k cluster groups. In a single iteration of the clustering procedure, each map cell is assigned to the closest (*i.e.*, environmentally most similar) centroid in terms of Euclidean distance. At the end of the iteration, once all map cells are assigned to a centroid, the coordinates of all map cells within each group are averaged to produce a new, adjusted centroid for each cluster, and another iteration of assigning map cells to these new centroids begins. The iterative process of classifying map cells and adjusting centroid locations continues until fewer than a pre-determined number of map cells change cluster assignments during an iteration. After the process has converged on a particular grouping scheme, the k ecoregions have been statistically defined.

Once cluster assignments have stabilized, map cells are re-assembled in geographic space, retaining their ecoregion classifications. Although geographic coordinates are not used directly in the classification, ecoregions tend to be geographically cohesive due to the spatial autocorrelation which is usually present in the environmental data. Because of the Euclidean distance assignment method, the k-means clustering algorithm tends to fit globular clusters of equal size in data space. Thus, all large ecoregions share a similar upper limit on within-group variance, and have a similar maximum radius around each centroid. This uniform heterogeneity across ecoregions prevents the creation of side-by-side ecoregions that have vastly different within-region variance.

We call this empirical process **Multivariate Geographic Clustering (MGC)**. We have implemented it in a parallel algorithm written in the C language using the Message Passing Interface (MPI). The code is dynamically load-balancing, fault-tolerant, and performs both initial seed-finding and iterative cluster assignment in parallel. Individual nodes independently classify subsets of cells, then combine results at the end of an iteration. As a result, the quantitative ecoregionalization algorithm can be used to analyze very large datasets quickly (Hoffman and Hargrove, 1999).

Ecoregions determined using MGC are self-describing in that the coordinates of the final centroids quantitatively define the synoptic conditions for each ecoregion. Nominative multivariate conditions within a particular ecoregion are described by the N coordinates of its centroid. The technique is parametric only in that means are used to calculate each new centroid. Rather than imposing a pre-conceived external grouping upon the map, the variance structure present in the environmental conditions is used, allowing an unbiased, uniform classification structure to emerge from the data.

Initially, we performed a number of empirical regionalizations for the conterminous United States at 1km^2 resolution, dividing the U.S. into as many as 3000 distinct ecoregions (Hargrove and Luxmoore, 1998). We included nine characteristics from three categories—elevation, edaphic factors, and climatic factors. The edaphic factors were 1) plant-available water capacity, 2) soil organic matter, 3) total Kjeldahl soil nitrogen, and 4) depth to seasonally-high water table. The climatic factors were 1) mean precipitation during the growing season, 2) mean solar insolation during the growing season, 3)

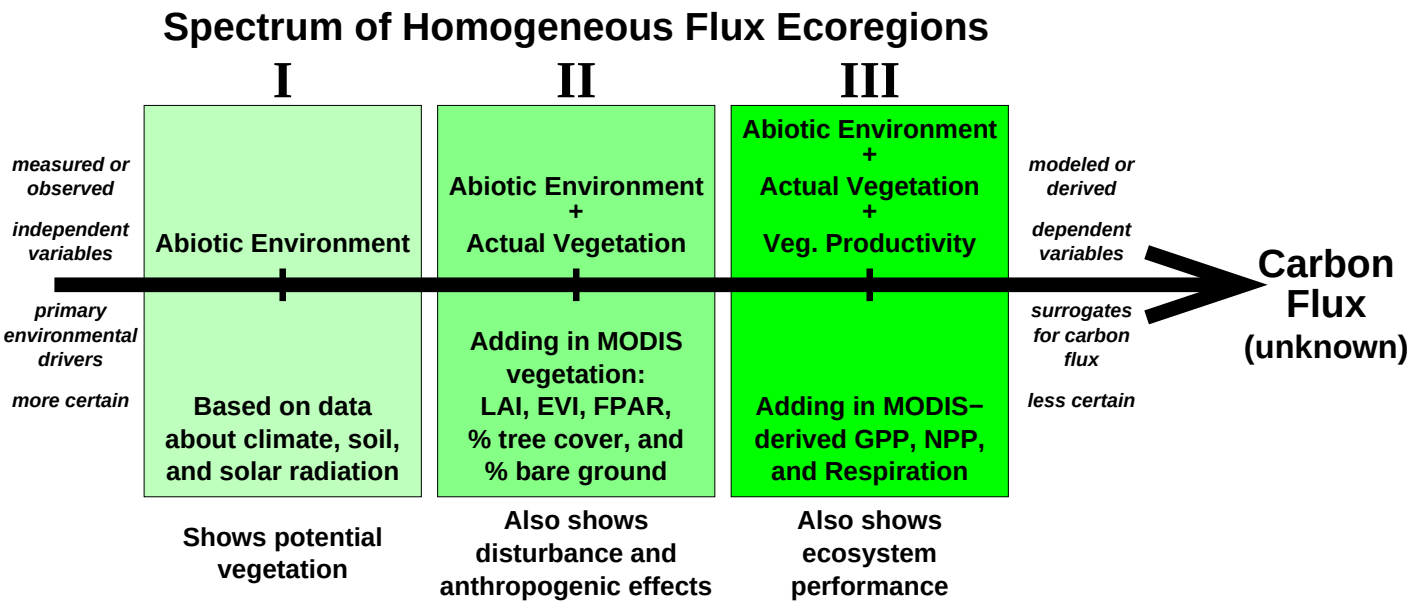

Figure 1.1: The spectrum of Homogeneous Flux Ecoregions

degree-day heat sum during the growing season, and 4) degree-day cold sum during the non-growing season. The growing season was defined by the frost-free period between mean day of first and last frost each year. A map for each of these characteristics was generated from best-available data at a 1km^2 resolution for input into the clustering process. Each of the input maps contained more than 7.8 million cells. Such map, data, and ecoregion resolution surpasses that usually accomplished by ecoregion experts using qualitative methods. These maps appear to capture the ecological relationships among the nine input variables. More recently, we have added new variables and divided the U.S. into as many as 5000 ecoregions. Twenty-five environmental factors, including elevation, mean and extremes of annual temperature, mean monthly precipitation, soil nitrogen, organic matter, water capacity, frost-free days, soil bulk density and depth, and solar aspect and insolation were included (Hargrove and Hoffman, 2004).

1.2 Conceptual Approach to Mapping Flux Ecoregions

The conceptual basis for development of the flux-relevant ecoregions is a spectrum or gradient starting from primary ecological forcing factors on the left, and building additively toward the right (Figure 1.1). Actual carbon flux, or NEE, forms the extreme right side of this continuum. NEE is unknown and is not directly measured for most ecosystems in the CONUS, and is what we are trying here to design a network to measure. If we knew the continuous map of NEE, we could design a perfect network to monitor and sample it. However, we wouldn't need to measure it, since we would know it already! So the extreme right hand side of this continuum is ultimate-but-unknown NEE.

Our approach has been to start with primary factors on the left, and then add further information about the primary characteristics of the existing vegetation, and finally to also add information about simulated surrogates of ecosystem performance. In this approach, then, we start with the simple, and add factors which are increasingly complex, building toward the unknown, NEE itself. Because uncertainty also increases from left to right along this continuum, this step-wise approach to regionalization initially

produces oversimplified, but more certain initial flux-relevant ecoregions, but ultimately produces more sophisticated, but less certain flux-ecoregions, all based on best-available data.

The left side of Figure 1.1 represents climatic, edaphic, and physiographic factors which might be considered, *a priori*, to impose limits on the amount and direction of carbon flux for a particular ecosystem. We will produce a set of regionalizations based solely on these primary drivers. However, consideration of primary forcing factors alone will produce ecoregions which reflect the carbon flux associated with **potential vegetation**. Anthropogenic effects, disturbance regimes, and history may have altered or reset the potential vegetation. The middle of this conceptual spectrum adds information about the characteristics of the vegetation that is actually existing in this ecosystem at this time. Finally, in a third set of flux regionalizations, we will add information about ecosystem gross primary production and respiration. These ecosystem activity values are not measurements, but are simulated based on measurements, and can be thought of as surrogates for the unknown carbon flux itself. Thus, we will create three sets of regionalizations, each time adding factors used as input, and increasing in sophistication (Figure 1.1).

Each of the input maps had to be developed before they could be used. These are valuable products in themselves. Each was constructed from the best-available data at a 1km^2 resolution. Most of the input maps are themselves synthetic aggregate products which were produced from map series through time, and were designed to summarize or integrate the most important aspects of that raw map series into a single component which is both immediately important to vegetation and independent of information contained in other input layers. For example, we did *not* include elevation, since elevation effects are confounded with (and probably act through) differences in temperature and precipitation. Variable selection represents a compromise between desirability and availability.

Remote sensing provides the only practical source of data which can be used to describe the characteristics of existing vegetation for the middle of the conceptual continuum. We are using data from NASA's new MODIS sensor, which is now operating on both the Terra and Aqua orbital platforms. Only MODIS Terra data were used here, since the Aqua platform has not been up long enough to produce a substantial data record. MODIS provides estimates of **Leaf Area Index (LAI)**, **Fraction of Photosynthetically Active Radiation (FPAR)**, and an **Enhanced Vegetation Index (EVI)** at 1km^2 resolution. EVI is provided once every 16 days, while LAI and FPAR are available every eight days. The **Continuous Vegetation Fields** product provides estimates of **percent tree cover** and **percent bare ground** in every cell across the CONUS.

MODIS was also used to provide indices of ecosystem performance for the third set of flux regionalizations. **Net Photosynthesis (PSNNET)** and **Gross Primary Production (GPP)** are produced every eight days. We have taken the eight-day difference of PSNNET from GPP as a **respiration index (RI)**, which we believe is a more relevant measure of ecosystem performance. The **Net Primary Productivity (NPP)** product is also available for the last two years. MODIS **Land Surface Temperature (LST)**, during both the day and the night, will be used in the initial flux regionalization using only environmental forcing factors. As the temperature of the vegetation canopy or soil surface, LST should be more meaningful than just the temperature of the ambient air.

1.3 Separation into Local Growing and Non-growing Seasons

We are using a consistent approach to integrate raw time series maps into input layers by dividing the annual cycle at every cell into a growing season and a non-growing season. The growing season is defined by the frost-free period between the median day of the last frost of the spring and the median day of the first frost of the fall, as measured over the 30-year climate normals period (1960–1990). We used these dates to divide the synoptic year into two temperature-defined periods customized for each cell location in the CONUS. These two seasons form a common basis for dividing many of the input variables into periods that should be relevant for vegetation growing across the CONUS.

All variables other than edaphic factors were integrated over the growing and non-growing seasons into two summary maps. For example, a heat sum was constructed from daytime LST over the local growing season, and a cold sum was constructed from nighttime LST over the non-growing season. Similarly, total precipitation was summed over the growing and non-growing seasons. Because these layers contain information about precipitation totals, but not the temporal distribution of precipitation events, another layer was included which counts number of measurable precipitation events during the growing and non-growing seasons.

1.4 Notation for Alternative Flux Ecoregions

This work has produced nine separate sets of flux ecoregions for the conterminous U.S. (three types of flux ecoregions × three seasons for each type). We have adopted a shorthand notation for distinguishing these alternative flux regionalizations which is shown in Figure 1.2. We use Roman numerals I, II, and III to refer to the three different stages along the conceptual continuum shown in Figure 1.1 from primary forcing factors to derived ecosystem flux surrogates. Within each of these, we use Arabic A, B, and C to refer to annual, growing season, and non-growing season divisions, respectively. Thus, "IIB" refers to the flux ecoregions created using abiotic environment and actual vegetation factors which were integrated over the growing season. We use this notation throughout the remainder of this report to refer to particular alternative flux ecoregions.

The type "A" annual regionalizations contain both growing season and non-growing season layers rather than a single annual layer, since the division into these two temperature-defined seasons is still a more relevant form than simply integrating across the entire year. This means that the "A" versions of each flux regionalization contain more input maps than the "B" and "C" versions (Figure 1.2).

Table 1.1 shows the list of input maps used to produce each set of flux ecoregions. We included 18 layers of primary forcing factors in developing the first set of flux regions (Series I). To these we added eight MODIS-derived layers from each of the two seasons to produce the regionalizations which consider existing vegetation (Series II). Finally, another four layers comprised of composite MODIS-derived flux surrogates were added to produce the most sophisticated flux regionalizations (Series III). Most of these input layers represent valuable products in themselves. But these groundbreaking products represent our starting point, not the finished product for this task.

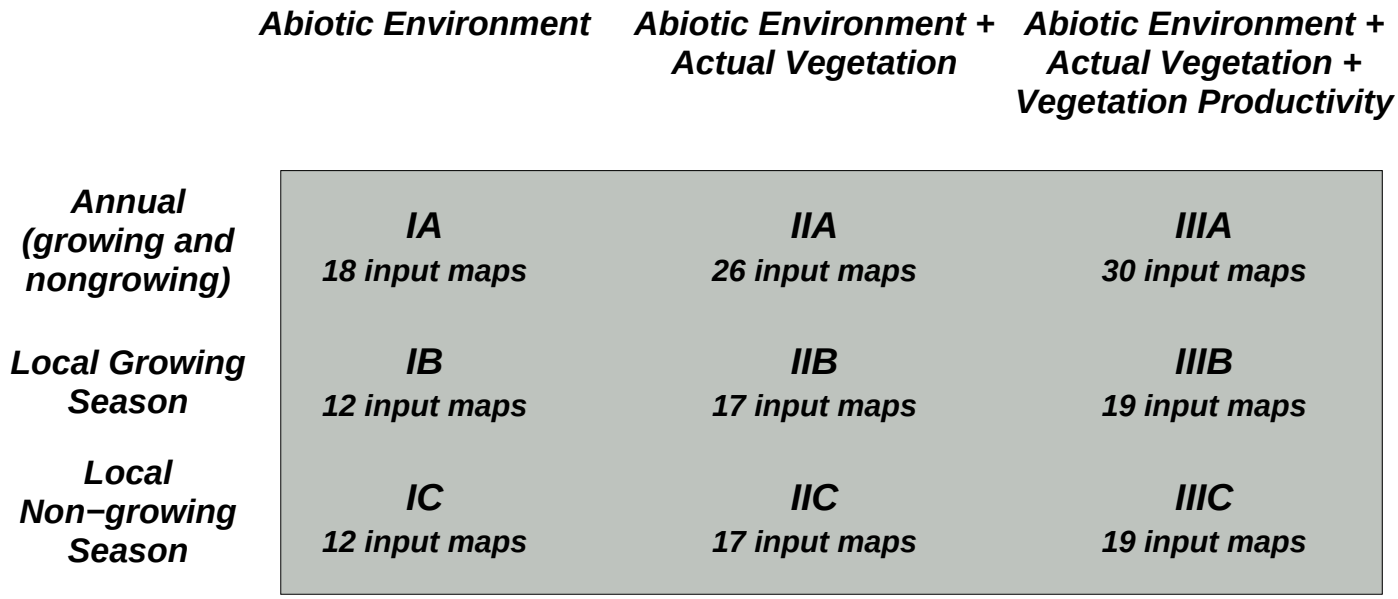

Figure 1.2: Shorthand notation for distinguishing alternative flux ecoregionalizations

Map Layer or Variable Name	IA	IB	IC	IIA	IIB	IIC	IIIA	IIIB	IIIC
Degree-days heat sum above 42°F from daytime land surface temperature during the local growing season	✓	✓		✓	✓		✓	✓	
Degree-days cold sum below 42°F from nighttime land surface temperature during the local non-growing season	✓		✓	✓		✓	✓		✓
Number of days above 90°F during the local growing season	✓	✓		✓	✓		✓	✓	
Number of days below 32°F during the local non-growing season	✓		✓	✓		✓	✓		✓
95^{th} percentile of maximum diurnal surface temperature difference during the local growing season	✓	✓		✓	✓		✓	✓	
95^{th} percentile of maximum diurnal surface temperature difference during the local non-growing season	✓		✓	✓		✓	✓		✓
Precipitation sum during the local growing season	✓	✓		✓	✓		✓	✓	
Precipitation sum during the local non-growing season	✓		✓	✓		✓	✓		✓
Number of days with measurable precipitation during the local growing season	✓	✓		✓	✓		✓	✓	
Number of days with measurable precipitation during the local non-growing season	✓		✓	✓		✓	✓		✓
Depth of mineral soil	✓	✓	✓	✓	✓	✓	✓	✓	✓
Depth to water table	✓	✓	✓	✓	✓	✓	✓	✓	✓
Soil Kjeldahl nitrogen to 50 cm depth	✓	✓	✓	✓	✓	✓	✓	✓	✓
Soil organic matter to 50 cm depth	✓	✓	✓	✓	✓	✓	✓	✓	✓
Soil plant-available water holding capacity to 1.5 m	✓	✓	✓	✓	✓	✓	✓	✓	✓
Compound Topographic Index (CTI)	✓	✓	✓	✓	✓	✓	✓	✓	✓
Total solar insolation during the local growing season, including clouds, aerosols, slope and aspect physiography	✓	✓		✓	✓		✓	✓	
Total solar insolation during the local non-growing season, including clouds, aerosols, slope and aspect physiography	✓		✓	✓		✓	✓		✓
Enhanced Vegetation Index (EVI) integrated over the local growing season				✓	✓		✓	✓	
Enhanced Vegetation Index (EVI) integrated over the local non-growing season				✓		✓	✓		✓
Fraction of Photosynthetically Active Radiation (FPAR) absorbed by vegetation integrated over the local growing season				✓	✓		✓	✓	
Fraction of Photosynthetically Active Radiation (FPAR) absorbed by vegetation integrated over the local non-growing season				✓		✓	✓		✓
Leaf Area Index (LAI) integrated over the local growing season				✓	✓		✓	✓	
Leaf Area Index (LAI) integrated over the local non-growing season				✓		✓	✓		✓
Percent tree cover				✓	✓	✓	✓	✓	✓
Percent bare cover				✓	✓	✓	✓	✓	✓
Gross Primary Production (GPP) integrated over the local growing season							✓	✓	
Gross Primary Production (GPP) integrated over the local non-growing season							✓		✓
Respiration Index (RI) integrated over the local growing season							✓	✓	
Respiration Index (RI) integrated over the local non-growing season							✓		✓

Table 1.1: Map Layers Used in Multivariate Geographic Clustering

1.5 Development of Input Maps

We have processed every MODIS granule over the United States, for every eight-day interval, for every year, for 2001, 2002, and 2003 for almost every MODIS product from the Terra platform. There are 14 granules for each of the 46 periods for each of the three years for most MODIS products. We are using Version 4 or later for all of these products (for PSNNET and GPP, we are using version 4.5, direct from Dr. Steve Running's lab). Just acquiring all of the primary MODIS files in HDF format (14 granules per date $\times$ 46 dates per year $\times$ three years $\times$ five MODIS product families = 9660 primary files) via ftp was an accomplishment. We wrote custom scripts to handle each type of MODIS product, mosaic the granules together, change them into GIS layers, and reproject them into the **Lambert Azimuthal Equal-Area (LAEA)** projection for the CONUS, using a 6,370,997m radius for the Earth and centered on latitude 45 and longitude -100.

MODIS quality control is provided by flags in bit fields of an image which is separate from the primary image. Unfortunately, there is little consistency among various MODIS products in how these flags are to be read. Furthermore, there is as yet little agreement among the MODIS community about which combinations of these flags produce the best quality assurance. We checked our interpretations of the MODIS quality assurance flags with Dr. Steve Running, who believes that we are using these flags appropriately for the carbon flux regionalization task. We masked most images with the quality assurance flags, using only data which are of sufficiently high quality.

MODIS images are always taken on the same Julian dates each year, usually every eight days, but every 16 days for vegetation indices, producing either 46 or 23 images per year. Because we processed three full years of MODIS images (2001–2003) for most products, we have three separate images for each date. Since our goal is to develop full coverages for a single average or synoptic year, we composited the three separate images together to produce a single, more complete image for each Julian date. For most products, this composite is formed by averaging the three available year images for that Julian day.

1.5.1 Filling Gaps in Images

Even after compositing, holes exist in the composite images due to the QA flags, clouds, snow, etc. We developed methods for filling in such gaps in the images. Some MODIS products like LAI/FPAR also have internal flags for lakes, urban areas, perennial ice, swamps, etc. We set such areas to zero.

We developed a mathematical procedure, based on the values in each cell through time, to perform a temporal interpolation to fill gaps one cell at a time. A spline with tension was fitted through the temporal sequence of values in each cell. In order to pre- and post-condition the spline curve, we duplicated the 46/23 values in the synoptic year, and added an extra copy of the year onto the front and back, so that the spline was actually developed to fit a three-year temporal sequence. Interpolated values taken from the middle year were used to fill the gaps to avoid edge effects.

The spline procedure has an adjustable tension, which acts to draw the curve back to trend. To avoid overshoots, we slightly expanded the range of the actual data values, and then fitted the spline repeatedly, starting with the lowest possible tension. If the interpolated values exceeded the new range of the data, we increased the tension and re-calculated the spline. In this way, the interpolated values were always near the range of the actual image values, and were obtained using the lowest possible tension setting.

Because of this limited overshoot, exclusively positive values may be caused to occasionally go slightly negative in a few cells. If the totals over time are still negative, we reset these few cells back to zero.

We believe that this temporal interpolation using splines is the most sophisticated procedure currently being used to fill gaps in MODIS products. Since most MODIS parameters are temporally autocorrelated, making use of the temporal sequence of information at a cell location is likely to be better than relying on spatial neighbors for interpolation. While some researchers are using temporal linear interpolation, we have seen many examples in temporal sequences of MODIS data where such linear models seem less appropriate than a spline curve.

Nevertheless, there are occasionally map cells which have three or fewer values over the entire 46/23 image synoptic year. A temporal spline would not likely have sufficient information to appropriately fill data gaps under such data-poor circumstances. In these cases, we switch to a spatial interpolation method to fill the holes in the maps. A weighted circular adaptive spatial filter with a radius of 3km replaces the focal center cell with the weighted mean of all data-containing cells within the current range of the filter. The filter is used in multiple passes until all remaining holes are filled.

1.5.2 Integration of Input Variables Through a Season

To increase relevance for vegetation and carbon flux, we integrated the area under the time curve by growing and non-growing season. Photosynthesis and respiration are proportional, for example, to the area of the leaf crop as indicated by LAI times the number of days that the vegetation had that leaf crop (Prince, 1991; Rasmussen, 1997). Carbon flux, in turn, should be related to photosynthesis and respiration. A similar conceptual argument can be made for integrating EVI, FPAR, PSNNET, and GPP by season.

Integration by season helps to distinguish not only evergreen from deciduous vegetation, but also mixtures of each type. We are using the spline with tension to turn the discrete values at each of the 46/23 image periods into a smooth curve with a unique value for each of the 365 days of the year. These daily values are then summed in the integration step to produce three maps: an annual integration, a growing season integration, and a non-growing season integration.

The growing and non-growing season maps sum to what would be full annual values (Figure 1.3). Sometimes this temperature-defined seasonal split causes surprising features in the map. For example, the non-growing season total solar insolation map shown in Figure 1.3 makes it appear that the southern tip of Florida does not receive much sun. This is because the southern tip of Florida has no non-growing season over which to integrate insolation. The summed map at the bottom has the appearance that we might intuitively expect. While such annual maps look more understandable, seasonally divided maps are likely to be more relevant for plants, and are a better match for the time-scales over which we will be using the flux ecoregions to estimate flux measurements.

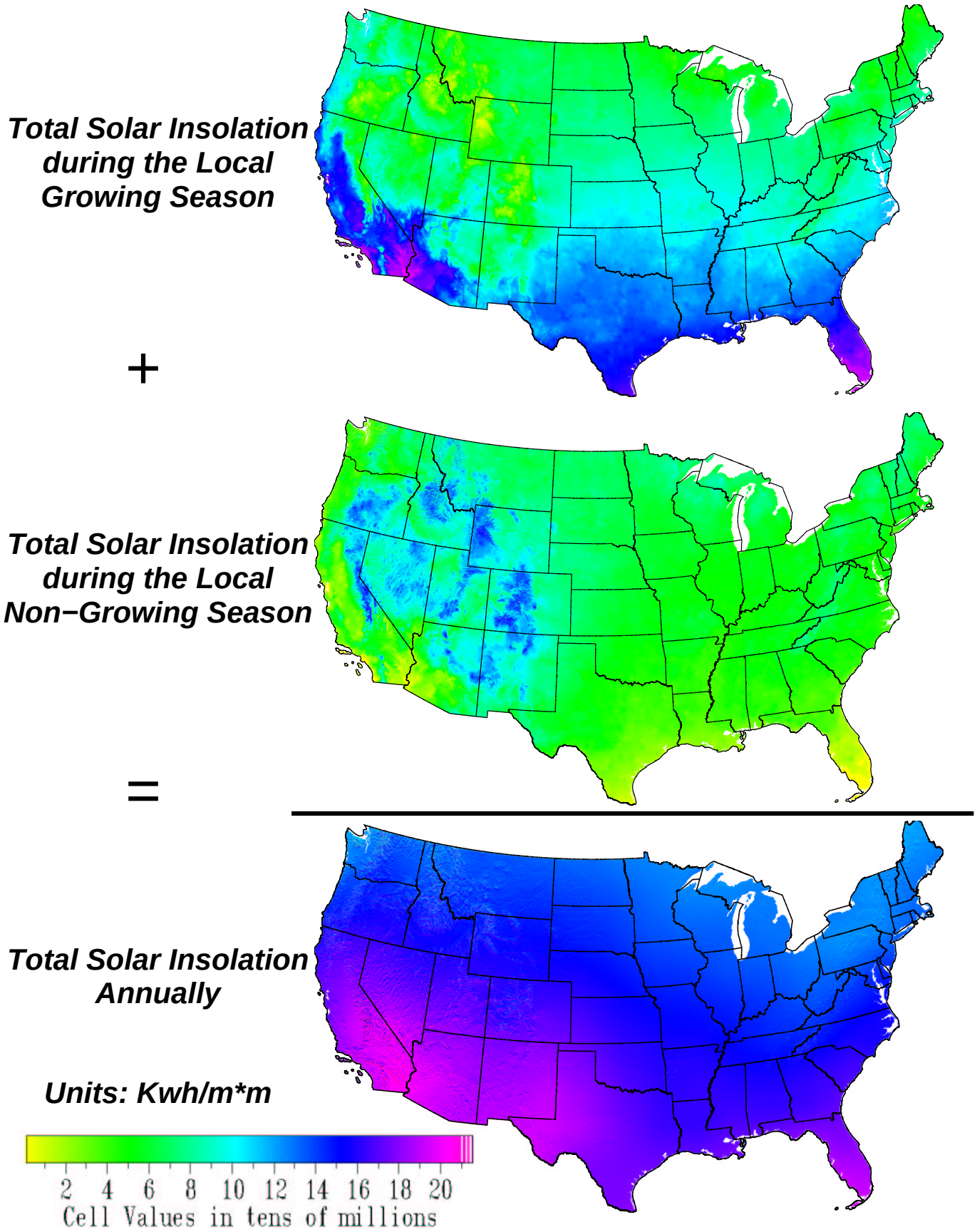

Figure 1.3: Annual Total Solar Insolation

While dividing these maps by the number of days in the growing season (or simply not time-integrating) would produce an instantaneous map which might be more intuitive, a map which is integrated through time is more useful for estimating seasonal carbon flux. For example, two different flux ecoregions might, over the course of a growing season, absorb roughly equal amounts of carbon, but one might do it in a short spike of fixation whereas the other does it with a small but constant fixation rate. Because we are interested in source/sink terms over seasonal intervals, and because we will be integrating measurements at flux towers over seasonal time scales, season-integrated maps are more relevant for the creation of these flux ecoregions.

We used a variation of the spline procedure to calculate 95^{th} percentile of maximum diurnal temperature difference in the growing and non-growing season. First, a spline was fitted to the 46 MODIS daytime Land Surface Temperature (LST) values, and was then used to estimate 365 daily values of daytime LST. This produced 365 maps of the CONUS, each with 7.8 million cells. Next, the splining procedure was repeated for MODIS nighttime LST values, producing another set of 365 CONUS maps. Finally, these maps were subtracted from each other, restricted cell-by-cell to the spatially unique growing and non-growing season, and the results sorted by cell to find the 95^{th} percentile value. We used the 95^{th} percentile value rather than the maximum diurnal difference to avoid any problems that could be caused by mapping anomalies.

In addition to MODIS products, we included layers that we have developed ourselves, along with a few that we have purchased. As with the MODIS products, most of these raw layers were not included as inputs to the MGC process directly. Rather, they were used as components in the construction of second-order products. These second-order products, which ostensibly contain more pertinent information about carbon flux, were the actual inputs into the clustering process. Even though the purchased maps are proprietary and cannot be distributed, the map products derived from them are not subject to this limitation (so long as the original map cannot be reverse-engineered back out).

We are also including monthly discrete counts of days with extreme events, *i.e.*, temperatures greater than 90°F or below 32°F. Days with measurable precipitation also fall into this category of counts of discrete events. Because of the limitations of the monthly data, we uniformly pro-rated these counts over the days of each month. For growing season periods beginning and ending on days other than month boundaries, we added these pro-rated partial sums over the appropriate number of days. In this way, total events were conserved and growing season counts plus non-growing season counts equaled annual counts. Including such extreme events (and the variance information that they convey) is important for carbon flux, even though these best-available data are temporally coarse.

1.6 Preparation of Input Layers for Multivariate Clustering

Before submitting them to the MGC procedure, all map layers were normalized by subtracting the mean from each observation, and dividing through by the standard deviation. This **normalization** is necessary, since absolute differences inherent in different units of measurement used for various map layers would otherwise unduly affect the clustering process. Only the variance information is used in the clustering process.

Consideration of this normalization process affected our treatment of a few map layers. For example, negative values of MODIS PSNNET indicate that maintenance respiration exceeds GPP, and this

difference between positive values and negative values has particular biological significance. Since normalization of PSNNET would have destroyed the significance of this zero point where production exceeds respiration, we subtracted PSNNET from GPP to produce a respiration index (RI). Since both GPP and RI are always positive, and since PSNNET is related by subtraction, the inclusion of GPP and RI rather than PSNNET provides the same information and eliminates the possibility of destroying negative values of PSNNET.

1.7 Correlations Among Inputs

Before performing the statistical clustering to produce flux ecoregions, we examined the degree to which all of the input layers were cross-correlated with each other. Even if two maps show 95% correlation with one another, however, it may not be prudent to eliminate one of them. If the additional information carried in the uncorrelated 5% serves to distinguish or separate two regions which have important differences in carbon flux, and which would otherwise be confounded, then it is important to retain both layers in the analysis. Thus, the inclusion decision for input layers cannot be distilled to a simple correlation analysis. Ecological expertise must be used in considering which layers to include in the MGC analysis.

Thus, layers selected for inclusion were not be entirely uncorrelated with one another. The MODIS MOD17A3 GPP and NPP averaged annual products from 2001 and 2002 were found to be so highly correlated with GPP and RI seasonal layers that these two input layers were dropped. Some remaining input layer pairs showed expected high correlations greater than 0.9: cold days with cold sum, wet days growing with precipitation growing, solar growing with cold days (negatively), LAI non-growing with FPAR non-growing, GPP growing with FPAR growing and LAI growing, RI growing with LAI growing, and RI non-growing with GPP non-growing. The highest of these was 0.96, most were below 0.93.

Cross-correlations do not strongly affect the MGC results, but are best avoided if possible. **Principal Component Analysis (PCA)** could be used to produce axes which are orthogonal (uncorrelated) to each other for clustering. However, results from clustering within a PCA space will be in PCA units, and cannot be transformed back into the original units of measurement if PCA axes that explain even small amounts of variance have been dropped.

Most applications of PCA are designed to reduce dimensionality by eliminating all but the three or four axes which explain the majority of the variability in the data. Although accounting for the majority of variability, less than 100% of the variance is explained by any subset of the axes. This loss of explanatory power means that it is impossible to convert values from the reduced PCA space back into the original units.

We used a unique statistical technique to ensure not only that the axes forming the data space within which the MGC procedure operates are orthogonal, but also that we can untransform the clustered units back into original measurement units for each axis. We performed a PCA analysis on all input layers included in each flux ecoregionalization, but retained all of the PCA axes in the analysis. Thus, if there were 26 input layers, we retained all 26 PCA axes that resulted. All PCA axes produced were guaranteed to be orthogonal and uncorrelated, but, because 100% of the variance in the original data was retained, we could still convert these PCA scores back into units that are ecologically relevant.

1.8 Resolution of Printed Maps

This report is severely limited by the size of its printed pages. Small printouts cannot show the full resolution contained within these maps. Each map would have to be printed as a wall-sized poster to easily see the single square kilometer-sized cells that they contain. However, digital files for each of the 48 high-resolution maps in this report would each be 85 MB at full resolution. As a compromise between size and quality, we have printed maps with a resolution degraded to 1500m rather than the full 1000m resolution. It is difficult to see the difference between these in a 10 inch map printed on a standard 600 dpi printer.

This document has been released in PDF and in PostScript formats. The PDF version is much smaller and can be emailed easily, but the maps are resampled. If printed, they will appear to be much coarser than they actually are. The PostScript format is much larger, but will produce maps of 1500m resolution if printed. Versions of this document in both formats are available at http://geobabble.ornl.gov/flux-ecoregions. Figure 1.4 shows a closeup of Nevada at full 1km^2 resolution as an example. The aspect of individual mountain ranges can be seen as differences in total solar insolation during the non-growing season in this figure. This layer carries information about slope and aspect into the flux ecoregion process.

Also available at http://geobabble.ornl.gov/flux-ecoregions are a variety of supporting imagergy, animations, and GIS maps. Maps of the homogeneous flux ecoregions and the interpolated and integrated input layers can be viewed using the Pan/Zoom/Scroll tool on the website at http://geobabble.ornl.gov/cgi-bin/pzs?conf=FluxEcoregionMaps/FluxEcoregionMaps.conf. Animations of the synoptic interpolated time series input data derived from MODIS products are available in AVI, QuickTime, and MPEG formats. Digital GIS map layers of the resulting homogeneous flux ecoregions can be downloaded also.

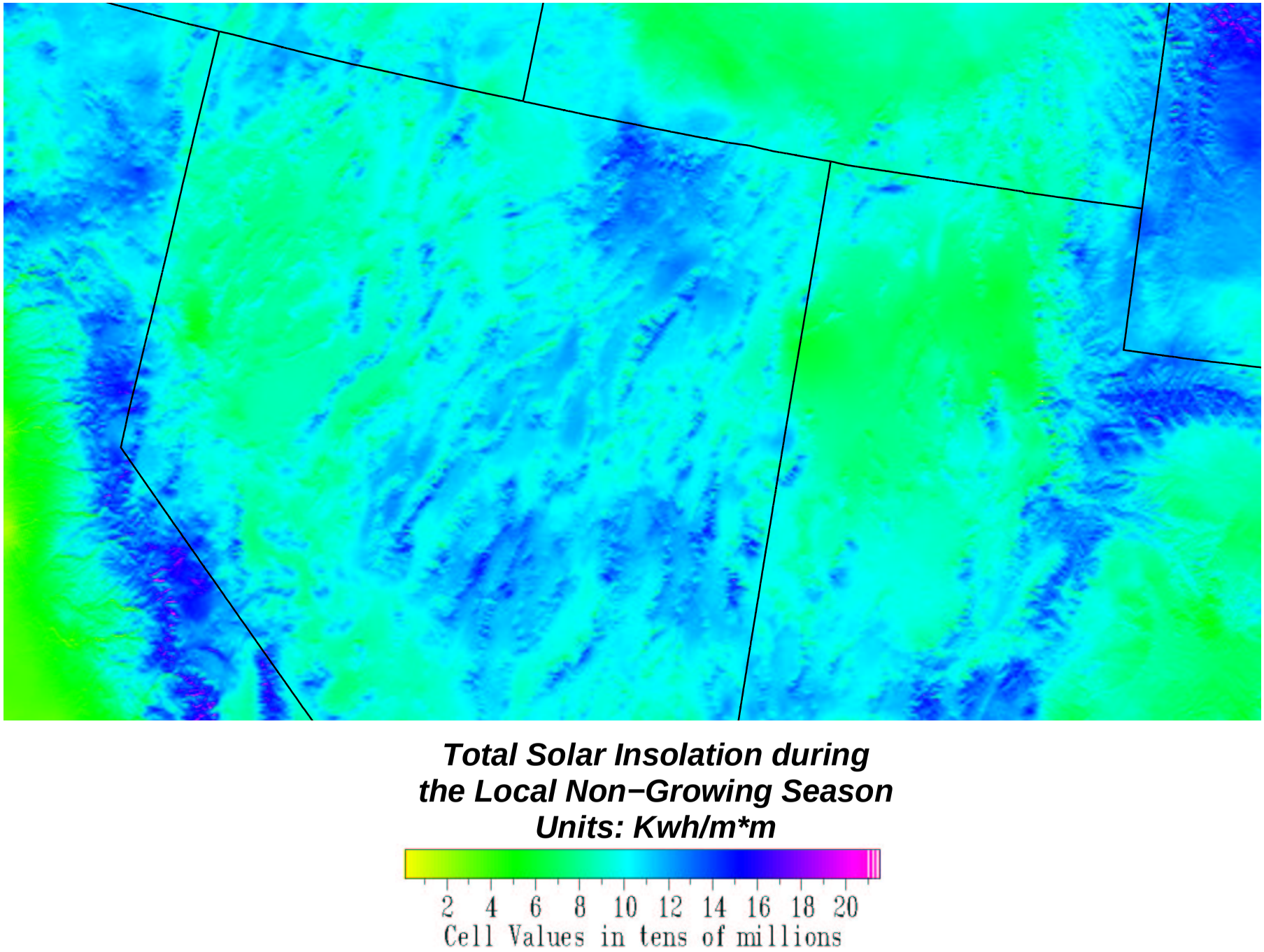

Figure 1.4: Total Solar Insolation During the Local Non-Growing Season in the Central Western United States

Chapter 2

Input Map Layers Used to Create Flux Ecoregions

The following pages contain a series of metadata sheets and maps used to produce flux ecoregions. Each metadata sheet describes the source of data and the method of processing for the maps that follow. Pairs of maps split into two seasons share a single metadata sheet.

2.1 Degree-days Heat Sum and Cold Sum

Name: Degree-days Heat Sum Above 42°F from Daytime Land Surface Temperature During the Local Growing Season, Degree-days Cold Sum Below 42°F from Nighttime Land Surface Temperature during the Local Non-growing Season

Data Sources: MODIS MOD11A2 Collection4 1km 8-day composites, 2000 through 2002; median day of last frost of spring, median day of first frost of fall, Climate Source, Inc., http://www.climatesource.com/

Description of Processing: 14 MODIS tiles comprising the CONUS at each date × 46 8-day composites per year × 3 years (2000,2001,2002) = 1932 MODIS tiles obtained from LPDAAC, mosaicked and reprojected using the MODIS Reprojection Tool v3.1c and nearest-neighbor resampling to 1km LAEA. Daytime Land surface temperature (SDS 1) and Nighttime Land surface temperature (SDS 5) were used for the heat sum and the cold sum, respectively. Although the Clear-sky flags for each of these (SDS 11 and 12) were consulted for Quality Control, it was decided that even a single clear-sky temperature was potentially better than an interpolated value. Therefore, land-surface temperature values were retained if the sensor saw even a single clear-sky view within the 8-day viewing period.

The 3 images from each of the 3 years were composited by averaging into a single sequence of 46 dates representing a nominal or synoptic year. Gaps were filled using a temporal spline with tension, using the lowest possible tension setting that did not cause data over- and undershoots (see Section 1.5 for details). Cells having 3 or fewer dates with data were filled by repeatedly applying a 7 × 7 cell weighted spatial adaptive filter. An animated sequence of the filled LST maps for the synoptic year is available at http://geobabble.ornl.gov/flux-ecoregions.

Daytime land surface temperatures were used to accumulate the heat sum, while nighttime land surface temperatures were used to accumulate the cold sum. This assumes that night temperatures are colder than day temperatures. The heat sum was calculated during the local growing season, while the cold sum was calculated during the local non-growing season. This assumes that the limiting factor for vegetation is heat during the growing season, but cold during the non-growing season. The same threshold of 42°F was used for the heat sum and the cold sum. Thus, this threshold forms the bottom/top of the integrated temperature sum curves.

Heat sum and cold sum were integrated over days of the growing season and non-growing season on a cell-by-cell basis, using the Julian days from the two Climate Source layers. A spline with tension was used to interpolate smoothed daily values for each cell, and then the portion above/below the temperature threshold was accumulated as Degrees Kelvin × days for the growing and non-growing seasons.

Measurement Units: Degrees Kelvin × Days

Conversion Factor: 0.02
The conversion factor used in the original MOD11A2 product was retained.

Expected Discriminatory Power: Temperature is of primary importance for carbon fixation and respiration rates. Degree-day integration is a well-established technique (Prince, 1991; Rasmussen, 1997), and developmental responses of many plants and animals are known to be well-predicted by degree-day trigger thresholds. Land surface temperature, as the directly sensed temperature of the vegetation canopy or soil, is more relevant than air temperature for expected carbon flux.

Comments/Observations: Midwestern cities can be seen as urban heat islands in both the heat sum and the cold sum maps. Most lakes and rivers are colder than ambient, but the Great Lakes are warmer than ambient during the local non-growing season.

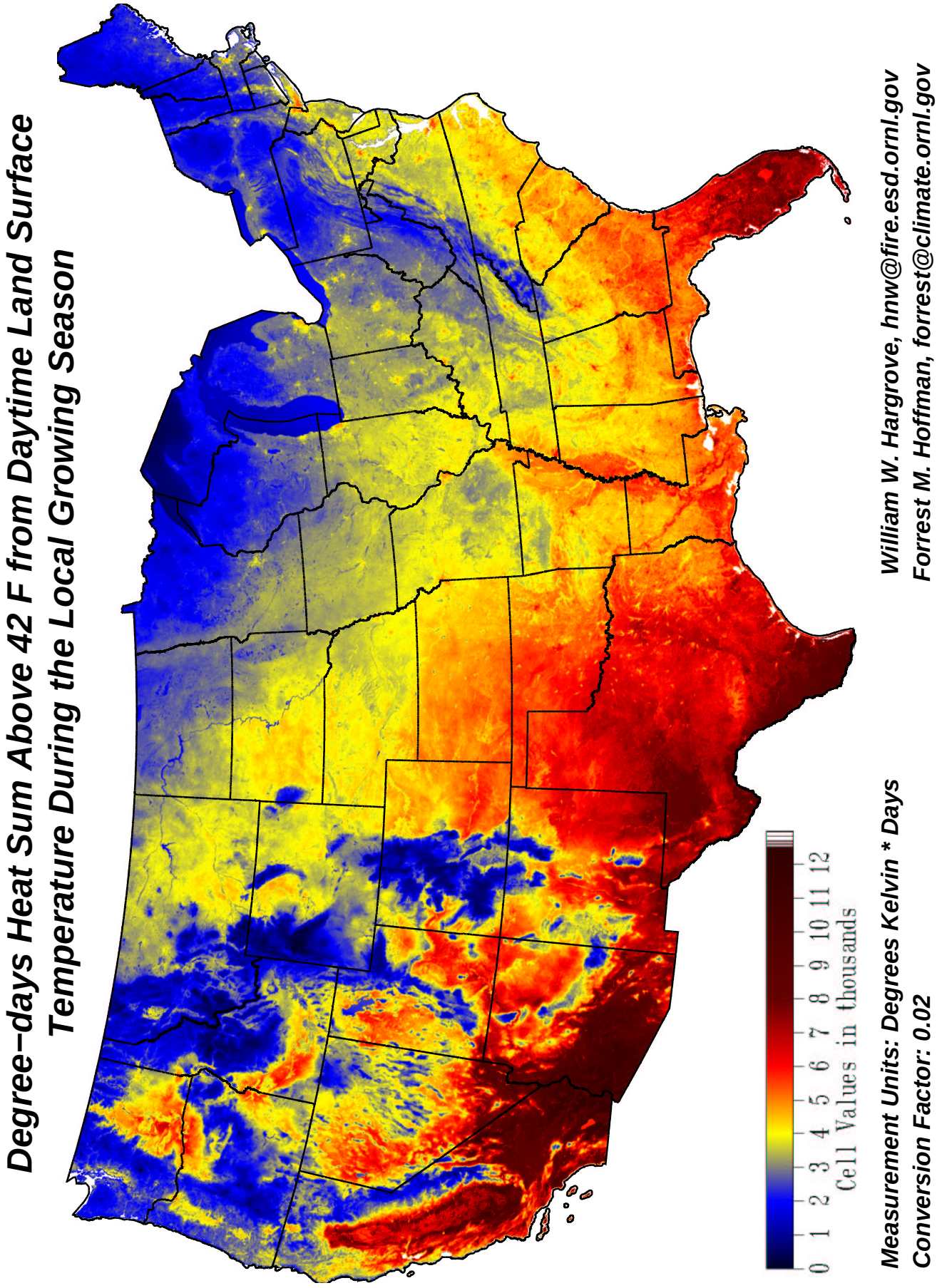

Figure 2.1: Degree-days Heat Sum Above 42°F from Daytime Land Surface Temperature During the Local Growing Season

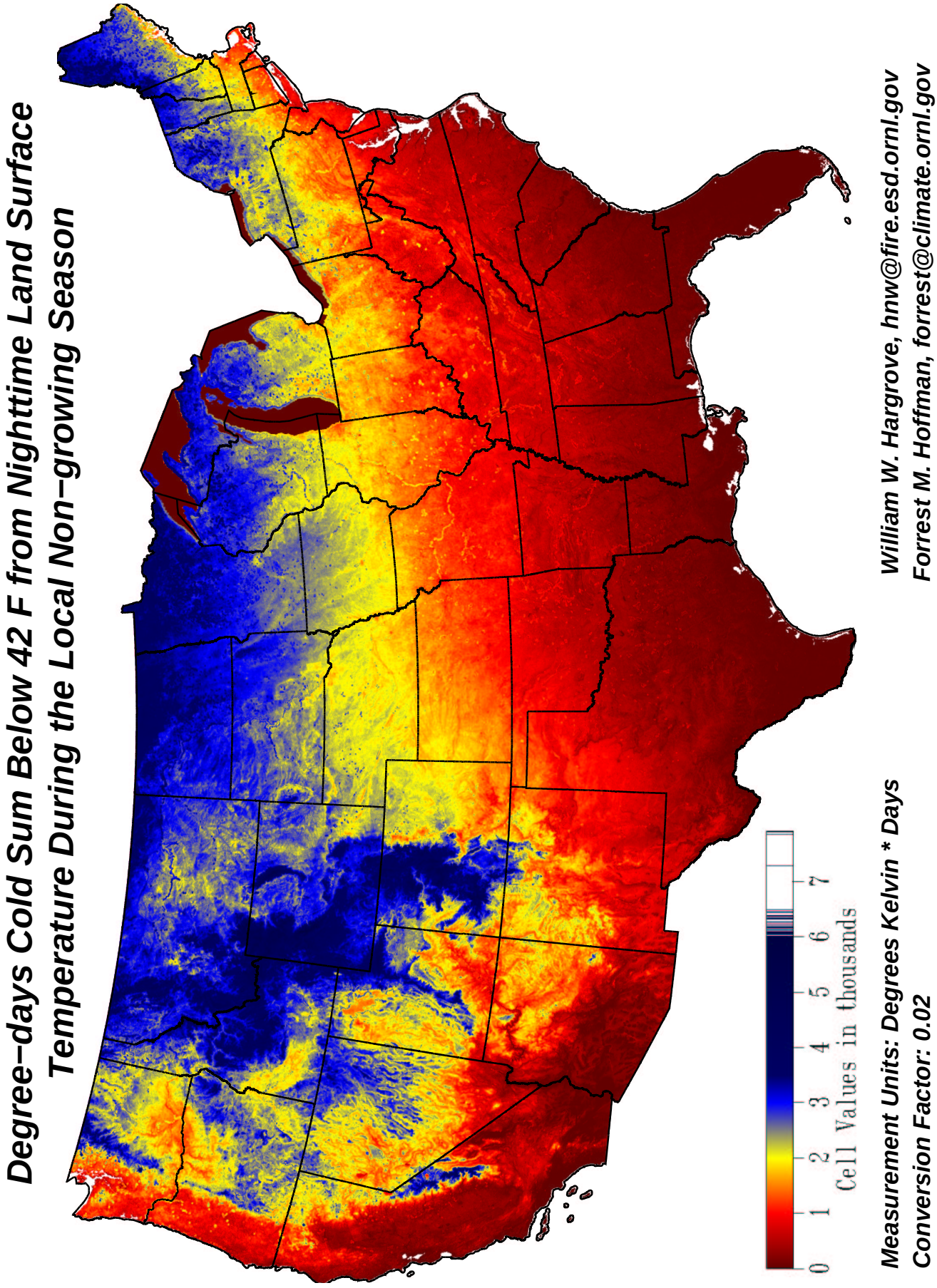

Figure 2.2: Degree-days Cold Sum Below 42°F from Nighttime Land Surface Temperature During the Local Non-growing Season

2.2 Number of Hot Days and Cold Days

Name: Number of Days Above 90°F During the Local Growing Season, Number of Days Below 32°F During the Local Non-growing Season

Data Sources: Monthly mean number of days maximum temperature $\geq$ 90°F, Monthly mean number of days minimum temperatures $\leq$ 32°F, Median day of last frost of spring, Median day of first frost of fall, all from 1961–1990 climate normals, Climate Source, Inc., http://www.climatesource.com/

Description of Processing: Reprojected 12 monthly maps for hot days and cold days from geographic coordinates to LAEA using nearest-neighbor resampling. A spline with tension was used to interpolate smoothed daily values for each cell, and then the number of days was summed for the growing and non-growing seasons, according to the two Climate Source frost layers.

Measurement Units: Days

Conversion Factor: 0.01

Expected Discriminatory Power: While degree-day sums carry information about mean temperature, information is also needed about variance and frequency of temperature extremes. Most vegetation stops photosynthesis at temperatures above 90°F and below 32°F, so the number of excursions into these extreme events is important for expected carbon flux.

Comments/Observations: These maps of frequencies of temperature extremes highlight maritime vs. continental differences, and also the effects of higher elevations.

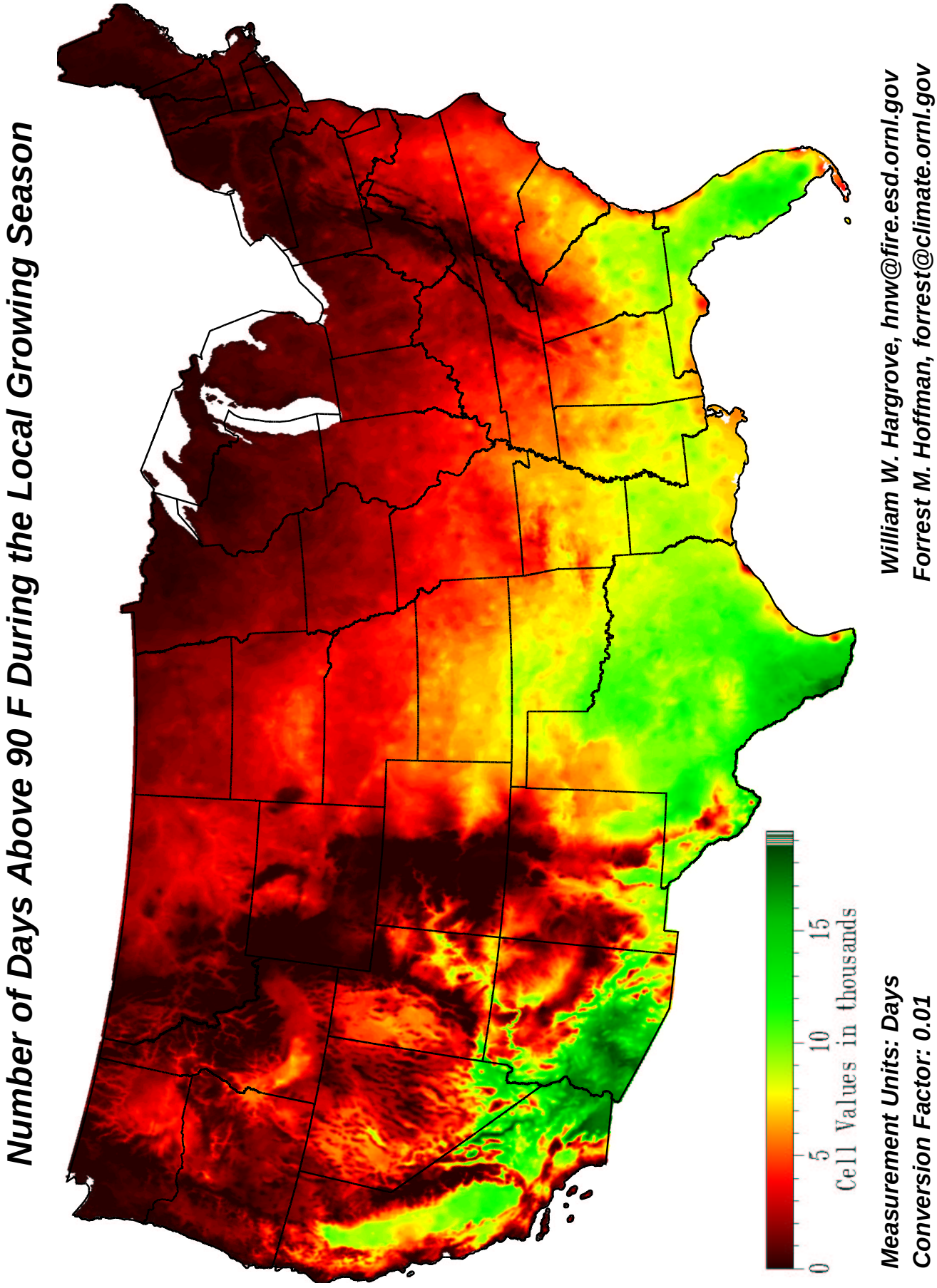

Figure 2.3: Number of Days Above 90°F During the Local Growing Season

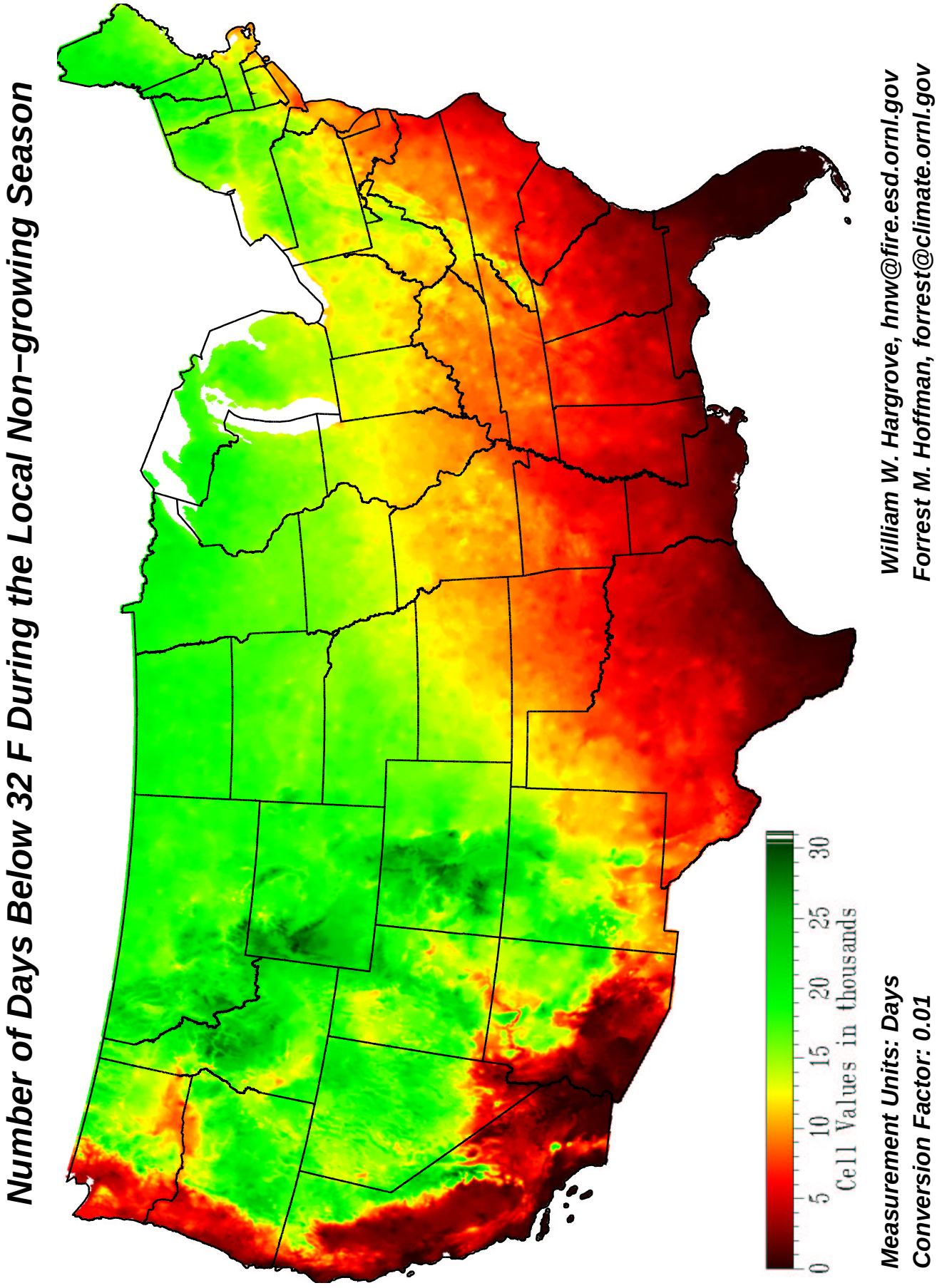

Figure 2.4: Number of Days Below 32°F During the Local Non-growing Season

2.3 Maximum Diurnal Surface Temperature Differences

Name: 95th Percentile of Maximum Diurnal Surface Temperature Difference During the Local Growing Season, 95th Percentile of Maximum Diurnal Surface Temperature Difference During the Local Non-growing Season

Data Sources: MODIS MOD11A2 Collection4 1km 8-day composites, 2000 through 2002; median day of last frost of spring, median day of first frost of fall, Climate Source, Inc., http://www.climatesource.com/

Description of Processing: 14 MODIS tiles comprising the CONUS at each date × 46 8-day composites per year × 3 years (2000,2001,2002) = 1932 MODIS tiles obtained from LPDAAC, mosaicked and reprojected using the MODIS Reprojection Tool v3.1c and nearest-neighbor resampling to 1km LAEA. Daytime Land surface temperature (SDS 1) and Nighttime Land surface temperature (SDS 5) were used as the starting points to calculate the diurnal surface temperature differences. Although the Clear-sky flags for each of these (SDS 11 and 12) were consulted for Quality Control, it was decided that even a single clear-sky temperature was potentially better than an interpolated value. Therefore, land-surface temperature values were retained if the sensor saw even a single clear-sky view within the 8-day viewing period.

The 3 images from each of the 3 years were composited by averaging into a single sequence of 46 dates representing a nominal or synoptic year. Gaps were filled using a temporal spline with tension, using the lowest possible tension setting that did not cause data over- and under-shoots (see Section 1.5 for details). Cells having 3 or fewer dates with data were filled by repeatedly applying a 7 × 7 cell weighted spatial adaptive filter.

Each of the 46 nighttime maps were subtracted from the 46 daytime maps to produce 46 diurnal surface temperature difference maps. A spline with tension was used to interpolate smoothed daily values of diurnal difference for each cell.

The maximum diurnal surface temperature difference values were split across days of the growing season and non-growing season on a cell-by-cell basis, using the Julian days from the two Climate Source frost layers. Because the greatest single diurnal surface temperature difference might be anomalous, we mapped the 95th percentile of the maximum diurnal surface temperature difference within each season instead. The 95th percentile is more robust to outlier values from either of the two surface temperature maps.

Measurement Units: Degrees Kelvin

Conversion Factor: 0.02
The conversion factor used in the original MOD11A2 product was retained.

Expected Discriminatory Power: The range of diurnal temperature provides information about daily extremes of surface temperature, which control the environments of photosynthesis and respiration. Continental and high-elevation locations will be distinguished from maritime and low-elevation locations by this diurnal thermal range. Wetter locations would also be expected to have more diurnal thermal inertia than drier locations.

Comments/Observations: High deserts show the greatest diurnal temperature ranges during both seasons, while the Great Lakes and wet places like the Mississippi Delta and the Everglades show the least diurnal temperature differences.

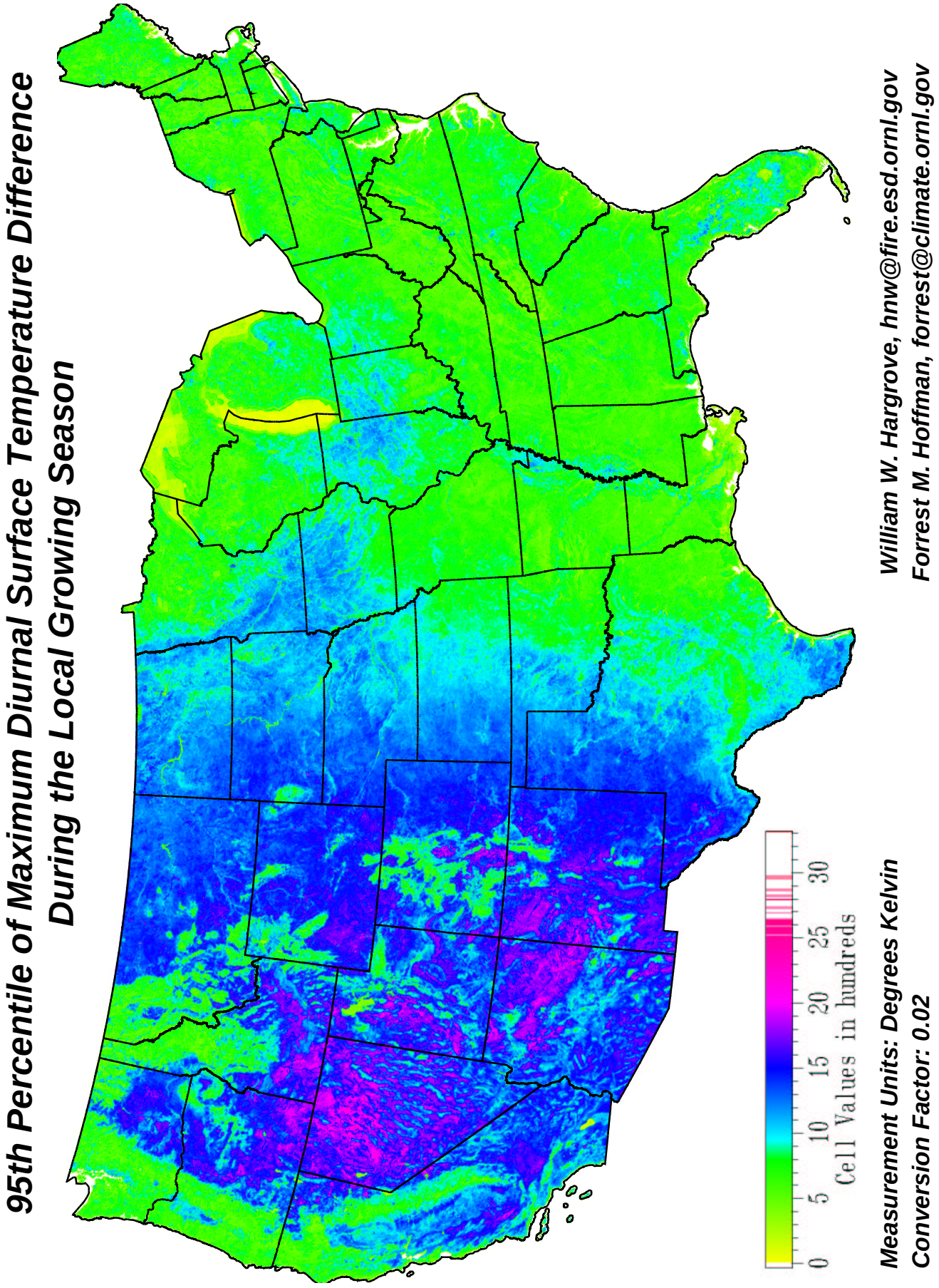

Figure 2.5: 95$^{\text{th}}$ Percentile of Maximum Diurnal Surface Temperature Difference During the Local Growing Season

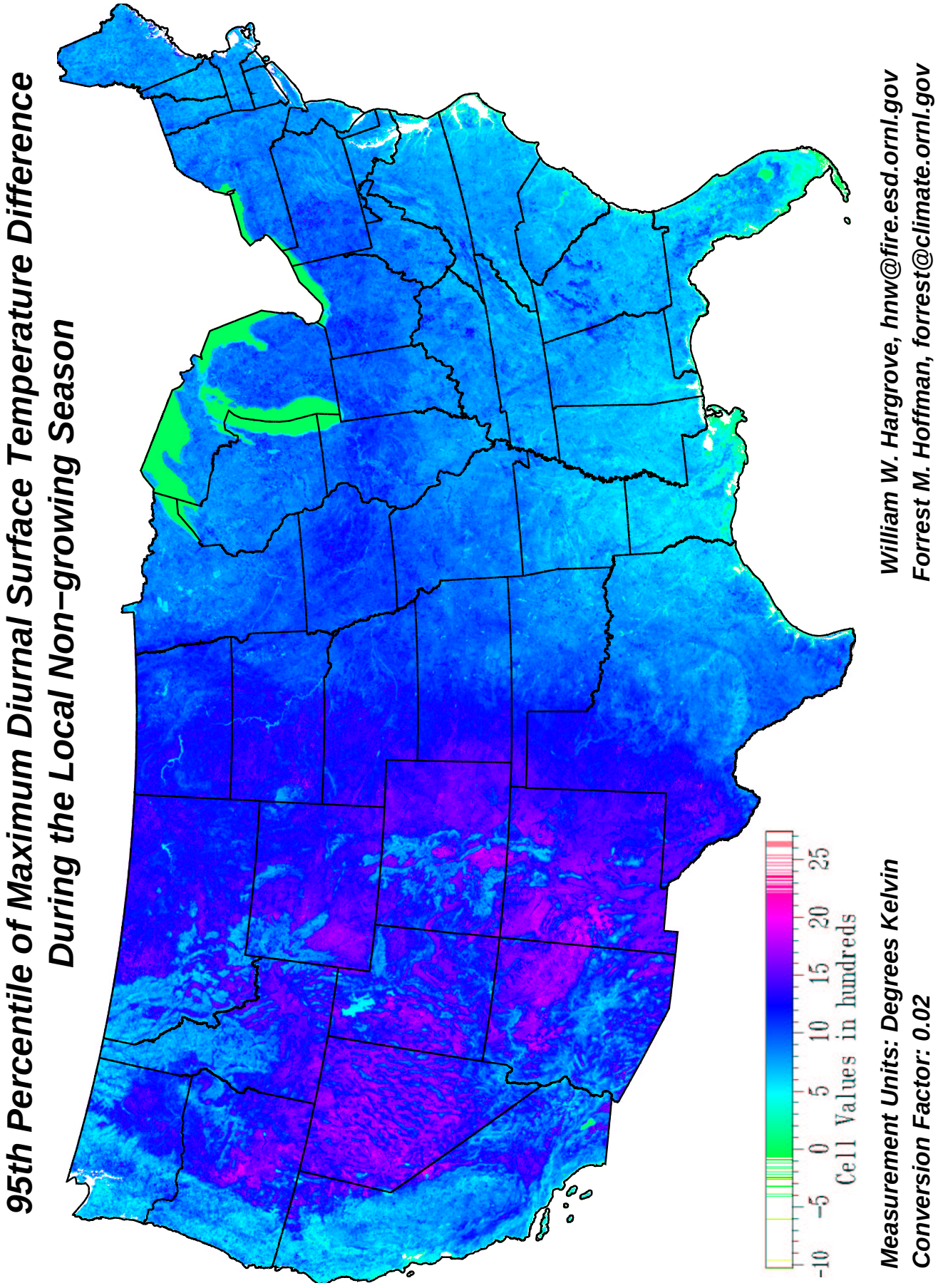

Figure 2.6: 95$^{\text{th}}$ Percentile of Maximum Diurnal Surface Temperature Difference During the Local Non-growing Season

2.4 Total Precipitation

Name: Total Precipitation During the Local Growing Season, Total Precipitation During the Local Non-growing Season

Data Sources: Monthly precipitation, Median day of last frost of spring, Median day of first frost of fall, all from 1961–1990 climate normals, Climate Source, Inc., http://www.climatesource.com/

Description of Processing: Reprojected 12 monthly precipitation maps for hot days and cold days from geographic coordinates to LAEA using nearest-neighbor resampling. A spline with tension was used to interpolate smoothed daily values for each cell, and then the daily precipitation was summed for the growing and non-growing seasons, according to the two Climate Source frost layers.

Measurement Units: Millimeters

Conversion Factor: 0.01

Expected Discriminatory Power: Mean precipitation may be the most important limiting factor for photosynthesis.

Comments/Observations: Coastal areas of the Pacific Northwest enjoy precipitation during the growing season, since temperatures in these areas are mediated by the ocean, allowing higher sums of precipitation to integrate. The crest of the Cascade Range through Washington and Oregon sharply divides the western slopes, which get a lot of precipitation, from the dry eastern slopes. Water budgets in the west depend on spring melt of a winter snowpack, because growing season precipitation is so small. Areas just east of the Smoky mountains (near the Georgia/North Carolina border) have subtropical amounts of annual precipitation.

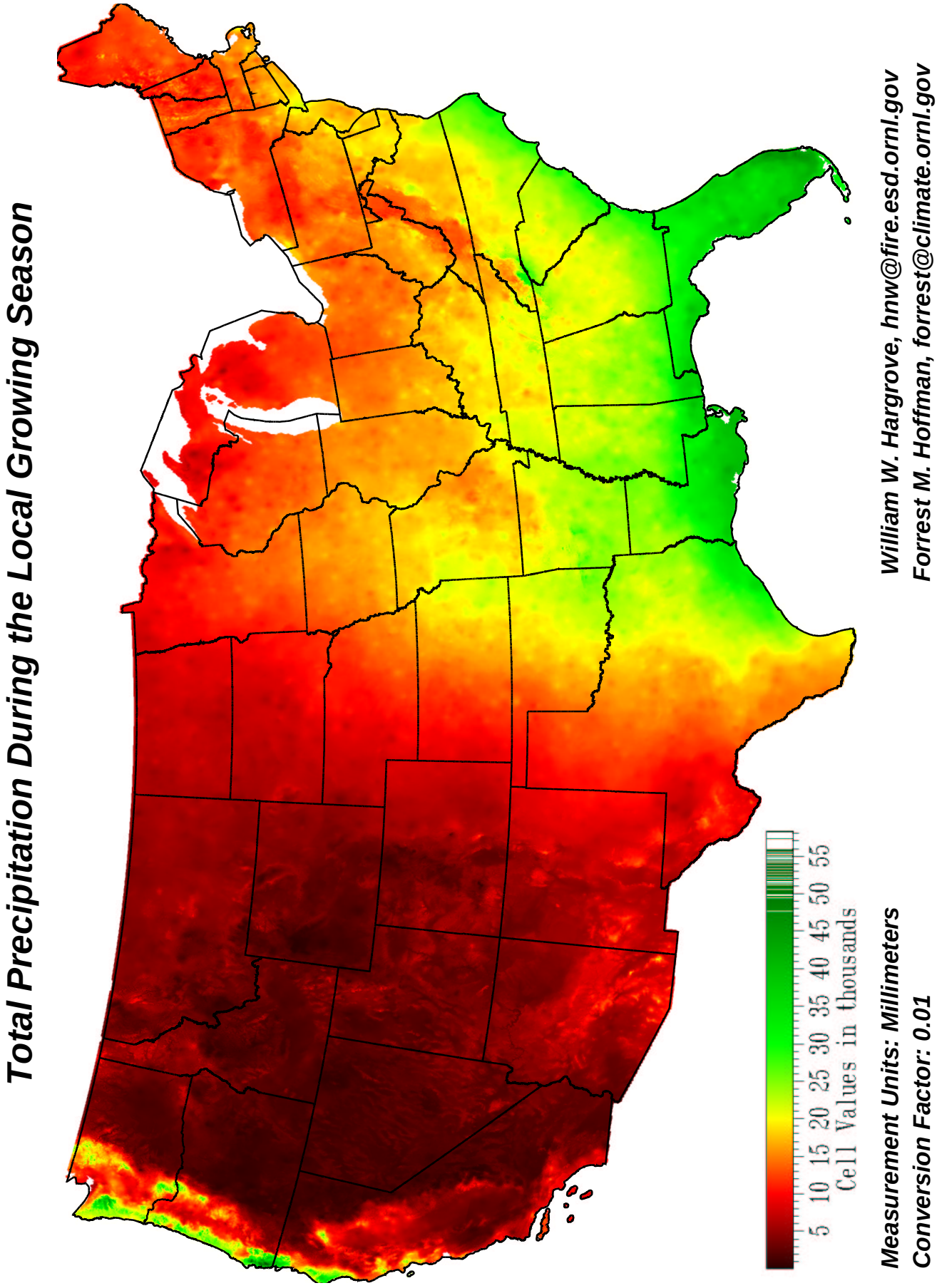

Figure 2.7: Total Precipitation During the Local Growing Season

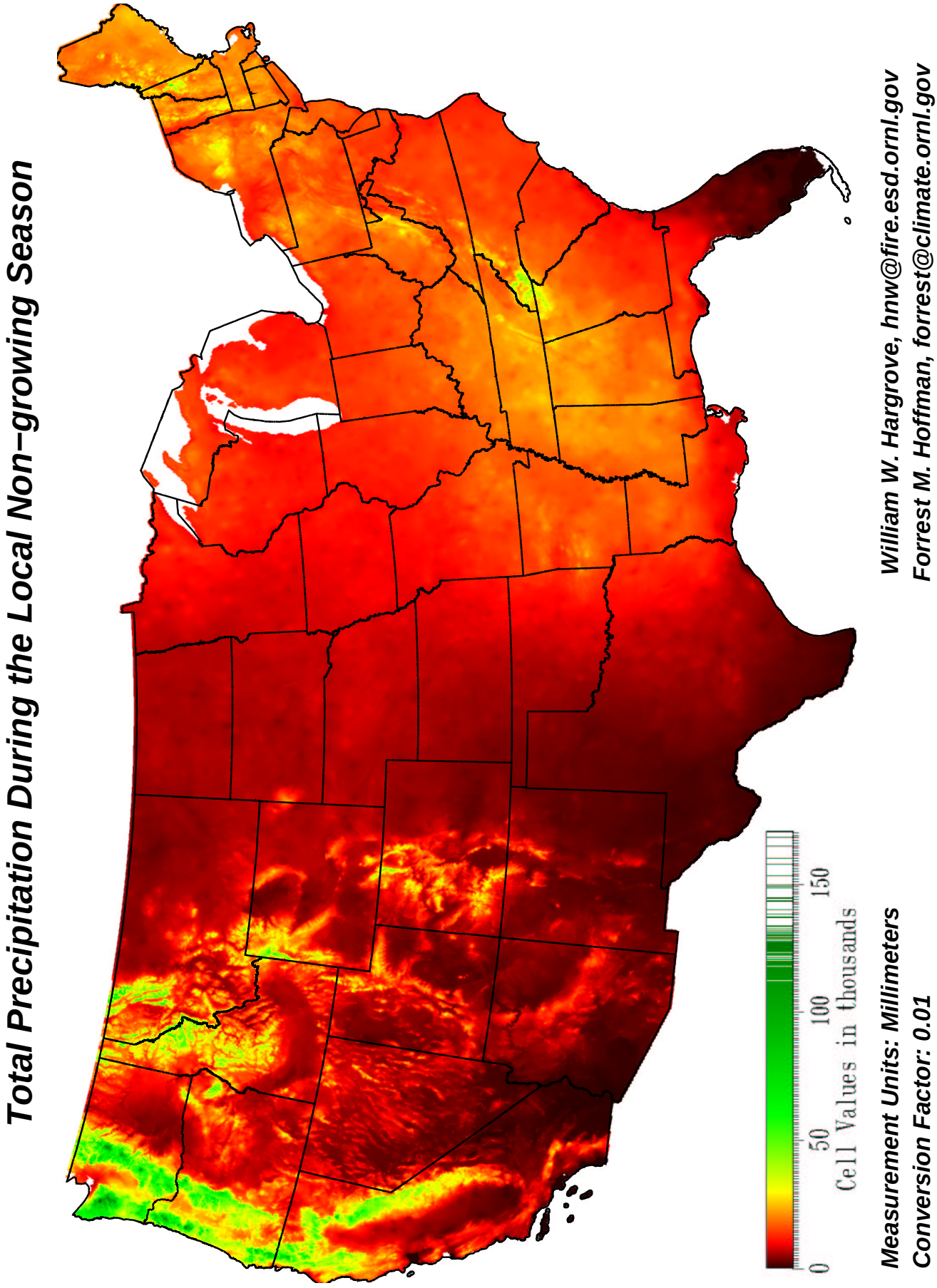

Figure 2.8: Total Precipitation During the Local Non-growing Season

2.5 Number of Days with Measurable Precipitation

Name: Number of Days with Measurable Precipitation During the Local Growing Season, Number of Days with Measurable Precipitation During the Local Non-growing Season

Data Sources: Monthly mean number of days with precipitation ≥ 0.01", Median day of last frost of spring, Median day of first frost of fall, all from 1961–1990 climate normals, Climate Source, Inc., http://www.climatesource.com/

Description of Processing: Reprojected 12 monthly maps for days with measurable precipitation from geographic coordinates to LAEA using nearest-neighbor resampling. A spline with tension was used to interpolate smoothed daily values for each cell, and then the number of days was summed for the growing and non-growing seasons, according to the two Climate Source frost layers.

Measurement Units: Days

Conversion Factor: 0.01

Expected Discriminatory Power: While total precipitation carries information of significance for vegetation, it is in the sense of a mean. Equally important to vegetation growth is the variance of precipitation, i.e., how it is distributed through time. These layers will distinguish places that receive their precipitation in only a few discrete events from those locations whose precipitation is spread evenly across time. Since precipitation events in the non-growing season can represent snowfall, this layer also carries information about snowpack.

Comments/Observations: The Pacific Northwest and the east coast of Florida have the greatest number of precipitation events during the growing season. The non-growing season clearly shows "lake-effect" snowfalls associated with the Great Lakes in Northern Michigan and the Upper Peninsula, Pennsylvania, and New York. This occurs when cold, dry Canadian air sweeps over the warmer Great Lakes, absorbing moisture which is then deposited as snow when the air mass passes over land.

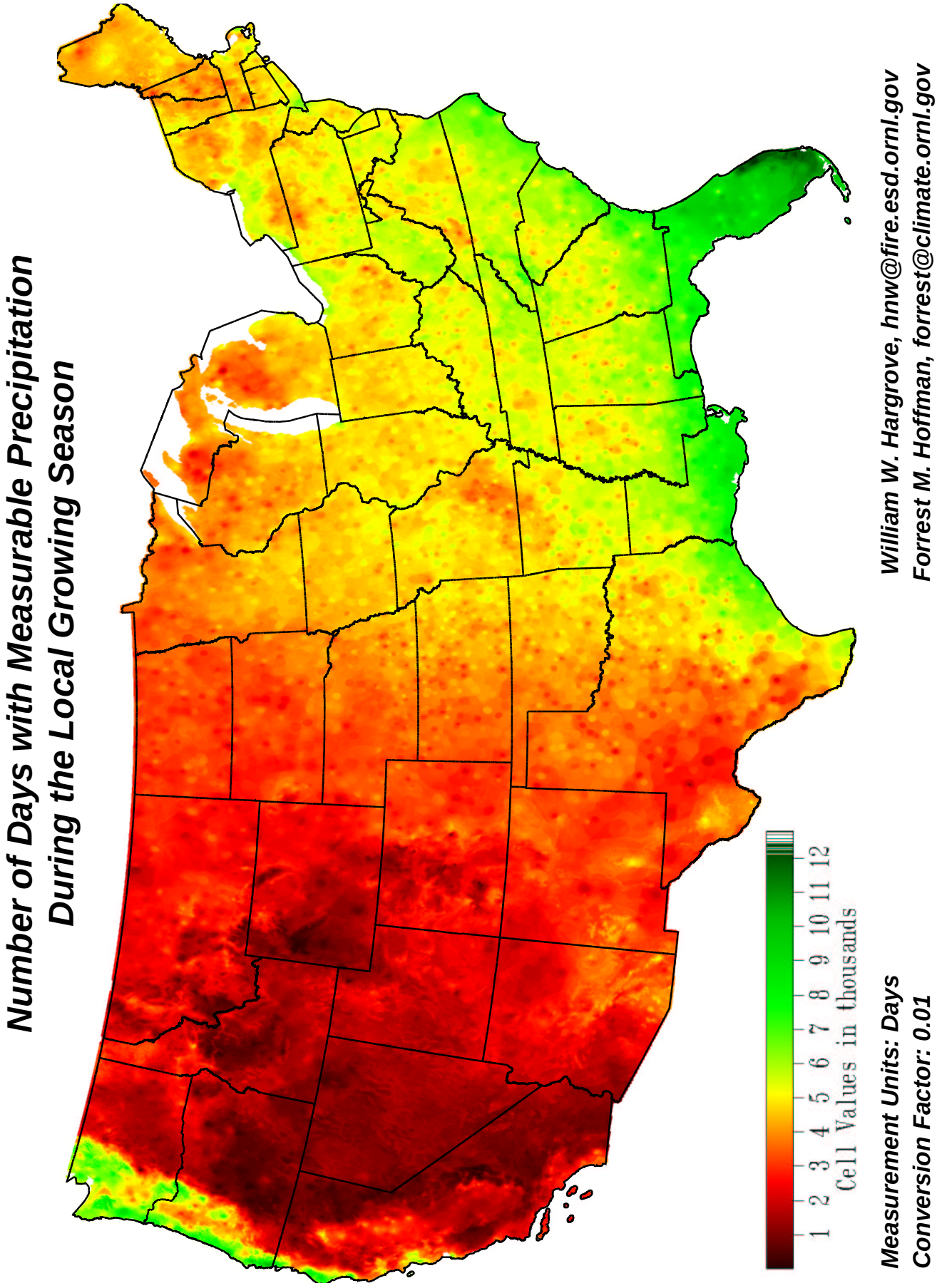

Figure 2.9: Number of Days with Measurable Precipitation During the Local Growing Season

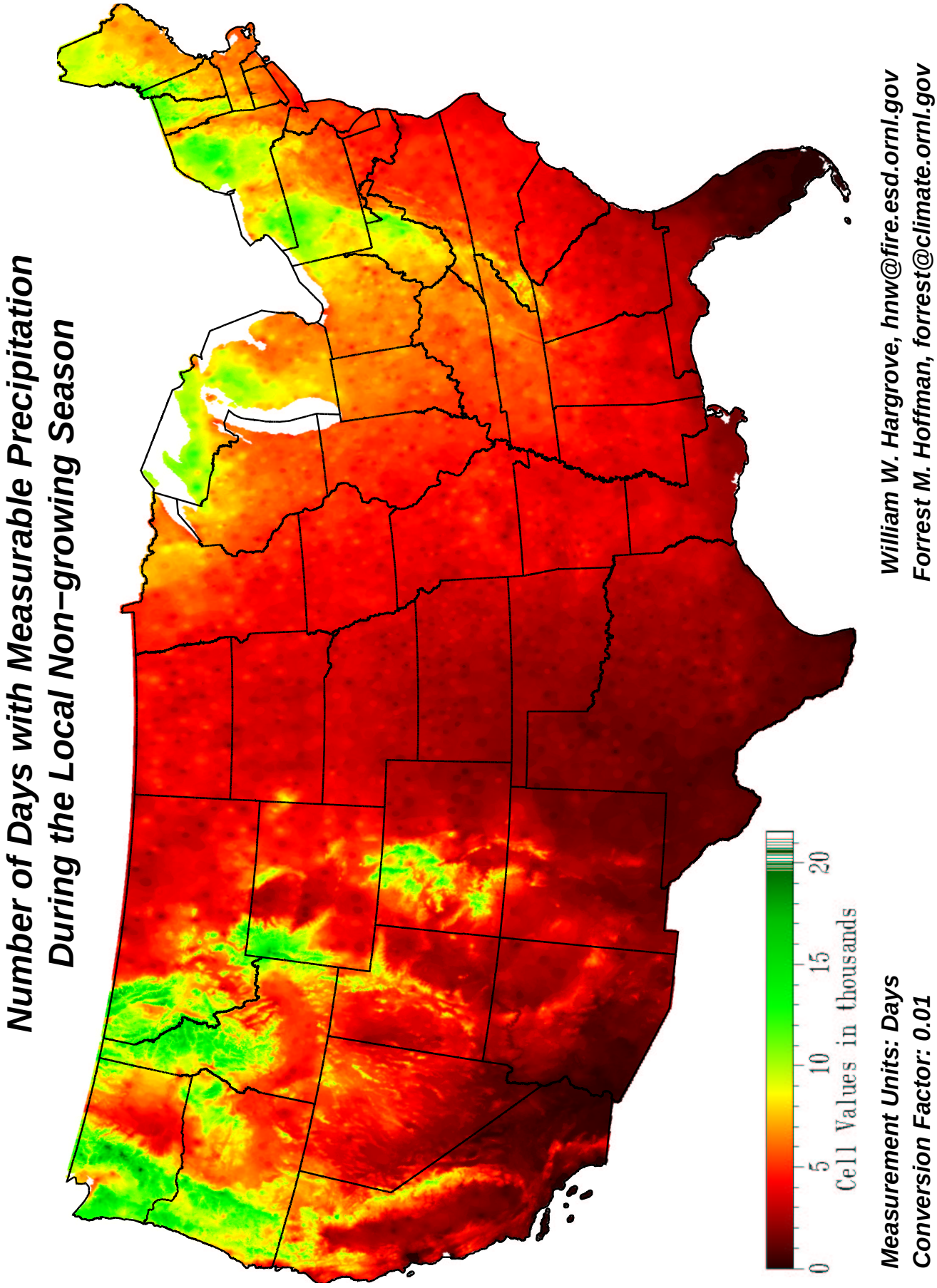

Figure 2.10: Number of Days with Measurable Precipitation During the Local Non-growing Season

2.6 Depth of Mineral Soil

Name: Depth of Mineral Soil

Data Sources: State Soil Geographic (STATSGO) Database, U.S. Depart of Agriculture, Natural Resources Conservation Service, National Soil Survey Center

Description of Processing: Vector Map Unit ID (muid) polygon vectors joined for all states in CONUS, reprojected to LAEA and converted to raster at 1km resolution. Average depth to bedrock calculated for each component of each muid polygon, then area-weighted by the contribution of that component to the muid polygon.

Measurement Units: Centimeters

Conversion Factor: None

Expected Discriminatory Power: Depth of mineral soil is an important ecosystem characteristic, and carries information on rooting zone and root drainage. This layer will distinguish areas where bedrock comes close to the surface from areas with deep soils from sandy or gravelly areas.

Comments/Observations: The Southern Appalachians show thin soils because of proximity of bedrock to the surface. Southern Nevada shows thin soils on top of sand and gravel, as does Eastern Texas.

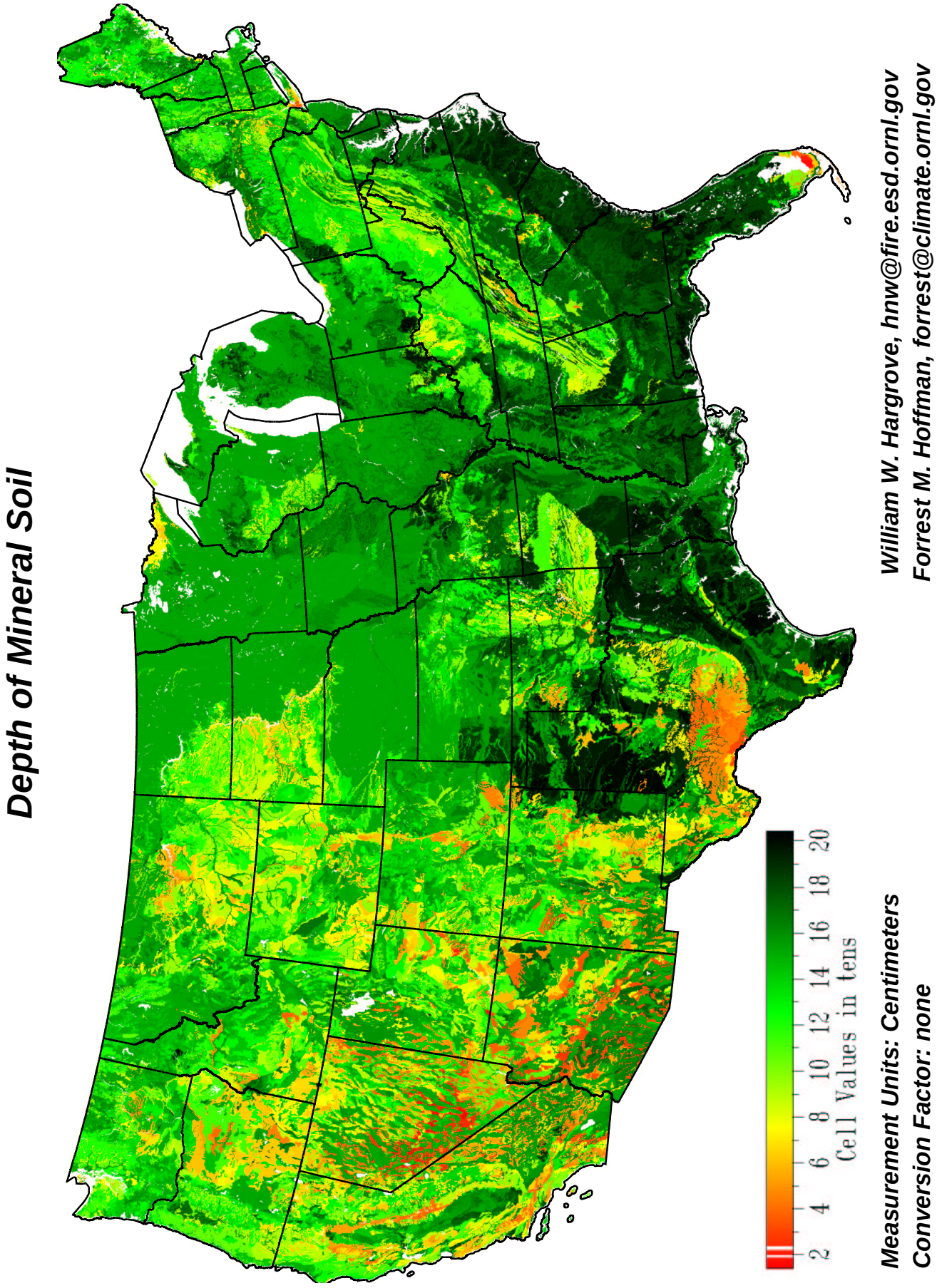

Figure 2.11: Depth of Mineral Soil

2.7 Depth to Water Table

Name: Depth to Water Table

Data Sources: State Soil Geographic (STATSGO) Database, U.S. Depart of Agriculture, Natural Resources Conservation Service, National Soil Survey Center

Description of Processing: Vector Map Unit ID (muid) polygon vectors joined for all states in CONUS, reprojected to LAEA and converted to raster at 1km resolution. Average depth to water table was calculated for each component of each muid polygon, then area-weighted by the contribution of that component to the muid polygon.

Measurement Units: Feet

Conversion Factor: 0.1

Expected Discriminatory Power: Depth to water table is a measure of water availability for vegetation at a site, and also contains information about root inundation and anoxia if too shallow.

Comments/Observations: Most of the western United States is beyond the range of this STATSGO parameter, so it serves to discriminate eastern locations from one another. The Mississippi Valley and Delta, the Florida Everglades the Okefenokee Swamp, and the Atlantic Coastal Plain have very shallow water tables. The Great Salt Lake also has a shallow water table.

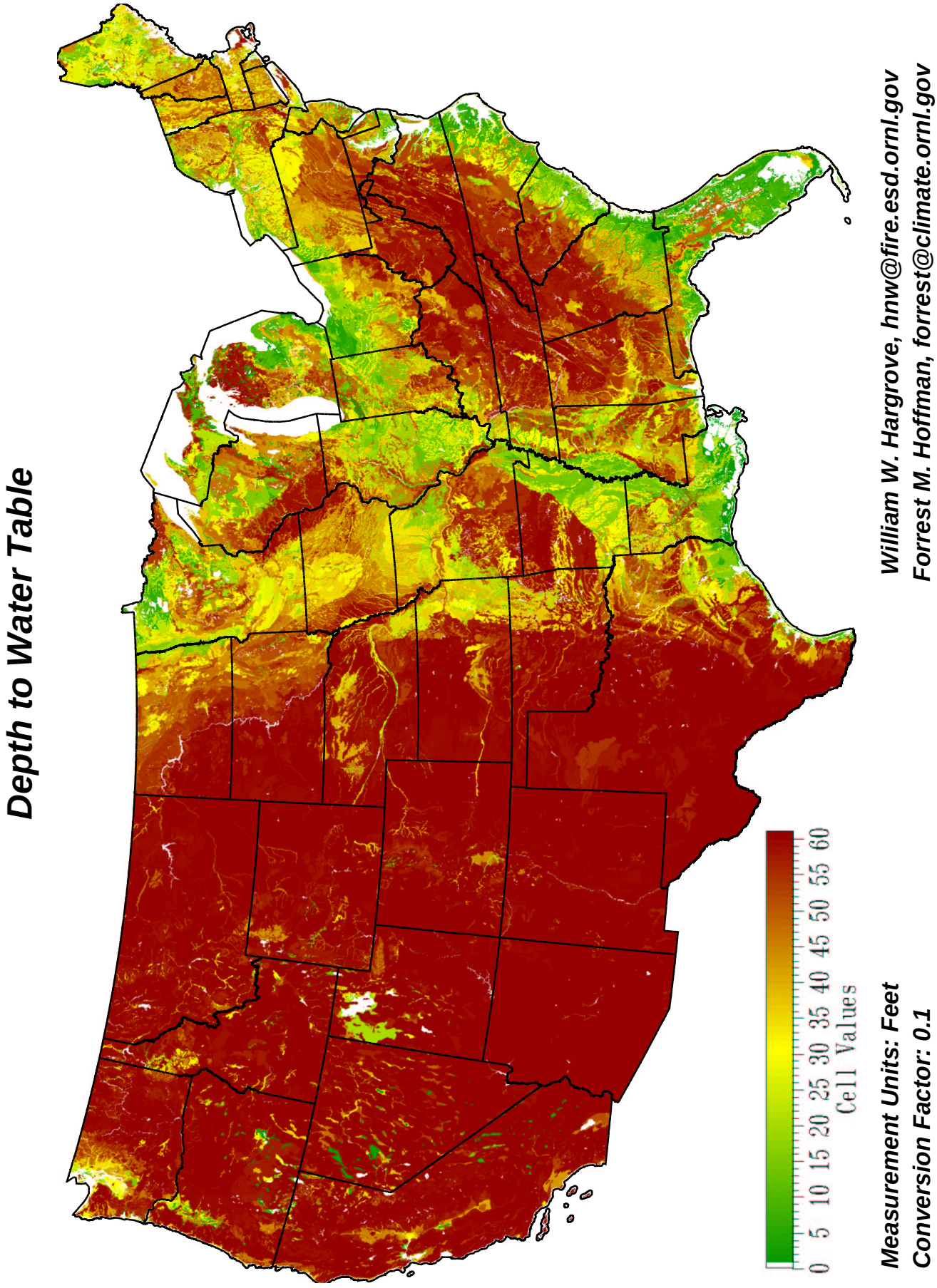

Figure 2.12: Depth to Water Table

2.8 Soil Kjeldahl Nitrogen to 50cm Depth

Name: Soil Kjeldahl Nitrogen to 50cm Depth

Data Sources: State Soil Geographic (STATSGO) Database, U.S. Depart of Agriculture, Natural Resources Conservation Service, National Soil Survey Center; National Soil Characterization Database (NSCD), National Soil Survey Center—Soil Survey Laboratory (SSL).

Description of Processing: The soil taxonomy specified for each component of each Map Unit ID (muid) polygon in STATSGO was used as a link into the NSCD database. All soil pedons fitting this soil taxonomy within NSCD are used. Soil Kjeldahl nitrogen was summed layer by layer, weighted for layer thickness, down to the cutoff depth of 50cm. All pedons with this taxonomy within NSCD that had information down to the cutoff depth were averaged together.

The average for each component of each muid polygon was then weighted spatially by the area of the muid comprised by that component. Thus, the single value for each STATSGO muid represents a vertical integration through all soil layers from all taxonomic matching pedons in NSCD down to the cutoff depth, followed by a horizontal area-weighting by the size of each component of the muid polygon.

If no pedons in the NSCD matched the full four-level taxonomic soil type called for by STATSGO, the least-significant subgroup designation was dropped, and the match was performed again. This process of dropping the least significant specifier in the soil taxonomy was repeated until all components of all STATSGO muid polygons were calculated.

Measurement Units: kg N/ha

Conversion Factor: None

Expected Discriminatory Power: Soil nitrogen limits productivity for many CONUS ecosystems. Estimates of soil nitrogen will discriminate areas having high potential vegetation productivity from those with lower potential productivity. Productivity of vegetation has a direct impact on expected carbon flux.

Comments/Observations: The cutoff depth for this map was chosen because nutrients present in the upper 50cm of soil are available to plants via fine roots. The Mississippi Delta, the Everglades, the Okefenokee and Atlantic Coastal swamps, and the wetlands of the Upper Peninsula are all high in soil nitrogen.

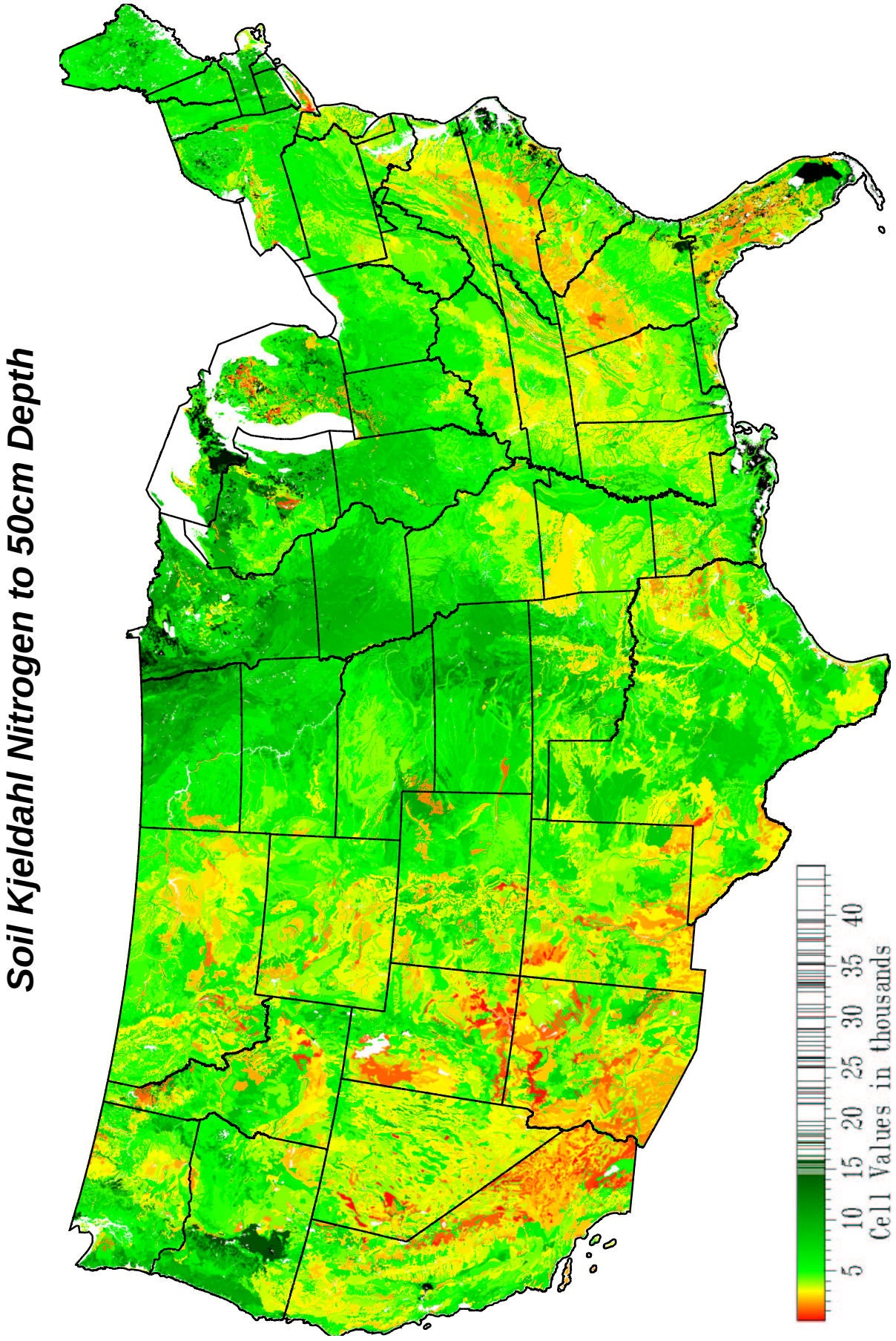

Figure 2.13: Soil Kjeldahl Nitrogen to 50cm Depth

2.9 Soil Organic Matter to 50cm Depth

Name: Soil Organic Matter to 50cm Depth

Data Sources: State Soil Geographic (STATSGO) Database, U.S. Depart of Agriculture, Natural Resources Conservation Service, National Soil Survey Center; National Soil Characterization Database (NSCD), National Soil Survey Center—Soil Survey Laboratory (SSL).

Description of Processing: The soil taxonomy specified for each component of each Map Unit ID (muid) polygon in STATSGO was used as a link into the NSCD database. All soil pedons fitting this soil taxonomy within NSCD are used. Soil organic matter was summed layer by layer, weighted for layer thickness, down to the cutoff depth of 50cm. All pedons with this taxonomy within NSCD that had information down to the cutoff depth were averaged together.

The average for each component of each muid polygon was then weighted spatially by the area of the muid comprised by that component. Thus, the single value for each STATSGO muid represents a vertical integration through all soil layers from all taxonomic matching pedons in NSCD down to the cutoff depth, followed by a horizontal area-weighting by the size of each component of the muid polygon.

If no pedons in the NSCD matched the full four-level taxonomic soil type called for by STATSGO, the least-significant subgroup designation was dropped, and the match was performed again. This process of dropping the least significant specifier in the soil taxonomy was repeated until all components of all STATSGO muid polygons were calculated.

Measurement Units: kg OM/ha

Conversion Factor: 0.01

Expected Discriminatory Power: Soil organic matter is both a plant nutrient and an indication of past vegetation productivity. It may also carry information about soil respiration.

Comments/Observations: The cutoff depth for this map was chosen because nutrients present in the upper 50cm of soil are available to plants via fine roots. The soils of the upper Midwest, the Mississippi Delta, the Atlantic Coastal Plain, and the Pacific Northwest are all high in organic matter content. In contrast, the sandy desert soils of Arizona are poor in organic matter.

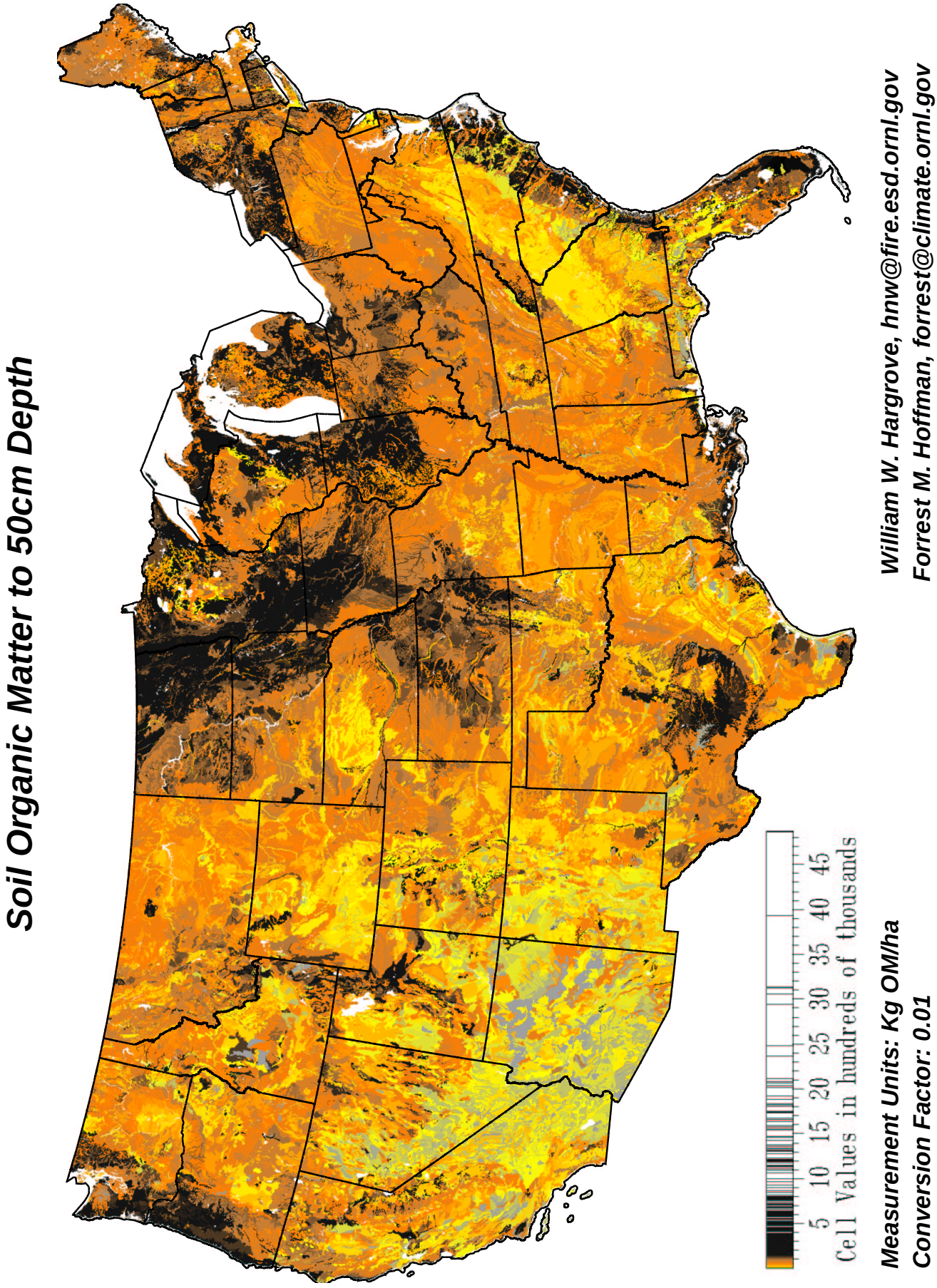

Figure 2.14: Soil Organic Matter to 50cm Depth

2.10 Soil Plant-Available Water Holding Capacity to 1.5m Depth

Name: Soil Plant-Available Water Holding Capacity to 1.5m Depth

Data Sources: State Soil Geographic (STATSGO) Database, U.S. Depart of Agriculture, Natural Resources Conservation Service, National Soil Survey Center; National Soil Characterization Database (NSCD), National Soil Survey Center - Soil Survey Laboratory (SSL).

Description of Processing: The soil taxonomy specified for each component of each Map Unit ID (muid) polygon in STATSGO was used as a link into the NSCD database. All soil pedons fitting this soil taxonomy within NSCD are used. Soil plant-available water was summed layer by layer, weighted for layer thickness, down to the cutoff depth of 1.5m. All pedons with this taxonomy within NSCD that had information down to the cutoff depth were averaged together.

The average for each component of each muid polygon was then weighted spatially by the area of the muid comprised by that component. Thus, the single value for each STATSGO muid represents a vertical integration through all soil layers from all taxonomic matching pedons in NSCD down to the cutoff depth, followed by a horizontal area-weighting by the size of each component of the muid polygon.

If no pedons in the NSCD matched the full four-level taxonomic soil type called for by STATSGO, the least-significant subgroup designation was dropped, and the match was performed again. This process of dropping the least significant specifier in the soil taxonomy was repeated until all components of all STATSGO muid polygons were calculated.

Measurement Units: Percent by weight

Conversion Factor: None

Expected Discriminatory Power: Plant-available soil water is a characteristic describing the water-holding capacity of soil, and describes the amount of water that vegetation could remove from that soil. That the soil has a particular water holding capacity is independent from the question of whether that water is actually present in that soil. In other words, this layer describes a characteristic of the soil rather than a characteristic of moisture or wetness itself.

Comments/Observations: The cutoff depth for this map was chosen because the water in the first 1.5m is available to plants via tap roots. The deep Molisols of the Midwest “breadbasket” and the Piedmont show the greatest water holding capacity. Soils in the Pacific Northwest and the Mississippi Delta also have high water holding capacity.

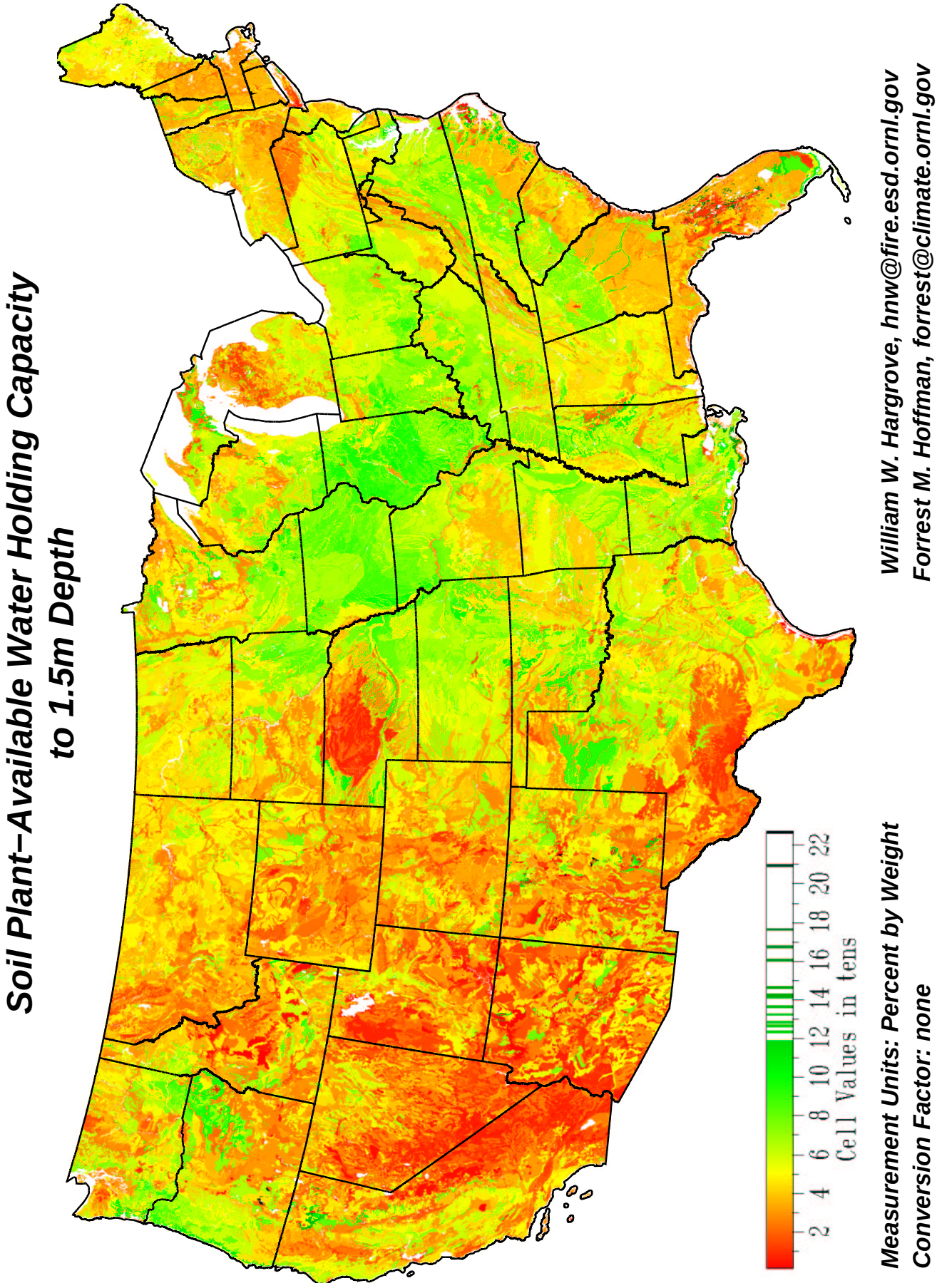

Figure 2.15: Soil Plant-Available Water Holding Capacity to 1.5m Depth

2.11 Compound Topographic Index (CTI)

Name: Compound Topographic Index

Data Sources: HYDRO1k, USGS, http://edcdaac.usgs.gov/gtopo30/hydro/namerica.asp

Description of Processing: Developed from the USGS' 30 arc-second digital elevation model (DEM) of the world (GTOPO30), HYDRO1k provides a standard suite of geo-referenced data sets at a resolution of 1 km regarding hydrologic information on a continental scale. Processing is described at http://edcdaac.usgs.gov/gtopo30/hydro/readme.asp

Measurement Units: Unitless

Conversion Factor: 0.01

Expected Discriminatory Power: The Compound Topographic Index (CTI), commonly referred to as the Wetness Index, is a function of the upstream contributing area and the slope of the landscape. The implementation used in the HYDRO1k data set is based on Moore et al (1991). The CTI is calculated using a flow accumulation (FA) layer along with the slope as:

$$\mathrm{CTI} = \frac{\ln(\mathrm{FA})}{\tan(\mathrm{slope})}$$

In areas of no slope, a CTI value is obtained by substituting a slope of 0.001. This value is smaller than the smallest slope obtainable from a 1000m data set with a 1m vertical resolution.

CTI carries information about relative landform (slope and drainage) position, differentiating hilltop locations from midslope locations from valley bottom locations. Landform position is a strong surrogate for relative wetness, although being at the bottom of a drainage is not a guarantee of the availability of water.

Moore, I.D., R.B. Grayson and A.R. Ladson, 1991, Digital Terrain Modelling: A Review of Hydrological, Geomorphological and Biological Applications. In: Hydrological Processes An International Journal, January–March, 1991, pp. 3–30.

Comments/Observations: Even rivers smaller than 1 km wide are visible in the CTI layer, because the river channels in which they flow are visible at this resolution. Since the technology does not exist to measure soil moisture over CONUS scales, CTI is probably the best surrogate that is obtainable. As an important limiting resource for photosynthesis, relative soil moisture is important for expected carbon flux.

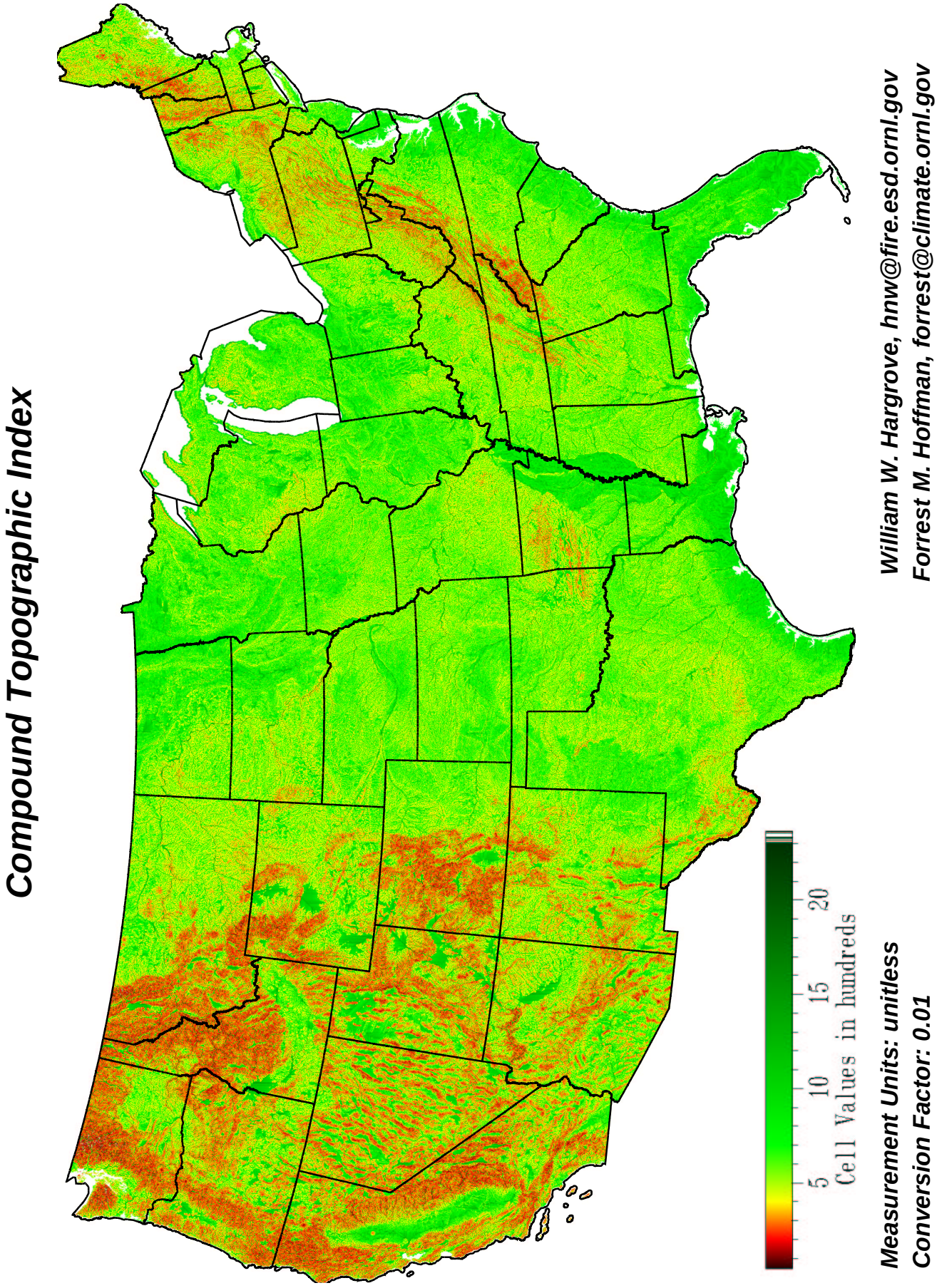

Figure 2.16: Compund Topographic Index (CTI)

2.12 Total Solar Insolation

Name: Total Solar Insolation During the Local Growing Season Including Clouds, Aerosols, Slope and Aspect Physiography, Total Solar Insolation During the Local Non-growing Season Including Clouds, Aerosols, Slope and Aspect Physiography

Data Sources: Surface Meteorology and Solar Energy (SSE) Data Set, 1 degree, NASA LARC, http://eosweb.larc.nasa.gov/cgi-bin/sse/global.cgi; USGS GTOPO30 1km elevation; Median day of last frost of spring, Median day of first frost of fall, all from 1961–1990 climate normals, Climate Source, Inc., http://www.climatesource.com/

Description of Processing: Constructed 12 monthly maps from SSE, representing monthly averages for July 1983–June 1993. SSE maps were resampled to 0.1 degree using a regularized spline with tension and smoothing. Splined 0.1 degree maps were reprojected to 1km LAEA using bilinear resampling. These maps represent instantaneous insolation on a theoretical horizontal surface, given in kWh/m^2/day.

Most land surfaces are not horizontal, but have a particular aspect, slope, and orientation. Reprojected the GTOPO30 30 arc-second digital elevation model (DEM) data to 1km LAEA using nearest neighbor resampling. Calculated Solar F, the ratio of solar insolation on a land surface with a particular slope and orientation to solar insolation on a theoretical horizontal surface. Solar F ratio can be greater than one for favorable solar aspects, to less than one or even zero for unfavorable orientations (Swift 1976). Using the DEM, calculated 12 monthly Solar F maps, using the solar position on the median day of each month.

Multiplied the monthly maps of instantaneous insolation on a horizontal surface by the monthly maps of average Solar F ratio to obtain monthly actual insolation on the land surface, given its aspect and slope. A spline with tension was used to interpolate smoothed daily values for each cell, and then the total solar insolation was summed for the growing and non-growing seasons, according to the two Climate Source frost layers.

Swift, L.W. 1976. Algorithm for Solar Radiation on Mountain Slopes. Water Resources Research 12(1):108-112.

Measurement Units: kWh/m^2

Conversion Factor: None

Expected Discriminatory Power: This total solar insolation layer carries information about slope, aspect, and solar orientation, as well as elevation and cloudiness. The total amount of energy impinging on the surface, corrected for surface orientation and summed over the growing and non-growing seasons, is important as the driving force behind carbon fixation and respiration temperature.

Comments/Observations: The Sonoran Desert area receives the most solar insolation annually. The aspect of individual mountain ranges can start to be seen in this area. West Texas and the Florida peninsula also receive large amounts of solar insolation. The Pacific Northwest and the Northeast receive somewhat less total insolation than the rest of the country.

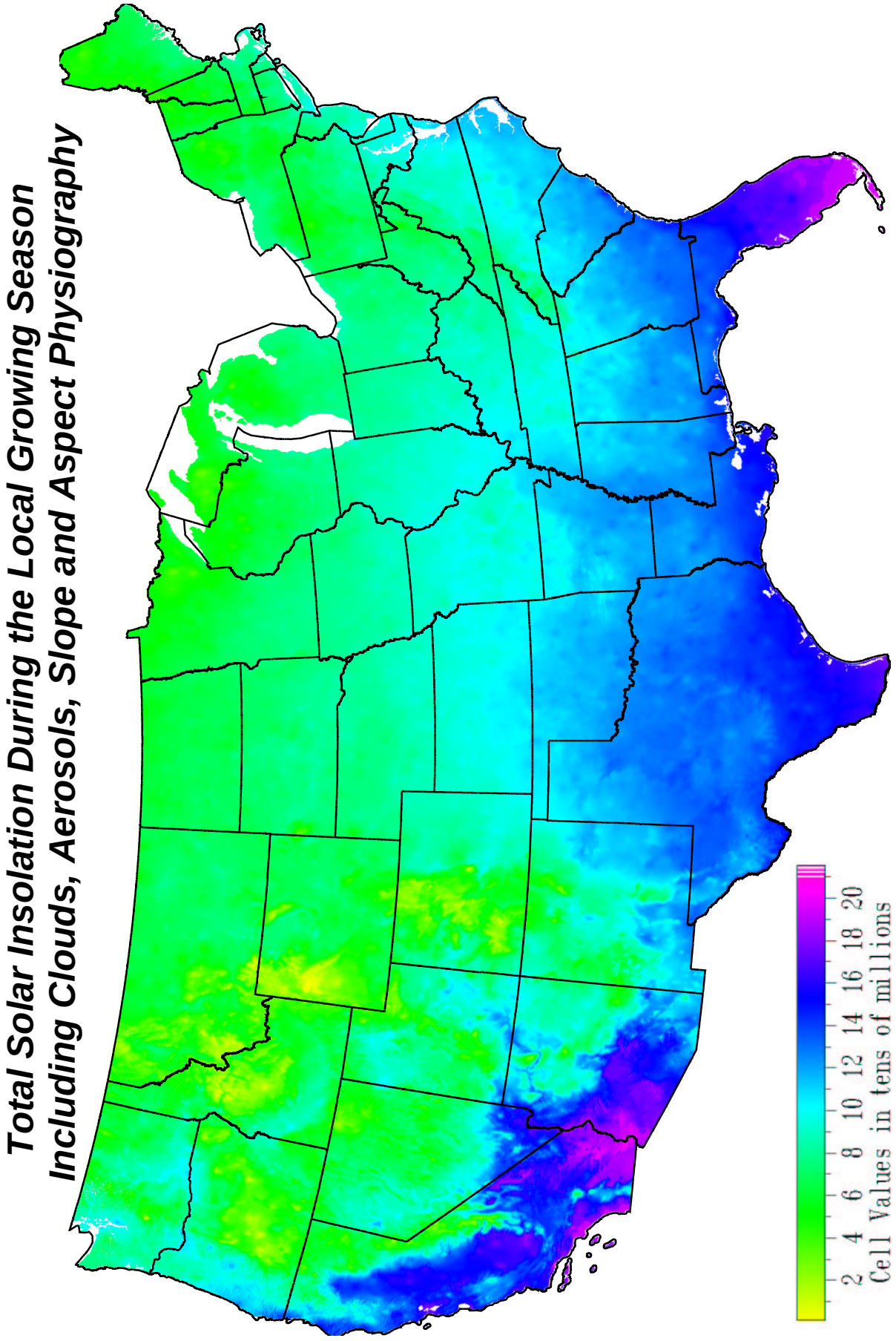

Figure 2.17: Total Solar Insolation During the Local Growing Season Including Clouds, Aerosols, Slope and Aspect Physiography

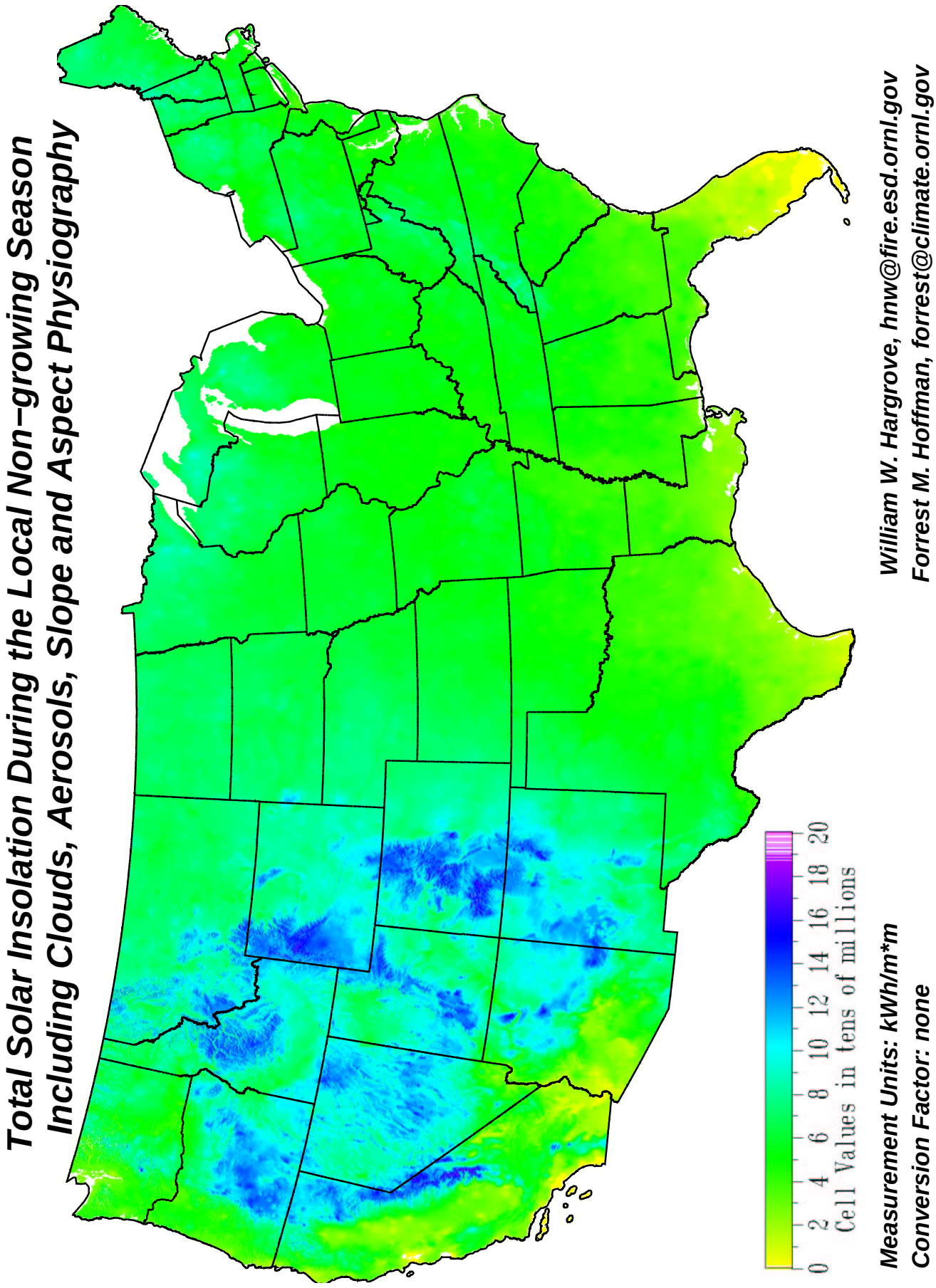

Figure 2.18: Total Solar Insolation During the Local Non-growing Season Including Clouds, Aerosols, Slope and Aspect Physiography

2.13 Enhanced Vegetation Index (EVI)

Name: Enhanced Vegetation Index (EVI) Integrated Over the Local Growing Season, Enhanced Vegetation Index (EVI) Integrated Over the Local Non-Growing Season

Data Sources: MODIS MOD13A2 v4 1km 16-day composites, 2000 through 2002; median day of last frost of spring, median day of first frost of fall, Climate Source, Inc., http://www.climatesource.com/

Description of Processing: 14 MODIS tiles comprising the CONUS at each date × 23 16-day composites per year × 3 years (2000,2001,2002) = 966 MODIS tiles obtained from LPDAAC, mosaicked and reprojected using the MODIS Reprojection Tool v3.1c and nearest-neighbor resampling to 1km LAEA. All images filtered using MODIS VI Usefulness Quality Control bits, range 0–13. Only cells with Usefulness ≤ 7 were retained.

The 3 images from each of the 3 years were composited by averaging into a single sequence of 23 dates representing a nominal or synoptic year. Gaps were filled using a temporal spline with tension, using the lowest possible tension setting that did not cause data over- and undershoots (see text for details). Cells having 3 or fewer dates with data were filled by repeatedly applying a 7×7 cell weighted spatial adaptive filter. An animated sequence of the filled EVI maps for the synoptic year is available at http://geobabble.ornl.gov/flux-ecoregions.

EVI was integrated over days of the growing season and non-growing season on a cell-by-cell basis, using the Julian days from the two Climate Source layers. A spline with tension was used to interpolate smoothed daily values for each cell, and then the EVI × days were accumulated for the growing and non-growing seasons.

Measurement Units: Unitless × Days

As a ratio of the sum and difference of two spectral reflectance bands, EVI is unitless. When integrated and accumulated over growing and non-growing seasons, we believe that the concept of "greenness days" is relevant for expected amounts of carbon flux that might be exchanged.

Conversion Factor: 0.0001

The conversion factor used in the original MOD13A2 product was retained.

Expected Discriminatory Power: Differences between growing season and non-growing season EVI will highlight differences between evergreen and deciduous ecosystems, and will carry information about relative mixtures of these life-strategies growing in each map cell.

Comments/Observations: Because EVI is said to be more responsive at the low and high ends of the vegetation spectrum than NDVI, we selected it for inclusion in the flux ecoregions. Unlike the LAI/FPAR product, nothing is pre-masked in the EVI layer. Hence, values of EVI are obtained for urban areas, bare ground, sand beaches, and ice. This makes EVI an important complement to the LAI/FPAR product when trying to capture information about existing vegetation for flux ecoregions.

Indeed, the non-growing EVI layer seems to highlight productive areas of conifer dominance in higher CONUS latitudes. Presence of such evergreens will strongly influence the seasonality of carbon flux in these areas.

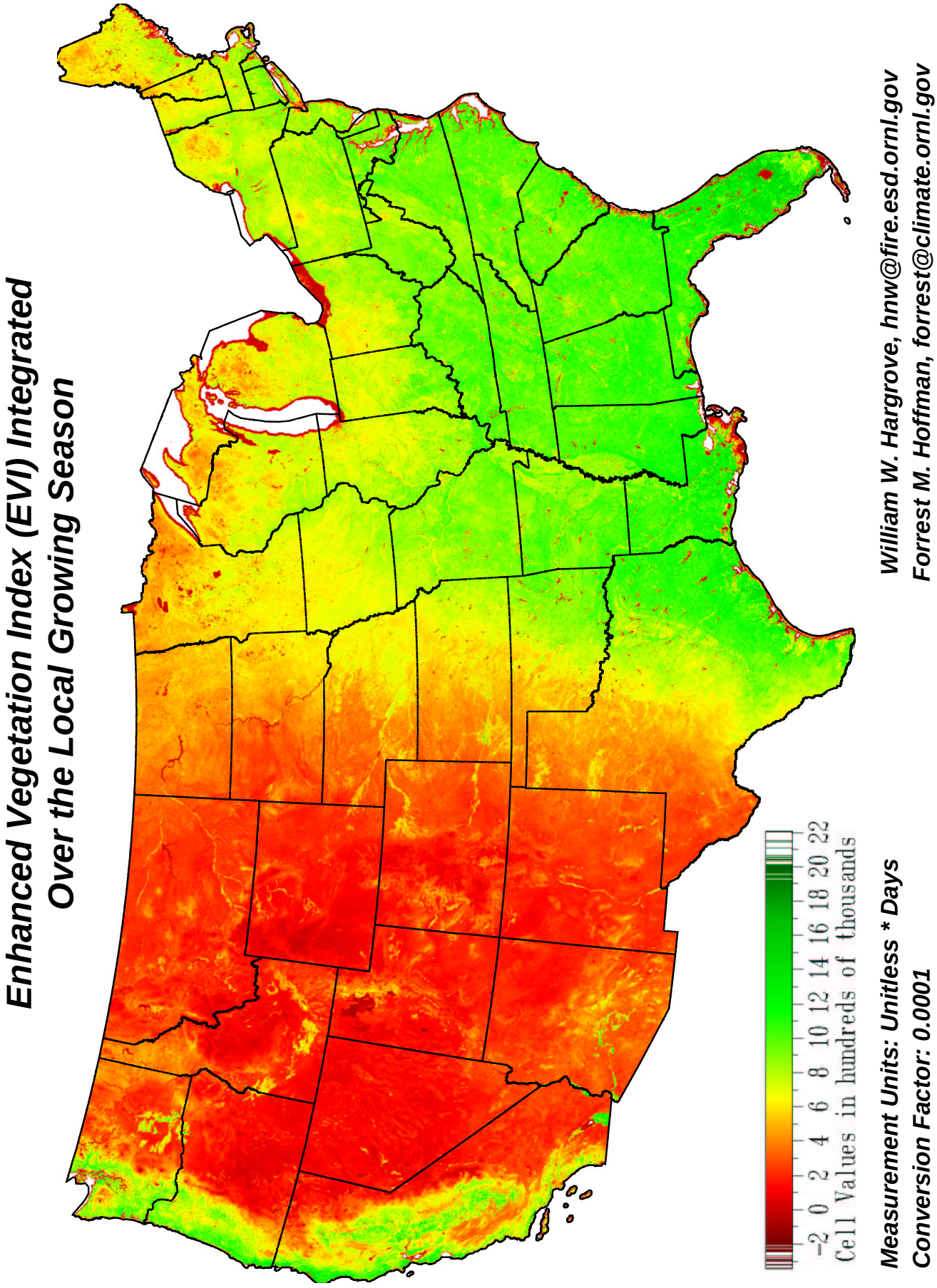

Figure 2.19: Enhanced Vegetation Index (EVI) Integrated Over the Local Growing Season

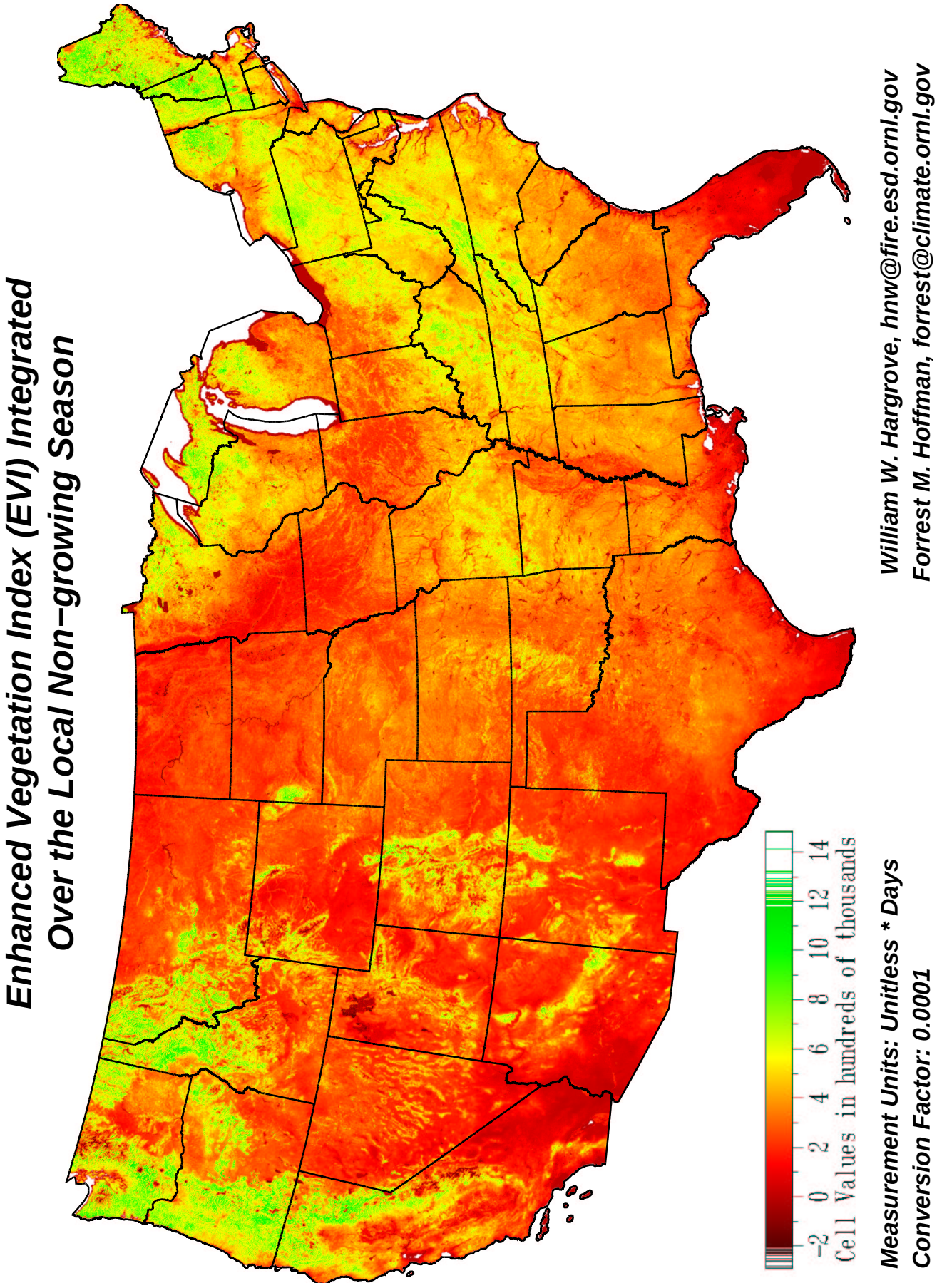

Figure 2.20: Enhanced Vegetation Index (EVI) Integrated Over the Local Non-Growing Season

2.14 Fraction of Photosynthetically Active Radiation (FPAR)

Name: Fraction of Photosynthetically Active Radiation (FPAR) Absorbed by Vegetation Integrated over the Local Growing Season, Fraction of Photosynthetically Active Radiation (FPAR) Absorbed by Vegetation Integrated over the Local Non-growing Season

Data Sources: MODIS MOD15A2 Collection4 1km 8-day composites, 2000 through 2002; median day of last frost of spring, median day of first frost of fall, Climate Source, Inc., http://www.climatesource.com/

Description of Processing: 14 MODIS tiles comprising the CONUS at each date × 46 8-day composites per year × 3 years (2000,2001,2002) = 1932 MODIS tiles obtained from LPDAAC, mosaicked and reprojected using the MODIS Reprojection Tool v3.1c and nearest-neighbor resampling to 1km LAEA. All images filtered using MODIS SCF_QC quality control bits, range 0–4. Only cells with SCF_QC ≤ 1 (i.e., Main (RT) algorithm used, R. Myneni, personal communication) were retained. The secondary algorithm is known (as of late 2003) to be unreliable.

The 3 images from each of the 3 years were composited by averaging into a single sequence of 46 dates representing a nominal or synoptic year. Gaps were filled using a temporal spline with tension, using the lowest possible tension setting that did not cause data over- and undershoots (see text for details). Cells having 3 or fewer dates with data were filled by repeatedly applying a 7×7 cell weighted spatial adaptive filter. An animated sequence of the filled FPAR maps for the synoptic year is available at http://geobabble.ornl.gov/flux-ecoregions.

FPAR was integrated over days of the growing season and non-growing season on a cell-by-cell basis, using the Julian days from the two Climate Source layers. A spline with tension was used to interpolate smoothed daily values for each cell, and then the FPAR × days were accumulated for the growing and non-growing seasons.

Measurement Units: Percent × Days
Integration over growing and non-growing seasons produces "percent absorbed days," which should be relevant for expected carbon flux.

Conversion Factor: 0.01
The conversion factor used in the original MOD15A2 product was retained.

Expected Discriminatory Power: Differences between growing season and non-growing season EVI will highlight differences between evergreen and deciduous ecosystems. FPAR also carries information about senescent foliage, which is alive but not actively fixing carbon. The respiration and shading costs of such foliage are important for expected carbon flux.

Comments/Observations: Areas that were pre-masked by the MODIS team, including water, barren, snow and ice, and urban, were set to zero. Areas with the fill value and indeterminate were set to missing and interpolated.

Our approach was to try to remove the presence of snow using our temporal spline method, i.e., to try to obtain the value of FPAR without snow. This approach is conceptually different than that used by Zhao at Numerical Terradynamics Simulation Group (NTSG), who tries to get the FPAR value with the snow present. We rely on other input layers to carry information about the presence of a snow pack.

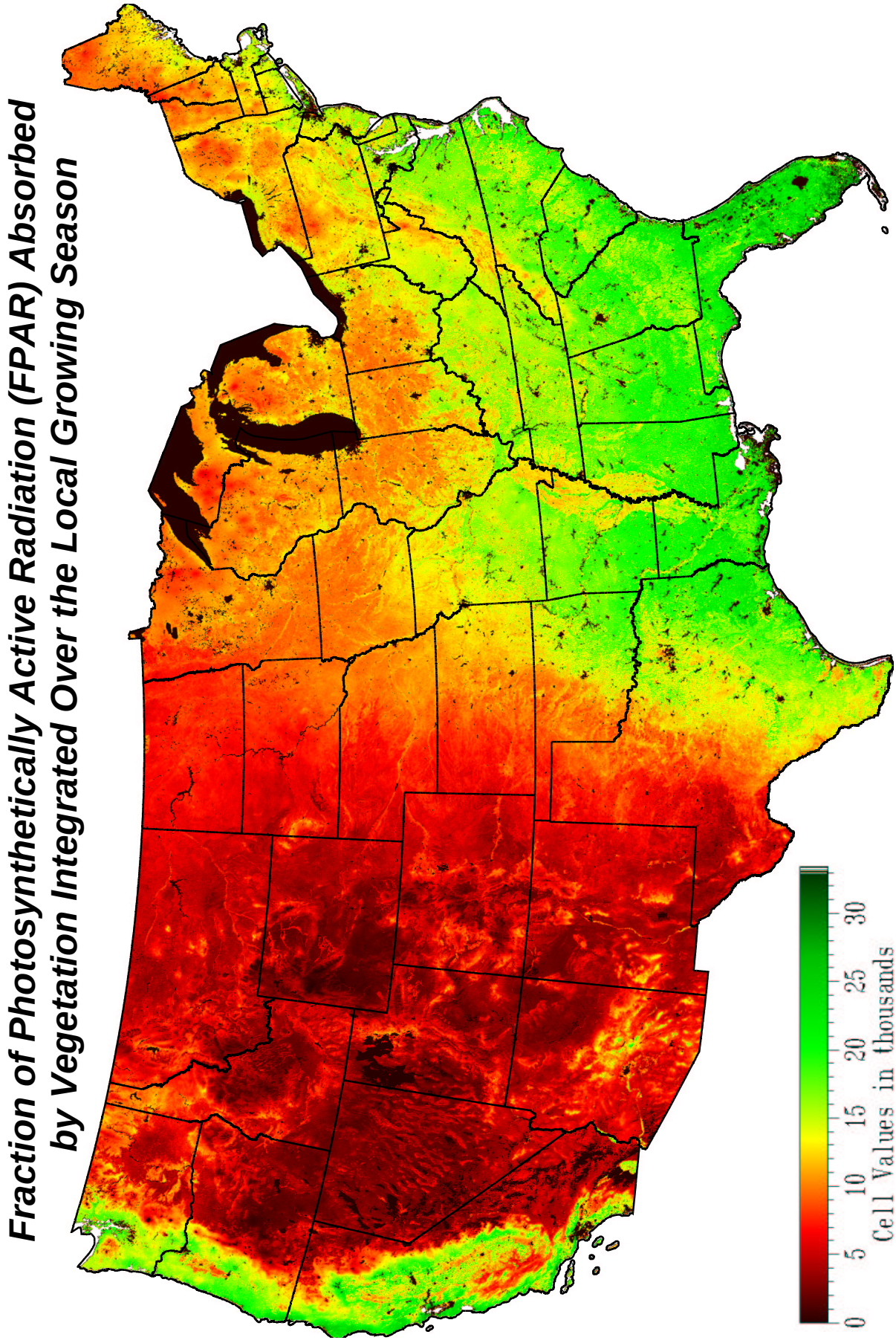

Figure 2.21: Fraction of Photosynthetically Active Radiation (FPAR) Absorbed by Vegetation Integrated Over the Local Growing Season

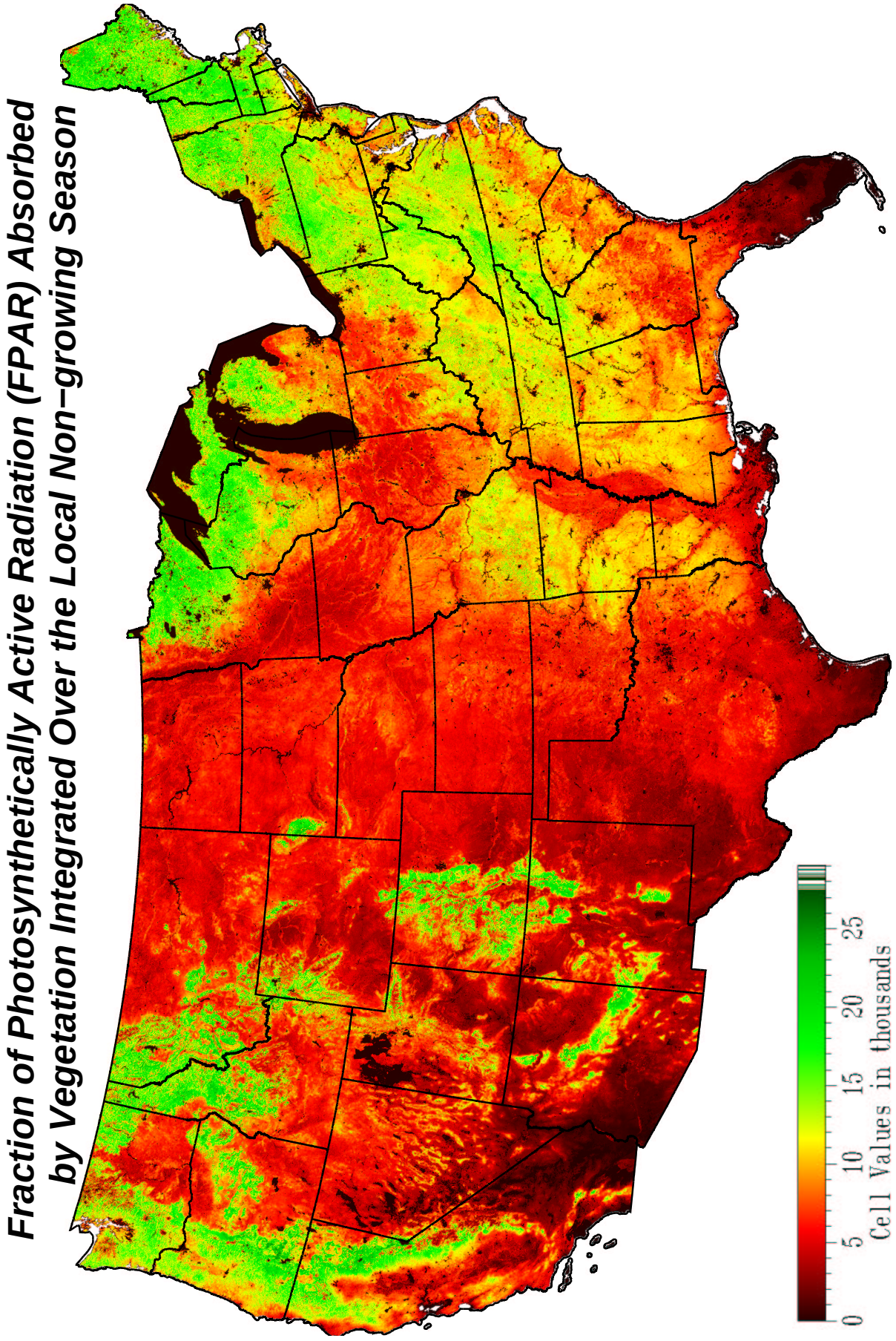

Figure 2.22: Fraction of Photosynthetically Active Radiation (FPAR) Absorbed by Vegetation Integrated Over the Local Non-Growing Season

2.15 Leaf Area Index (LAI)

Name: Leaf Area Index (LAI) Integrated Over the Local Growing Season, Leaf Area Index (LAI) Integrated Over the Local Non-growing Season

Data Sources: MODIS MOD15A2 Collection4 1km 8-day composites, 2000 through 2002; median day of last frost of spring, median day of first frost of fall, Climate Source, Inc., http://www.climatesource.com/

Description of Processing: 14 MODIS tiles comprising the CONUS at each date × 46 8-day composites per year × 3 years (2000,2001,2002) = 1932 MODIS tiles obtained from LPDAAC, mosaicked and reprojected using the MODIS Reprojection Tool v3.1c and nearest-neighbor resampling to 1km LAEA. All images filtered using MODIS SCF_QC quality control bits, range 0–4. Only cells with SCF_QC ≤ 1 (i.e., Main (RT) algorithm used, R. Myneni, personal communication) were retained. The secondary algorithm is now known (as of late 2003) to be unreliable.

The 3 images from each of the 3 years were composited by averaging into a single sequence of 46 dates representing a nominal or synoptic year. Gaps were filled using a temporal spline with tension, using the lowest possible tension setting that did not cause data over- and undershoots (see text for details). Cells having 3 or fewer dates with data were filled by repeatedly applying a 7×7 cell weighted spatial adaptive filter. An animated sequence of the filled LAI maps for the synoptic year is available at http://geobabble.ornl.gov/flux-ecoregions.

LAI was integrated over days of the growing season and non-growing season on a cell-by-cell basis, using the Julian days from the two Climate Source layers. A spline with tension was used to interpolate smoothed daily values for each cell, and then the FPAR × days were accumulated for the growing and non-growing seasons.

Measurement Units: $(m^2/m^2) \times$ Days

Units are one-sided leaf area per area of ground. Integration over growing and non-growing seasons produces "leaf area days," which should be relevant for expected carbon flux, both in terms of carbon fixation and maintenance respiration.

Conversion Factor: 0.10

The conversion factor used in the original MOD15A2 product was retained.

Expected Discriminatory Power: Integration of the crop of leaves times how long this crop is held should provide information about vegetation status that is important both in terms of the photosynthetic "organs" and also in terms of respiration to maintain those organs. Vegetation leaf crop should also carry information on disturbed areas, agriculture, urban, and other anthropogenic effects on carbon flux (excluding direct anthropogenic emissions).

Comments/Observations: Similar, but not identical to, the appearance of the FPAR input layers.

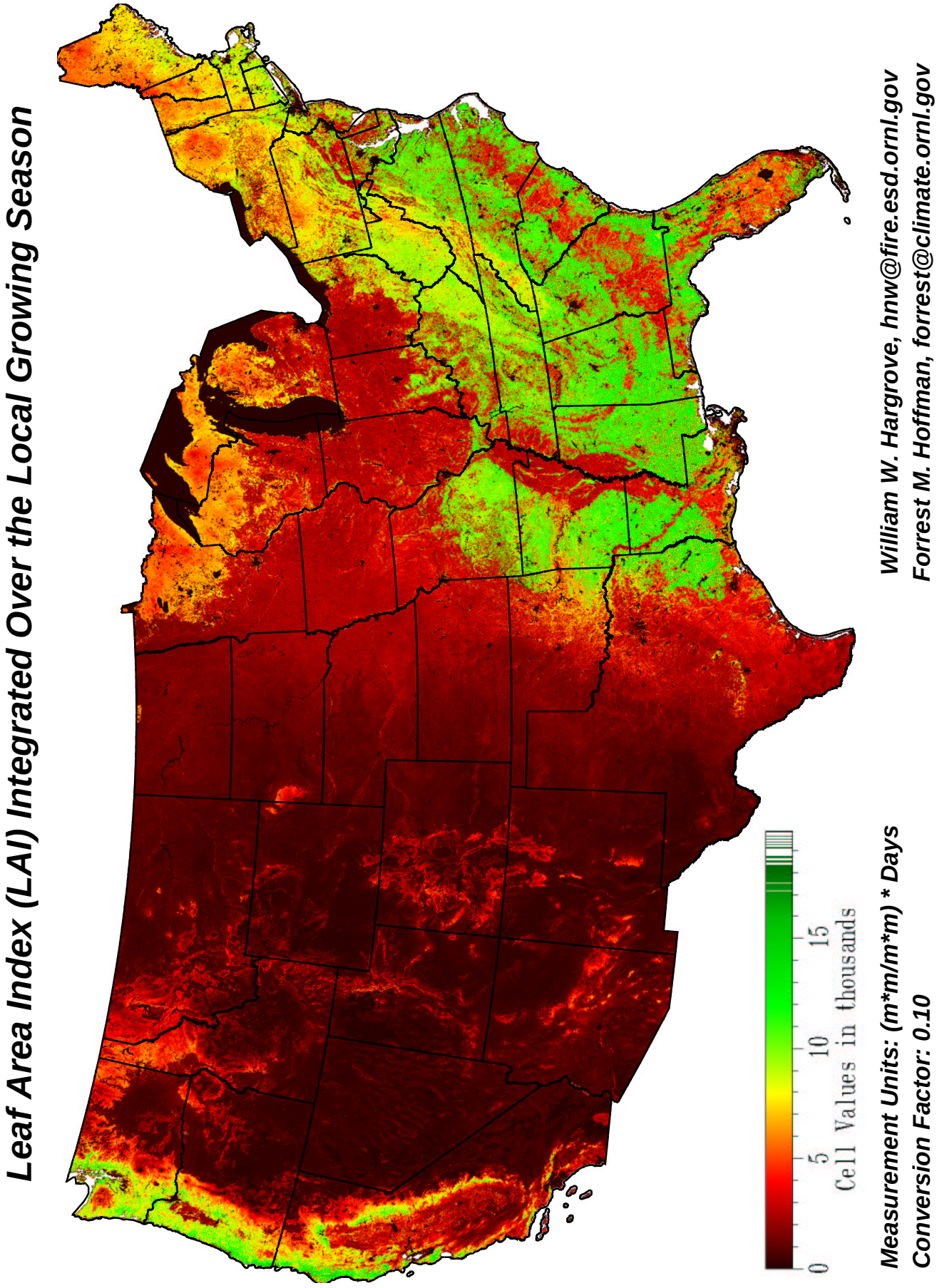

Figure 2.23: Leaf Area Index (LAI) Integrated Over the Local Growing Season

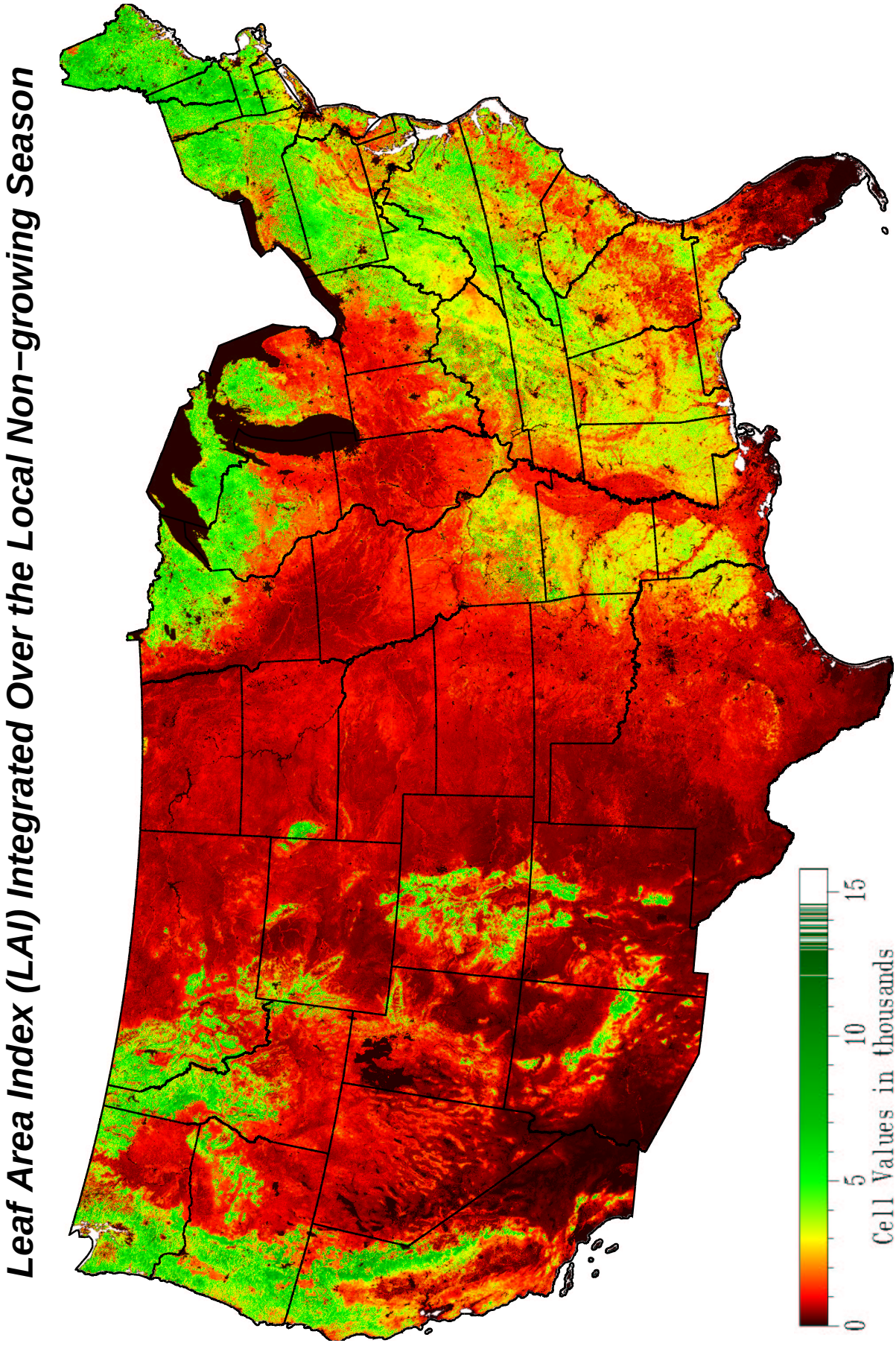

Figure 2.24: Leaf Area Index (LAI) Integrated Over the Local Non-growing Season

2.16 Continuous Vegetation Fields

Name: Percent Bare Ground, Percent Tree Cover

Data Sources: MODIS MOD44B 500m resolution Continuous Vegetation Fields, 2000–2001

Description of Processing: Obtained North American continent from http://modis.umiacs.umd.edu/vcfdistribution.htm in geographic coordinates, reprojected to 1km LAEA using nearest-neighbor resampling

Measurement Units: Percent

Conversion Factor: None

Expected Discriminatory Power: Since the %tree, %shrub, and %bare layers sum to 100%, and since we suspect that Hansen and Defries, et. al actually modeled %tree and %bare, and calculated %shrub by difference, we selected only %tree and %bare as the input layers containing the most non-correlated information here.

Since there is only a single annual layer for each of these, and since there is no seasonality to the presence of bare ground and tree cover, these layers were included in both growing and non-growing season flux ecoregionalizations. The presence of trees, even in the non-growing season, is potentially important for respiration components of carbon flux.

Comments/Observations: Eastern cities and urban areas are visible as dark spots in the %bare ground layer where they interrupt the vegetation field.

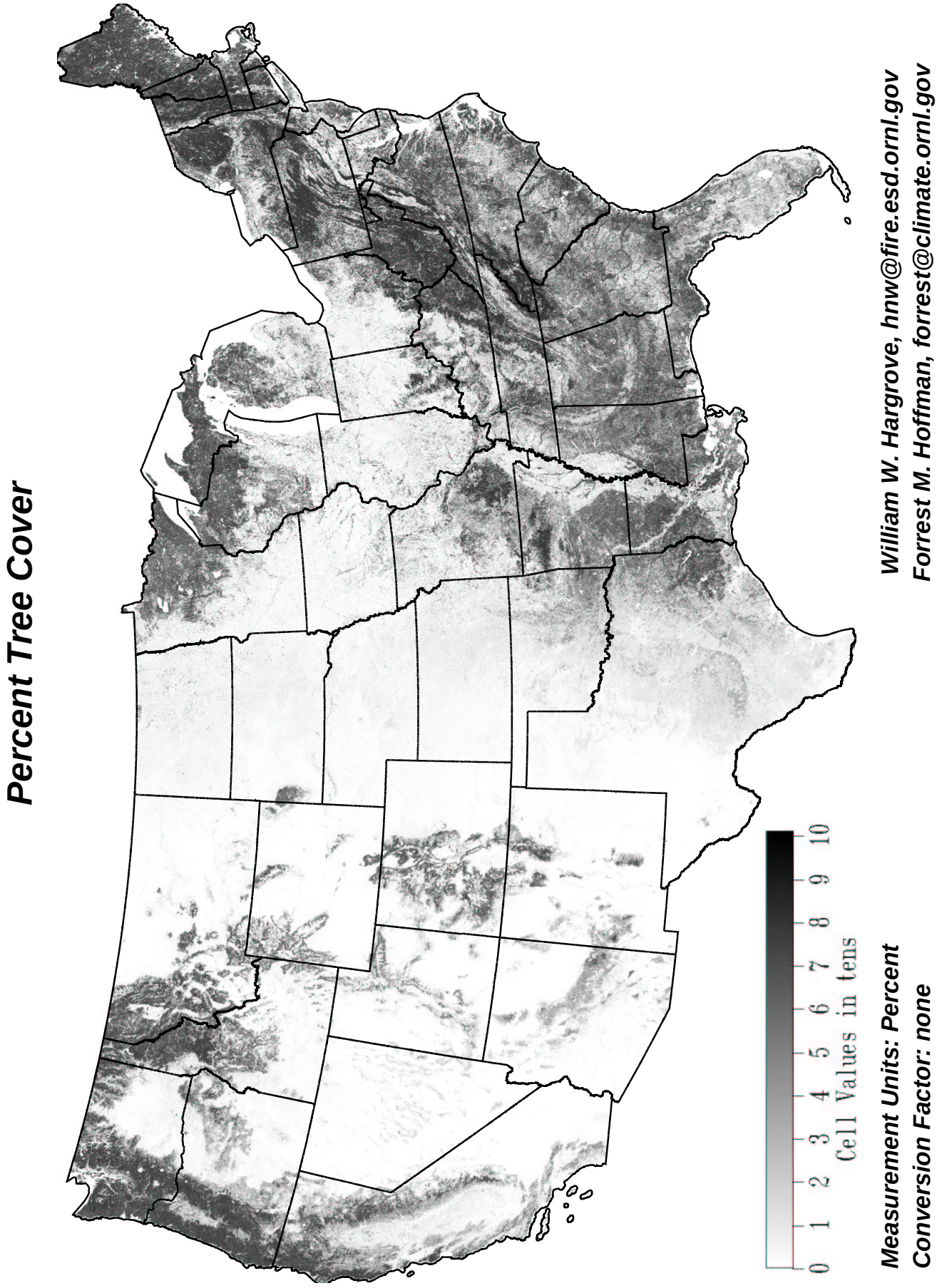

Figure 2.25: Percent Tree Cover

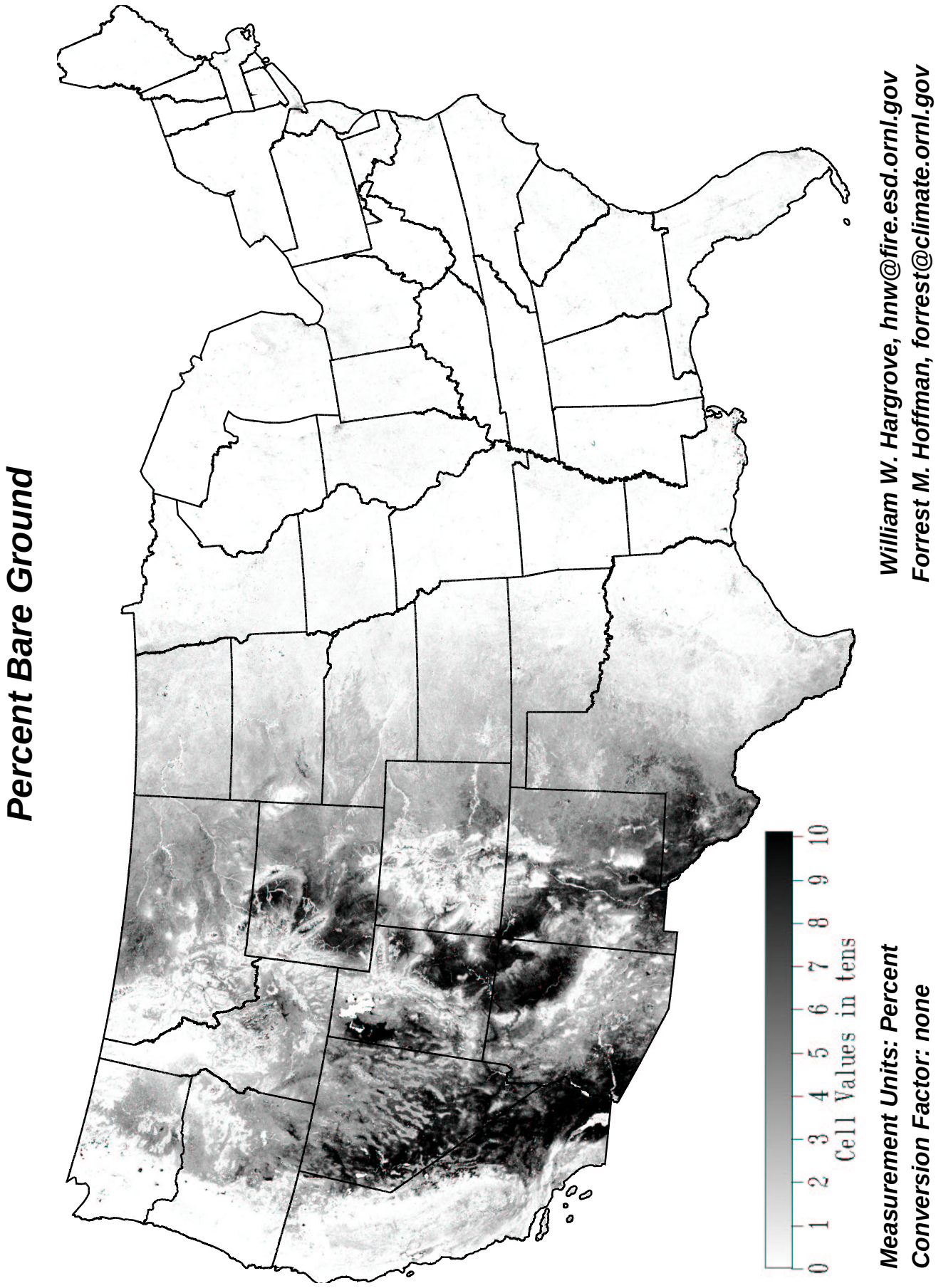

Figure 2.26: Percent Bare Ground

2.17 Gross Primary Production (GPP)

Name: Gross Primary Production (GPP) Integrated Over the Local Growing Season, Gross Primary Production (GPP) Integrated Over the Local Non-growing Season

Data Sources: MODIS MOD17A2 Collection4.5 1km 8-day composites, 2000 through 2002 from Maosheng Zhao, NTSG, Steve Running's group; median day of last frost of spring, median day of first frost of fall, Climate Source, Inc., http://www.climatesource.com/

Description of Processing: Zhao used a temporal linear interpolation to fill FPAR, and a spatial smoothing filter to smooth daily meteorology data from DAO, resulting in a customized MOD17A2 product which is better than the general Collection4 release.

14 MODIS tiles comprising the CONUS at each date × 46 8-day composites per year × 2 years (2000,2001) = 1288 MODIS tiles mosaicked and reprojected using the MODIS Reprojection Tool v3.1c and nearest-neighbor resampling to 1km LAEA. Unlike all other MODIS products, this custom product has been gap-filled. Therefore, there is no need to examine Quality Control flags; every cell can be used as is. The 2 images from each of 2 years were composited by averaging into a single sequence of 46 dates representing a nominal or synoptic year. An animated sequence of the filled GPP maps for the synoptic year is available at http://geobabble.ornl.gov/flux-ecoregions.

GPP was integrated over days of the growing season and non-growing season on a cell-by-cell basis, using the Julian days from the two Climate Source layers. A spline with tension was used to interpolate smoothed values for each day for each cell, and then the GPP × days were accumulated for the growing and non-growing seasons.

Measurement Units: (kg C/m^2/8 days) × Days
Units for MOD17A2 are estimated carbon fixation totals over the 8-day observation interval. Therefore, users can multiply by 8 to obtain kg C/m^2.

Conversion Factor: 0.0001
The conversion factor used in the original MOD17A2 product was retained.

Expected Discriminatory Power: GPP, as a higher-order measure of ecosystem activity and carbon "velocity," is expected to carry critical information about expected carbon flux.

Comments/Observations: Areas that were pre-masked by the MODIS team, including water, barren, snow and ice, and urban, were set to zero. The Mississippi Valley and the Piedmont are particularly visible as lower-productivity areas in the growing season map. The Appalachians, Adirondacks, and Allegheny Mountains show up in the non-growing season map, as do the Black Hills, the Bitterroot Mountains, and the Cascades.

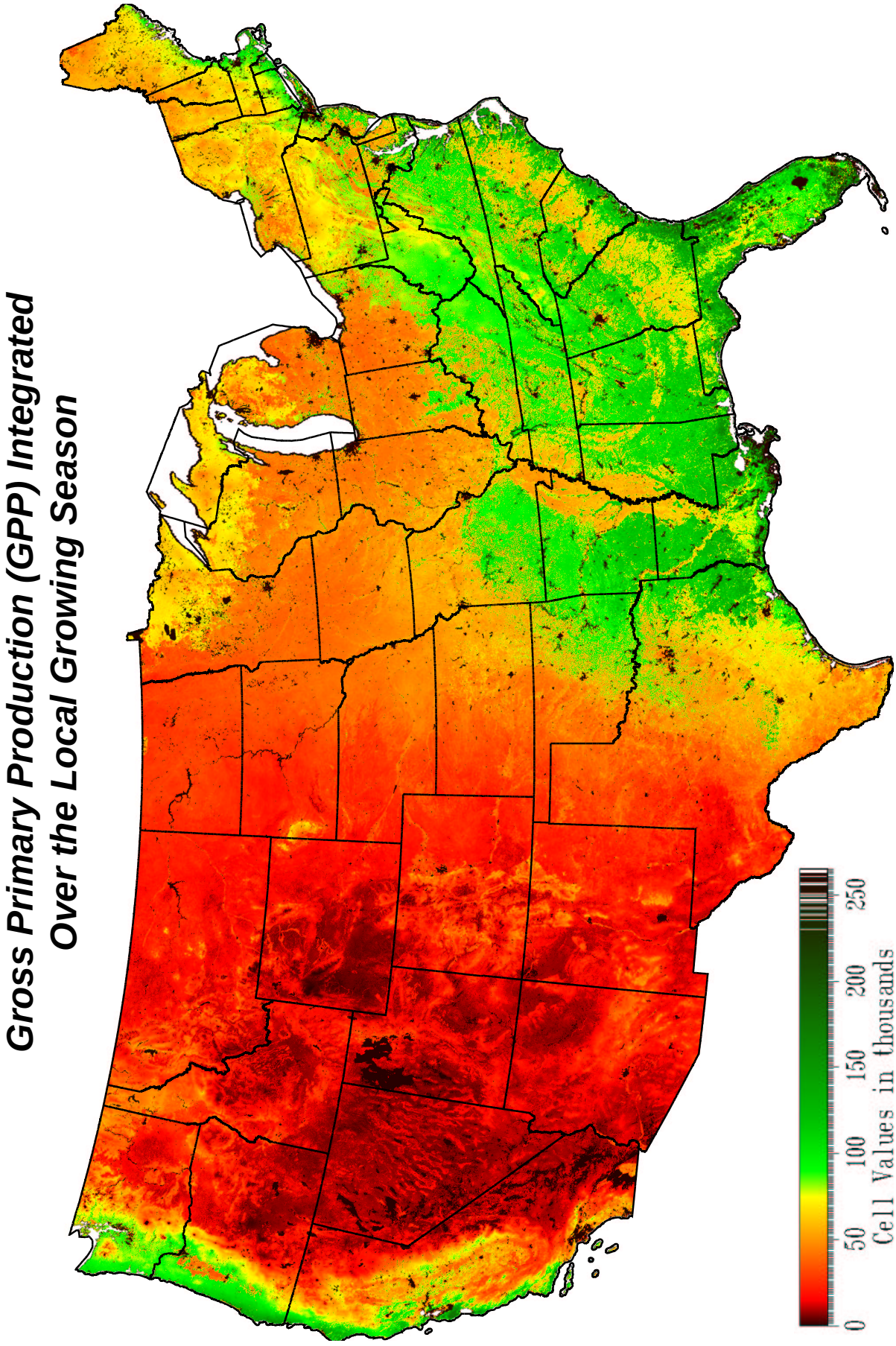

Figure 2.27: Gross Primary Production (GPP) Integrated Over the Local Growing Season

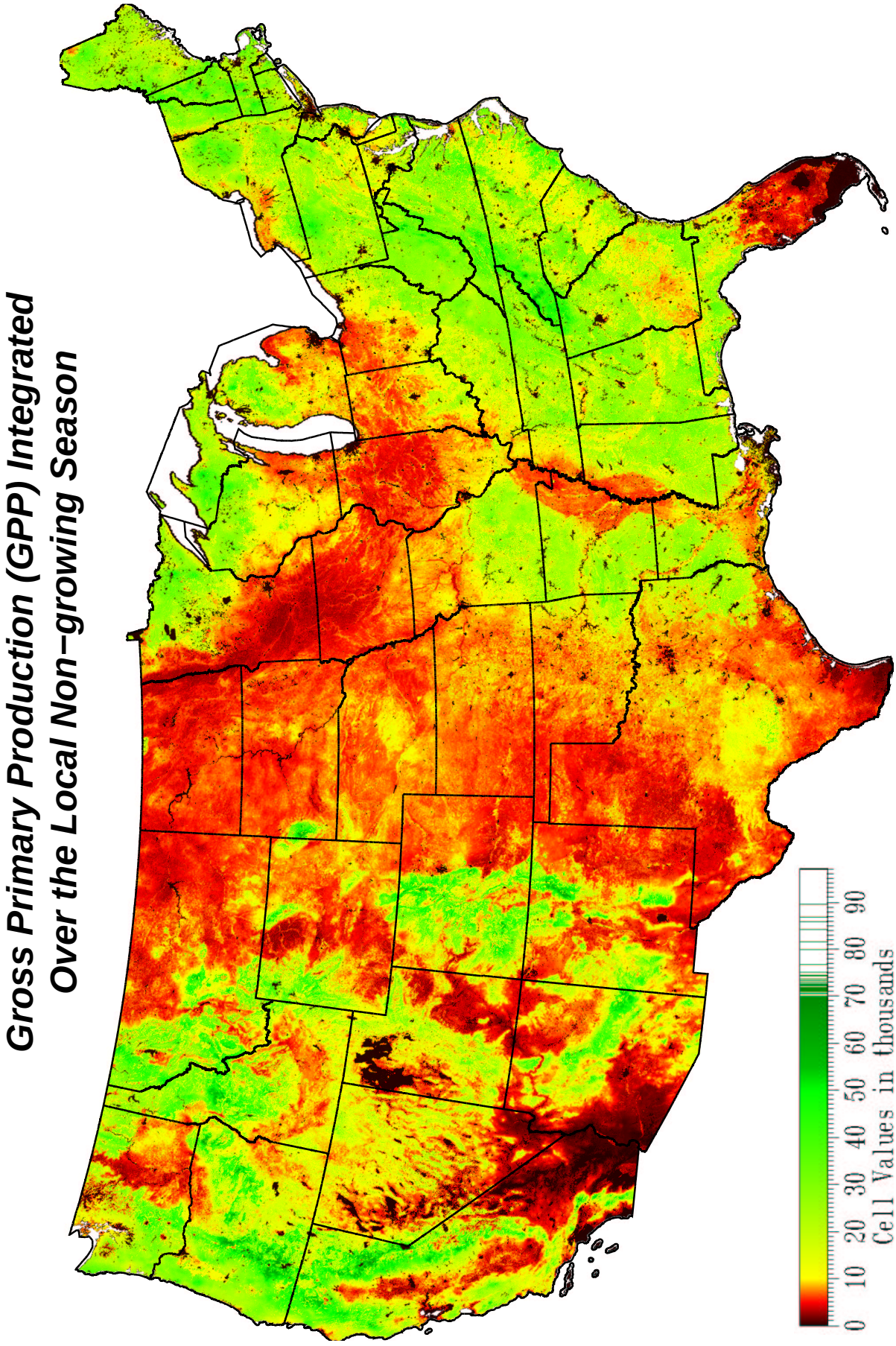

Figure 2.28: Gross Primary Production (GPP) Integrated Over the Local Non-growing Season

2.18 Respiration Index (RI)

Name: Respiration Index (RI) Integrated over the Local Growing Season, Respiration Index (RI) Integrated over the Local Non-growing Season

Data Sources: MODIS MOD17A2 Collection4.5 1km 8-day composites, 2000 through 2002 from Maosheng Zhao, NTSG, Steve Running's group; median day of last frost of spring, median day of first frost of fall, Climate Source, Inc., http://www.climatesource.com/

Description of Processing: Zhao used a temporal linear interpolation to fill FPAR, and a spatial smoothing filter to smooth daily meteorology data from DAO, resulting in a customized MOD17A2 product which is better than the general Collection4 release.

14 MODIS tiles comprising the CONUS at each date × 46 8-day composites per year × 2 years (2000,2001) = 1288 MODIS tiles mosaicked and reprojected using the MODIS Reprojection Tool v3.1c and nearest-neighbor resampling to 1km LAEA. Unlike all other MODIS products, this custom product has been gap-filled. Therefore, there is no need to examine Quality Control flags; every cell can be used as is.

The 2 PSNNET images from each of 2 years were composited by averaging into a single sequence of 46 dates representing a nominal or synoptic year. Then, each of the 46 PSNNET dates for the synoptic year were subtracted from the 46 GPP synoptic dates to produce 46 maps we call Respiration Index (RI) over a synoptic year. An animated sequence of the filled RI maps for the synoptic year is available at http://geobabble.ornl.gov/flux-ecoregions.

RI was integrated over days of the growing season and non-growing season on a cell-by-cell basis, using the Julian days from the two Climate Source layers. A spline with tension was used to interpolate smoothed values for each day for each cell, and then the RI × days were accumulated for the growing and non-growing seasons.

Measurement Units: (kg C/m^2/8 days) × Days
Units for MOD17A2 are estimated carbon respiration totals over the 8-day observation interval. Therefore, users can multiply by 8 to obtain kg C/m^2.

Conversion Factor: 0.0001
The conversion factor used in the original MOD17A2 product was retained.

Expected Discriminatory Power: PSNNET (SDS 2) from MOD17A2 has both positive and negative values. The zero point for this variable has ecological meaning, since this is the balance point where GPP equals respiration. Since we must standardize units to mean of zero and uniary std. deviation prior to clustering, we would lose the significance of the biological "break even" point at zero PSNNET.

Since GPP, PSNNET, and RI are related by subtraction, including any two of them as inputs will make all of the ecosystem productivity information available for flux ecoregionalization. Because GPP and RI are always positive, these two are not adversely affected by the standardization process. Therefore, we have included GPP and RI, as calculated from the other two MODIS-provided members of the triad of derived ecosystem performance measures.

Comments/Observations: Areas that were pre-masked by the MODIS team, including water, barren, snow and ice, and urban, were set to zero.

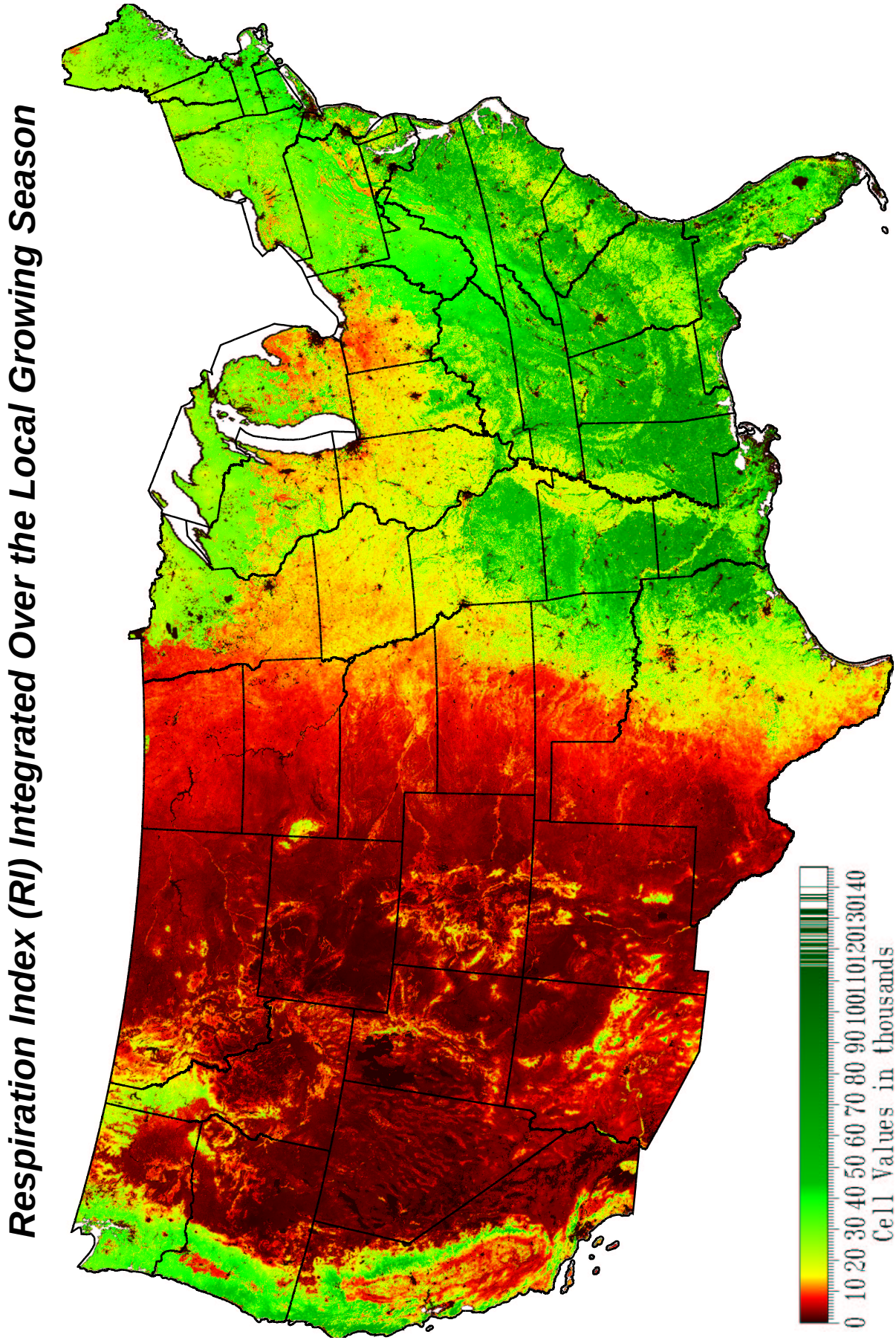

Figure 2.29: Respiration Index (RI) Integrated Over the Local Growing Season

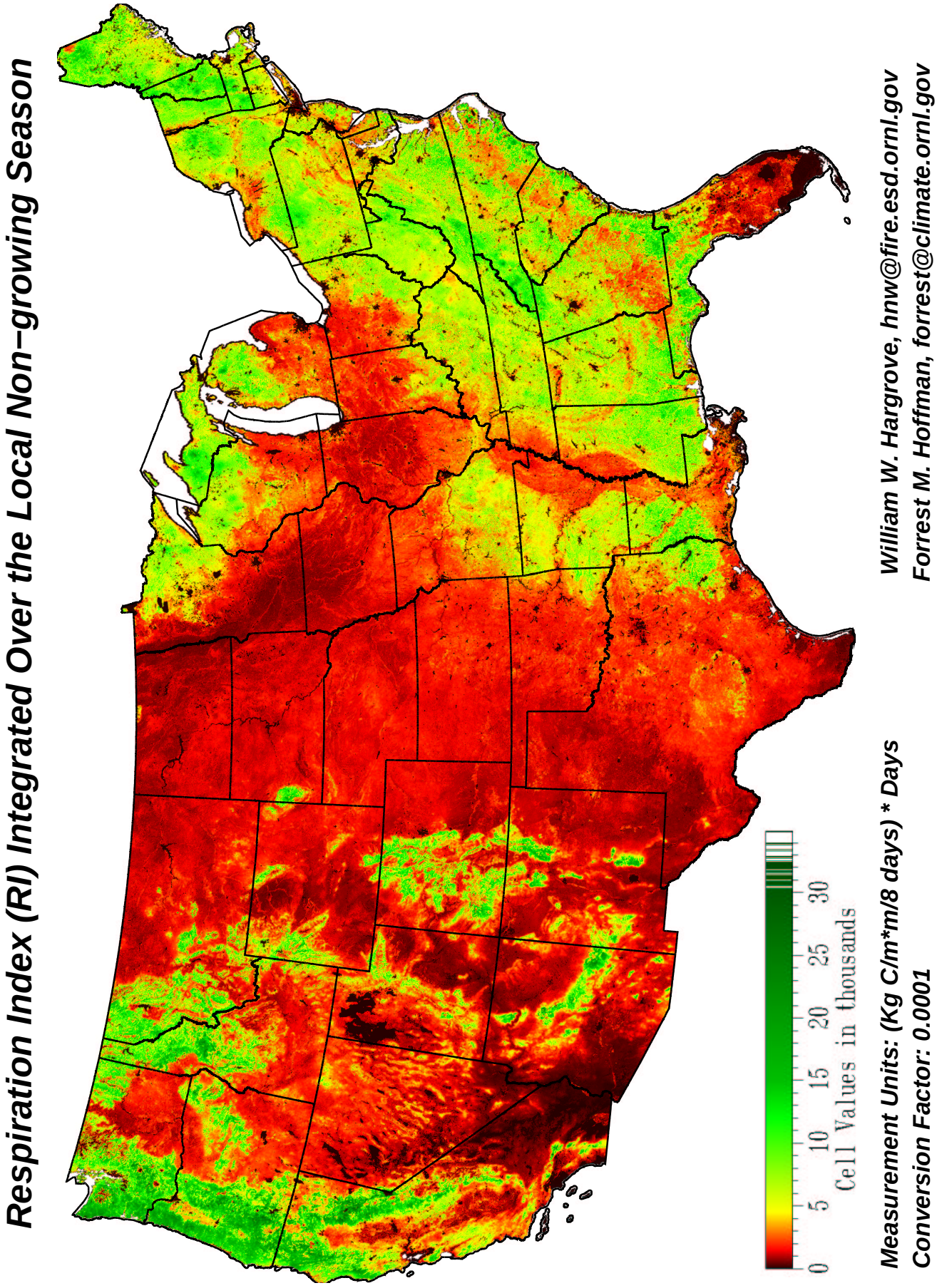

Figure 2.30: Respiration Index (RI) Integrated Over the Local Non-growing Season

Chapter 3

Results

For MGC, every included cell must have a value for every input variable. We calculated separate GIS masks for I, II, and III consisting of the largest geographic area which still had values for each input map in the list. These masks defined a minimum inclusive border around coastline and major lakes which was contained in all map layers. Soil parameters within lakes and rivers were set to zero so that these potentially important flux environments would also be clustered, based solely on their climatic characteristics.

We performed a PCA using **varimax rotation** on all standardized variables, and then performed MGC on the factor scores. All factors that were produced were retained for clustering, so that we had as many factors as original variables. By doing this, 100% of the variability in the original data was explained, yet all PCA factors were orthogonal and uncorrelated with each other. This process ensured a statistically clean environment for clustering, yet it also allowed the conversion of final cluster centroids back into original measurement units.

We continued the clustering process for each set of flux ecoregions until a convergence criterion was met. At convergence, fewer than 0.5% of the cells in the CONUS changed flux ecoregion assignment from this iteration to the last. This means that fewer than 39,000 square kilometers within the CONUS were in transition when each flux ecoregion classification process was stopped.

We tried several levels of division for each set of flux ecoregions, and picked one that seemed most appropriate overall relative to the general appearance of the maps and the number of existing flux towers. There are 52 unique locations at $1km^2$ resolution within the CONUS having actively reporting AmeriFlux towers (AmeriFlux has "clusters" of towers near each other within different land cover treatments at several locations; however, these "clusters" are considered here as a single unique $1km^2$ cell).

Dividing the CONUS each time into the 90 most-different homogeneous flux ecoregions produced interpretable maps which should provide enough spatial resolution for continental flux estimates without overspecifying flux ecoregions relative to the number of measurement locations. Even if we had created exactly 52 ecoregions, it is likely that some would have multiple flux towers while others would have none. While pseudostatistical methods can be used to estimate the "naturalness" of a particular level of division, we have not used those here. In all of the alternative flux ecoregion maps produced, the western U.S. is divided into more, smaller flux ecoregions than the east, ostensibly because of elevation and coastal gradients. Nevertheless, the statistical clustering process ensures that the within-ecoregion

variance in flux environments is held constant across all flux ecoregions of substantial size.

3.1 The Challenge of Multivariate Presentation

This is a highly multivariate investigation. The challenge is to depict these multivariate results in an understandable and interpretable way. Within a GIS, it is easy to inquire to which flux ecoregion a particular cell belongs. On the printed page in a small format, this is much harder. We have tried to be creative in our solutions to this challenge of visualization and presentation of results. Some of our approaches may seem unusual initially. However, once familiar, these presentation methods make it possible to extract much information from the printed flux ecoregion maps.

Each of the nine flux ecoregionalizations is shown as a set of five items: a color table legend which specifies average conditions within each flux ecoregion, a randomly colored map of flux ecoregions, a schematic map showing cluster numbers for larger flux ecoregions, a map of the flux ecoregions colored using Similarity Colors, and a table showing the loadings of each input layer on the first three PCA scores used for the Similarity Colors. By cross-referencing among these five items, it is possible to identify many of the flux ecoregions that have been specified. Each of the components is explained in greater detail below.

3.1.1 Color Table Legends

Since the final location of the cluster centroid is, by definition, the most centrally located point inside each cluster, the data space coordinates of each centroid provide a description of the average ecological conditions in this cluster ecoregion. These are the synoptic conditions that would be experienced by plants and animals living within each of these homogeneous flux ecoregions. Comparison of the centroid coordinates from two ecoregions quantifies the differences between the average environments found in each cluster ecoregion. The units for each variable are as shown on the input maps and their corresponding metadata tables, but conversion factors have already been applied for ease of use.

The random color and the Similarity Color of each homogeneous flux ecoregion are shown at the left. Color table legends are not in order by flux ecoregion number, since these are simply labels used to distinguish flux ecoregions. Rather, the color table legends are sorted by Similarity Color, in red-green-blue (RGB) order. Thus, Similarity Colors go generally from blues to reds. That this color ordering is not exact is a testament to the multivariate nature of these results; no single sorted ordering based on any one variable can fully explain these multivariate results. Lake and river flux ecoregions are easy to identify in the color table legends, since they have values near zero for all soil properties.

3.1.2 Random Colors

While it is impossible to pick a set of random colors that eliminate possible confusion between flux ecoregions, we have attempted to do so. Random colors emphasize the border edges between adjacent flux ecoregions. The random colors serve only to distinguish different flux ecoregions from each other. Random colors portray the borders between adjacent flux ecoregions. While different flux ecoregions may

happen to have the same carbon flux over a given interval, it would be the same for different reasons.

3.1.3 Schematic Maps

If the random colors are close, it may be difficult to see where one flux ecoregion ends and another begins. It may also be difficult to associate a particular random color with a numbered flux ecoregion in the color table legend. We resampled the randomly colored flux ecoregion maps at 75km^2 resolution, numbered all spatially-disjoint flux ecoregions thus created, and plotted vector borders which separate each of these discrete areas. We call these coarsened and labeled maps schematic maps, since they provide a kind of simplified version of the original flux maps.

By comparing the schematic map and the original flux map at the same geographic location, looking for a match in the random color, and noting the number, particular larger flux ecoregions can be identified. Nearby flux ecoregions with slightly different random colors can be identified as distinct. Schematic maps are also useful to find other discrete occurrences of a particular flux ecoregion. While unusual in appearance, the schematic maps are valuable once their use is understood.

3.1.4 Visualizing Flux Similarity using Similarity Colors

Randomly colored ecoregion maps emphasize the location of borders between ecoregions. However, ecologists might also wish for some indication of just how different the mixture of environmental conditions is across the border between neighboring flux ecoregions.

If another, separate PCA from the one used before MGC is used to condense the larger number of "raw" environmental variables into only three orthogonal principal component axes, we can perform a one-to-one scalar mapping of the first, second, and third principal component scores to a red-green-blue (RGB) color triplet. The combination of values for the three coordinates for each cluster centroid can be used to specify a unique color for that ecoregion which indicates the relative mixture of each environmental factor. A red-green-blue visualization based on the first three PCA scores of flux ecoregion centroids indicates with color the relative combination of environmental conditions found within that flux ecoregion. Comparison of adjacent ecoregions in such visualizations is simple; ecoregions containing similar environmental combinations are colored similarly.

The same flux ecoregion map colored with Similarity Colors appears strikingly different from its randomly colored counterpart, even though the underlying raster is identical. Individual ecoregion borders disappear, and the map changes into a smooth gradient of colors which reflect the dominant suites of variables affecting carbon flux in each region of the country.

A color wheel in the lower left corner of each Similarity Color map indicates the factor assignments for each color. Lighter colors represent high values of all three colors, while darker colors represent low values of all three colors.

3.1.5 Factor Loading Patterns

Finally, a table that shows quantitatively how each flux-relevant variable loads onto each of the three PCA factors is shown. Check marks (✓) indicate the PCA factor onto which the majority of each flux-relevant variable loads. At the bottom of this table, interpretive names are given to the ecological meanings of each factor. Sometimes factor color order assignment was altered for a more intuitive color mapping, *i.e.*, red for temperature, blue for precipitation.

3.2 Homogeneous Flux Ecoregions IA

Table 3.1: Average Conditions Within the 90 Homogeneous Flux Ecoregions for IA

	Rand color	Sim color	Heat sum	Cold sum	Hot days	Cold days	Di-urnal diff grow	Di-urnal diff non-grow	Precip grow	Precip non-grow	Wet days grow	Wet days non-grow	Soil depth	Water table depth	Soil N	Organic matter	Soil avail water	CTI	Solar grow $\times 10^7$	Solar non-grow $\times 10^7$
58			28.36	58.52	1.41	165.72	13.49	15.03	101.15	729.22	32.40	161.60	114.6	5.54	5895	766	33.52	2.70	5.81	7.90
84			32.46	41.43	0.77	104.76	13.27	13.28	291.46	1086.20	63.34	160.50	114.5	5.79	6339	887	39.42	2.67	7.23	5.67
87			23.28	70.88	1.18	220.62	14.79	15.39	42.25	443.25	17.64	146.68	125.6	5.77	5265	527	31.47	3.12	3.87	10.40
50			19.03	74.16	1.48	247.28	15.86	17.36	23.48	226.61	13.27	110.84	128.9	5.75	4170	641	30.78	3.59	2.96	13.10
10			23.43	79.27	1.34	232.29	17.32	17.31	38.21	291.67	16.33	113.01	122.0	5.65	4619	658	29.21	3.26	3.54	11.10
44			25.26	61.24	4.01	218.16	13.59	15.26	38.88	283.84	17.80	118.26	132.4	5.74	4782	622	32.33	3.25	3.80	8.36
88			24.42	76.52	1.08	237.95	18.07	18.67	32.48	207.71	16.10	81.68	128.9	5.80	4472	780	30.61	2.88	3.92	13.70
23			36.89	44.37	4.55	147.33	13.57	14.58	65.29	423.15	26.80	125.93	125.3	5.87	12710	870	48.71	3.17	6.71	7.68
41			40.31	40.19	4.06	97.79	12.82	18.21	154.22	544.59	49.84	133.86	124.6	5.48	7092	1058	49.88	3.16	8.38	6.25
20			30.58	66.13	2.81	219.05	17.07	17.35	35.96	162.65	18.25	75.60	136.2	5.90	4202	775	32.33	3.30	4.41	10.50
69			40.60	30.11	2.08	79.46	13.69	13.86	205.05	631.37	58.72	133.93	121.6	5.22	7704	1282	42.38	3.55	7.87	4.35
40			48.91	23.08	6.35	66.10	13.47	14.09	287.81	789.84	63.64	128.65	107.9	5.80	6034	1052	46.52	3.07	9.01	4.72
70			44.40	22.05	1.84	58.53	13.30	15.00	215.33	640.49	61.31	132.35	119.3	5.69	9800	2307	84.28	4.18	8.54	4.77
79			38.78	53.11	10.71	185.60	15.85	16.43	37.79	193.68	20.96	97.44	137.8	5.74	4625	716	38.65	3.75	5.46	8.71
31			44.64	40.12	8.42	176.49	17.69	16.67	22.15	309.25	8.04	71.13	111.7	5.83	2948	721	26.68	3.49	6.85	11.60
85			43.71	49.43	12.11	177.53	20.26	19.34	24.17	175.46	13.56	88.36	118.8	5.67	5609	565	84.32	4.30	5.34	9.92
1			39.60	60.25	3.29	178.39	13.34	16.54	116.33	167.92	42.81	81.78	143.6	2.74	6295	1440	50.53	5.26	5.71	6.92
54			42.99	26.18	3.12	74.24	13.18	13.73	160.73	464.85	54.82	122.11	116.6	4.74	6250	1373	47.02	3.62	8.04	4.22
18			50.91	68.06	6.85	203.91	27.08	26.24	31.01	121.90	17.96	68.36	119.4	5.87	5596	862	42.33	4.23	5.41	10.80
72			44.05	39.00	17.92	170.73	20.66	20.20	70.70	170.82	21.09	75.59	155.8	4.17	14948	499	54.10	6.05	5.48	10.00
29			45.82	53.97	5.99	164.30	14.97	18.53	109.92	152.44	40.95	88.48	156.4	5.05	4907	1071	32.66	6.32	6.22	6.69
4			52.98	49.40	19.12	148.14	14.15	16.24	141.14	125.01	45.17	64.35	157.3	1.04	23771	10579	75.22	7.56	7.33	6.33
86			36.60	68.86	6.74	182.13	13.03	14.96	100.59	106.42	37.91	59.22	0.0	0.45	0	0	0.00	8.44	5.98	6.96
17			48.55	41.30	5.19	150.41	13.22	19.00	133.64	180.03	48.39	93.66	142.2	3.19	5227	1186	52.82	5.12	6.58	6.23
75			30.66	54.31	5.05	154.11	11.33	14.17	116.03	132.03	44.91	80.29	0.2	0.17	9	2	0.09	9.62	6.79	6.11
83			46.43	66.80	9.17	183.63	16.82	19.03	98.03	91.30	36.11	53.86	147.9	3.39	10392	1546	45.34	7.33	6.05	7.05
7			57.50	47.97	18.08	183.34	31.00	28.61	12.51	95.02	8.69	61.97	79.7	5.85	4557	677	32.75	5.32	5.15	10.80
13			68.40	36.25	23.25	118.35	15.15	16.46	176.42	120.67	53.36	61.84	165.5	0.34	35687	19472	65.20	7.80	8.95	5.28
3			61.72	21.38	31.56	101.40	14.17	13.67	70.97	422.94	17.89	80.98	106.7	5.91	3655	968	45.67	3.56	9.30	7.24
47			59.51	42.57	21.92	133.23	13.93	14.84	165.95	121.17	48.46	56.69	165.9	0.64	9069	19919	48.39	7.66	7.97	6.18
28			52.20	36.46	8.30	148.29	12.97	15.68	142.68	193.52	46.23	68.42	142.1	3.99	6314	913	36.49	4.98	7.04	5.96
12			56.40	21.70	15.62	74.86	13.26	14.76	86.94	283.17	35.54	100.07	117.5	5.77	6683	1076	55.92	3.97	9.14	5.76
63			52.48	17.94	5.38	45.54	13.55	13.86	187.81	379.08	62.66	101.76	119.5	5.79	9792	1781	71.43	4.30	9.97	4.17
57			57.51	44.49	19.60	174.77	19.95	18.48	41.08	111.43	21.47	58.74	121.0	5.88	3986	621	33.45	3.27	6.38	7.27
59			66.61	62.93	11.20	187.48	30.44	28.47	30.46	70.74	18.95	46.08	122.5	5.89	3839	483	32.79	5.25	6.19	9.28
15			55.35	27.60	5.15	55.16	15.15	19.27	137.66	282.06	58.51	101.61	123.6	4.14	6016	1307	53.83	5.02	9.31	4.10
90			57.93	14.57	-0.00	32.86	16.03	11.70	105.66	112.34	71.60	63.40	140.1	0.20	33085	20659	117.00	5.81	10.00	2.41
67			59.56	31.62	14.17	183.79	22.27	21.24	68.94	86.21	31.11	41.50	123.0	5.96	3970	384	36.64	3.89	7.09	11.20
8			46.97	25.81	11.58	111.59	6.53	21.52	159.97	194.10	50.27	59.99	8.8	0.53	322	73	2.54	1.47	8.71	4.92
45			60.58	63.40	19.21	179.56	22.16	22.85	78.82	66.30	32.51	41.05	147.0	5.31	6424	1192	47.20	6.35	6.80	6.90
52			56.27	20.29	15.74	118.90	11.60	16.15	161.30	183.08	53.04	70.18	113.6	5.51	5230	689	49.31	4.65	7.98	5.93
16			70.26	22.02	10.60	57.59	18.74	16.56	98.80	248.44	46.79	97.49	145.4	3.70	6390	1776	58.82	7.07	9.16	4.46
5			79.43	47.66	32.29	180.64	34.55	30.15	20.67	73.24	13.86	49.96	116.4	5.87	3724	509	37.35	5.04	6.59	9.71
65			41.12	16.34	0.73	39.85	11.08	14.13	128.07	184.62	64.67	78.67	39.1	1.40	1690	377	12.08	2.39	9.72	3.01
6			67.31	50.30	26.92	153.51	21.41	26.65	75.40	84.98	30.96	49.70	144.0	5.41	4643	754	44.86	6.03	7.64	6.94
77			76.55	52.46	29.81	175.99	26.34	24.88	57.67	63.05	28.14	40.26	90.6	5.94	4417	659	45.52	5.29	7.15	7.39
24			67.57	46.83	22.96	154.93	22.34	20.23	131.22	90.26	42.40	43.09	152.7	4.39	8387	1694	68.39	6.48	8.00	6.12
42			77.44	33.86	26.56	159.24	23.90	22.42	42.56	73.64	20.50	37.22	72.4	5.99	4202	517	24.45	3.26	8.16	9.99
68			79.65	47.64	37.50	166.68	29.70	28.37	20.81	59.54	14.66	43.31	155.0	2.08	4004	657	27.01	8.30	7.35	9.13
32			70.67	30.85	24.10	120.52	17.02	18.34	157.13	140.52	48.59	56.41	159.3	1.91	6387	1210	68.96	6.94	8.76	5.28
14			89.16	40.46	29.21	131.82	29.22	24.49	25.56	84.17	18.63	58.79	112.0	5.84	4801	596	48.27	4.86	7.85	6.59
25			80.17	41.94	35.85	162.23	24.38	24.18	88.37	71.53	33.26	36.32	150.7	5.60	4675	475	25.15	5.77	7.97	7.21
53			74.43	20.92	32.13	94.23	12.99	13.63	210.95	143.11	55.47	49.26	165.1	1.44	7689	7661	44.25	7.49	9.88	4.93
43			76.85	32.73	35.99	126.02	17.08	19.87	169.86	99.77	45.47	39.78	146.7	4.63	7234	1061	75.73	5.87	9.18	5.66
22			75.77	14.85	33.63	88.73	14.19	15.39	193.28	180.28	53.71	52.47	156.6	5.34	3302	537	63.61	5.81	9.60	5.32
89			72.65	26.98	49.36	104.54	15.47	16.09	158.74	130.28	44.27	43.99	0.4	0.13	23	13	0.28	6.43	9.80	5.52
27			64.70	25.44	63.27	119.16	11.51	11.45	38.73	58.29	20.61	35.98	4.5	0.12	36	9	0.22	9.50	10.30	6.62
9			77.49	10.55	24.93	78.32	10.85	11.31	212.53	146.48	57.87	46.37	12.2	0.75	327	96	4.58	5.15	10.20	4.41
46			71.12	8.60	14.51	24.16	13.50	12.99	303.36	322.01	64.79	55.77	118.8	5.52	5272	1108	53.19	3.52	13.00	3.02
33			78.46	28.89	42.96	113.83	16.87	17.87	156.26	120.74	44.78	45.03	149.6	4.61	5551	842	53.55	13.10	9.38	5.60
49			76.99	14.27	50.99	84.62	12.61	16.52	200.60	181.73	48.56	44.04	155.8	5.32	3478	526	52.30	5.25	10.40	5.26
11			69.58	27.78	46.24	103.26	13.67	14.34	166.27	120.45	47.36	44.29	1.0	1.42	50	11	0.36	15.11	9.85	5.25
38			101.84	29.56	40.21	147.92	30.24	29.03	75.08	43.01	31.86	26.65	135.4	5.93	5411	473	63.12	5.67	9.19	8.96
76			97.67	39.98	48.39	156.40	30.25	29.16	49.29	45.78	23.91	31.10	134.1	5.78	3821	399	31.11	11.32	8.58	8.46
62			105.98	26.75	46.18	141.59	29.83	27.96	52.23	44.31	24.36	26.48	50.3	5.99	3620	266	19.47	4.62	9.30	8.87
66			97.34	33.64	60.20	142.43	24.65	26.32	97.31	50.48	34.63	24.60	155.4	5.86	6245	723	50.16	6.08	9.53	7.04
39			100.02	11.09	59.67	56.74	18.30	14.23	64.64	185.21	19.16	45.69	87.9	5.93	3890	542	36.17	3.92	11.90	5.21
19			100.73	12.98	43.12	65.25	18.30	16.08	52.22	142.64	15.86	34.01	80.4	5.96	3560	463	27.28	2.99	13.20	6.73
64			111.62	28.76	53.18	139.41	31.08	29.70	60.30	37.73	25.30	24.14	160.0	5.94	3505	348	27.33	5.42	9.61	8.60
55			93.42	9.95	71.32	61.79	14.34	14.02	232.19	161.65	53.13	37.78	170.4	2.22	5056	639	62.17	7.10	11.60	4.39
74			102.76	4.01	69.27	27.12	10.33	10.68	345.40	106.55	76.33	27.44	175.5	0.13	28840	5081	74.24	8.25	14.00	2.90
80			95.02	5.49	79.94	45.92	13.48	13.61	248.78	162.30	58.31	36.10	180.5	4.97	3639	495	47.44	6.02	12.30	4.19
81			98.36	4.53	73.51	44.44	14.57	13.49	250.30	136.45	63.10	35.74	185.3	2.39	4656	801	37.17	7.06	12.30	4.23
51			78.91	0.82	9.58	6.08	9.45	7.78	123.14	64.39	36.67	14.34	45.1	2.80	2163	261	15.41	1.53	16.70	1.71
21			117.03	3.91	29.45	19.80	19.79	13.75	91.22	100.86	28.51	23.60	95.2	5.75	4977	608	38.08	4.30	15.00	3.10
35			115.23	8.23	89.12	63.59	17.50	17.35	177.14	76.24	41.32	23.50	75.4	5.82	5563	836	37.15	5.57	12.30	4.87
36			104.68	0.08	71.63	11.38	6.57	5.15	345.55	75.73	76.45	18.48	3.6	0.16	110	34	0.82	2.91	15.30	2.22
26			148.81	11.75	85.08	79.62	29.74	27.59	80.25	25.16	32.21	15.07	129.4	5.97	3698	475	35.12	5.57	12.30	6.75
34			113.26	2.14	78.48	23.00	13.65	12.80	330.32	108.31	69.92	25.69	178.6	2.46	5400	1006	48.97	7.95	14.10	2.97
78			132.55	0.12	94.63	3.50	12.19	10.10	366.62	26.44	98.37	7.29	163.3	0.18	32143	17468	144.50	8.05	17.30	1.25

continued on next page

continued from previous page

	Rand color	Sim color	Heat sum	Cold sum	Hot days	Cold days	Diurnal diff grow	Diurnal diff non-grow	Precip grow	Precip non-grow	Wet days grow	Wet days non-grow	Soil depth	Water table depth	Soil N	Organic matter	Soil avail water	CTI	Solar grow $\times 10^7$	Solar non-grow $\times 10^7$
30			155.32	11.99	78.08	53.25	28.08	23.46	33.28	41.26	13.25	14.92	112.0	5.86	2872	218	21.89	4.58	14.00	5.49
37			129.11	7.28	102.83	51.04	19.47	18.26	182.36	55.59	42.82	19.54	174.2	5.57	6119	674	52.95	6.24	13.10	4.20
61			171.01	5.89	89.53	29.91	28.24	17.98	46.88	57.10	19.40	19.47	114.8	5.87	3572	324	40.71	5.33	15.10	3.53
2			144.65	5.96	103.87	23.65	22.27	15.93	45.64	46.57	20.56	18.51	148.6	5.45	4191	405	43.97	8.00	15.90	2.88
48			161.38	0.46	21.90	3.53	22.38	14.46	91.05	25.57	28.71	6.10	114.4	5.09	3730	494	42.39	5.77	17.90	1.21
60			174.35	4.02	129.39	31.69	23.83	16.97	50.37	24.66	21.71	11.10	50.9	5.99	2472	164	12.48	3.94	15.60	3.76
56			140.86	0.21	105.22	3.93	16.35	13.89	358.64	32.51	93.72	9.10	182.6	1.85	3879	928	30.84	7.86	16.70	1.62
73			182.03	3.88	147.09	29.52	26.81	21.55	88.38	21.65	31.33	11.56	154.0	5.92	3333	364	35.99	6.74	15.10	3.67
71			144.43	0.00	93.33	0.27	12.69	7.33	397.01	5.34	107.21	1.75	48.0	0.51	2911	645	15.44	7.71	18.70	0.36
82			211.81	2.78	158.64	13.90	27.63	20.64	28.71	8.68	13.66	4.77	143.8	5.78	2200	124	17.34	5.75	17.80	2.32

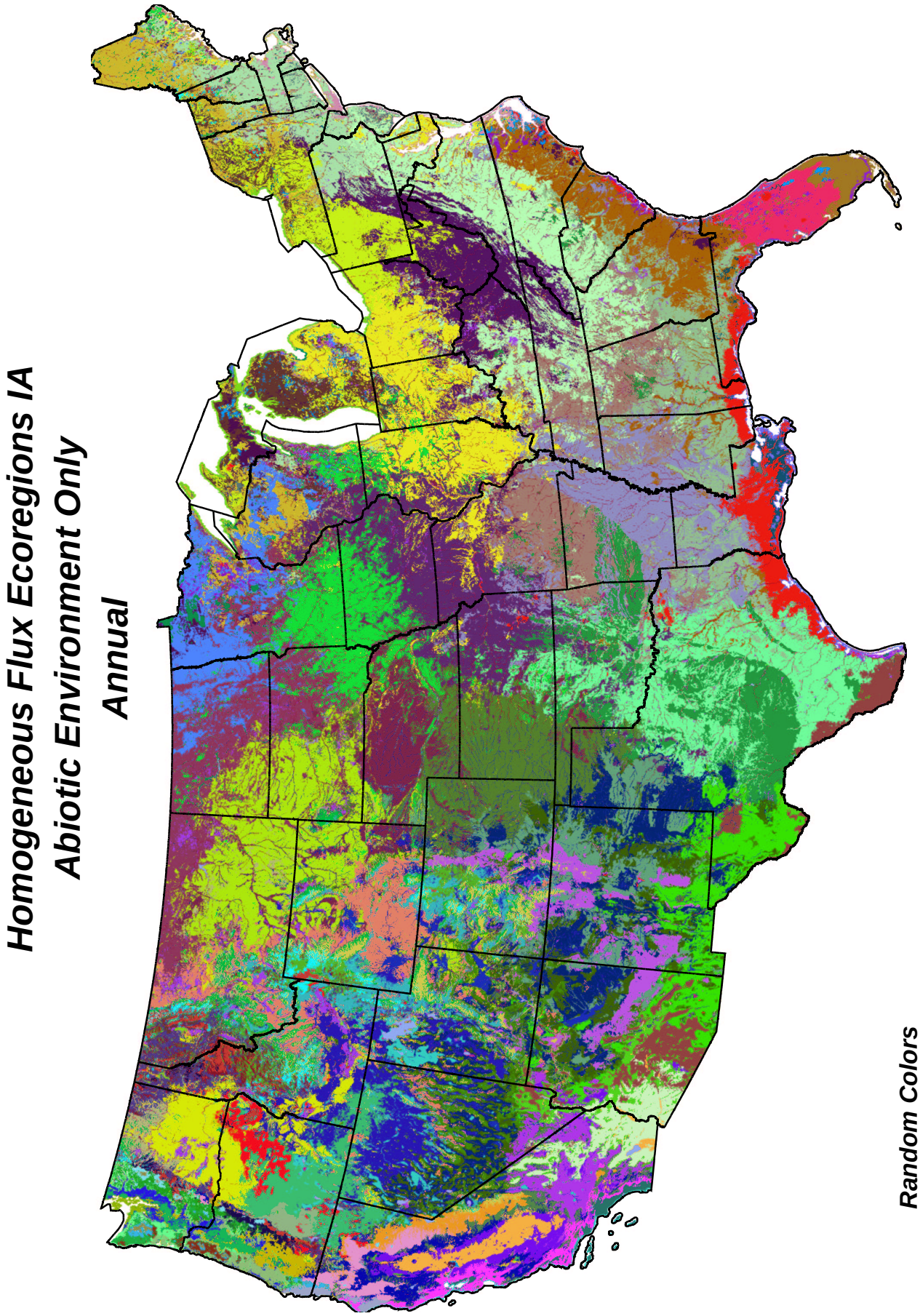

Figure 3.1: Homogeneous Flux Ecoregions IA Random Colors

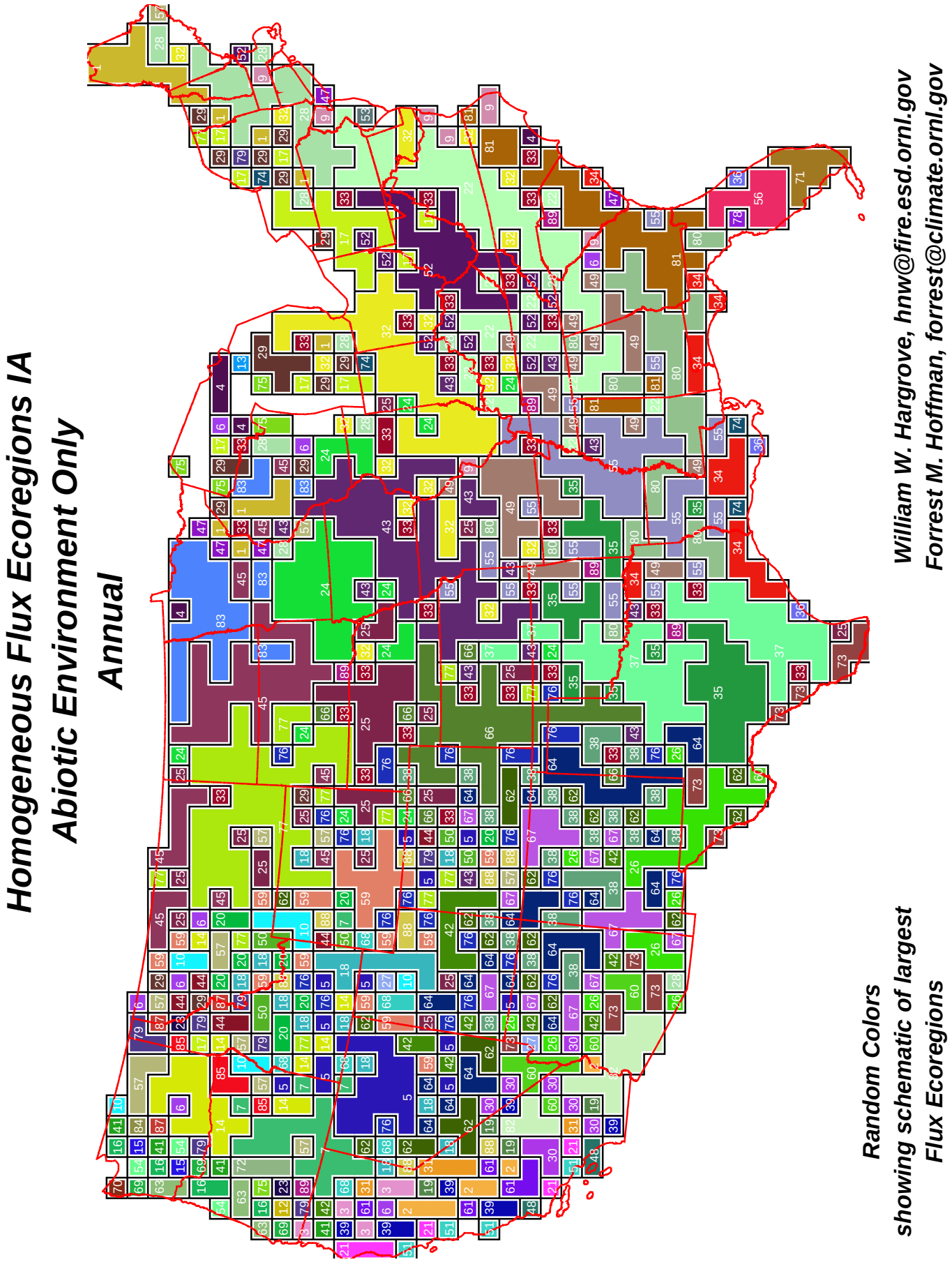

Figure 3.2: Homogeneous Flux Ecoregions IA Schematic

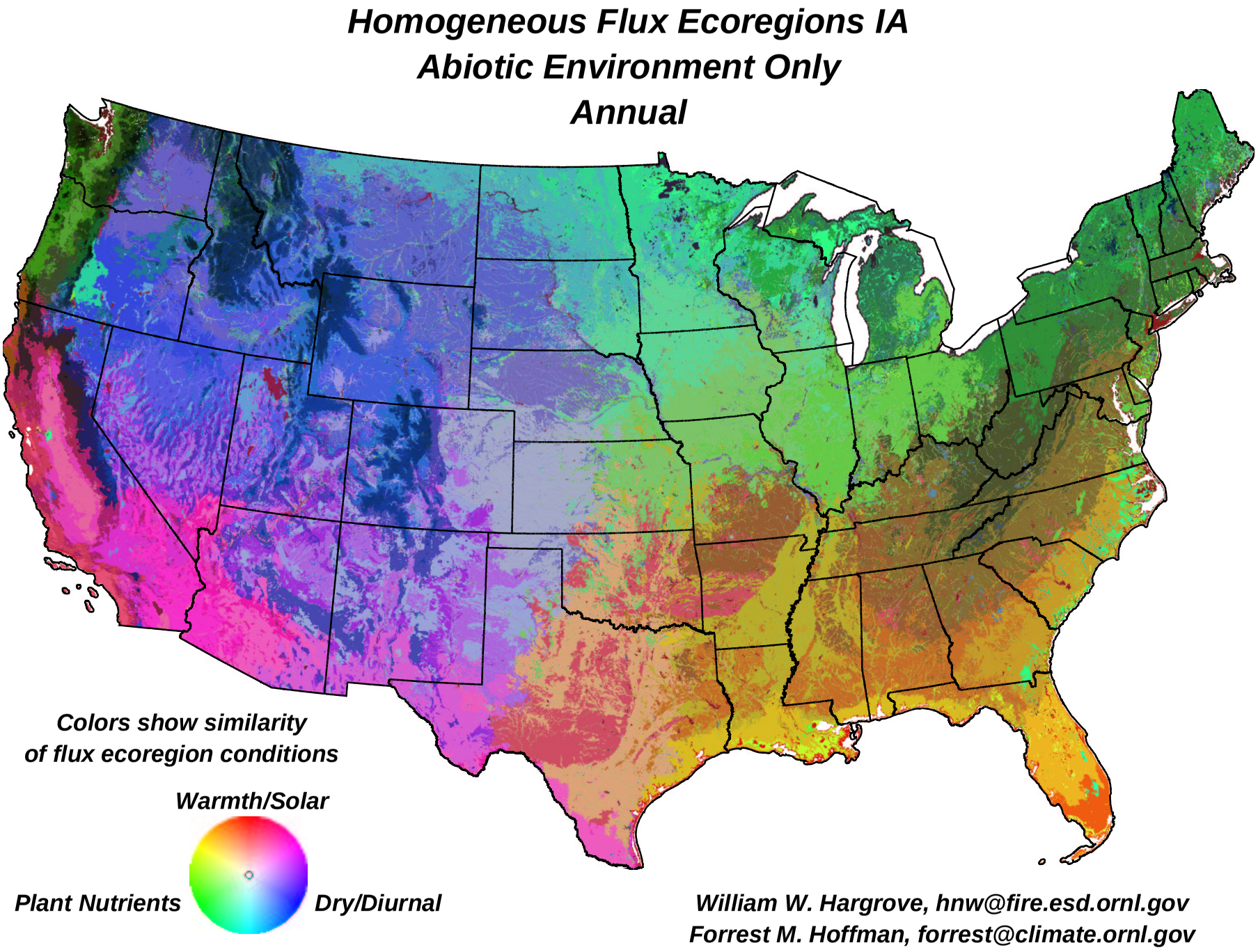

Figure 3.3: Homogeneous Flux Ecoregions IA Similarity Colors

Map Layer	Factor 1	Factor 2	Factor 3
Degree-days heat sum above 42°F from daytime land surface temperature during the local growing season	0.94155 ✓	0.20816	-0.05942
Degree-days cold sum below 42°F from nighttime land surface temperature during the local non-growing season	-0.81975 ✓	0.39945	0.07470
Number of days above 90°F during the local growing season	0.91870 ✓	0.00974	-0.04167
Number of days below 32°F during the local non-growing season	-0.84475 ✓	0.46816	-0.00529
95th percentile of maximum diurnal surface temperature difference during the local growing season	0.13328	0.91768 ✓	-0.07905
95th percentile of maximum diurnal surface temperature difference during the local non-growing season	-0.07284	0.89898 ✓	-0.00791
Precipitation sum during the local growing season	0.39686	-0.77884 ✓	0.28939
Precipitation sum during the local non-growing season	-0.51727	-0.64461 ✓	-0.13071
Number of days with measurable precipitation during the local growing season	0.29426	-0.76371 ✓	0.32854
Number of days with measurable precipitation during the local non-growing season	-0.84761 ✓	-0.33655	-0.08007
Depth of mineral soil	0.13663	-0.13956	0.52476 ✓
Depth to water table	-0.00671	0.50523 ✓	-0.39437
Soil Kjeldahl nitrogen to 50 cm depth	-0.18252	-0.01213	0.78779 ✓
Soil organic matter to 50 cm depth	-0.13503	-0.05658	0.70470 ✓
Soil plant-available water holding capacity to 1.5 m	-0.05480	-0.18775	0.61696 ✓
Compound Topographic Index (CTI)	0.23900	0.02433	0.42996 ✓
Total solar insolation during the local growing season, including clouds, aerosols, slope and aspect physiography	0.94712 ✓	-0.23542	-0.00571
Total solar insolation during the local non-growing season, including clouds, aerosols, slope and aspect physiography	-0.67209 ✓	0.57144	-0.19336
Factor 1: warmth/solar **Factor 2: precip/diurnal** **Factor 3: plant nutrients**			

Table 3.2: Homogeneous Flux Ecoregions IA Rotated Factor Pattern

3.3 Homogeneous Flux Ecoregions IB

Table 3.3: Average Conditions Within the 90 Homogeneous Flux Ecoregions for IB

	Rand color	Sim color	Heat sum	Hot days	Diurnal diff grow	Precip grow	Wet days grow	Soil depth	Water table depth	Soil N	Organic matter	Soil avail water	CTI	Solar grow $\times 10^7$
29			21.58	2.06	16.44	24.81	12.30	129.3	5.83	4340	650	27.95	3.23	3.16
2			31.57	7.42	10.20	90.81	34.26	0.0	0.05	1	0	0.01	10.20	5.90
76			29.84	5.60	19.77	20.85	10.05	134.1	5.86	13434	451	55.78	4.09	4.12
45			32.21	7.03	11.37	119.76	46.33	0.1	0.03	4	1	0.03	9.94	7.27
12			37.73	3.98	12.76	108.21	38.48	146.8	2.25	6334	1158	54.16	5.71	5.42
6			38.39	8.44	15.76	47.83	24.06	138.2	5.86	4300	699	35.45	3.02	5.70
85			54.29	15.25	6.03	181.64	54.10	0.3	0.20	8	6	0.08	0.03	9.33
1			48.18	11.40	13.52	135.23	46.02	0.2	0.17	5	1	0.05	6.07	7.20
73			42.93	3.60	12.49	126.47	45.96	141.6	3.33	5639	1085	38.48	4.19	6.13
27			41.70	0.77	11.48	119.77	65.67	43.9	1.61	1971	432	13.92	2.49	9.93
55			50.66	11.30	14.96	115.39	39.18	153.3	0.57	31316	11761	66.39	8.03	6.90
34			51.05	13.54	14.13	150.40	47.35	161.7	0.97	24171	12288	89.18	7.21	7.14
33			47.35	7.75	14.95	114.52	40.72	154.0	3.57	10116	3869	52.76	6.36	6.39
38			57.23	15.06	14.84	148.96	46.80	162.4	0.46	33813	17230	81.41	7.62	7.72
17			52.62	18.38	20.50	33.41	16.44	123.4	5.82	4693	675	86.00	4.34	6.28
43			50.75	9.92	14.93	119.14	40.05	150.3	4.55	8888	842	38.41	6.06	6.72
61			49.48	9.06	13.45	105.35	40.17	119.2	5.89	10352	1147	57.39	3.51	8.64
58			53.80	13.75	11.88	160.51	51.47	97.8	5.61	5971	739	42.33	4.36	7.71
60			54.88	13.10	12.69	147.67	50.34	129.9	4.88	4534	736	62.83	4.60	7.47
67			46.55	4.38	13.97	206.02	63.23	119.7	5.57	8295	1595	59.16	3.49	9.15
65			57.75	21.63	13.11	171.01	48.54	161.3	0.57	9598	15457	38.72	7.77	7.96
75			52.32	12.05	14.30	128.01	42.99	160.7	5.26	4226	732	29.83	6.29	6.97
81			59.99	19.52	33.07	15.62	10.35	96.3	5.88	4062	617	38.87	4.98	5.18
72			56.08	16.05	19.38	107.31	38.03	153.5	2.38	11525	1469	49.21	7.49	6.89
87			56.70	6.78	15.72	122.61	52.91	132.3	4.50	5566	1284	56.13	5.10	8.94
57			68.73	38.54	23.14	45.51	23.55	0.2	0.03	15	5	0.11	6.84	7.83
37			58.64	30.73	15.47	131.66	41.02	2.2	5.12	135	19	0.67	7.02	8.26
10			75.94	22.39	28.17	26.49	14.97	58.2	5.97	4395	542	23.60	3.64	7.20
90			63.79	14.58	16.46	140.78	48.49	159.2	1.71	5864	1189	57.00	6.53	7.98
66			61.65	20.57	23.94	79.46	33.29	148.2	5.37	6764	1095	44.96	5.41	7.02
82			65.15	30.37	15.93	52.94	16.24	104.8	5.92	3536	775	38.13	3.45	9.29
28			69.35	21.45	25.61	45.90	23.93	135.2	5.90	4180	654	47.50	4.23	6.91
53			72.89	4.78	7.70	117.48	35.94	15.5	1.03	493	47	3.82	0.77	16.80
18			67.72	21.56	21.48	141.54	43.58	154.6	4.33	8559	1694	76.44	6.18	8.15
3			83.33	35.66	16.23	205.72	61.60	165.3	0.14	38169	24162	46.87	8.31	10.50
24			82.68	34.20	25.91	57.17	28.42	68.7	5.97	4270	507	28.12	4.21	7.85
20			80.24	25.88	32.01	27.64	16.75	147.4	5.88	3557	387	27.37	4.51	6.99
44			83.41	33.63	27.71	56.45	27.88	97.3	5.96	4434	648	56.97	5.03	7.60
15			77.01	36.08	29.58	20.88	14.65	154.9	2.08	4136	678	29.07	8.04	7.16
8			69.82	29.30	23.26	75.86	31.60	149.8	5.47	6223	978	47.10	9.39	7.50
50			64.26	41.45	13.44	155.53	45.86	0.5	0.73	19	6	0.21	16.80	9.41
51			68.25	26.98	14.51	169.03	49.73	143.5	5.22	4599	736	64.60	9.72	8.80
70			76.46	26.03	14.98	191.42	52.92	159.6	4.92	3765	629	54.77	5.52	9.27
69			75.27	32.99	17.09	172.74	48.61	157.8	2.29	6597	1223	81.93	6.34	9.33
74			75.02	32.84	13.06	211.31	55.50	167.8	1.49	7313	6238	43.81	7.49	9.92
13			88.01	23.19	33.58	55.70	28.96	114.0	5.98	4528	411	39.85	5.08	7.78
83			73.34	35.64	14.29	185.35	50.97	159.8	5.28	3739	547	72.85	5.30	9.55
89			79.08	28.14	32.45	31.01	18.21	145.6	5.72	3615	375	29.61	9.90	6.91

continued on next page

continued from previous page

	Rand color	Sim color	Heat sum	Hot days	Diurnal diff grow	Precip grow	Wet days grow	Soil depth	Water table depth	Soil N	Organic matter	Soil avail water	CTI	Solar grow $\times 10^7$
22			85.43	44.68	14.74	232.27	61.46	182.6	0.69	6006	31688	79.73	8.04	10.90
39			72.48	33.90	16.47	164.45	47.13	158.5	2.35	6783	1113	62.80	12.19	9.04
21			86.76	38.88	26.34	74.69	31.36	149.9	5.75	4286	401	21.91	5.42	8.20
41			88.61	36.86	29.04	47.46	24.50	78.4	5.95	4004	484	36.94	9.53	7.87
19			83.24	73.02	11.52	228.46	53.69	1.3	0.11	71	38	0.82	7.38	11.90
5			79.08	86.85	10.65	36.79	20.57	3.3	0.29	102	5	0.54	9.65	12.30
11			89.25	24.97	14.97	124.70	34.23	100.3	5.80	4674	700	40.79	3.45	14.50
62			95.04	44.71	10.57	279.94	67.14	7.9	0.62	192	65	2.34	7.90	12.50
42			96.77	61.97	5.77	354.62	76.71	6.0	0.12	178	40	1.08	0.05	14.60
71			86.24	62.11	13.72	211.23	48.98	97.0	5.66	4114	507	49.23	5.29	10.90
56			92.80	58.60	16.36	212.09	50.18	164.3	2.34	6430	879	48.99	6.70	10.90
79			82.12	49.28	18.47	137.80	40.47	152.4	5.12	4988	711	41.71	14.42	9.45
84			94.11	69.80	9.60	328.71	86.33	3.8	0.17	91	17	0.83	0.23	15.60
31			87.00	44.95	14.11	330.77	69.49	154.4	5.24	5156	949	44.41	5.18	12.20
80			113.25	76.87	7.26	213.38	52.86	2.9	0.16	70	10	0.25	0.99	15.90
86			101.48	67.17	23.70	111.48	36.44	161.1	5.83	7131	801	54.35	5.93	9.98
88			120.69	47.86	21.80	56.61	18.21	68.5	5.95	3824	357	24.67	3.59	13.60
36			96.59	71.82	14.55	214.03	47.31	180.6	5.10	3753	513	48.72	5.99	11.60
23			93.93	78.13	13.12	245.13	54.99	173.4	2.34	4588	575	68.45	6.83	12.10
68			133.29	65.47	27.54	79.57	31.43	60.7	5.96	3957	385	21.31	4.48	11.60
52			94.10	81.19	13.40	227.06	53.87	179.9	5.24	3515	515	54.00	5.73	12.10
14			105.40	72.99	9.75	359.08	78.29	177.1	0.13	28288	4633	75.70	8.27	14.50
30			101.66	75.10	15.65	237.06	59.40	182.6	4.83	4245	496	37.14	6.40	12.20
32			112.51	80.66	19.67	172.20	41.52	145.5	5.65	7778	940	68.23	6.00	11.50
48			99.44	82.55	13.82	258.59	62.69	183.3	1.93	4653	747	37.46	6.95	12.70
49			127.75	64.55	29.44	83.94	31.45	167.3	5.91	5226	500	63.99	5.85	11.10
26			131.32	57.00	7.09	357.19	103.36	4.0	0.14	430	136	2.95	1.64	19.20
46			148.31	21.50	22.69	81.25	26.39	115.8	5.31	4346	578	41.10	5.58	16.80
40			112.23	74.76	13.33	335.71	71.38	175.6	1.56	5570	1087	48.95	8.34	14.00
54			130.46	101.53	19.33	150.98	36.08	62.6	5.97	6378	1089	27.06	5.54	13.10
16			117.75	86.30	12.93	323.71	85.02	156.2	0.56	15727	8560	73.50	7.93	15.50
4			139.58	81.05	28.60	84.55	29.89	167.7	5.95	3376	452	28.00	5.69	11.90
78			128.12	103.12	13.63	352.67	93.13	171.6	0.00	38629	20432	167.09	8.57	16.20
7			165.75	82.81	29.03	33.61	14.48	125.8	5.86	3197	263	32.74	4.94	14.50
63			143.51	102.19	22.24	46.04	20.54	149.8	5.45	4215	414	44.64	7.93	15.80
35			139.44	101.00	12.46	391.39	105.38	29.0	0.30	2772	479	12.65	9.24	18.30
64			173.35	124.59	23.86	44.88	19.03	51.5	5.99	2496	162	13.51	3.79	15.70
47			153.36	81.93	16.16	387.95	103.12	160.1	1.65	3933	961	28.00	8.36	17.50
9			137.19	107.62	16.35	352.20	92.21	184.6	1.88	3772	782	30.79	7.71	16.50
59			155.03	113.76	26.61	86.03	29.16	153.6	5.87	3682	432	33.68	11.33	13.50
25			170.16	141.02	25.16	106.83	33.94	152.7	5.91	3847	478	38.73	5.99	14.60
77			206.57	154.72	27.92	31.09	14.81	155.2	5.82	2195	130	20.30	5.57	17.10

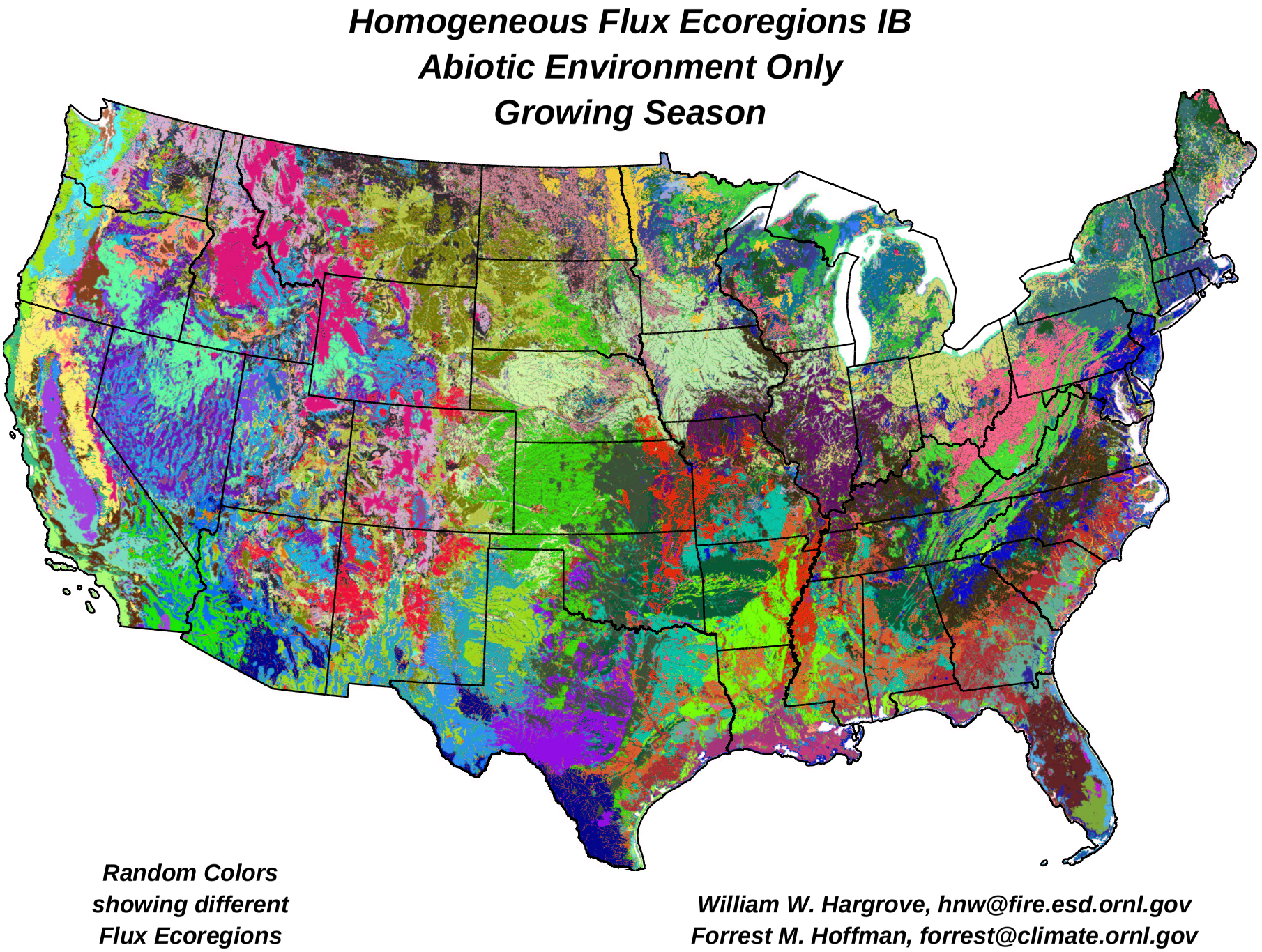

Figure 3.4: Homogeneous Flux Ecoregions IB Random Colors

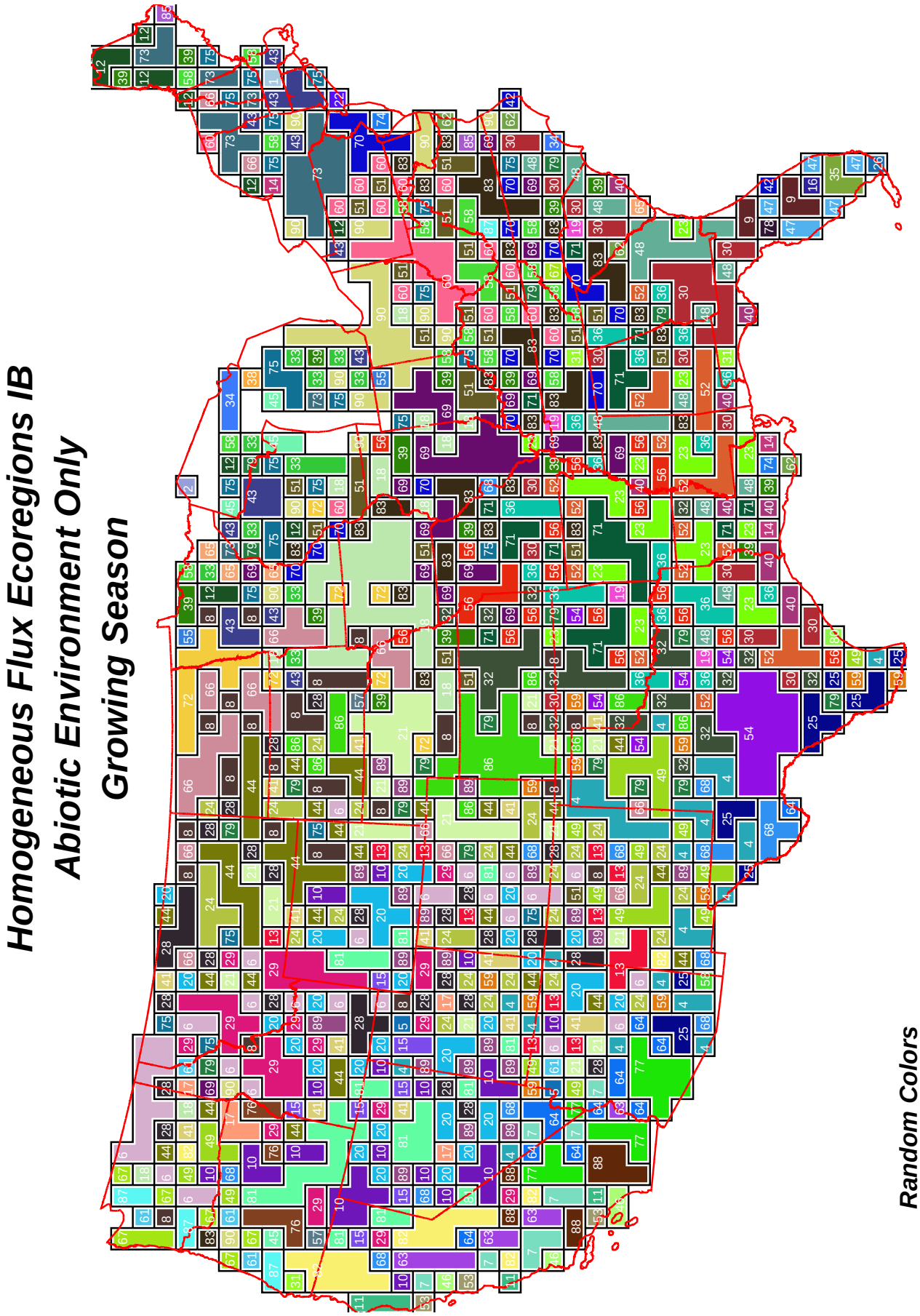

Figure 3.5: Homogeneous Flux Ecoregions IB Schematic

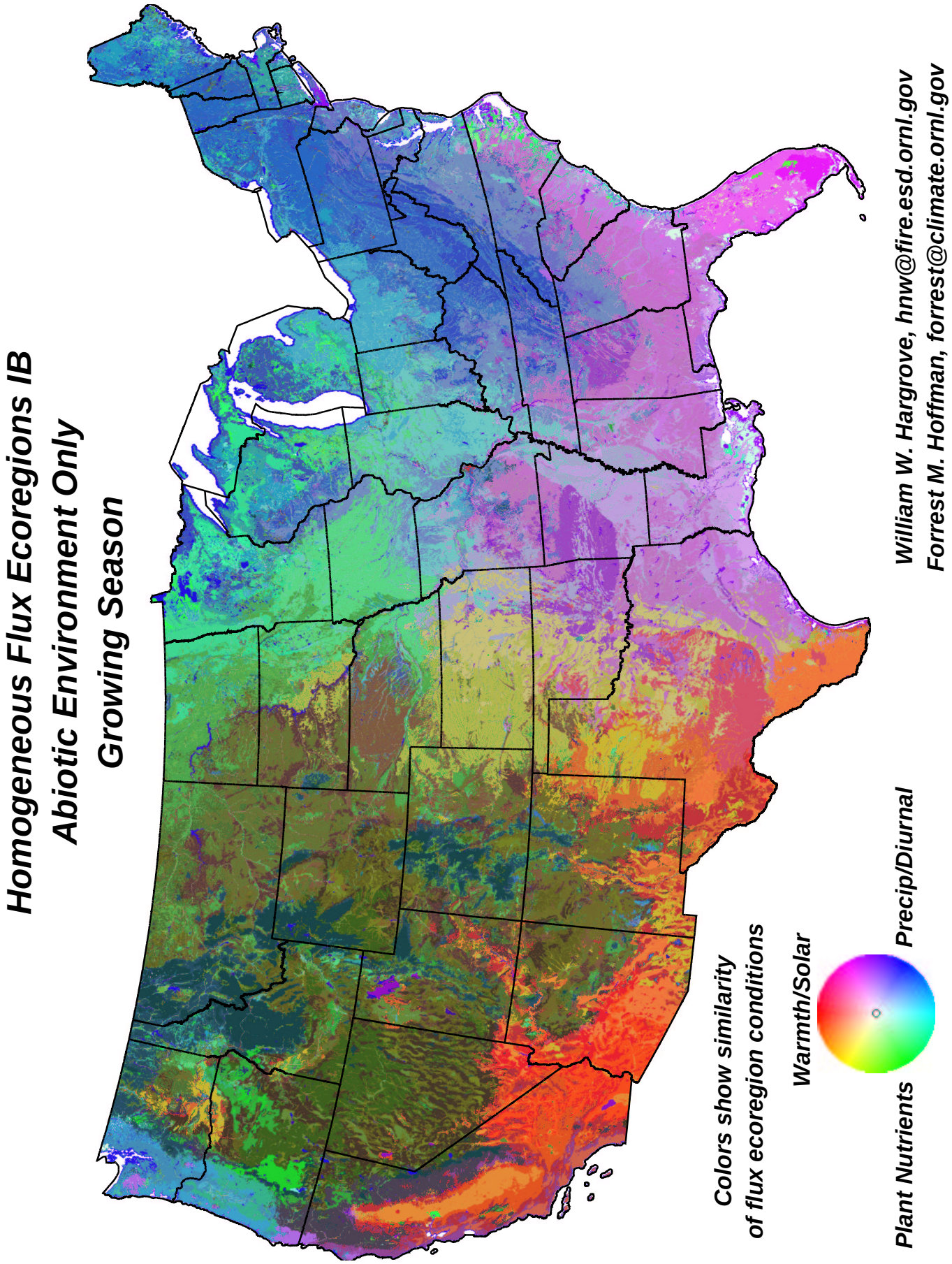

Figure 3.6: Homogeneous Flux Ecoregions IB Similarity Colors

Map Layer	Factor 1	Factor 2	Factor 3
Degree-days heat sum above 42°F from daytime land surface temperature during the local growing season	0.96209 ✓	-0.17149	-0.05792
Number of days above 90°F during the local growing season	0.95105 ✓	0.01761	-0.04781
95th percentile of maximum diurnal surface temperature difference during the local growing season	0.19930	-0.85344 ✓	-0.03341
Precipitation sum during the local growing season	0.33306	0.88405 ✓	0.16620
Number of days with measurable precipitation during the local growing season	0.21999	0.89417 ✓	0.18368
Depth of mineral soil	0.21063	0.18707	0.53253 ✓
Depth to water table	0.05865	-0.66698 ✓	-0.22345
Soil Kjeldahl nitrogen to 50 cm depth	-0.15862	0.01820	0.83625 ✓
Soil organic matter to 50 cm depth	-0.12570	0.06240	0.73911 ✓
Soil plant-available water holding capacity to 1.5 m	-0.03655	0.19172	0.65644 ✓
Compound Topographic Index (CTI)	0.26431	0.14935	0.29998 ✓
Total solar insolation during the local growing season, including clouds, aerosols, slope and aspect physiography	0.92426 ✓	0.25974	-0.03814
Factor 1: warmth/solar **Factor 2: precip/diurnal** **Factor 3: plant nutrients**			

Table 3.4: Homogeneous Flux Ecoregions IB Rotated Factor Pattern

3.4 Homogeneous Flux Ecoregions IC

Table 3.5: Average Conditions Within the 90 Homogeneous Flux Ecoregions for IC

	Rand color	Sim color	Cold sum	Cold days	Diurnal diff non-grow	Precip non-grow	Wet days non-grow	Soil depth	Water table depth	Soil N	Organic matter	Soil avail water	CTI	Solar non-grow $\times 10^7$
38			0.19	12.30	4.06	62.54	16.28	5.2	0.12	139	32	1.08	0.04	1.90
88			0.08	4.47	6.92	26.23	7.24	19.4	0.34	1792	341	8.84	8.84	1.05
13			4.05	33.02	13.57	101.56	26.54	182.2	1.50	4071	889	36.49	7.36	3.35
66			2.74	16.81	18.25	24.01	10.10	168.4	5.63	3124	366	20.96	5.92	2.60
9			3.58	21.44	15.48	42.83	13.63	61.5	5.90	3071	316	22.39	4.10	2.86
84			11.46	61.85	14.19	126.44	35.34	1.0	0.23	40	21	0.46	7.75	4.42
82			3.44	23.77	17.31	46.74	17.56	166.2	5.67	4968	542	53.97	6.56	3.11
23			17.87	45.54	14.68	367.01	94.99	2.0	0.20	81	17	0.55	1.89	3.83
39			8.41	55.69	13.46	160.37	38.23	171.9	2.25	4590	648	68.31	6.73	4.20
14			6.28	50.89	14.70	125.26	32.81	183.6	4.80	3966	447	39.46	6.10	4.34
52			3.18	24.52	10.98	104.58	26.80	156.2	0.23	29329	1838	74.14	8.73	2.74
2			10.52	60.20	14.92	120.95	32.30	167.2	1.72	8752	918	44.57	7.18	4.20
30			11.69	50.97	13.57	260.73	53.62	98.8	5.87	3917	724	43.32	3.62	5.02
41			10.88	70.21	14.99	192.64	43.18	176.9	5.14	3443	584	51.23	5.57	4.91
85			19.83	109.77	13.12	161.38	53.17	5.9	0.57	157	54	1.76	4.04	5.05
70			26.51	99.49	14.44	116.37	42.89	1.3	1.40	59	13	0.46	15.99	5.10
3			17.92	83.27	15.44	147.03	42.43	163.7	2.33	5787	846	62.58	11.85	4.77
19			13.39	68.10	17.40	97.65	30.91	154.8	5.33	4375	551	43.88	13.58	4.73
60			5.74	56.00	17.75	51.98	19.08	61.9	5.95	6314	980	25.75	5.65	4.96
35			17.54	79.07	13.42	121.23	42.43	163.0	1.29	7597	5954	50.29	7.63	4.39
22			13.80	86.24	15.57	170.78	50.07	164.0	5.42	3047	495	71.29	5.66	5.31
75			13.69	85.43	15.23	195.47	48.43	99.6	5.62	4038	551	49.06	5.07	5.30
72			17.20	43.32	13.83	408.43	101.25	116.6	5.86	10281	1943	79.88	4.34	4.17
81			33.85	90.49	16.11	154.36	83.84	17.9	0.97	820	246	6.87	3.23	4.29
31			11.08	62.36	20.11	59.82	21.86	62.1	5.98	3531	314	20.80	3.26	6.22
53			26.99	141.52	11.20	89.70	48.40	0.3	0.04	3	1	0.03	9.32	7.81
76			10.99	58.41	27.35	28.93	13.66	159.0	5.91	3149	387	35.48	5.95	5.50
12			29.21	121.23	21.45	182.08	57.69	1.1	0.16	30	7	0.31	1.91	5.14
8			21.94	69.22	14.56	291.69	102.64	120.8	5.68	7316	1248	57.02	4.22	5.33
61			16.93	90.83	18.98	81.52	28.46	111.1	5.57	6189	825	69.09	5.71	5.42
20			26.95	73.30	16.68	428.12	120.56	127.9	4.96	6580	1438	53.79	4.06	4.74
73			31.09	73.89	19.71	222.66	96.42	140.4	3.35	6088	1339	57.67	6.50	4.78
86			40.03	100.82	13.31	1087.50	158.61	114.2	5.81	6333	894	39.85	2.67	5.59
27			33.98	95.84	14.20	809.23	141.21	109.6	5.71	5991	999	42.42	2.91	5.63
89			31.93	83.93	15.97	653.55	138.04	121.6	5.42	8034	1447	53.11	3.56	4.99
17			21.84	111.42	13.50	443.14	82.42	106.3	5.92	3746	959	43.26	3.50	7.71
77			16.83	93.12	22.61	44.79	19.09	181.2	5.84	7599	702	63.09	6.30	5.94
42			32.79	123.07	19.14	123.84	47.08	155.9	2.52	6801	1257	74.90	5.97	5.45
63			21.78	125.96	15.39	183.66	67.60	105.8	5.63	5811	669	43.04	3.90	6.17
43			30.10	130.29	17.71	155.98	65.32	135.5	5.00	5082	875	50.40	10.05	5.97
49			5.78	29.87	13.18	77.69	24.17	176.6	0.32	36200	18825	142.26	8.50	2.96
21			36.24	134.09	19.73	141.09	68.07	156.1	1.68	6375	1227	57.67	7.00	5.48
15			58.52	167.69	12.99	102.97	57.04	0.0	0.45	0	0	0.00	9.73	6.41
1			41.50	104.81	15.19	525.00	125.10	123.7	5.47	5643	973	42.44	3.10	6.15
16			8.24	65.51	12.84	142.07	45.53	182.6	0.69	6006	31688	79.73	8.04	4.74
67			29.62	86.22	12.89	95.77	35.76	172.9	0.37	27971	8815	73.42	8.11	4.55
68			29.50	136.60	18.41	181.44	85.75	130.5	4.62	4663	811	57.09	4.70	6.11
4			57.93	157.90	15.08	140.74	87.85	0.7	0.20	29	8	0.29	10.06	6.40

continued on next page

continued from previous page

	Rand color	Sim color	Cold sum	Cold days	Diurnal diff non-grow	Precip non-grow	Wet days non-grow	Soil depth	Water table depth	Soil N	Organic matter	Soil avail water	CTI	Solar non-grow $\times 10^7$
18			40.78	156.50	15.85	204.85	71.57	142.4	3.52	6311	904	36.30	4.75	6.16
87			34.40	114.72	14.86	115.03	51.36	160.9	1.70	17994	8116	71.91	7.28	5.28
26			39.88	149.69	18.53	112.54	52.13	147.6	5.37	5098	907	46.14	4.76	6.27
55			63.05	173.51	18.01	106.21	56.66	0.1	0.22	4	1	0.04	6.06	6.80
62			43.39	147.99	20.51	97.08	44.57	151.2	4.98	6870	1155	81.34	5.85	6.12
56			37.03	122.79	15.05	503.03	131.07	117.3	5.93	13908	1058	51.65	3.17	6.88
71			39.26	146.93	22.69	70.71	32.01	149.7	5.24	8402	1257	61.13	6.09	6.46
32			26.40	126.05	29.18	41.21	25.15	57.0	5.98	3386	317	22.21	5.26	8.10
47			42.65	134.02	24.46	97.24	64.31	117.6	5.77	4800	653	57.39	4.72	6.63
7			57.29	171.40	17.14	172.74	90.74	147.2	2.59	5988	1608	45.86	5.04	6.76
78			47.38	138.25	14.77	112.27	55.36	161.3	0.57	9598	15457	38.72	7.77	6.13
69			38.23	157.69	26.25	57.89	29.91	151.8	5.72	4632	476	27.65	5.83	7.40
50			28.61	140.59	29.85	38.51	25.29	158.5	5.93	3393	324	25.47	5.07	8.70
80			32.80	144.15	29.88	40.42	26.74	148.3	5.78	3773	375	29.34	10.61	8.41
29			27.46	155.75	24.40	55.87	31.27	57.0	5.99	3906	339	19.95	3.77	9.42
46			54.65	166.22	18.34	162.01	92.83	155.2	5.33	4361	920	31.59	5.75	6.94
33			53.25	168.98	23.30	70.72	39.77	132.2	5.37	5942	970	49.58	11.03	6.96
37			56.35	174.85	17.11	140.55	73.30	143.4	4.85	9485	868	38.55	6.13	7.12
44			53.56	200.85	14.96	190.72	94.35	141.8	5.77	4246	653	32.22	3.16	7.85
45			65.97	180.61	20.07	84.71	49.87	151.8	2.51	11285	1476	49.98	7.48	6.85
58			66.67	181.50	19.40	81.56	48.06	148.0	4.52	8108	1749	46.56	6.71	6.87
79			52.56	175.96	25.06	63.91	40.68	85.2	5.95	4330	655	43.46	4.93	7.41
40			42.50	179.72	16.90	297.58	70.40	111.3	5.86	3016	736	25.58	3.38	11.80
90			32.13	187.45	20.55	92.00	43.10	123.0	5.95	3947	418	36.22	3.72	11.40
6			33.52	158.88	30.85	47.32	30.98	125.1	5.96	4067	422	53.22	5.13	9.63
65			63.57	202.91	14.70	378.23	130.63	128.4	5.76	5338	559	31.09	3.00	8.07
28			62.42	181.51	25.51	57.62	38.20	145.0	5.64	5253	858	44.16	5.61	7.07
34			51.39	176.26	30.02	56.59	42.81	154.2	2.26	3836	572	25.13	7.92	9.66
24			49.42	181.38	19.32	172.58	86.79	117.1	5.75	5613	519	88.32	4.11	10.20
10			56.04	177.67	28.05	71.13	50.04	145.1	5.87	3990	519	33.46	4.88	8.53
11			46.50	178.30	27.72	96.67	61.34	71.7	5.90	4669	686	30.26	4.36	10.40
25			67.19	221.26	17.16	171.81	77.27	135.1	5.87	4012	728	31.51	3.22	10.40
51			51.77	191.72	23.88	112.82	55.64	109.4	5.93	5085	808	38.89	3.31	11.40
57			58.46	187.61	30.09	73.39	52.40	120.6	5.67	4033	536	41.15	9.85	10.00
5			34.41	113.63	18.05	98.75	52.80	162.6	0.16	38451	24705	47.57	8.21	4.65
83			45.37	143.04	16.60	134.03	75.23	159.2	0.23	35643	15878	63.60	7.42	6.04
74			68.62	192.68	27.69	97.88	57.17	114.0	5.87	4720	696	40.19	4.48	9.83
59			65.55	226.74	17.04	204.36	104.31	133.9	5.86	4383	663	31.44	3.57	11.80
54			60.82	176.08	16.67	150.29	85.05	151.6	1.02	26154	13802	83.44	7.05	6.91
48			76.94	222.89	17.23	331.12	121.57	123.9	5.79	4778	624	29.10	3.27	11.30
36			48.95	204.83	21.98	200.63	90.11	145.5	5.67	15239	415	57.26	4.83	11.80
64			79.05	241.11	18.38	213.08	86.05	129.5	5.76	4376	750	29.88	2.93	13.70

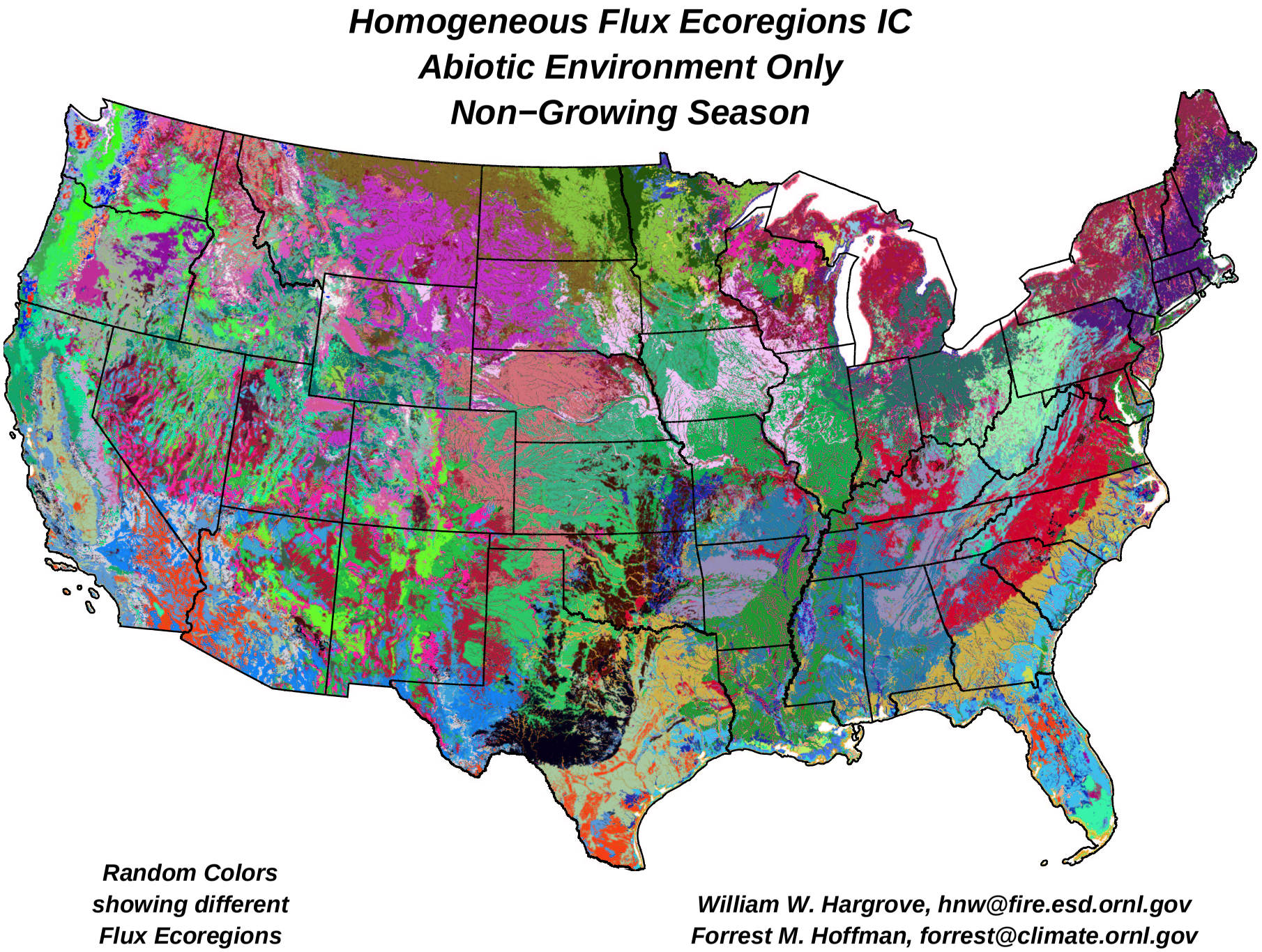

Figure 3.7: Homogeneous Flux Ecoregions IC Random Colors

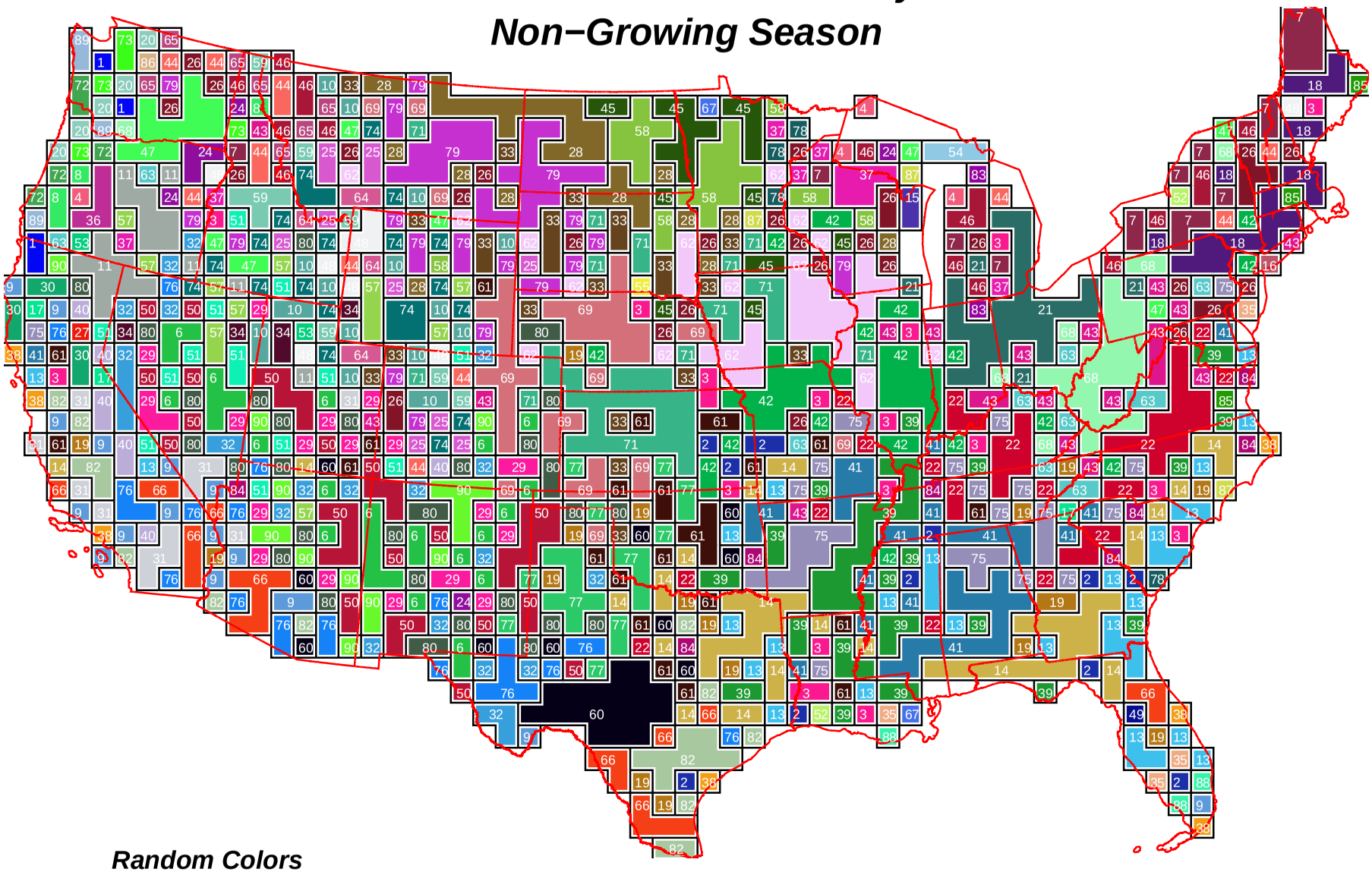

Figure 3.8: Homogeneous Flux Ecoregions IC Schematic

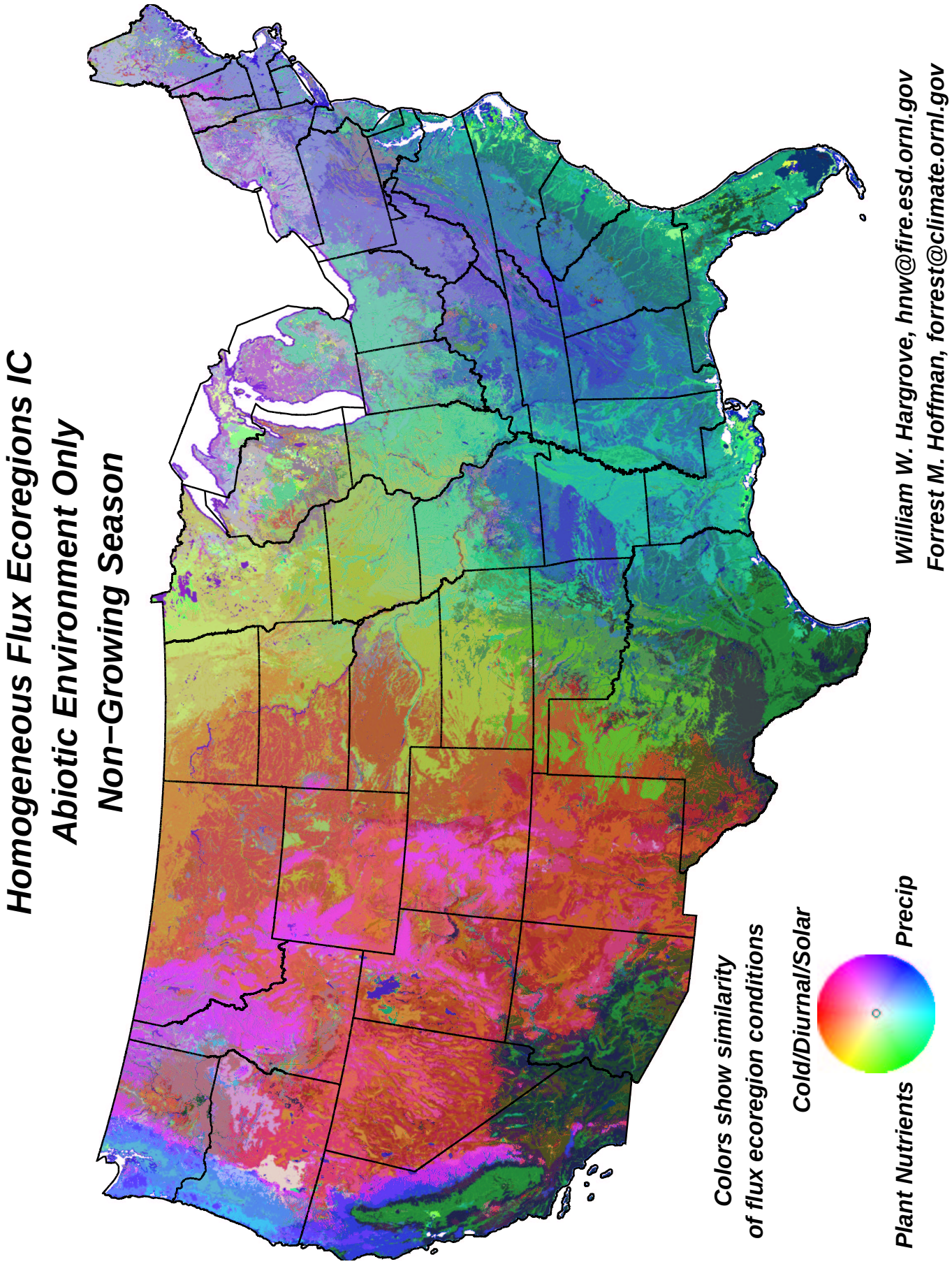

Figure 3.9: Homogeneous Flux Ecoregions IC Similarity Colors

Map Layer	Factor 1	Factor 2	Factor 3
Degree-days cold sum below 42°F from nighttime land surface temperature during the local non-growing season	0.89220 ✓	0.08324	0.17827
Number of days below 32°F during the local non-growing season	0.95417 ✓	-0.01148	0.13806
95^{th} percentile of maximum diurnal surface temperature difference during the local non-growing season	0.64257 ✓	-0.15662	-0.60385
Precipitation sum during the local non-growing season	-0.03168	0.04525	0.91830 ✓
Number of days with measurable precipitation during the local non-growing season	0.41592	0.07427	0.85470 ✓
Depth of mineral soil	-0.18117	0.52057 ✓	-0.07136
Depth to water table	0.33142	-0.45100 ✓	-0.24131
Soil Kjeldahl nitrogen to 50 cm depth	0.16448	0.81555 ✓	0.03377
Soil organic matter to 50 cm depth	0.09031	0.74197 ✓	0.05891
Soil plant-available water holding capacity to 1.5 m	-0.07934	0.63957 ✓	0.07727
Compound Topographic Index (CTI)	-0.17516	0.37571 ✓	-0.33402
Total solar insolation during the local non-growing season, including clouds, aerosols, slope and aspect physiography	0.88959 ✓	-0.21638	0.03882
Factor 1: cold/diurnal/solar **Factor 2: plant nutrients** **Factor 3: precip**			

Table 3.6: Homogeneous Flux Ecoregions IC Rotated Factor Pattern

3.5 Homogeneous Flux Ecoregions IIA

Table 3.7: Average Conditions Within the 90 Homogeneous Flux Ecoregions for IIA

	Rand color	Sim color	Heat sum	Cold sum	Hot days	Cold days	Di-urnal diff grow	Di-urnal diff non-grow	Precip grow	Precip non-grow	Wet days grow	Wet days non-grow	Soil depth	Water table depth	Soil N	Organic matter	Soil avail wa-ter	CTI	Solar grow $\times 10^7$	Solar non-grow $\times 10^7$	EVI grow	EVI non-grow	FPAR grow	FPAR non-grow	LAI grow	LAI non-grow	% tree	% bare
4			29.30	49.35	6.26	206.34	22.70	22.42	13.59	199.05	7.16	89.56	145.8	5.51	15328	422	61.28	5.04	3.62	11.80	15.27	66.47	41.47	166.62	137.92	425.95	29.2	7.4
29			20.49	84.52	0.43	247.60	17.98	17.77	24.36	274.00	11.55	94.63	124.2	5.71	3897	618	19.04	2.64	3.41	14.00	10.05	15.45	21.62	55.09	36.59	83.96	3.5	44.3
18			21.66	78.93	1.38	242.10	17.59	17.80	27.06	271.36	13.48	113.83	123.2	5.69	4446	679	28.70	3.25	3.20	12.40	14.85	38.07	34.66	87.81	95.49	172.85	22.6	14.6
38			19.62	71.24	1.36	243.59	15.26	16.54	25.58	213.15	13.92	99.41	133.1	5.84	4005	625	31.38	3.52	3.15	12.30	15.47	64.37	44.34	170.35	175.77	464.80	55.4	3.0
53			38.11	68.51	3.81	190.41	14.79	17.21	103.16	117.11	37.13	68.24	151.2	0.79	10468	15716	45.89	7.34	5.30	7.50	50.46	53.97	96.81	161.33	532.81	457.18	50.5	0.2
7			29.88	74.75	2.47	221.97	19.65	19.71	37.43	249.98	17.49	104.46	127.7	5.65	5047	758	35.40	3.92	4.13	11.30	22.80	41.52	53.70	164.08	206.63	404.37	25.8	10.9
55			24.50	67.26	2.06	216.49	14.33	15.03	39.35	386.95	17.27	134.39	129.1	5.81	5695	566	31.45	3.02	4.01	9.36	21.31	44.94	55.56	113.02	213.27	262.44	51.1	5.2
31			40.36	61.96	5.58	209.54	20.32	20.81	35.71	154.40	18.37	67.58	124.0	5.90	4945	906	36.33	3.09	5.41	12.20	24.45	43.09	53.52	91.12	138.14	170.79	20.9	13.9
30			56.83	48.14	17.53	185.50	31.13	28.81	12.14	93.69	8.49	61.76	81.3	5.75	4627	687	32.30	5.25	5.05	11.00	10.40	31.72	24.54	76.30	33.76	105.92	3.8	38.6
65			27.25	63.90	1.25	171.19	14.50	14.69	96.70	692.86	31.19	158.48	116.9	5.61	5538	633	28.70	2.49	5.67	8.52	25.56	18.78	60.01	77.75	203.41	178.69	29.6	19.0
72			61.28	64.94	9.38	193.61	29.63	27.54	29.14	94.83	17.90	57.19	119.5	5.88	4666	640	36.42	4.78	5.91	9.99	17.59	24.78	35.48	62.34	55.23	83.57	2.2	37.7
17			53.41	48.80	19.65	147.05	14.10	16.20	142.88	125.46	45.46	64.23	157.4	1.02	23917	10638	75.33	7.56	7.38	6.31	67.78	48.61	124.57	127.68	649.33	374.05	51.8	0.3
87			20.14	60.26	2.00	178.67	12.76	14.12	93.88	153.63	37.67	98.33	0.0	-0.00	0	0	-0.00	12.04	5.14	7.43	18.14	186.36	-0.00	-0.00	-0.00	-0.00	-0.0	0.0
85			80.00	30.31	39.55	98.05	15.05	15.88	208.44	103.36	61.00	52.32	165.2	0.27	36272	19923	89.49	8.02	10.40	4.62	89.88	35.24	150.78	85.53	637.35	230.52	41.7	0.4
78			32.28	55.33	7.21	200.25	14.11	15.27	36.70	217.78	19.35	99.92	137.0	5.86	4440	632	34.32	3.19	4.63	7.55	26.71	58.83	70.62	142.37	295.36	383.94	58.0	2.6
56			34.92	57.00	4.49	188.72	14.22	16.92	77.83	214.63	30.46	100.56	137.6	4.60	5522	955	41.96	4.52	5.10	8.68	48.33	71.47	88.64	196.35	511.14	804.50	50.3	0.7
14			51.12	49.61	14.62	166.68	21.44	20.40	29.19	163.84	17.19	86.68	121.7	5.52	5465	655	68.20	4.45	5.98	9.05	28.13	53.11	63.49	110.35	170.59	217.63	25.1	9.2
83			40.98	47.48	11.89	180.01	17.33	17.35	31.32	169.44	16.85	84.18	126.5	5.75	4539	736	47.87	4.11	5.46	9.15	30.74	70.65	80.88	187.62	361.51	587.23	40.7	2.1
64			39.52	61.11	5.55	190.28	16.45	17.25	64.41	148.03	27.95	73.07	135.6	5.35	4928	910	35.39	4.13	5.54	8.30	37.51	51.52	78.85	109.09	287.42	237.48	51.1	3.6
13			35.58	58.52	3.60	181.76	12.94	17.09	95.01	187.21	36.58	102.61	145.7	4.51	5449	1216	37.85	5.19	5.29	7.62	56.49	65.31	96.44	143.90	569.44	469.42	62.9	0.2
24			82.05	47.22	34.05	176.08	34.65	29.99	20.98	73.77	14.05	50.16	114.0	5.80	3736	520	36.19	5.30	6.76	9.42	15.36	27.59	30.76	63.25	42.19	83.50	1.8	39.9
41			38.36	64.99	4.01	185.12	13.57	17.14	108.21	122.64	38.30	68.27	144.7	3.76	7938	1359	45.84	6.51	5.56	7.31	57.48	52.26	103.16	157.28	613.04	446.42	54.3	0.2
5			55.87	65.76	16.05	180.03	20.47	21.00	89.54	68.57	34.65	42.11	151.2	4.01	9628	1713	48.71	7.41	6.70	6.80	51.13	22.59	80.23	57.57	174.65	75.09	6.2	7.4
49			70.00	51.17	31.61	168.81	26.79	27.90	30.19	64.72	18.71	47.31	146.8	4.82	4562	650	38.86	7.62	7.21	8.68	46.36	47.21	65.03	85.25	125.75	129.58	3.4	11.2
3			66.23	61.78	20.65	180.89	25.27	26.08	57.56	59.76	27.71	39.84	140.3	5.74	4947	775	42.98	5.65	6.67	7.25	32.21	23.96	57.85	57.03	101.04	71.85	2.7	26.7
1			49.04	58.76	12.80	165.77	18.30	19.22	93.46	131.07	36.27	68.00	116.3	3.89	4951	924	35.65	6.55	6.60	7.08	47.93	40.46	0.30	0.31	1.68	1.08	24.8	5.3
77			55.31	32.73	12.32	184.56	21.13	20.15	71.76	95.08	31.46	43.35	121.8	5.96	3948	375	38.39	3.83	6.98	11.10	29.48	53.38	79.82	150.17	234.68	362.46	33.3	7.4
8			38.03	54.38	2.70	179.19	12.51	15.33	119.03	212.69	42.93	84.13	136.1	3.35	6408	937	44.04	4.81	5.69	6.91	67.23	71.71	108.69	166.52	668.40	590.88	70.0	0.0
32			85.79	35.11	22.99	172.10	31.68	30.41	59.32	53.87	29.23	32.95	123.7	5.94	4660	399	42.46	5.43	7.79	10.40	21.98	28.90	45.85	61.86	65.02	80.18	3.4	38.2
71			76.48	51.96	29.96	176.49	26.45	24.70	56.53	62.91	27.97	40.70	93.4	5.95	4501	664	45.94	5.27	7.13	7.43	27.26	27.16	52.99	59.14	83.51	74.79	2.2	30.0
26			40.15	38.99	3.97	107.39	12.98	17.62	133.51	543.86	44.20	134.27	122.8	5.61	8942	1056	51.00	3.31	7.95	6.34	57.69	63.04	125.27	137.90	604.00	432.13	66.9	0.2
39			78.36	33.45	27.36	164.96	25.03	23.44	41.33	70.65	20.55	37.14	64.7	5.99	4036	443	21.52	3.51	7.94	9.92	22.20	34.76	50.79	76.97	78.80	110.98	5.6	34.5
86			88.20	40.35	28.37	132.17	28.82	24.32	25.87	83.20	18.91	58.74	115.5	5.87	4823	598	48.36	4.81	7.78	6.46	25.33	32.85	51.25	64.51	83.64	91.84	4.6	27.7
11			85.73	7.97	45.51	64.44	14.62	12.77	233.94	141.23	61.57	45.06	182.6	0.67	6724	31604	77.33	8.08	10.90	4.72	99.43	43.88	171.39	104.19	839.22	301.25	42.1	0.1
52			37.95	51.07	14.91	155.35	11.92	13.80	99.73	111.93	38.84	65.00	5.7	0.21	93	23	0.69	9.75	7.17	6.51	6.05	2.39	1.72	0.95	3.29	1.31	2.7	1.3
57			100.09	38.39	45.95	156.96	31.77	29.74	30.84	39.22	18.75	29.01	117.4	5.66	2872	270	26.22	6.16	8.48	8.96	14.33	18.11	22.56	31.50	25.10	34.65	0.0	87.9
81			56.55	23.76	24.39	128.91	15.07	14.53	41.50	331.99	11.90	70.20	113.5	5.91	3704	968	47.48	3.74	8.56	9.33	49.80	74.02	121.94	181.76	622.06	724.82	45.8	0.4
28			46.33	40.27	5.03	150.14	12.47	19.05	137.50	186.37	49.00	94.42	138.5	3.67	5044	1034	49.94	5.06	6.56	6.28	77.92	54.07	122.43	136.33	728.39	403.96	65.7	0.1
42			67.80	44.98	22.65	149.89	21.36	20.75	141.78	93.42	43.74	42.98	154.6	4.32	8230	1653	74.10	6.42	8.19	5.95	66.43	22.89	100.02	55.74	241.35	70.56	3.4	2.4
20			58.82	42.09	12.30	144.51	16.15	18.87	134.18	135.35	45.74	67.71	155.2	4.63	6023	1292	49.00	6.16	7.52	5.89	70.82	40.91	108.50	90.08	298.38	151.15	9.2	1.9
73			37.94	37.62	3.43	97.46	12.70	14.07	162.85	542.70	51.15	130.23	117.9	5.26	6481	1046	43.74	2.82	7.40	4.23	51.73	40.54	116.03	89.39	469.41	224.20	67.1	1.1
48			45.09	27.65	5.67	81.54	13.09	15.93	147.36	492.04	48.66	125.25	121.9	5.45	7853	1381	58.33	3.80	8.70	6.06	81.08	82.51	147.37	164.78	828.37	830.44	64.5	0.2
80			87.41	38.19	43.57	156.66	24.93	25.18	87.60	61.94	32.92	31.80	152.2	5.63	4456	448	24.81	5.88	8.50	7.35	40.03	30.23	71.35	56.47	120.96	69.82	2.7	21.8
23			55.95	35.73	11.72	135.37	13.76	17.43	144.53	164.16	49.54	73.83	140.8	4.04	5135	1035	48.58	5.66	7.42	5.81	80.43	49.25	140.00	133.34	854.82	401.43	18.7	0.2
88			61.66	24.69	29.40	109.58	15.26	14.32	61.74	378.07	16.22	76.13	104.1	5.89	3340	817	36.18	3.51	9.09	7.74	51.46	53.20	127.75	126.74	561.92	371.39	44.5	3.3
60			69.04	34.00	22.34	126.65	17.02	19.15	153.65	132.84	47.82	56.87	157.8	1.90	6634	1245	67.59	6.88	8.55	5.41	72.95	34.93	112.75	77.09	281.83	119.11	7.3	1.4
89			52.48	34.76	8.71	143.12	13.12	15.71	148.24	193.63	47.21	66.95	141.9	3.67	6264	1054	37.61	5.25	7.25	5.82	82.33	50.88	137.38	135.06	836.87	397.69	64.4	0.0
27			98.17	33.85	59.14	142.82	25.07	26.55	96.35	49.49	34.65	24.50	156.0	5.87	6657	750	56.26	6.29	9.54	7.11	41.63	31.83	71.69	52.98	111.06	63.77	2.2	22.1
75			42.78	28.97	3.91	78.47	13.49	13.75	299.14	910.61	65.50	140.83	109.9	5.79	6076	985	43.65	2.91	8.31	4.80	61.04	50.82	128.01	105.90	554.98	343.86	65.1	1.9
62			43.82	22.57	2.44	63.15	13.52	14.27	222.55	649.22	61.69	131.13	120.6	5.34	8515	1831	60.62	4.17	8.44	4.66	85.15	73.12	155.88	135.41	846.05	545.25	66.9	0.0
51			83.99	34.55	44.63	130.82	21.02	21.36	118.55	89.58	37.67	39.81	142.8	5.02	5167	732	46.21	13.55	9.04	6.43	54.96	31.70	95.45	68.42	280.12	118.96	12.9	17.1
19			54.32	20.85	9.88	63.43	13.52	15.14	115.68	318.26	45.18	104.29	123.1	5.34	6803	1372	58.46	4.37	9.30	5.19	83.90	71.06	160.59	143.08	892.34	602.35	60.7	0.0
37			82.94	23.33	26.03	109.14	16.72	17.62	168.89	144.35	51.44	54.50	141.8	3.66	4796	944	51.42	6.56	9.06	5.14	69.87	36.02	0.00	0.00	0.00	0.00	15.9	4.7
76			65.34	23.69	8.66	55.12	17.39	17.33	108.99	244.52	51.15	96.03	131.2	3.59	5892	1469	53.10	6.27	9.27	4.20	76.81	56.11	140.38	104.53	612.57	301.65	39.9	0.8
67			51.21	19.59	6.46	53.26	13.15	14.19	166.91	374.22	57.43	105.25	121.4	5.67	9079	1638	65.03	4.04	9.55	4.29	86.25	57.66	168.14	112.86	871.95	378.49	68.1	0.1
9			56.06	17.76	16.49	114.98	11.08	15.29	168.54	189.76	53.56	67.91	117.9	5.57	5001	693	51.38	4.55	8.15	5.96	92.62	49.47	146.53	122.37	895.72	348.63	71.3	0.0
61			72.68	24.19	31.03	106.73	14.86	17.07	178.40	161.44	50.25	52.46	150.1	4.89	4352	661	62.18	5.95	9.14	5.41	88.89	52.24	130.87	99.40	377.99	185.72	12.8	0.4
47			67.65	36.27	33.41	120.68	15.60	16.36	150.41	124.58	44.99	49.75	0.5	0.37	19	7	0.20	7.64	8.90	5.74	57.89	30.37	119.88	79.90	482.64	185.76	28.2	6.7
22			131.58	15.21	66.44	98.50	28.75	26.85	79.49	31.13	31.68	17.76	63.8	5.98	3940	379	26.14	5.04	11.40	7.46	27.88	21.00	53.27	39.46	69.47	48.07	1.2	54.1
44			71.94	20.33	31.43	101.40	14.53	16.58	180.68	174.66	50.40	54.62	151.3	4.93	3963	646	57.80	5.93	9.16	5.58	92.16	61.13	162.81	141.31	1014.80	540.18	19.1	0.1
59			38.32	15.78	0.96	39.37	10.09	14.63	143.11	221.78	65.20	82.56	25.0	1.03	1051	220	7.88	2.00	9.73	3.14	36.13	19.22	66.83	31.06	223.98	72.72	23.8	1.8
15			138.26	16.02	79.48	95.38	28.88	27.43	92.38	27.50	31.89	15.64	172.4	5.94	4252	506	42.59	6.21	11.80	6.87	32.40	20.90	56.35	34.39	71.22	39.54	0.8	47.0

continued on next page

continued from previous page

	Rand color	Sim color	Heat sum	Cold sum	Hot days	Cold days	Diurnal diff grow	Diurnal diff non-grow	Precip grow	Precip non-grow	Wet days grow	Wet days non-grow	Soil depth	Water table depth	Soil N	Organic matter	Soil avail water	CTI	Solar grow $\times 10^7$	Solar non-grow $\times 10^7$	EVI grow	EVI non-grow	FPAR grow	FPAR non-grow	LAI grow	LAI non-grow	% tree	% bare
63			106.25	19.09	73.29	94.51	19.51	19.30	171.79	70.91	41.87	25.37	151.5	5.33	7790	961	65.98	6.12	11.00	5.40	64.01	36.51	113.03	63.97	222.50	91.99	6.6	10.4
58			71.04	11.92	41.27	75.57	8.61	11.94	209.72	146.60	54.94	43.47	27.3	0.75	904	199	8.12	5.00	10.70	4.44	13.92	4.15	11.70	3.80	23.31	5.95	7.4	3.5
82			77.12	17.66	45.40	88.39	13.49	15.79	200.12	160.94	51.85	46.64	157.0	4.53	4204	656	61.57	6.00	10.10	5.08	96.37	42.81	147.31	93.86	490.56	188.06	55.5	0.0
25			92.10	6.49	48.77	47.60	11.15	10.92	276.52	117.01	66.49	34.90	177.9	0.33	7542	12555	33.44	8.20	12.40	3.83	75.29	22.73	147.89	53.95	573.97	129.92	43.0	2.9
21			102.27	3.77	67.72	27.44	10.28	10.59	343.44	107.44	76.13	27.83	176.6	0.14	29168	5418	71.21	8.17	14.00	2.94	86.17	19.35	154.54	45.41	589.40	113.12	42.0	1.5
68			95.56	12.28	65.95	68.14	15.95	14.82	223.13	155.40	52.39	38.34	167.6	2.08	5580	745	57.83	7.44	11.40	4.49	90.07	36.36	143.04	74.31	366.88	132.37	15.2	1.2
36			95.78	12.14	70.45	56.51	14.44	15.15	227.44	130.40	54.92	34.62	136.7	3.75	4273	686	44.74	7.31	12.10	4.15	86.42	28.02	0.05	0.04	0.21	0.10	23.3	2.5
69			157.68	12.05	87.14	53.29	27.61	22.71	27.03	30.18	12.27	12.76	106.6	5.91	2443	168	18.61	4.36	14.20	5.42	23.58	13.69	43.56	22.98	49.86	26.13	0.1	80.3
16			117.19	8.12	62.79	45.96	20.46	15.31	64.27	129.89	20.17	33.17	81.2	5.93	3963	432	32.29	3.98	13.20	4.90	61.14	35.50	150.89	83.63	413.40	205.10	22.7	8.9
70			77.51	11.74	52.45	77.33	12.55	15.00	209.26	181.71	51.84	44.72	156.1	5.37	3466	497	56.58	5.65	10.50	5.08	100.34	42.59	181.50	109.52	1069.40	309.65	63.5	0.0
6			84.47	11.15	58.54	71.30	13.47	14.90	220.04	172.91	53.57	42.51	161.9	4.88	3741	535	52.81	5.98	10.90	4.85	99.10	42.49	188.75	107.60	1091.40	310.61	32.4	0.1
45			120.55	7.46	93.56	60.67	18.11	17.68	169.21	62.13	39.55	20.78	72.2	5.83	5698	908	34.68	5.58	12.60	4.83	70.71	31.54	130.54	59.68	292.99	94.91	14.0	11.3
34			169.27	6.91	85.36	35.41	29.08	19.63	43.21	59.05	18.00	20.14	111.1	5.86	3691	309	38.98	5.24	14.70	4.00	45.15	29.45	93.50	53.01	155.78	117.85	4.1	21.5
35			91.96	6.12	29.80	30.61	14.92	12.36	107.05	144.22	30.70	31.72	91.8	5.74	4479	631	36.98	3.25	14.60	4.05	88.37	33.64	199.55	73.16	777.53	227.39	41.9	3.4
74			135.44	3.35	27.82	17.39	21.99	15.18	76.79	69.74	24.50	16.45	101.1	5.64	4657	547	36.50	4.77	15.90	2.84	69.91	20.65	158.47	45.16	342.78	103.13	15.7	12.1
66			69.25	8.50	11.87	22.27	13.26	12.87	318.94	338.22	67.21	57.62	120.8	5.46	5436	1164	54.73	3.52	12.90	2.91	108.65	40.55	220.64	77.49	1097.60	302.08	64.9	0.1
40			85.48	1.76	60.86	13.71	7.92	7.40	86.09	41.40	29.53	12.13	16.1	0.74	497	60	3.18	4.52	16.40	1.99	13.57	2.81	19.58	3.41	30.65	5.56	3.1	9.9
2			101.45	4.77	76.30	43.71	15.34	14.26	248.35	143.40	62.63	35.55	183.6	3.90	4075	559	38.72	6.63	12.30	4.21	99.72	35.93	165.35	75.68	452.27	154.57	30.9	0.9
10			164.97	0.75	38.51	5.10	22.06	14.13	100.09	31.36	31.92	8.07	114.2	4.58	3283	494	42.53	5.98	17.50	1.27	61.07	7.72	0.58	0.06	0.79	0.11	5.0	23.4
84			147.01	5.83	106.59	23.19	22.72	16.41	42.91	43.48	19.91	18.07	154.3	5.42	4330	395	44.98	8.18	16.00	2.82	87.87	24.00	143.65	41.06	286.40	81.59	5.2	8.3
43			93.72	4.76	77.56	44.28	12.54	12.63	263.26	148.44	61.15	35.21	180.4	2.21	4780	726	53.16	7.20	12.40	4.06	106.33	36.93	210.32	95.31	1158.80	300.99	59.2	0.0
54			179.22	3.85	140.79	32.34	26.47	20.91	82.14	25.18	30.73	12.60	132.5	5.95	3252	323	31.62	5.95	15.00	3.94	43.82	14.66	78.86	26.50	106.77	33.92	2.1	38.9
79			131.05	3.51	110.71	31.45	17.56	17.06	202.06	58.53	46.61	19.63	179.7	5.35	4912	565	48.26	6.44	13.90	3.38	94.12	26.62	156.37	46.93	331.18	74.63	14.5	5.5
46			206.03	3.16	155.76	16.39	27.08	19.76	29.08	9.81	14.33	5.52	125.3	5.84	2210	125	17.01	5.58	17.40	2.55	25.48	5.70	36.80	7.38	40.34	7.99	0.0	93.2
50			114.85	1.65	78.19	20.78	13.73	12.65	335.09	106.48	70.97	25.16	175.6	2.43	5288	1014	47.93	7.95	14.20	2.88	106.03	25.05	187.35	54.23	552.59	126.32	31.6	1.4
90			109.63	0.03	75.22	7.75	6.64	3.86	352.74	56.04	83.40	13.75	23.3	0.21	777	284	5.24	3.64	16.20	1.70	6.90	1.05	4.74	0.74	7.73	1.13	5.1	5.3
12			143.49	0.05	89.22	1.92	13.26	8.74	387.68	18.83	101.75	5.18	94.3	1.33	3414	1173	22.03	8.02	17.80	0.83	100.29	5.48	0.07	0.00	0.11	0.00	18.6	4.6
33			145.33	0.09	104.35	2.04	15.76	12.56	374.64	20.15	98.92	5.82	149.4	1.29	4293	1175	30.55	8.16	17.50	1.12	125.23	8.63	227.60	18.27	648.01	42.40	26.6	1.5

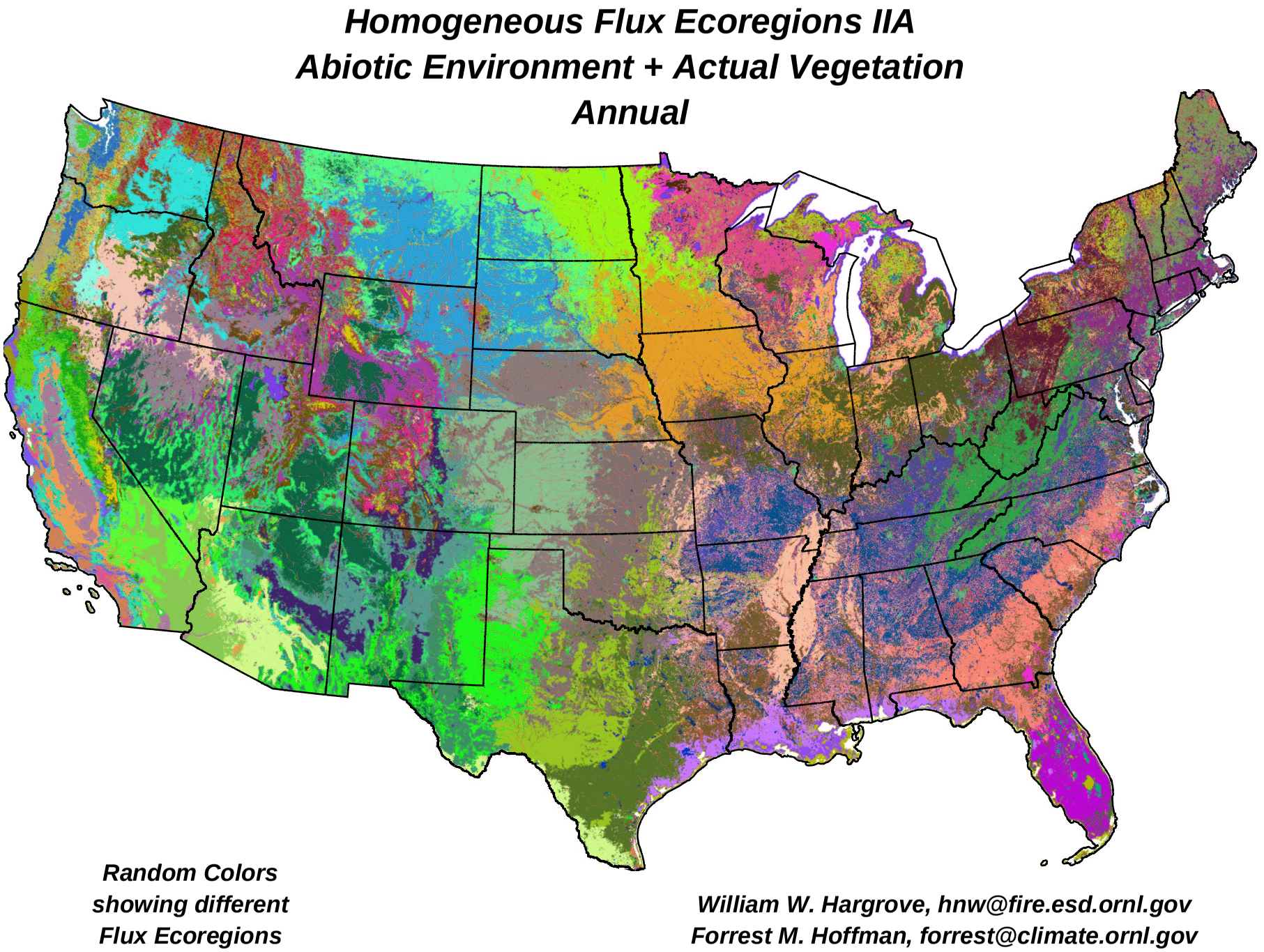

Figure 3.10: Homogeneous Flux Ecoregions IIA Random Colors

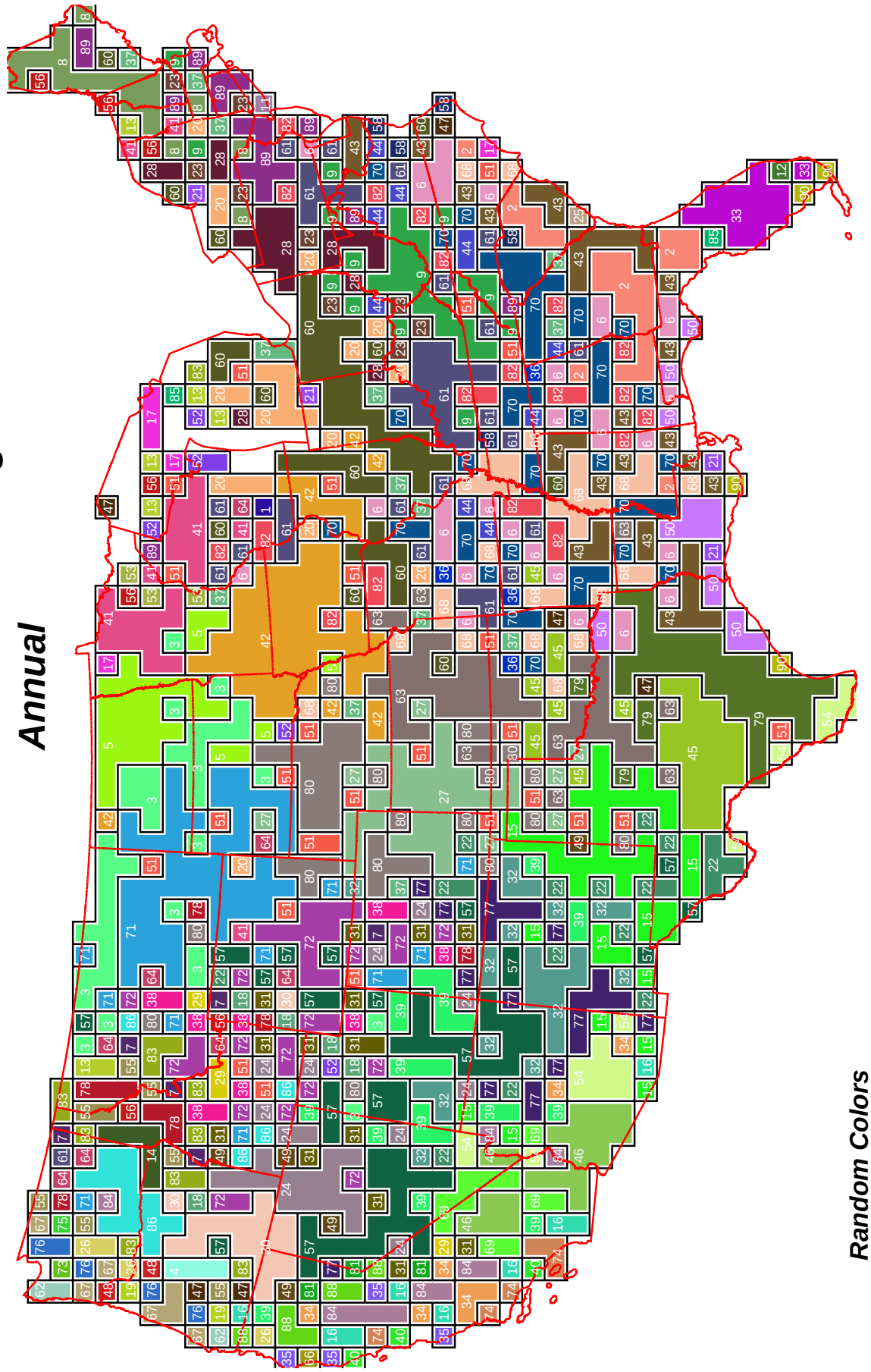

Figure 3.11: Homogeneous Flux Ecoregions IIA Schematic

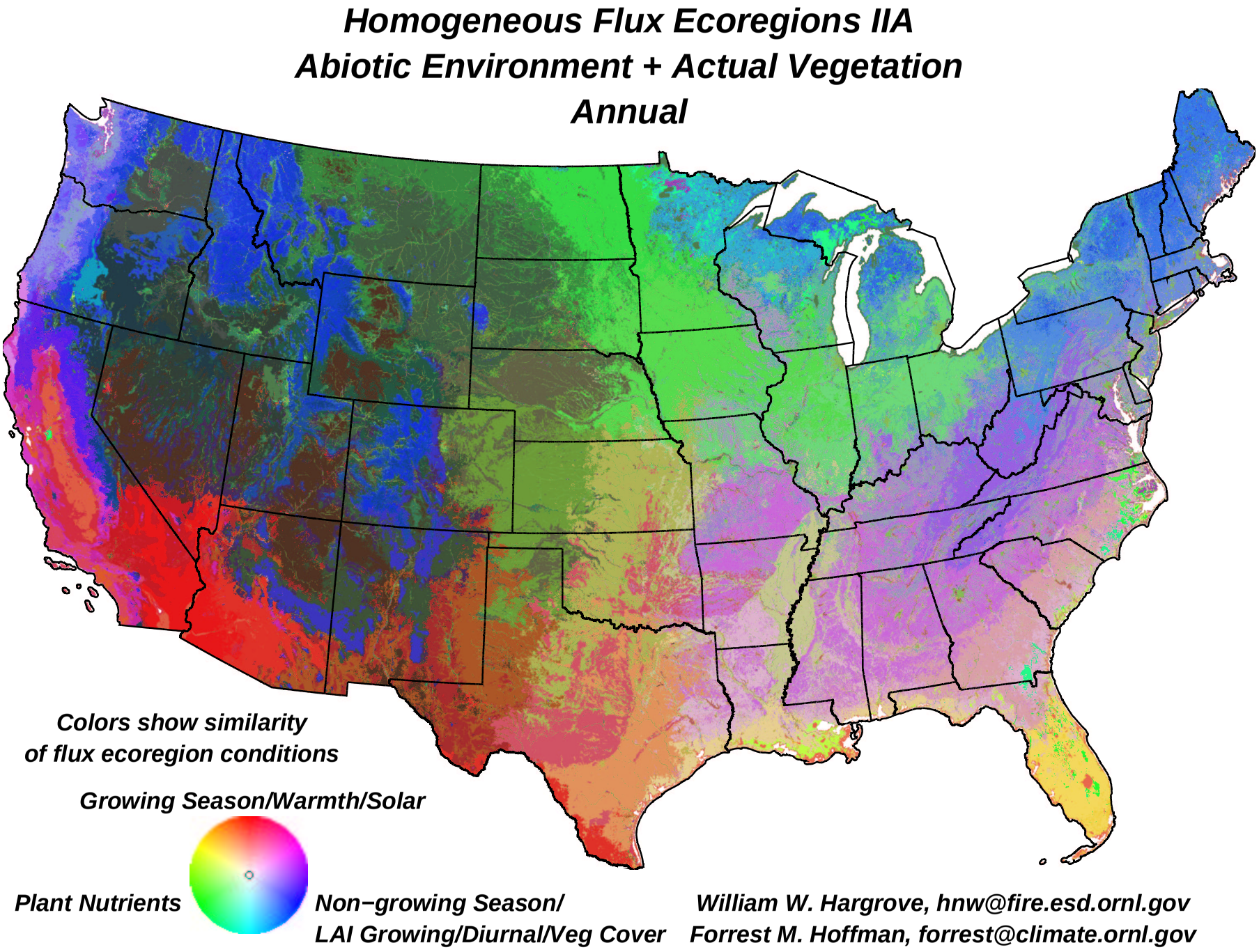

Figure 3.12: Homogeneous Flux Ecoregions IIA Similarity Colors

Map Layer	Factor 1	Factor 2	Factor 3
Degree-days heat sum above 42°F from daytime land surface temperature during the local growing season	-0.55692	0.73383 ✓	-0.18689
Degree-days cold sum below 42°F from nighttime land surface temperature during the local non-growing season	-0.03092	-0.91663 ✓	0.06218
Number of days above 90°F during the local growing season	-0.37486	0.80616 ✓	-0.12331
Number of days below 32°F during the local non-growing season	-0.01171	-0.96202 ✓	-0.05563
95^{th} percentile of maximum diurnal surface temperature difference during the local growing season	-0.76803 ✓	-0.29441	-0.31609
95^{th} percentile of maximum diurnal surface temperature difference during the local non-growing season	-0.65020 ✓	-0.46345	-0.23378
Precipitation sum during the local growing season	0.35836	0.69324 ✓	0.47691
Precipitation sum during the local non-growing season	0.78663 ✓	-0.14404	0.01768
Number of days with measurable precipitation during the local growing season	0.36787	0.59017 ✓	0.52702
Number of days with measurable precipitation during the local non-growing season	0.66596 ✓	-0.59035	0.02701
Depth of mineral soil	0.09982	0.17953	0.44385 ✓
Depth to water table	-0.15639	-0.17472	-0.59233 ✓
Soil Kjeldahl nitrogen to 50 cm depth	-0.00364	-0.20837	0.72554 ✓
Soil organic matter to 50 cm depth	0.00075	-0.14717	0.65600 ✓
Soil plant-available water holding capacity to 1.5 m	0.16511	0.01911	0.58009 ✓
Compound Topographic Index (CTI)	-0.22631	0.16188	0.42994 ✓
Total solar insolation during the local growing season, including clouds, aerosols, slope and aspect physiography	-0.23544	0.94151 ✓	-0.00780
Total solar insolation during the local non-growing season, including clouds, aerosols, slope and aspect physiography	-0.08002	-0.83933 ✓	-0.31347
Enhanced Vegetation Index (EVI) integrated over the local growing season	0.52293	0.63166 ✓	0.43750
Enhanced Vegetation Index (EVI) integrated over the local non-growing season	0.80607 ✓	-0.24806	-0.01325
Fraction of Photosynthetically Active Radiation (FPAR) absorbed by vegetation integrated over the local growing season	0.58254	0.61114 ✓	0.32133
Fraction of Photosynthetically Active Radiation (FPAR) absorbed by vegetation integrated over the local non-growing season	0.84942 ✓	-0.29513	-0.01234
Leaf Area Index (LAI) integrated over the local growing season	0.76104 ✓	0.38490	0.18911
Leaf Area Index (LAI) integrated over the local non-growing season	0.87381 ✓	-0.14189	-0.04594
Percent tree cover	0.82699 ✓	0.10072	0.05003
Percent bare cover	-0.67436 ✓	-0.10572	-0.47159
Factor 1: nongrowing season/LAIgrowing/diurnal/tree cover **Factor 2: growing season/warmth/solar** **Factor 3: plant nutrients**			

Table 3.8: Homogeneous Flux Ecoregions IIA Rotated Factor Pattern

3.6 Homogeneous Flux Ecoregions IIB

Table 3.9: Average Conditions Within the 90 Homogeneous Flux Ecoregions for IIB

	Rand color	Sim color	Heat sum	Hot days	Diurnal diff grow	Precip grow	Wet days grow	Soil depth	Water table depth	Soil N	Organic matter	Soil avail water	CTI	Solar grow $\times 10^7$	EVI grow	FPAR grow	LAI grow	% tree	% bare
53			23.23	2.82	15.33	28.28	14.07	131.5	5.83	4346	676	32.28	3.43	3.48	17.90	47.93	183.16	54.4	3.4
60			34.96	6.98	17.35	51.89	20.21	138.9	4.93	13309	574	54.37	4.77	5.06	32.25	73.62	339.61	46.9	3.5
34			45.34	7.78	14.44	121.94	41.24	156.7	0.78	27968	12959	83.83	7.62	6.35	59.63	108.59	570.59	52.0	0.4
1			41.81	6.03	14.74	109.33	37.95	153.5	0.77	10047	14890	45.98	7.37	5.71	51.09	96.15	509.63	47.9	0.6
90			54.02	11.92	15.14	128.17	44.37	154.8	0.34	35556	19607	62.65	7.65	7.30	68.83	117.43	532.08	40.6	0.4
40			34.87	5.53	19.61	30.14	15.07	123.1	5.85	4842	780	30.58	3.07	4.50	19.04	43.24	111.50	8.6	21.4
61			42.74	8.49	16.80	59.27	27.56	134.7	5.80	4372	666	42.80	3.49	6.23	33.90	85.21	329.04	52.7	2.5
15			41.62	4.38	12.80	123.89	44.19	144.3	2.71	6178	1180	47.83	5.02	6.03	70.26	113.99	687.81	66.6	0.0
64			43.43	5.81	12.86	121.73	41.67	150.2	4.67	6401	1061	33.53	6.10	6.17	67.21	115.42	695.74	61.2	0.0
62			48.06	13.86	12.15	145.20	47.39	0.6	0.54	24	7	0.20	7.05	7.70	27.46	1.55	3.05	55.3	2.9
79			31.31	6.07	10.60	119.03	44.64	0.2	0.08	7	2	0.05	10.18	6.81	4.39	1.42	2.72	0.5	0.9
32			50.38	10.01	15.06	134.15	47.09	139.8	3.92	5916	1091	45.71	5.83	7.27	65.51	2.95	14.50	59.3	0.3
63			47.36	5.04	13.21	175.85	56.95	120.4	5.69	9290	1560	62.80	3.64	9.17	80.41	157.14	805.08	67.2	0.3
5			39.17	2.35	10.07	136.13	66.68	25.4	1.08	1032	210	7.90	1.63	10.10	41.84	85.98	296.03	22.6	1.7
69			55.21	15.93	11.51	166.57	52.42	116.4	5.43	4982	693	52.47	4.50	7.98	90.89	144.85	893.34	70.3	0.0
4			64.21	20.43	31.96	17.51	11.30	81.7	5.93	4300	646	34.91	4.57	5.67	13.39	28.91	41.87	3.6	36.2
7			72.52	24.44	15.47	164.53	49.73	155.5	0.52	35924	12503	55.54	7.79	9.49	71.31	123.23	445.67	28.3	1.2
82			55.92	6.25	15.14	128.98	55.22	127.7	4.26	5969	1363	54.37	5.16	9.11	87.06	163.72	877.17	55.6	0.2
36			59.58	21.20	7.40	180.77	53.34	0.8	0.15	27	7	0.16	2.07	9.64	9.28	2.87	4.53	1.9	2.0
10			57.05	16.05	19.90	101.02	36.85	153.3	3.18	10774	1555	45.98	7.51	6.90	55.21	87.47	222.39	7.6	6.6
28			64.00	27.65	13.76	179.72	53.00	161.9	1.79	15565	7498	66.69	7.17	8.70	80.67	145.96	749.45	50.8	0.2
16			53.59	42.95	12.30	35.20	20.91	14.1	0.24	108	30	0.74	9.65	8.82	3.77	3.27	5.06	0.5	1.8
45			61.09	24.98	14.37	158.15	47.64	1.1	0.55	44	17	0.49	8.12	8.38	67.05	132.96	611.38	52.6	3.1
12			67.62	35.98	23.29	48.71	23.76	0.3	0.05	16	5	0.14	7.32	7.62	21.54	29.43	54.80	3.4	13.7
46			76.31	38.71	16.62	57.15	17.26	97.6	5.92	3685	744	39.31	3.58	10.20	55.07	136.00	551.01	38.2	3.6
39			68.53	28.43	31.38	20.49	13.38	153.2	2.33	5317	806	40.74	7.96	6.29	21.30	35.49	71.49	4.0	34.8
31			76.19	21.24	32.13	38.12	21.29	143.2	5.89	4266	490	33.85	4.94	6.82	19.48	38.72	58.55	3.0	36.6
21			68.02	28.23	19.61	98.14	37.48	143.4	4.73	5852	1011	43.89	6.15	8.19	40.14	0.39	1.06	4.8	8.5
3			79.32	29.43	26.94	54.49	27.07	107.5	5.95	4479	637	59.43	4.77	7.43	26.83	53.49	88.49	3.8	30.1
65			68.59	30.28	23.83	82.52	32.88	151.1	5.36	6632	1139	49.87	6.32	7.67	53.64	80.88	166.46	3.5	8.7
38			68.68	30.16	13.84	176.96	50.41	148.5	5.06	4193	691	60.87	5.64	9.03	90.18	133.81	443.26	54.0	0.0
43			66.33	21.82	15.32	159.78	48.47	151.4	4.93	5072	938	59.67	5.57	8.41	81.45	120.63	338.17	9.1	0.8
24			63.15	31.32	13.35	163.70	48.10	1.6	0.57	59	17	0.63	6.89	8.90	62.19	133.14	537.18	7.2	3.3
41			69.19	22.82	21.03	149.23	44.76	155.3	3.90	8428	1712	79.86	6.14	8.36	67.43	102.15	246.53	3.5	2.1
68			85.43	44.68	14.74	232.27	61.46	182.6	0.69	6006	31688	79.73	8.04	10.90	99.77	170.81	838.73	41.4	0.1
49			68.49	22.13	16.77	149.50	47.79	158.9	1.83	6162	1190	64.34	6.68	8.48	73.85	113.21	286.97	8.3	1.5
56			88.80	33.53	26.38	57.57	26.87	61.6	5.98	4446	491	24.95	4.09	8.41	26.74	57.39	92.99	5.0	30.9
57			68.61	28.95	13.96	174.70	50.66	150.3	4.54	4416	771	53.49	5.78	8.89	89.30	160.11	976.01	19.6	0.2
11			82.95	17.88	17.67	158.58	52.15	134.3	2.35	4636	1091	49.45	6.58	8.63	59.42	0.03	0.10	8.9	7.4
80			79.81	34.37	24.56	75.75	31.53	148.8	5.75	4676	546	29.63	5.34	7.87	35.17	66.36	118.96	3.8	23.4
37			80.27	29.75	29.08	50.41	25.47	121.8	5.88	4580	590	43.38	9.59	7.34	25.17	48.13	75.95	2.9	32.6
48			74.21	4.95	7.81	117.34	36.56	27.2	1.21	798	89	6.18	1.25	16.70	23.51	45.57	74.65	5.1	11.8
9			69.32	25.66	13.49	321.33	68.84	136.5	5.50	5416	906	46.60	4.19	11.00	90.49	174.34	797.51	61.7	0.5
13			79.51	28.95	33.38	22.68	15.24	122.9	5.78	3233	298	31.66	8.51	6.76	11.75	19.16	21.69	0.0	83.9
59			70.24	28.51	17.65	145.40	43.99	154.0	4.23	6824	1202	67.77	10.77	8.54	69.16	109.58	276.17	8.2	3.7
70			71.52	45.98	13.44	187.85	51.05	0.5	0.78	22	5	0.20	7.67	10.10	65.16	0.37	1.15	10.1	1.6
26			87.60	29.76	15.16	111.77	30.55	94.8	5.81	4306	621	37.05	3.27	13.90	85.84	192.51	772.75	42.1	3.8
88			84.34	47.81	22.30	28.46	18.31	119.1	4.57	2025	304	13.59	6.03	8.42	12.67	18.12	22.05	0.3	91.7
55			92.65	39.95	16.22	187.99	52.09	150.7	4.57	4763	791	54.48	6.03	9.96	80.82	0.07	0.24	16.3	3.3
30			74.85	38.40	16.04	154.78	46.39	134.6	4.46	4962	850	45.36	14.40	9.42	60.75	0.51	1.72	14.0	5.1
77			87.29	49.74	19.07	126.99	38.70	70.1	5.68	4347	554	32.93	11.38	9.53	59.09	109.10	413.90	22.7	15.9
81			82.31	60.50	12.82	221.33	53.22	163.1	5.34	3421	487	54.32	5.75	11.00	100.83	189.09	1098.00	56.3	0.0
66			83.63	47.79	20.01	120.15	37.76	158.9	4.99	5026	706	40.37	13.94	9.16	57.46	102.09	328.78	17.9	13.4
72			112.21	53.22	30.19	44.13	22.45	60.4	5.99	3145	299	23.92	4.80	9.61	18.12	31.15	35.39	0.0	80.5
73			70.84	44.50	7.85	279.30	65.68	73.2	1.93	2511	573	19.19	4.33	12.00	3.78	12.37	23.73	2.8	89.3
33			89.99	56.51	9.36	265.58	64.19	167.1	2.32	5304	1427	43.50	6.63	12.70	21.40	12.90	21.53	15.4	5.7
52			85.41	72.89	9.43	242.51	57.30	0.3	0.46	17	2	0.15	8.99	12.50	11.37	1.93	3.00	3.4	1.8
19			110.06	52.08	32.19	41.85	22.23	148.7	5.92	3124	325	30.31	5.13	9.15	17.50	28.78	32.76	0.0	81.6
78			93.55	55.68	8.96	288.58	68.34	7.4	0.51	271	191	1.76	4.91	13.10	47.85	146.89	393.14	24.0	4.2
18			98.91	72.33	12.97	295.37	70.59	179.7	0.29	32467	4790	31.75	8.06	13.20	105.78	200.14	938.17	53.8	0.5
87			89.89	69.74	13.14	254.60	62.06	156.0	3.73	3989	660	48.69	6.98	12.30	106.03	0.02	0.07	54.3	0.1
35			93.88	69.01	15.83	190.12	48.78	150.9	4.61	4881	695	52.52	6.34	11.70	83.01	0.06	0.14	7.1	3.2
44			100.07	59.64	9.68	313.91	72.41	183.3	0.14	8178	15218	22.90	8.68	13.60	77.66	157.11	598.61	46.3	3.2
58			97.76	63.85	5.46	349.54	75.95	3.1	0.07	104	26	0.65	2.04	14.80	1.57	2.72	4.03	3.3	1.7
83			131.12	32.80	22.24	67.21	21.88	94.9	5.76	4560	501	34.39	4.48	15.10	65.50	151.21	332.41	16.2	12.7
23			96.24	63.74	16.18	223.62	50.85	161.4	2.67	6206	844	61.35	6.80	11.20	87.26	141.19	348.40	11.0	1.5
75			108.95	74.30	22.21	138.07	38.53	161.6	5.82	7652	829	63.65	6.14	10.80	51.85	92.83	156.10	4.3	17.1
76			93.46	77.47	12.62	259.81	60.39	179.5	2.08	4674	699	53.98	7.17	12.40	106.74	209.62	1164.30	56.5	0.0
47			106.37	72.29	7.19	386.19	81.89	184.6	0.06	27037	5665	98.79	8.02	15.10	51.12	0.63	1.00	32.1	4.9
6			98.50	78.22	13.96	253.37	59.58	177.7	2.27	4754	750	50.61	7.30	12.40	105.77	172.17	520.81	49.0	0.1
54			118.42	90.57	18.16	169.58	39.79	78.5	5.84	5841	903	38.76	5.41	12.40	70.68	129.49	289.13	13.4	11.1
25			108.85	73.91	9.07	383.72	81.16	172.1	0.07	26502	4047	90.07	8.53	14.90	96.02	206.07	702.04	43.7	0.5
89			105.96	81.51	15.65	227.85	54.02	182.6	4.94	4075	502	43.79	6.28	12.40	97.13	159.57	415.46	22.4	2.2
8			127.19	77.47	11.08	339.18	92.73	150.2	0.64	27953	15129	111.35	7.69	17.20	101.56	0.00	0.00	30.4	1.6
50			137.64	76.71	28.68	95.30	32.33	171.0	5.95	4404	519	40.85	6.09	11.90	33.72	60.01	77.31	1.1	41.7
22			134.73	101.77	14.73	361.22	95.86	177.4	0.00	39508	22684	134.59	8.70	16.70	133.17	233.62	834.17	40.0	0.4
71			159.38	79.12	28.94	41.83	17.97	107.0	5.89	3793	325	38.06	5.06	13.90	42.36	89.84	150.86	5.1	22.1
42			112.78	69.75	13.26	328.48	72.33	179.5	1.80	5448	1340	40.91	8.29	14.00	96.47	189.92	616.33	34.2	1.9
85			167.32	29.65	22.60	95.07	30.16	109.0	4.67	3204	482	44.00	5.95	17.70	60.00	3.18	4.07	4.8	25.3
74			154.97	81.64	26.97	28.02	12.36	96.9	5.96	2473	168	17.30	4.05	14.20	23.89	45.64	52.95	0.2	78.0

continued on next page

continued from previous page

	Rand color	Sim color	Heat sum	Hot days	Di-urnal diff grow	Precip grow	Wet days grow	Soil depth	Water table depth	Soil N	Organic matter	Soil avail wa-ter	CTI	Solar grow $\times 10^7$	EVI grow	FPAR grow	LAI grow	% tree	% bare
29			120.41	83.62	7.92	356.71	96.88	3.8	0.10	168	84	0.90	3.79	18.00	6.16	1.75	2.64	1.9	0.8
84			139.22	97.78	22.77	41.73	19.91	152.5	5.44	4223	407	44.47	8.07	15.20	86.40	140.61	283.56	5.4	7.6
20			130.46	77.24	14.00	336.11	76.39	174.9	2.08	4878	1316	37.51	7.61	15.00	96.93	0.02	0.03	17.1	4.5
14			123.23	163.08	10.15	31.61	16.38	26.7	1.43	680	23	4.24	9.30	17.20	10.16	7.72	9.08	0.4	12.5
2			180.04	138.20	27.40	68.39	27.77	123.9	5.98	2985	279	30.65	5.70	14.80	35.76	65.72	82.50	1.5	43.1
51			154.45	137.10	20.18	170.47	43.03	168.7	5.72	5313	652	44.83	6.63	14.90	90.24	148.81	264.47	8.2	11.1
27			147.28	87.14	13.88	402.87	108.56	46.9	1.12	2244	562	13.14	8.16	18.30	88.97	0.10	0.17	15.9	5.5
17			139.76	105.02	16.78	352.17	92.42	181.8	1.93	3831	853	30.97	7.74	16.50	125.64	214.22	562.17	25.6	1.3
86			146.53	96.55	13.89	401.65	108.22	60.7	0.57	4245	993	21.17	8.90	18.50	107.93	232.44	694.10	29.1	2.1
67			198.74	149.45	27.26	31.35	15.03	131.2	5.84	2315	179	19.32	5.66	16.80	25.02	35.69	38.92	0.0	92.7

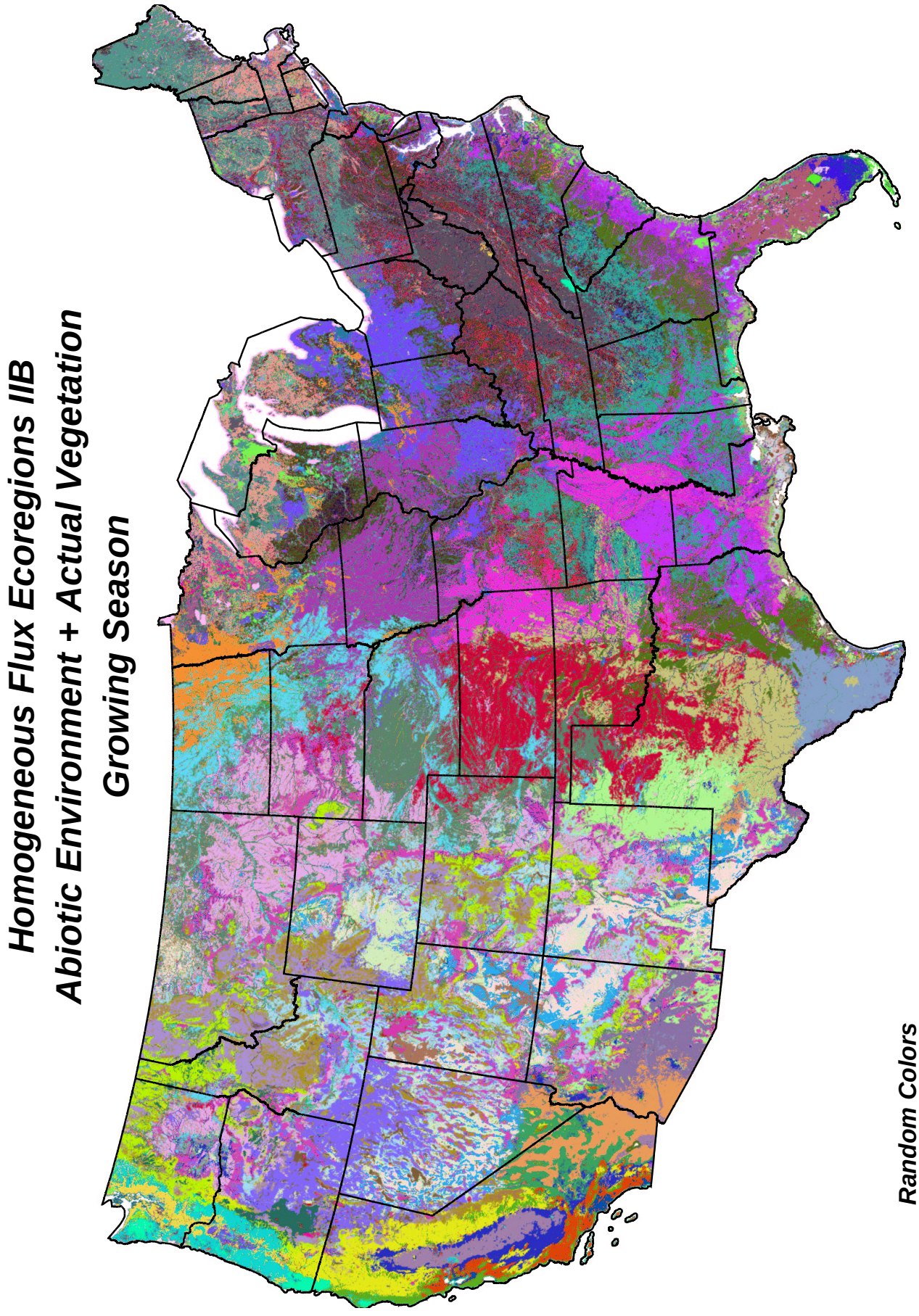

Figure 3.13: Homogeneous Flux Ecoregions IIB Random Colors

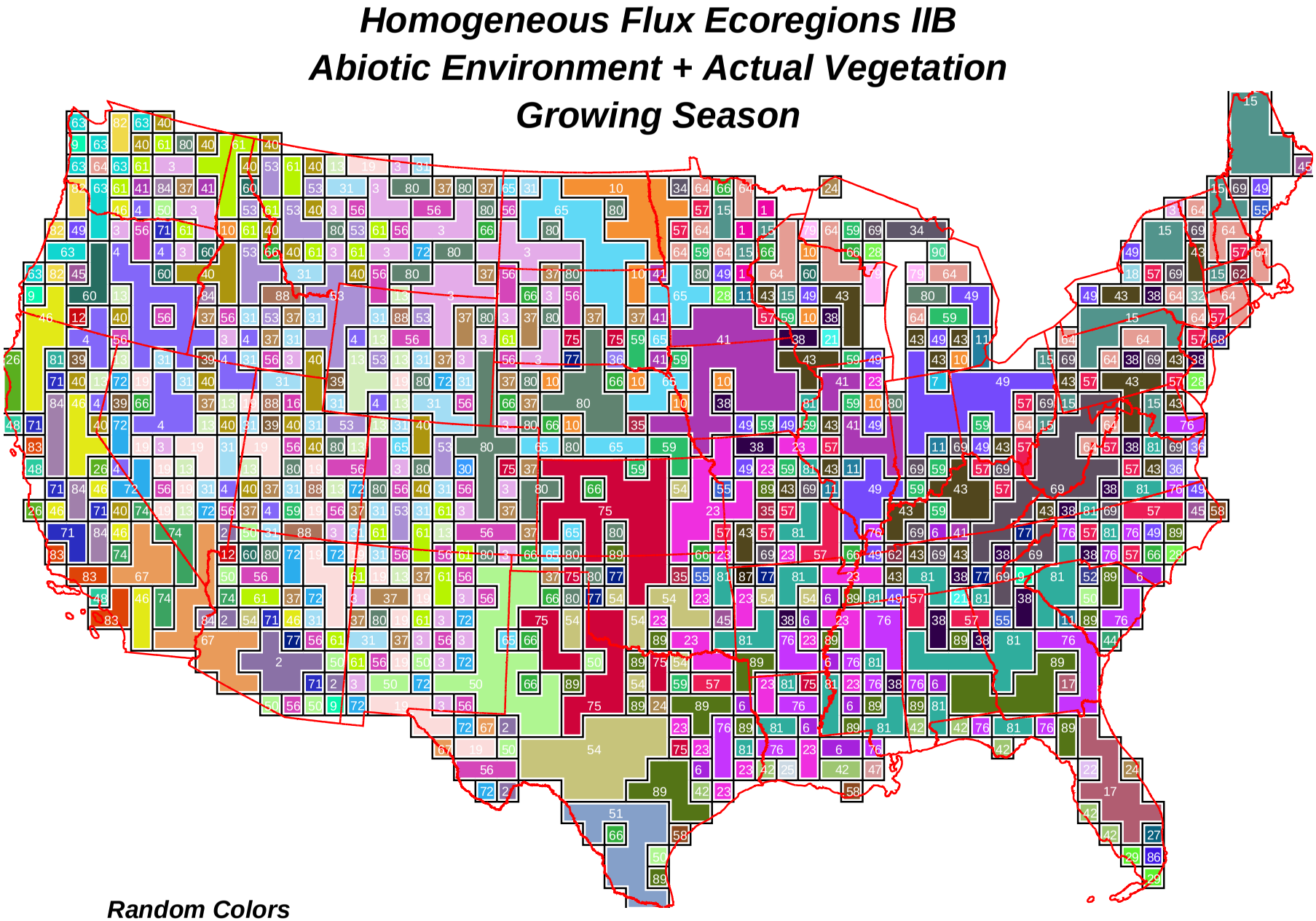

Figure 3.14: Homogeneous Flux Ecoregions IIB Schematic

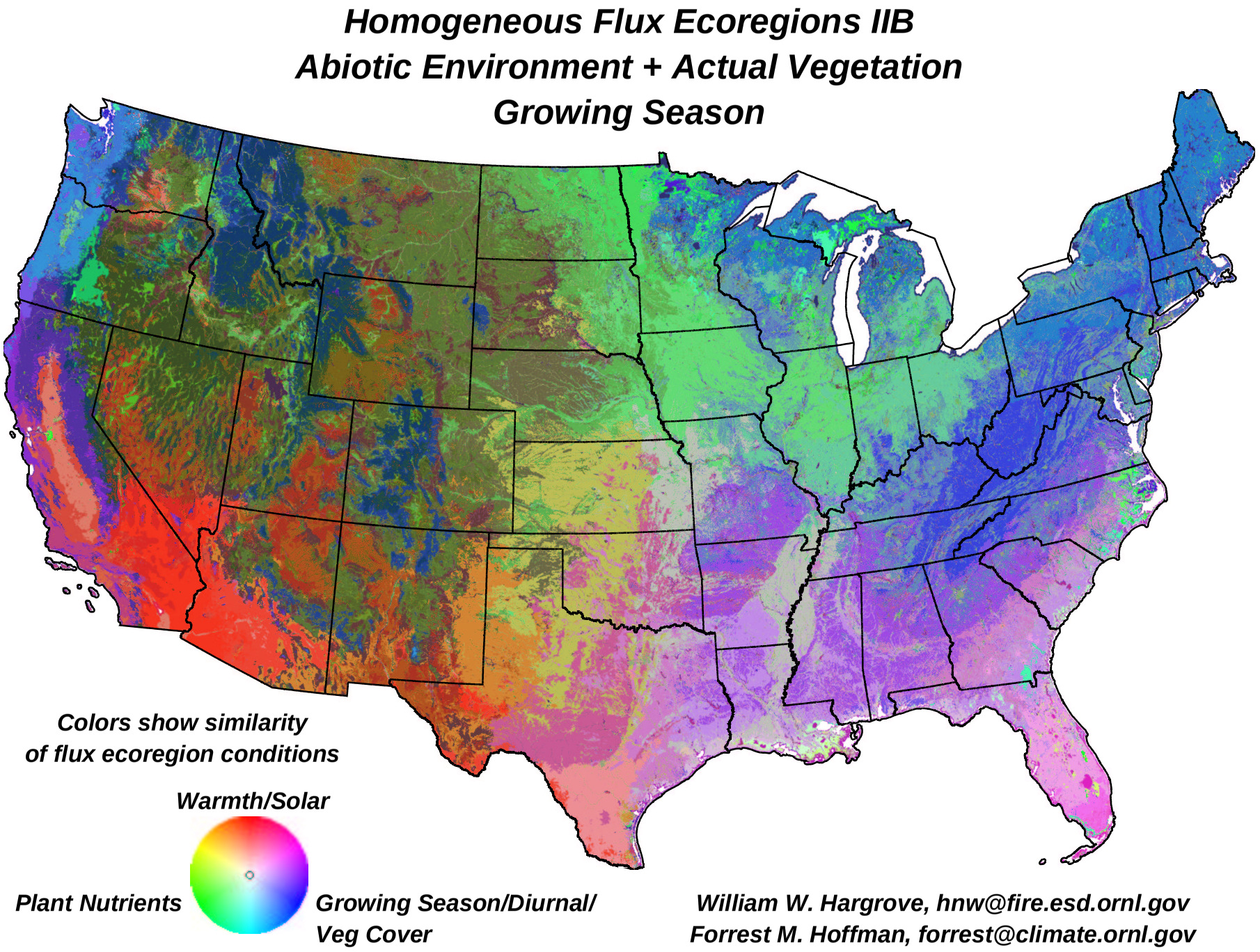

Figure 3.15: Homogeneous Flux Ecoregions IIB Similarity Colors

Map Layer	Factor 1	Factor 2	Factor 3
Degree-days heat sum above 42°F from daytime land surface temperature during the local growing season	-0.18828	0.94992 ✓	-0.06827
Number of days above 90°F during the local growing season	0.01930	0.93427 ✓	-0.05754
95th percentile of maximum diurnal surface temperature difference during the local growing season	-0.86388 ✓	0.18303	-0.07387
Precipitation sum during the local growing season	0.80697 ✓	0.37438	0.24734
Number of days with measurable precipitation during the local growing season	0.78991 ✓	0.26853	0.27913
Depth of mineral soil	0.25938	0.18908	0.46229 ✓
Depth to water table	-0.40511	-0.00668	-0.40566 ✓
Soil Kjeldahl nitrogen to 50 cm depth	0.00548	-0.18132	0.81624 ✓
Soil organic matter to 50 cm depth	0.01884	-0.14030	0.73784 ✓
Soil plant-available water holding capacity to 1.5 m	0.25439	-0.05067	0.59987 ✓
Compound Topographic Index (CTI)	0.01403	0.28812	0.40366 ✓
Total solar insolation during the local growing season, including clouds, aerosols, slope and aspect physiography	0.24101	0.92683 ✓	-0.01829
Enhanced Vegetation Index (EVI) integrated over the local growing season	0.87213 ✓	0.27069	0.24175
Fraction of Photosynthetically Active Radiation (FPAR) absorbed by vegetation integrated over the local growing season	0.86942 ✓	0.24067	0.15045
Leaf Area Index (LAI) integrated over the local growing season	0.87068 ✓	-0.04023	0.01597
Percent tree cover	0.73041 ✓	-0.32160	-0.09123
Percent bare cover	-0.74734 ✓	0.29143	-0.25908
Factor 1: growing season/diurnal/veg cover **Factor 2: warmth/solar** **Factor 3: plant nutrients**			

Table 3.10: Homogeneous Flux Ecoregions IIB Rotated Factor Pattern

3.7 Homogeneous Flux Ecoregions IIC

Table 3.11: Average Conditions Within the 90 Homogeneous Flux Ecoregions for IIC

	Rand color	Sim color	Cold sum	Cold days	Diurnal diff non-grow	Precip non-grow	Wet days non-grow	Soil depth	Water table depth	Soil N	Organic matter	Soil avail water	CTI	Solar non-grow $\times 10^7$	EVI non-grow	FPAR non-grow	LAI non-grow	% tree	% bare
4			0.47	10.33	4.82	47.90	12.87	8.9	0.21	560	124	3.25	3.50	1.60	2.60	5.22	11.06	6.2	3.3
43			1.92	21.78	13.08	86.71	22.36	181.6	1.30	4974	948	35.94	7.62	2.86	25.69	60.06	179.78	42.6	0.8
58			6.35	49.91	12.60	153.34	36.65	173.4	1.97	4879	775	67.55	7.65	4.07	34.25	87.55	235.54	58.3	0.1
62			3.41	24.01	18.23	39.98	15.63	171.7	5.63	4705	537	44.76	6.59	3.12	20.61	35.61	57.45	8.0	14.7
88			8.39	59.87	14.41	168.86	39.15	179.7	5.09	3559	518	47.06	5.82	4.56	38.23	95.13	249.23	61.8	0.0
2			5.04	25.27	19.55	15.05	7.63	120.6	5.92	2237	146	17.80	5.09	3.20	7.44	11.42	12.64	0.1	90.7
5			5.59	33.18	16.51	65.00	19.56	69.0	5.87	3611	405	29.53	4.05	3.84	23.29	48.95	103.76	11.7	20.6
16			0.32	12.58	8.83	94.54	21.34	175.8	0.07	26641	4524	93.47	8.36	2.35	13.26	29.02	62.49	40.3	1.9
83			8.51	61.57	14.26	185.40	41.35	177.8	4.76	3494	541	51.88	5.75	4.71	42.42	107.34	320.14	41.2	0.1
90			7.01	53.66	15.64	117.78	31.46	181.2	4.68	4161	526	39.94	6.16	4.47	35.04	68.28	121.09	17.5	4.9
12			19.68	90.71	14.86	171.29	55.54	1.8	0.22	50	14	0.46	3.19	4.65	6.97	9.89	18.30	5.8	2.4
31			30.70	99.99	15.64	113.31	44.31	0.6	0.39	32	11	0.31	8.25	4.94	28.02	74.72	175.27	31.3	4.9
53			1.94	33.62	9.61	105.42	31.64	191.0	0.09	8968	17321	16.41	8.18	3.72	18.85	45.61	108.43	43.6	4.3
55			12.39	79.45	15.10	187.41	45.48	97.2	5.68	4087	532	47.77	4.95	5.16	42.23	104.33	271.91	54.7	0.2
63			13.07	85.98	15.07	169.59	49.55	157.1	5.45	3117	462	72.23	5.80	5.37	46.76	117.74	344.28	60.3	0.3
35			13.08	67.09	12.38	122.49	39.42	167.1	0.69	6933	9619	45.39	8.08	4.30	27.81	64.98	159.46	40.6	2.0
52			6.67	58.77	18.29	55.81	20.34	61.5	5.96	6052	900	26.15	5.34	5.28	32.12	60.96	100.12	11.2	16.0
10			19.14	86.61	16.08	143.59	41.33	164.2	2.13	5775	838	63.35	6.94	4.82	37.69	78.33	137.52	10.3	1.2
46			40.30	124.29	16.00	134.83	55.66	3.5	0.56	83	21	0.88	7.68	5.82	24.50	1.70	6.19	21.0	2.8
54			21.21	59.31	14.53	320.06	101.17	118.8	5.47	8306	1403	61.06	4.10	4.51	55.13	109.20	342.73	66.2	0.2
79			19.42	100.49	15.95	175.74	53.41	144.7	5.00	4084	645	55.98	5.78	5.57	54.18	132.20	434.96	21.1	0.3
29			24.63	63.68	15.72	456.47	109.97	123.2	5.30	7100	1474	58.13	3.93	4.62	62.02	119.61	421.08	68.1	0.1
22			28.93	103.39	17.63	105.85	41.25	149.4	4.29	5184	903	46.47	6.05	5.42	19.57	1.59	6.37	9.5	8.5
49			45.61	143.57	12.70	115.21	62.97	1.4	0.17	14	4	0.12	10.14	6.24	1.08	1.24	1.87	1.7	1.0
7			24.42	63.12	17.05	279.34	102.58	125.7	4.73	6270	1362	57.40	5.15	4.86	64.51	135.92	513.85	52.4	0.2
57			22.85	104.30	16.88	161.60	51.74	150.1	5.01	4204	669	67.56	6.08	5.40	51.30	97.97	181.49	13.2	0.9
21			31.31	111.67	17.63	123.96	48.74	134.9	4.50	4674	789	43.76	12.91	5.65	29.03	0.84	2.99	14.5	6.8
36			18.76	121.13	15.67	187.87	73.11	116.5	5.55	5192	711	50.06	4.54	6.05	49.23	121.64	342.83	71.9	0.0
70			26.17	112.08	17.98	146.13	56.59	147.8	3.77	4984	953	53.50	6.00	5.38	40.44	0.26	0.95	11.9	3.8
69			24.00	68.34	14.94	668.35	130.01	119.1	5.46	8036	1628	57.87	3.87	5.11	75.79	142.70	616.90	65.8	0.1
76			38.16	120.43	16.67	163.50	61.52	142.7	4.26	5055	880	46.55	5.96	5.81	44.68	1.06	3.28	54.0	0.6
47			29.43	114.69	19.57	97.63	39.15	144.3	4.95	5224	743	47.54	13.29	5.81	32.80	71.53	132.84	15.0	12.6
72			24.14	72.68	15.26	426.82	115.38	124.6	5.49	7869	1442	60.77	4.00	5.69	79.18	154.92	764.45	64.4	0.1
73			24.10	109.52	14.25	383.34	76.40	101.6	5.91	3436	803	35.11	3.42	7.75	52.15	126.50	364.22	44.3	3.5
34			10.37	55.42	13.79	130.50	39.89	177.5	0.27	33728	7108	31.35	7.83	4.02	30.55	74.02	200.48	44.7	0.8
32			36.30	95.87	15.68	630.00	136.88	119.2	5.42	7004	1102	45.43	3.01	5.12	48.02	105.12	281.56	67.4	0.5
86			37.38	138.22	17.44	141.75	58.87	141.8	4.35	5427	913	56.75	5.29	5.98	46.51	98.53	190.05	57.1	0.4
48			35.14	147.22	15.92	197.53	68.80	136.5	4.01	6344	949	35.63	4.82	5.96	52.74	138.85	413.79	65.2	0.1
3			28.76	118.23	20.55	96.36	39.06	152.0	5.24	5324	669	42.98	6.30	6.29	55.33	87.14	145.41	8.6	6.7
13			27.71	121.72	16.80	183.52	65.72	143.3	5.11	4296	714	54.25	5.30	6.68	72.18	161.72	671.52	22.2	0.2
27			25.85	116.10	21.25	65.58	26.17	147.2	5.62	7901	957	66.68	6.11	6.04	35.04	61.54	82.49	5.2	13.7
11			39.46	104.71	13.71	940.71	151.69	111.8	5.73	5799	869	38.55	2.72	5.67	39.91	93.55	281.32	55.0	9.2
71			22.25	120.02	14.21	340.08	69.11	111.7	5.92	3725	975	46.82	3.69	8.99	72.07	175.48	702.24	46.1	0.4
8			36.31	132.93	19.80	137.34	64.20	154.8	1.67	6754	1360	60.40	7.24	5.47	32.66	75.44	116.30	6.0	2.0
33			0.24	5.71	12.23	40.61	11.25	171.7	0.00	38604	20400	166.78	8.57	1.89	14.87	32.31	90.90	43.1	0.5
85			30.72	102.95	14.50	109.19	47.58	159.4	1.45	17245	7968	71.92	7.45	4.85	39.25	100.38	297.56	47.4	0.4
56			35.36	133.53	25.84	39.08	30.31	137.3	1.33	1068	217	7.92	8.81	7.48	9.72	5.71	6.30	0.2	96.7
65			40.48	149.55	18.98	184.77	94.60	140.3	3.28	5083	1086	53.57	4.92	6.24	55.38	138.76	423.81	66.6	0.0
51			43.16	145.52	20.76	95.90	42.84	154.8	4.10	8164	1614	77.63	6.39	5.86	23.32	56.35	72.37	3.6	2.2
89			41.03	148.73	19.52	123.88	61.52	148.6	5.12	5772	1102	45.62	5.44	6.25	37.80	85.40	140.91	7.0	8.4
68			42.33	138.21	20.50	158.20	83.48	146.2	3.18	5517	1223	52.29	6.30	6.59	57.71	104.46	194.70	15.7	3.9
9			23.50	133.96	26.90	43.71	25.45	55.1	5.98	3874	333	21.70	4.31	8.59	24.39	48.92	60.05	1.3	48.7
15			34.89	147.79	26.85	52.38	27.73	157.0	5.77	4663	485	29.80	5.89	7.41	28.61	51.04	61.11	2.0	25.2
6			8.24	65.51	12.84	142.07	45.53	182.6	0.69	6006	31688	79.73	8.04	4.74	44.46	105.25	304.89	41.4	0.1
14			44.35	154.89	18.04	170.56	87.79	141.8	4.05	5022	1098	45.06	5.24	6.54	54.54	153.03	482.05	23.9	0.7
41			54.54	178.94	15.42	208.78	82.46	137.7	3.29	6447	927	43.59	4.85	6.90	72.22	167.04	595.83	69.1	0.0
77			28.35	128.99	30.16	32.71	23.18	152.2	5.89	3046	321	28.52	5.87	8.26	18.51	30.99	34.12	0.0	82.9
74			60.26	178.67	14.12	153.63	98.33	0.0	0.00	0	0	-0.00	12.04	7.43	186.36	-0.00	-0.00	-0.0	0.0
23			27.47	136.58	29.31	41.14	25.67	151.0	5.92	4879	478	55.33	5.32	8.50	23.80	44.60	52.74	1.1	40.3
82			56.05	167.25	18.50	161.69	93.16	155.4	5.31	4138	847	28.50	5.88	6.93	51.11	126.65	336.17	53.4	1.3
42			43.27	135.22	24.02	102.06	67.87	121.5	5.78	5004	615	62.42	4.87	6.90	37.65	74.52	119.42	8.2	21.9
39			38.88	133.25	14.58	472.16	128.64	121.1	5.92	14046	991	51.81	3.17	7.19	61.68	142.52	430.66	63.8	0.7
1			36.37	146.61	28.31	38.14	27.02	77.1	5.98	3031	298	29.02	5.90	8.37	17.95	32.85	36.26	0.0	85.6
40			54.64	204.66	14.82	189.51	90.41	137.8	5.84	4244	617	32.05	3.04	7.94	57.76	139.50	361.25	54.6	4.1
26			65.10	185.27	17.10	124.41	68.33	143.1	3.75	7705	1304	45.52	6.42	7.31	52.64	157.91	449.11	55.4	0.2
19			56.16	183.54	16.06	195.95	100.93	138.7	4.62	5642	1182	42.59	4.62	7.94	71.69	159.56	547.47	64.8	0.1
80			30.33	175.03	23.53	75.28	38.35	96.8	5.97	4244	416	30.30	3.94	10.70	42.00	104.18	175.56	14.1	22.0
81			52.09	175.46	24.96	63.31	40.77	89.3	5.96	4398	653	45.51	5.20	7.40	26.71	58.54	74.17	2.2	30.5
75			61.88	196.17	14.33	384.04	130.82	130.4	5.78	5374	591	32.24	2.89	7.46	46.07	110.38	258.64	60.8	2.6
60			61.18	179.65	24.62	61.36	39.25	145.3	5.57	5569	972	45.07	5.91	7.04	24.09	58.72	75.03	3.4	20.5
66			66.55	180.50	20.92	69.04	42.90	151.2	3.78	10206	1689	47.22	7.64	6.78	22.14	56.70	74.36	6.5	7.5
67			42.26	163.46	31.28	51.95	36.28	139.7	5.62	4064	447	35.65	10.22	9.40	26.23	52.68	65.73	1.3	42.6
44			41.44	200.07	18.17	131.62	58.48	127.4	5.94	3984	486	40.76	3.66	11.70	64.20	182.56	531.64	40.5	2.7
61			60.69	186.57	17.70	206.96	98.78	140.3	4.42	5650	1021	41.09	4.70	8.38	59.08	191.40	776.03	38.2	1.2
50			40.07	170.78	20.01	172.71	76.35	155.1	4.02	14991	548	57.04	6.15	9.91	58.55	147.13	374.46	34.4	5.6
28			46.75	174.14	28.11	91.17	57.50	73.0	5.93	4424	645	31.02	4.58	9.93	29.97	72.51	100.94	3.6	35.8
20			71.00	193.10	14.99	520.78	145.54	117.1	5.70	4992	552	26.91	2.62	9.27	17.69	77.75	168.57	21.2	18.9
17			50.46	188.27	23.34	112.50	53.26	105.6	5.90	4977	822	36.17	3.15	11.40	37.89	82.37	130.70	10.3	23.3
37			68.64	221.92	17.15	171.34	75.71	132.8	5.85	4045	697	30.77	3.35	10.80	55.36	126.58	291.88	49.6	5.5
45			65.63	189.71	28.41	88.80	56.09	130.9	5.77	4540	640	39.32	4.92	9.62	26.30	64.14	87.54	2.9	34.8

continued on next page

continued from previous page

	Rand color	Sim color	Cold sum	Cold days	Diurnal diff non-grow	Precip non-grow	Wet days non-grow	Soil depth	Water table depth	Soil N	Organic matter	Soil avail water	CTI	Solar non-grow $\times 10^7$	EVI non-grow	FPAR non-grow	LAI non-grow	% tree	% bare
64			67.38	188.54	16.89	116.17	66.46	150.9	0.79	10482	15734	46.46	7.23	7.35	51.81	145.17	386.62	55.6	0.2
38			63.62	218.06	18.40	181.70	97.00	127.7	5.86	4796	666	42.08	3.84	11.70	57.60	127.51	290.81	37.4	7.2
25			31.14	103.47	17.46	95.41	49.64	164.1	0.28	38215	23231	51.79	8.31	4.38	28.44	69.14	136.17	27.8	0.6
84			72.05	230.79	16.64	302.27	117.64	127.5	5.82	5059	651	29.60	3.05	11.30	38.22	96.69	201.46	30.9	13.2
24			73.19	219.85	20.06	219.01	97.26	126.9	5.76	5089	764	38.50	4.09	11.40	43.70	157.23	378.16	24.6	11.3
59			70.63	193.20	17.63	117.65	70.69	151.5	0.77	10508	15777	45.23	7.50	7.69	56.59	181.90	550.53	43.5	0.2
87			62.97	171.80	17.34	93.34	55.46	148.8	0.64	30090	11686	73.46	8.21	6.77	42.99	115.83	286.90	40.1	0.9
30			52.86	157.51	16.45	144.90	81.32	157.4	0.74	29998	15381	83.60	7.26	6.58	52.68	135.40	410.03	55.6	0.1
78			77.08	235.83	18.79	227.82	89.78	127.8	5.78	4564	833	31.04	2.90	13.50	37.42	85.99	166.44	18.4	16.8
18			84.70	248.31	17.05	288.30	94.27	127.6	5.71	3418	536	15.69	2.66	13.80	9.97	47.58	67.37	2.2	54.3

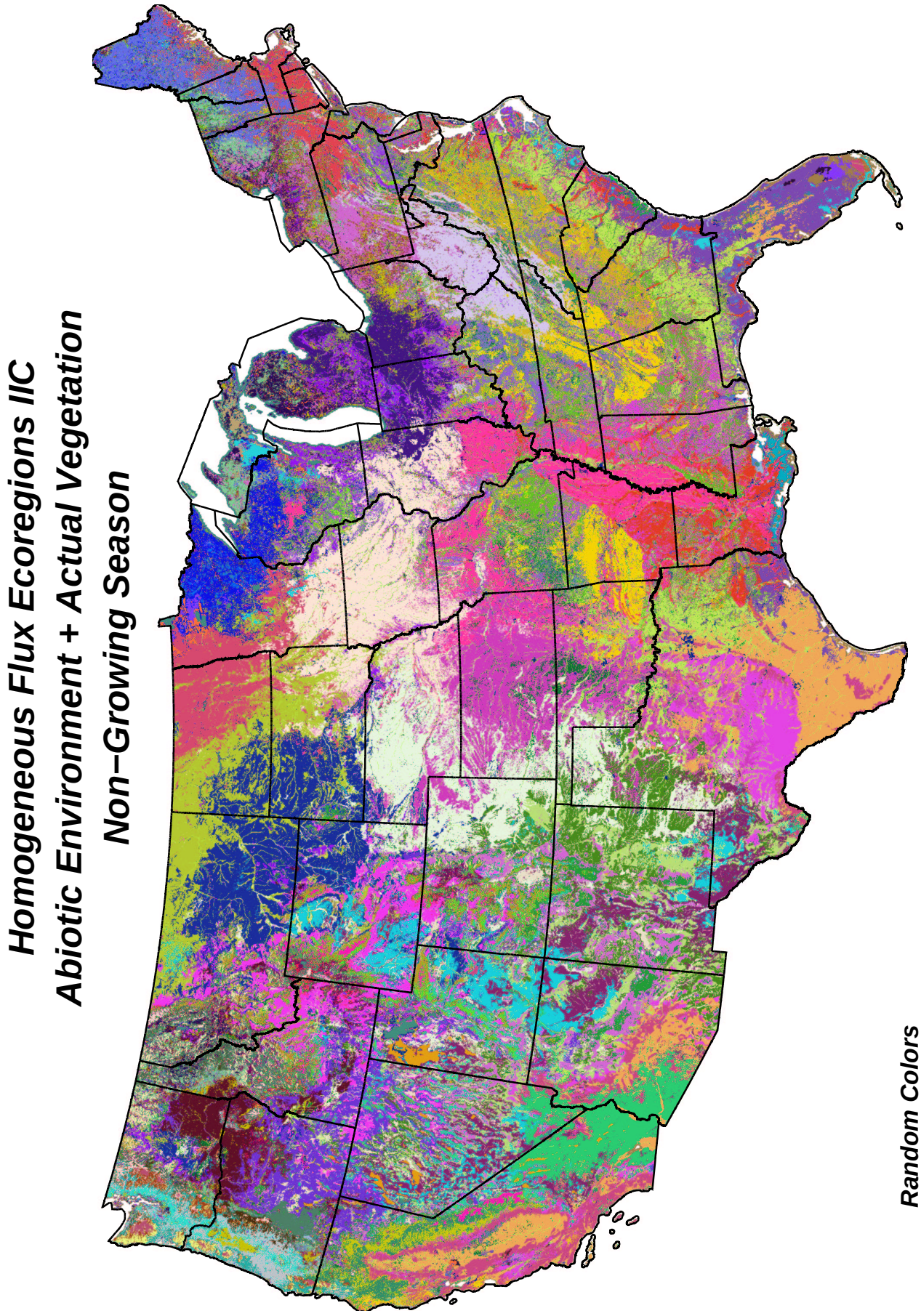

Figure 3.16: Homogeneous Flux Ecoregions IIC Random Colors

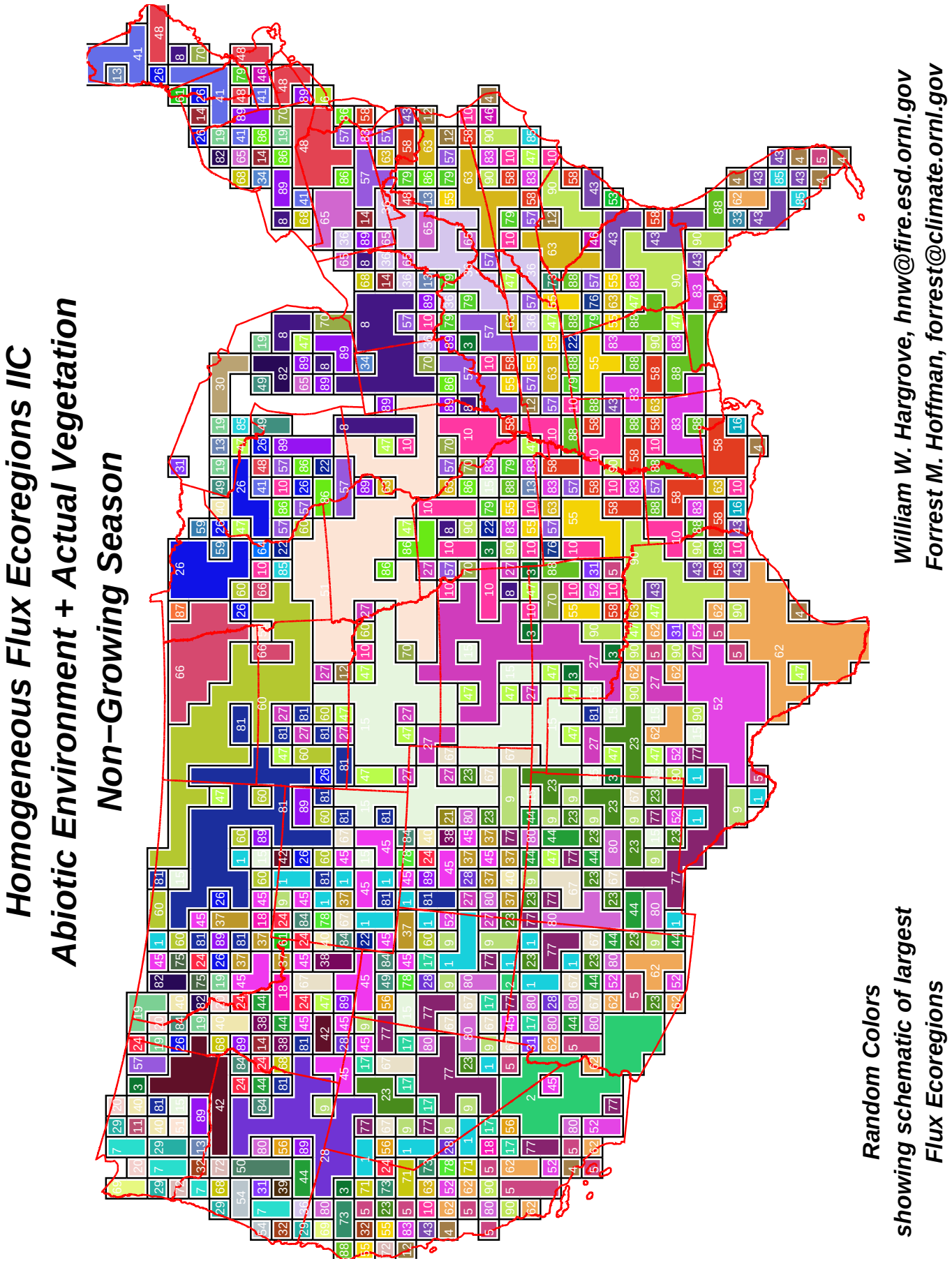

Figure 3.17: Homogeneous Flux Ecoregions IIC Schematic

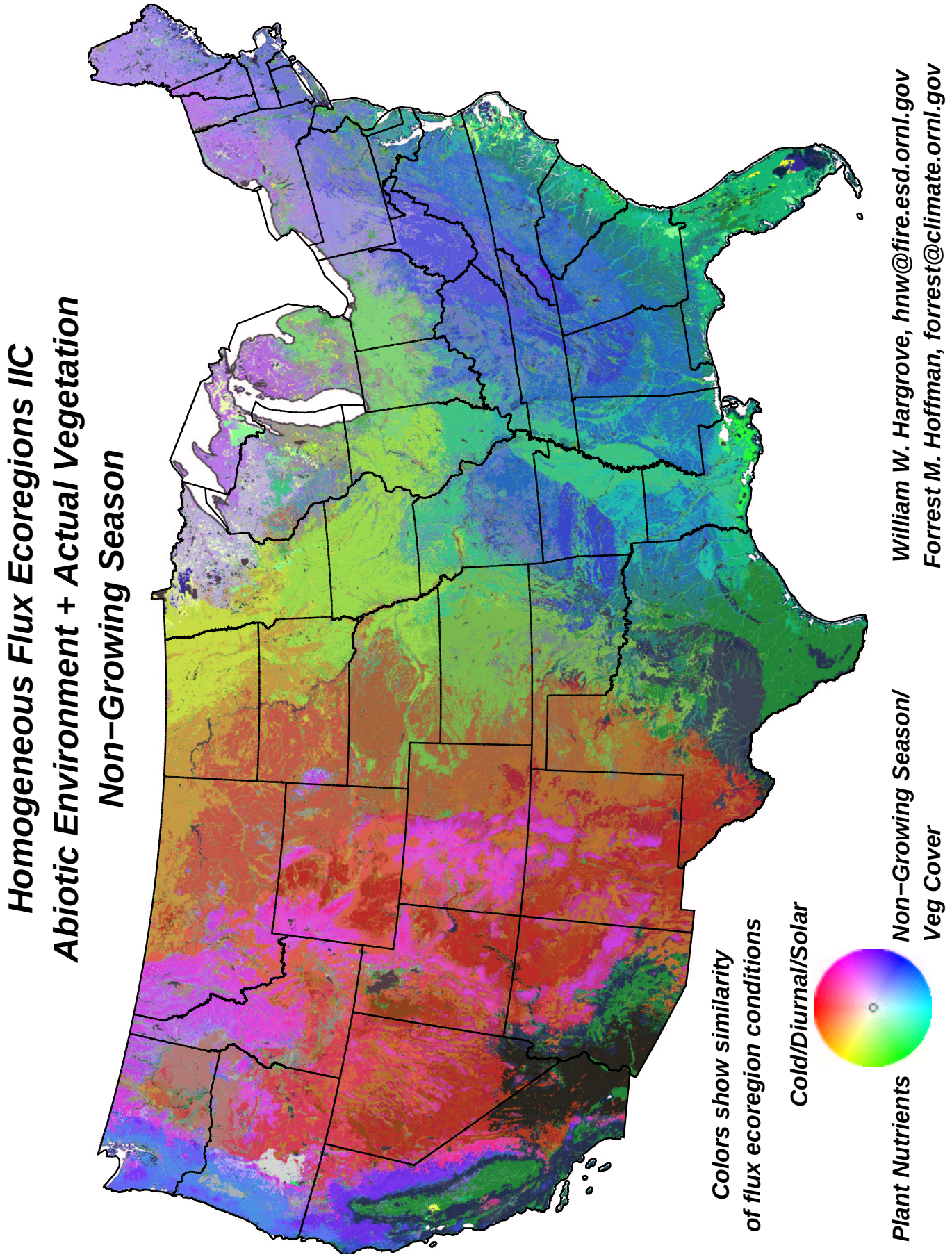

Figure 3.18: Homogeneous Flux Ecoregions IIC Similarity Colors

Map Layer	Factor 1	Factor 2	Factor 3
Degree-days cold sum below 42°F from nighttime land surface temperature during the local non-growing season	0.10049	0.89079 ✓	0.07673
Number of days below 32°F during the local non-growing season	0.12616	0.94943 ✓	-0.03039
95th percentile of maximum diurnal surface temperature difference during the local non-growing season	-0.56135	0.63236 ✓	-0.18035
Precipitation sum during the local non-growing season	0.81388 ✓	-0.01235	0.01838
Number of days with measurable precipitation during the local non-growing season	0.76474 ✓	0.43228	0.04571
Depth of mineral soil	0.07304	-0.17248	0.48914 ✓
Depth to water table	-0.10584	0.30856	-0.49526 ✓
Soil Kjeldahl nitrogen to 50 cm depth	0.04544	0.19153	0.80463 ✓
Soil organic matter to 50 cm depth	0.03891	0.12039	0.72825 ✓
Soil plant-available water holding capacity to 1.5 m	0.15873	-0.05914	0.62346 ✓
Compound Topographic Index (CTI)	-0.26601	-0.17278	0.39643 ✓
Total solar insolation during the local non-growing season, including clouds, aerosols, slope and aspect physiography	0.06170	0.88254 ✓	-0.25313
Enhanced Vegetation Index (EVI) integrated over the local non-growing season	0.86413 ✓	0.13558	0.06199
Fraction of Photosynthetically Active Radiation (FPAR) absorbed by vegetation integrated over the local non-growing season	0.89801 ✓	0.18685	0.06301
Leaf Area Index (LAI) integrated over the local non-growing season	0.90395 ✓	0.02809	0.02794
Percent tree cover	0.79659 ✓	-0.22901	0.06461
Percent bare cover	-0.62618 ✓	0.26993	-0.41356
Factor 1: nongrowing season/precip/veg cover **Factor 2: cold/diurnal/solar** **Factor 3: plant nutrients**			

Table 3.12: Homogeneous Flux Ecoregions IIC Rotated Factor Pattern

3.8 Homogeneous Flux Ecoregions IIIA

Table 3.13: Average Conditions Within the 90 Homogeneous Flux Ecoregions for IIIA

	Rand color	Sim color	Heat sum	Cold sum	Hot days	Cold days	Di-urnal diff grow	Di-urnal diff non-grow	Precip grow	Precip non-grow	Wet days grow	Wet days non-grow	Soil depth	Water table depth	Soil N	Organic matter	Soil avail wa-ter	CTI	Solar grow $\times 10^7$	Solar non-grow $\times 10^7$	EVI grow	EVI non-grow	FPAR grow	FPAR non-grow	LAI grow	LAI non-grow	% tree	% bare	GPP grow	GPP non-grow	RI grow	RI non-grow
2			19.55	84.90	0.47	249.43	17.77	17.67	24.42	279.30	11.79	101.99	121.9	5.62	3918	609	20.31	2.75	3.20	13.80	10.19	17.82	22.01	58.13	40.27	91.14	5.4	38.4	0.95	1.35	0.19	0.23
6			62.81	43.14	19.41	134.54	15.34	17.17	155.53	119.83	49.97	66.14	160.0	0.39	34966	19678	64.61	7.76	8.24	5.64	75.29	41.18	124.37	102.96	541.03	269.12	40.0	0.3	6.49	1.55	2.69	0.46
81			38.10	68.53	3.68	190.29	14.75	17.20	103.59	117.45	37.23	68.37	151.2	0.80	10830	15705	46.33	7.33	5.30	7.49	50.57	53.95	97.28	162.20	536.78	460.97	50.7	0.2	6.19	2.50	2.41	0.62
90			23.21	72.68	1.88	228.29	15.81	16.13	34.13	349.85	15.36	129.12	126.0	5.79	5168	590	30.18	3.11	3.61	10.50	18.16	41.35	46.41	102.79	161.85	225.39	39.1	9.5	2.05	2.38	0.70	0.52
55			21.52	72.68	0.85	241.85	16.58	17.50	30.22	191.90	16.02	89.33	133.1	5.78	3875	645	32.20	3.66	3.39	12.00	16.63	59.64	46.53	151.05	174.69	387.99	50.0	4.6	2.38	3.76	0.72	0.89
22			31.34	71.38	2.84	214.71	18.18	18.77	47.19	237.70	20.93	103.15	130.7	5.45	4904	797	34.95	3.98	4.40	10.80	28.47	44.19	62.15	167.23	271.66	426.84	31.9	8.2	2.96	2.56	1.10	0.61
49			35.88	66.33	4.19	217.20	19.99	20.53	32.79	173.22	16.95	76.37	124.9	5.87	5074	914	36.60	3.09	4.87	12.40	22.44	41.89	48.47	89.38	125.14	167.37	20.2	14.0	1.81	1.92	0.60	0.43
85			39.04	47.24	11.13	187.94	21.55	20.78	16.83	173.44	9.51	84.09	122.7	5.69	8084	539	61.78	4.54	4.68	10.70	20.13	64.20	56.97	168.65	192.99	446.62	27.6	6.6	2.39	4.12	0.85	0.97
66			26.75	55.84	5.47	209.82	13.17	15.57	37.48	227.93	17.31	106.50	132.7	5.50	4979	886	42.12	3.82	4.09	9.65	27.25	72.71	64.10	172.69	314.37	542.11	60.8	0.6	3.18	4.36	1.53	1.53
69			31.46	59.24	5.67	206.87	15.18	16.09	36.75	220.25	18.38	97.25	133.9	5.81	4529	658	32.85	3.14	4.33	7.78	23.95	52.87	64.56	129.52	254.73	325.20	52.4	4.4	2.99	3.08	1.12	0.77
79			61.38	64.69	9.80	192.92	29.52	27.44	29.51	96.43	18.06	58.08	119.4	5.88	4712	651	36.75	4.79	5.93	9.96	18.13	25.39	36.71	63.96	58.53	86.86	2.4	36.4	1.27	1.05	0.29	0.19
73			30.09	59.19	1.68	155.45	14.38	14.32	106.19	620.14	34.87	148.80	119.1	5.58	5828	699	31.83	2.52	6.20	7.67	30.47	22.02	71.41	77.83	250.04	175.70	37.0	12.9	3.30	1.05	1.01	0.30
47			36.55	58.51	4.71	186.13	14.44	16.64	82.78	215.07	32.42	96.81	136.1	4.44	5642	984	41.66	4.60	5.37	8.38	50.71	68.79	93.47	195.63	531.98	803.22	51.9	0.9	4.92	3.06	2.29	0.99
27			41.10	59.09	7.22	184.47	17.15	17.88	55.97	161.78	26.25	84.77	134.7	5.45	4954	861	38.16	4.16	5.60	8.47	37.19	54.43	75.77	104.71	276.47	227.56	44.7	4.4	3.41	1.83	1.22	0.48
59			70.37	47.80	26.78	182.18	33.43	29.77	15.85	81.48	11.00	54.93	98.0	5.79	4068	581	34.50	5.23	5.93	10.20	12.32	28.81	26.30	67.55	34.29	89.29	2.4	40.6	0.90	1.29	0.21	0.21
28			39.87	34.55	9.57	191.62	17.55	17.10	49.91	190.97	20.07	62.53	128.5	5.89	4347	592	41.77	3.72	5.92	11.90	30.29	73.55	80.88	197.24	355.88	668.40	42.5	1.2	2.79	4.96	1.89	1.82
57			30.84	50.25	1.54	126.52	13.49	13.40	239.43	1017.70	54.15	163.76	115.0	5.70	5217	734	31.57	2.53	6.91	6.40	39.29	27.34	85.20	79.17	328.65	221.42	45.2	14.6	4.41	1.10	1.48	0.44
31			37.69	65.82	3.64	186.47	13.60	17.04	105.50	121.59	38.00	68.64	137.1	3.66	7768	1389	42.48	6.57	5.48	7.36	54.87	52.92	101.50	157.28	591.71	444.03	54.9	0.3	6.63	2.47	2.62	0.61
35			39.07	53.98	8.85	179.51	14.36	16.23	58.85	176.31	27.67	92.26	145.5	5.62	4343	730	34.55	4.49	5.71	7.91	42.29	69.33	94.61	174.88	484.06	560.06	55.4	0.7	4.80	2.87	2.11	0.96
39			56.30	65.42	16.48	179.79	20.51	21.13	89.37	68.97	34.60	42.09	150.8	4.11	9382	1696	48.90	7.33	6.72	6.81	51.03	22.91	80.29	58.28	175.17	76.49	6.4	7.3	3.33	0.58	0.90	0.11
76			66.41	61.33	20.03	180.92	25.65	26.12	54.67	60.44	27.00	40.50	140.7	5.77	4734	711	41.42	5.54	6.63	7.30	30.26	24.00	55.24	56.48	95.01	71.55	2.5	29.5	2.17	0.64	0.46	0.13
63			69.55	51.75	31.14	169.38	27.06	27.79	30.17	67.21	18.57	48.47	139.9	4.48	4456	645	37.86	7.64	7.14	8.71	44.60	46.37	63.16	84.33	124.28	128.96	3.6	11.8	2.47	1.35	0.75	0.29
38			38.00	54.42	2.64	178.93	12.50	15.37	119.15	213.99	42.99	85.14	134.7	3.39	6366	945	43.34	4.83	5.69	6.91	67.37	71.27	108.70	165.62	667.40	585.80	69.9	0.0	6.21	2.92	2.94	0.93
80			59.87	32.44	13.87	181.51	22.53	21.45	70.03	86.33	31.36	41.50	118.6	5.95	4043	389	39.13	4.00	7.15	10.90	28.73	49.89	76.99	138.46	201.68	304.42	28.8	10.2	3.30	3.08	1.01	0.68
5			40.18	50.70	16.24	154.40	12.45	14.18	100.99	111.76	38.76	63.64	5.0	0.20	79	20	0.58	9.54	7.24	6.50	9.34	4.20	9.59	5.03	25.56	7.94	4.1	2.0	0.50	0.09	0.14	0.02
84			69.82	33.24	34.79	106.46	13.04	14.48	208.52	121.95	55.33	52.83	164.4	0.70	26849	9093	74.94	7.82	9.53	5.21	76.48	39.78	146.38	102.96	674.06	293.76	50.1	0.5	8.89	1.99	3.71	0.58
17			77.01	51.65	30.57	176.12	26.45	24.82	57.24	62.52	28.17	40.32	93.7	5.94	4546	666	46.22	5.30	7.18	7.44	27.59	27.16	53.34	58.97	83.96	74.42	2.3	29.6	2.12	0.72	0.42	0.15
68			38.74	40.52	2.86	108.64	13.12	16.10	136.67	531.54	45.51	132.97	123.0	5.53	8722	1051	49.37	3.10	7.69	5.74	54.40	55.50	121.58	123.40	554.18	359.01	67.7	0.2	6.45	2.28	2.64	0.96
43			42.09	46.46	3.54	161.24	12.36	18.58	127.69	190.30	45.97	99.22	138.6	3.67	5306	1129	47.29	5.07	6.04	6.67	72.18	57.44	114.89	140.12	710.76	438.89	63.3	0.1	6.82	2.81	2.95	0.76
71			89.24	35.42	25.63	169.21	32.22	30.86	58.52	51.21	29.03	32.02	125.7	5.94	4652	408	42.58	5.55	7.94	10.10	21.69	27.13	43.66	55.87	59.26	69.26	2.2	41.0	1.69	1.04	0.34	0.17
58			41.60	38.83	5.32	108.85	13.69	16.00	132.68	510.72	44.64	130.22	119.2	5.43	7420	1075	48.63	3.20	8.18	7.13	66.39	69.83	132.21	171.06	720.21	821.28	57.3	1.4	6.57	2.28	2.78	1.05
44			86.18	41.22	28.40	136.03	28.70	24.33	26.08	89.04	18.73	60.94	115.5	5.83	4818	602	49.09	4.83	7.66	6.76	25.17	34.14	51.11	67.87	83.40	97.98	5.4	26.2	1.83	0.94	0.39	0.20
72			85.73	7.97	45.51	64.44	14.62	12.77	233.94	141.23	61.57	45.06	182.6	0.67	6724	31604	77.33	8.08	10.90	4.72	99.43	43.88	171.39	104.19	839.22	301.25	42.1	0.1	9.23	2.11	4.41	0.64
34			77.14	33.68	26.45	165.47	24.63	23.11	42.14	70.95	21.08	37.60	73.5	5.98	4049	464	22.95	3.48	7.92	9.99	22.62	35.33	51.44	77.30	79.77	110.79	6.3	32.8	1.68	1.42	0.47	0.26
19			68.43	37.32	18.45	133.68	17.08	18.17	140.11	140.47	46.18	60.87	134.2	3.76	5024	972	46.61	6.53	7.97	5.84	62.61	38.83	0.01	0.01	0.06	0.04	19.5	4.4	0.00	0.00	0.00	0.00
89			68.25	43.96	22.96	147.63	21.12	20.74	143.89	95.87	44.14	43.62	154.8	4.23	8168	1642	74.82	6.42	8.26	5.90	66.97	23.34	100.95	56.34	243.37	71.72	3.4	2.3	4.29	0.55	1.37	0.11
7			64.57	36.43	15.33	132.65	17.01	19.22	141.62	141.01	47.97	66.24	155.4	1.98	6534	1331	59.59	7.00	8.04	5.47	71.01	35.81	108.45	80.13	276.67	127.82	7.3	1.5	4.52	0.85	1.49	0.23
9			58.07	30.36	21.91	127.93	16.50	15.12	51.56	378.57	14.14	76.90	104.8	5.85	3149	754	32.48	3.48	8.65	8.95	43.93	49.18	111.29	120.50	429.12	319.62	36.9	6.0	4.06	2.80	1.96	0.72
23			100.31	38.27	46.24	156.61	31.78	29.74	30.88	39.23	18.73	28.97	116.4	5.64	2862	269	26.03	6.17	8.50	8.95	14.33	18.09	22.60	31.51	25.15	34.68	0.0	87.9	0.76	0.53	0.16	0.08
20			75.43	23.90	13.96	58.49	20.12	18.19	93.82	234.47	45.02	93.39	142.1	3.57	6236	1548	58.29	7.25	9.35	4.61	66.28	57.05	87.99	75.66	199.47	160.77	24.1	1.9	3.48	0.91	0.77	0.34
62			91.97	36.74	50.88	151.85	25.09	26.30	90.33	55.51	33.62	28.09	154.8	5.76	5276	562	35.99	6.08	8.94	7.27	41.20	30.65	71.66	54.05	116.45	65.21	2.3	21.3	3.01	0.72	0.61	0.14
25			53.74	23.59	28.60	111.50	12.83	13.62	63.25	387.54	18.44	87.99	106.3	5.87	4363	907	41.38	3.37	8.22	6.86	52.87	64.87	126.91	145.18	639.71	481.75	59.7	0.1	5.55	4.51	3.46	1.85
77			84.22	35.34	44.64	132.69	21.37	21.64	115.71	86.84	37.08	39.54	141.3	4.96	5178	731	45.20	13.55	9.00	6.49	53.23	30.96	92.16	65.99	249.03	108.25	10.9	17.8	4.10	0.93	1.32	0.21
26			44.60	21.92	2.53	61.64	13.70	14.36	220.16	633.68	61.97	129.78	122.9	5.31	8537	1956	62.68	4.29	8.59	4.78	89.40	76.45	160.12	146.17	905.39	664.75	66.3	0.0	9.20	2.88	3.47	1.73
3			52.83	34.75	9.76	140.92	13.02	15.66	149.48	188.40	48.08	67.05	136.9	3.51	6067	1006	38.11	5.17	7.33	5.76	83.24	49.50	140.27	131.78	868.29	384.83	65.3	0.0	7.97	2.42	3.62	0.61
70			49.97	22.14	10.71	75.24	12.60	14.88	116.87	373.68	42.17	110.27	121.5	5.62	6978	1224	57.00	3.84	9.11	5.92	79.60	78.48	151.48	156.40	829.59	718.84	66.0	0.0	7.86	3.18	3.68	1.77
53			44.14	22.76	3.88	63.11	12.63	14.56	218.36	604.76	60.69	126.41	117.8	5.44	8059	1588	57.53	3.73	8.50	4.27	78.63	63.75	151.84	115.17	746.39	380.21	70.7	0.0	9.04	2.82	3.60	1.81
46			68.17	29.22	24.76	117.87	15.13	17.43	165.71	154.75	49.27	57.06	151.5	4.95	4823	833	57.85	6.00	8.63	5.54	84.32	50.01	124.62	97.83	356.56	177.70	10.6	0.5	5.38	1.20	2.01	0.35
48			49.46	22.98	6.48	66.52	13.46	14.03	298.23	806.13	64.46	127.90	107.8	5.78	5978	1012	46.46	3.05	8.98	4.54	67.34	55.91	143.50	113.28	638.69	386.78	67.5	0.0	8.67	2.62	3.29	1.38
61			51.05	19.85	13.11	75.79	11.77	13.58	101.16	323.89	37.22	100.58	118.0	5.68	6270	1119	53.64	3.73	8.98	5.29	70.21	64.20	145.89	125.12	717.36	415.27	69.1	0.0	7.88	3.30	3.81	1.87
52			38.10	16.66	1.07	41.55	10.03	15.05	150.03	244.11	64.97	84.93	22.1	0.92	957	212	7.32	2.10	9.64	3.25	27.93	15.22	49.93	22.70	133.14	45.03	19.5	2.2	2.86	0.42	0.64	0.17
88			57.96	23.72	6.60	55.32	15.43	16.85	125.60	272.38	54.80	99.63	121.6	4.23	6508	1453	53.59	5.18	9.29	4.19	83.71	56.36	168.65	125.09	878.90	427.98	51.2	0.2	8.50	1.95	2.96	0.89
50			63.67	32.63	25.95	122.41	13.93	16.58	163.92	149.74	48.32	58.71	153.7	4.00	5284	974	53.19	6.29	8.44	5.68	86.64	46.96	152.29	128.08	934.04	379.46	40.0	0.1	5.93	1.28	4.32	0.61
13			69.43	27.20	31.24	111.93	14.05	16.67	176.28	145.54	49.63	52.55	152.0	4.29	4890	845	59.16	6.12	9.07	5.42	87.20	43.25	136.40	92.16	440.41	170.28	52.6	0.1	5.88	1.12	2.46	0.33
11			73.59	17.42	33.67	93.38	15.48	14.40	61.49	268.77	16.71	55.49	103.5	5.96	3813	799	41.26	3.53	10.50	7.53	59.57	58.59	150.24	146.35	706.86	531.14	41.6	1.1	4.56	3.87	3.52	1.24
64			51.03	18.85	5.44	48.97	13.18	14.16	169.68	363.06	59.67	103.52	119.5	5.29	8366	1643	63.73	4.28	9.57	4.10	92.66	60.07	175.17	113.93	959.13	407.55	68.4	0.0	9.50	2.36	3.87	1.49
29			68.06	25.65	27.12	112.24	14.62	17.29	168.46	173.40	48.97	60.03	148.7	4.68	4258	747	54.23	5.68	8.67	5.73	88.23	61.76	155.11	144.76	974.06	561.35	15.0	0.2	8.74	2.80	3.96	0.83
54			57.71	16.79	18.26	111.40	11.35	15.38	173.19	192.05	53.81	66.85	122.9	5.56	4680	670	53.53	4.79	8.31	5.94	93.11	49.63	150.13	123.22	925.96	356.81	71.4	0.0	8.91	3.03	4.24	0.73
30			72.06	11.63	42.39	74.56	8.69	11.84	210.61	144.07	54.94	42.76	28.4	0.78	934	204	8.47	5.12	10.80	4.41	14.08	4.14	12.15	3.76	23.81	5.79	7.9	3.5	0.70	0.09	0.15	0.02
56			108.96	21.06	76.19	102.41	21.39	20.58	148.88	59.99	39.39	23.38	157.8	5.78	7724	882	64.11	6.27	10.90	5.76	55.11	37.11	98.40	61.67	170.86	85.53	5.0	15.1	4.27	0.82	0.96	0.18
74			131.18	15.07	66.12	97.62	28.50	26.54	78.75	32.76	31.28	18.19	61.6	5.95	3943	368	24.24	4.95	11.40	7.42	28.13	21.28	54.34	40.58	72.03	50.12	1.4	52.8	2.00	0.80	0.46	0.13
86			88.49	20.05	53.58	89.08	15.96	16.65	209.65	132.30	50.57	38.48	159.8	2.45	6120	883	65.70	6.83	10.60	4.86	84.81	36.99	136.32	75.16	339.68	124.67	10.8	1.2	6.00	0.89	2.01	0.24

continued on next page

continued from previous page

	Rand color	Sim color	Heat sum	Cold sum	Hot days	Cold days	Diurnal diff grow	Diurnal diff non-grow	Precip grow	Precip non-grow	Wet days grow	Wet days non-grow	Soil depth	Water table depth	Soil N	Organic matter	Soil avail water	CTI	Solar grow $\times 10^7$	Solar non-grow $\times 10^7$	EVI grow	EVI non-grow	FPAR grow	FPAR non-grow	LAI grow	LAI non-grow	% tree	% bare	GPP grow	GPP non-grow	RI grow	RI non-grow
87			91.34	6.93	47.81	49.20	11.16	10.95	274.03	118.30	65.93	35.50	178.7	0.31	7581	12793	32.82	8.25	12.30	3.88	74.54	22.43	144.90	52.40	559.99	123.14	42.9	3.0	8.49	1.25	3.30	0.32
82			93.68	13.19	67.54	63.49	14.82	15.70	214.35	136.75	52.82	36.53	136.0	3.95	4139	608	46.01	7.11	11.70	4.43	83.82	29.56	0.02	0.01	0.08	0.02	22.4	2.8	0.00	0.00	0.00	0.00
41			138.44	15.79	81.00	94.63	28.53	27.21	94.88	26.87	32.05	15.27	173.6	5.93	4364	515	44.50	6.27	11.90	6.76	33.31	20.98	57.38	34.08	72.71	38.91	0.8	46.1	2.30	0.59	0.44	0.10
75			71.68	18.97	33.54	97.77	13.80	15.82	185.72	174.88	52.33	55.17	148.1	4.73	3991	657	53.57	6.07	9.30	5.40	90.17	47.44	166.18	120.02	992.58	356.98	26.8	0.3	9.60	2.70	4.53	0.66
51			62.80	15.18	11.16	42.12	14.26	14.85	174.29	321.86	53.38	84.05	126.2	5.14	6568	1539	59.08	4.62	11.00	4.33	101.47	61.69	190.09	119.68	1082.70	541.68	57.4	0.0	13.20	2.77	3.35	1.09
24			131.51	0.16	97.41	3.98	12.62	10.79	364.39	29.51	97.35	8.16	167.3	0.11	33699	18165	149.69	8.31	17.00	1.40	130.87	10.95	228.07	24.09	876.80	67.49	44.9	0.6	12.68	0.70	6.01	0.23
4			82.61	10.90	57.19	69.89	12.92	14.57	224.29	176.40	55.25	44.98	157.8	4.45	4103	635	54.06	6.04	10.90	4.79	104.65	43.09	154.94	101.84	592.25	244.23	49.4	0.1	8.82	1.83	4.38	0.54
32			158.01	11.92	87.68	52.84	27.57	22.60	27.50	29.79	12.49	12.70	106.6	5.91	2435	168	18.71	4.34	14.20	5.37	23.68	13.62	44.07	22.98	50.51	26.13	0.1	79.9	1.01	0.40	0.35	0.07
83			127.88	7.69	37.64	39.70	21.95	17.00	57.81	82.38	18.86	20.81	86.2	5.76	4184	434	28.83	4.06	14.70	4.68	56.54	24.78	130.50	54.69	265.92	104.78	14.7	17.2	4.15	1.21	1.42	0.27
37			118.08	8.71	90.75	64.55	18.05	17.85	171.83	64.74	40.04	21.48	78.9	5.76	5810	902	38.57	5.62	12.40	4.89	70.81	31.50	131.15	59.85	298.19	93.47	13.5	10.7	5.88	0.99	1.73	0.22
8			78.30	12.59	55.68	79.55	12.43	15.14	208.10	177.43	49.75	42.85	157.7	4.65	3811	537	54.57	5.86	10.60	5.06	99.43	40.17	180.60	102.80	1063.00	272.91	57.4	0.0	10.40	2.33	5.31	0.52
33			119.90	7.20	70.73	37.66	20.19	14.43	74.67	141.30	22.91	35.18	88.7	5.85	3940	456	37.22	4.53	13.60	4.19	69.42	36.55	168.59	84.94	476.65	221.21	23.3	5.6	6.48	1.58	1.78	0.44
65			84.90	1.81	59.47	13.92	7.95	7.45	87.14	42.80	29.78	12.45	16.7	0.78	556	64	3.45	4.46	16.40	2.01	14.75	3.16	22.75	4.25	39.42	7.60	3.4	10.0	1.13	0.10	0.18	0.02
42			168.35	6.63	84.18	35.16	29.11	19.50	40.98	60.03	17.38	20.61	112.0	5.86	3771	325	40.29	5.24	14.70	4.00	45.66	30.41	94.10	54.49	155.19	122.55	4.3	19.9	3.42	1.00	0.71	0.28
67			101.70	4.99	74.98	44.46	15.41	14.16	250.20	144.78	61.89	35.73	182.0	3.52	4316	616	40.21	6.85	12.30	4.19	97.97	35.42	163.32	73.23	429.12	144.71	29.8	0.9	6.97	1.15	2.62	0.34
60			165.33	0.78	38.07	5.15	22.19	14.16	96.56	31.03	31.25	8.00	113.2	4.63	3239	485	42.66	5.94	17.50	1.26	60.51	7.71	2.88	0.17	3.77	0.34	4.8	23.6	0.11	0.00	0.02	0.00
36			110.66	2.36	19.67	12.97	17.75	12.32	99.61	85.38	30.86	20.10	94.8	5.66	5213	615	36.69	3.90	15.60	2.53	86.68	23.32	199.44	51.77	584.25	141.58	29.9	4.7	9.86	1.21	2.17	0.35
12			72.54	6.68	14.21	19.80	13.33	12.15	261.43	267.27	59.31	48.77	120.8	5.56	5108	1069	54.23	3.72	13.50	2.84	111.90	38.51	229.68	74.24	1152.00	289.63	64.6	0.1	11.50	1.79	5.00	0.97
16			109.41	0.02	74.96	7.89	6.63	3.91	355.66	57.73	83.67	14.02	33.3	0.20	2298	637	11.07	3.90	16.20	1.72	7.55	1.15	2.94	0.43	4.31	0.61	6.3	5.7	0.17	0.01	0.03	0.00
21			147.13	5.74	106.84	23.10	22.73	16.43	41.27	42.37	19.50	17.89	155.2	5.40	4349	394	44.77	8.22	16.00	2.83	87.83	23.69	141.11	39.89	272.16	76.67	5.1	8.4	5.11	0.56	1.35	0.16
78			89.72	5.77	74.15	51.57	12.61	13.43	241.53	175.02	56.35	38.49	170.2	4.38	3788	501	55.20	6.27	11.90	4.40	104.47	39.15	204.32	103.71	1143.50	309.46	54.1	0.0	11.42	2.61	7.00	0.74
1			134.39	0.17	84.82	6.35	12.69	9.67	369.91	44.57	91.04	11.52	121.9	1.44	5934	1533	32.94	8.15	16.60	1.45	99.37	10.05	0.01	0.00	0.02	0.00	21.5	4.1	0.00	0.00	0.00	0.00
15			178.74	3.84	139.90	31.67	26.45	20.90	84.02	25.64	31.12	12.69	133.0	5.94	3287	322	31.77	5.94	15.00	3.91	44.77	14.74	80.96	26.83	110.70	34.54	2.2	37.9	2.39	0.56	0.74	0.10
14			130.38	3.34	107.83	30.17	17.37	16.73	212.99	61.29	48.32	19.92	179.6	5.18	5029	600	48.72	6.60	14.00	3.30	95.33	26.39	157.85	46.33	332.08	73.88	14.8	5.1	6.41	0.75	2.01	0.19
18			206.02	3.19	155.75	16.46	27.10	19.81	29.07	9.83	14.31	5.52	125.5	5.84	2209	125	17.06	5.59	17.40	2.55	25.50	5.72	36.66	7.34	40.19	7.93	0.0	93.2	0.75	0.12	0.30	0.02
10			98.66	2.87	82.14	33.49	12.57	12.47	290.55	133.40	67.52	31.61	180.3	2.39	4821	895	45.96	7.21	13.10	3.74	109.77	37.26	220.48	92.39	1190.10	323.85	60.0	0.0	13.10	2.65	7.70	1.01
40			105.75	2.46	72.93	26.87	11.81	10.95	318.47	100.64	76.37	25.74	144.3	1.54	4464	1100	34.68	7.41	14.10	3.02	102.72	27.71	219.43	68.34	1039.00	233.01	50.3	0.5	15.75	2.23	6.07	0.68
45			146.67	0.14	105.82	2.52	16.71	13.59	370.36	23.73	96.95	6.73	158.5	1.52	3905	953	29.41	8.15	17.30	1.27	124.98	9.64	215.61	19.54	522.28	39.78	23.0	1.9	9.13	0.43	3.30	0.14

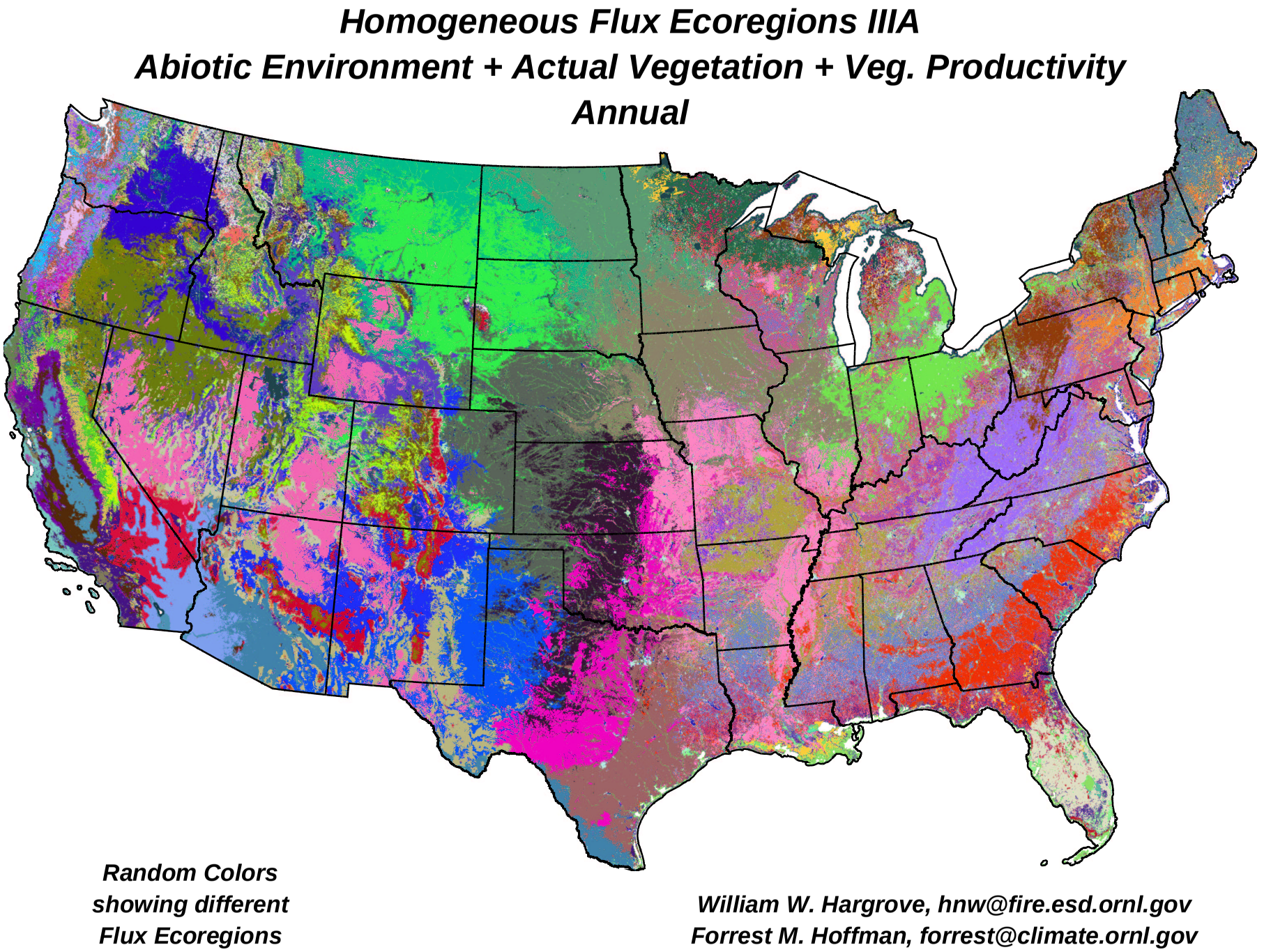

Figure 3.19: Homogeneous Flux Ecoregions IIIA Random Colors

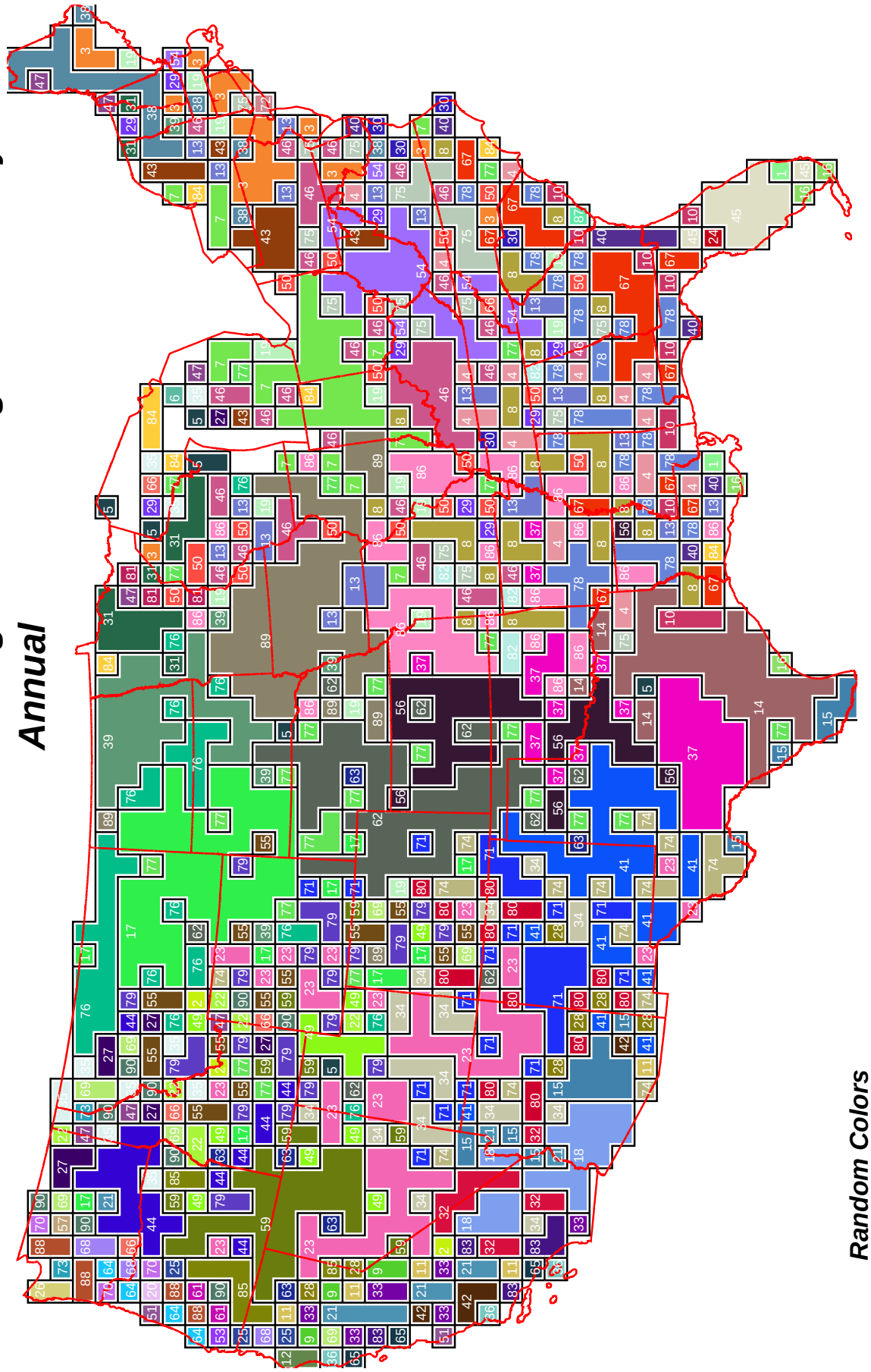

Figure 3.20: Homogeneous Flux Ecoregions IIIA Schematic

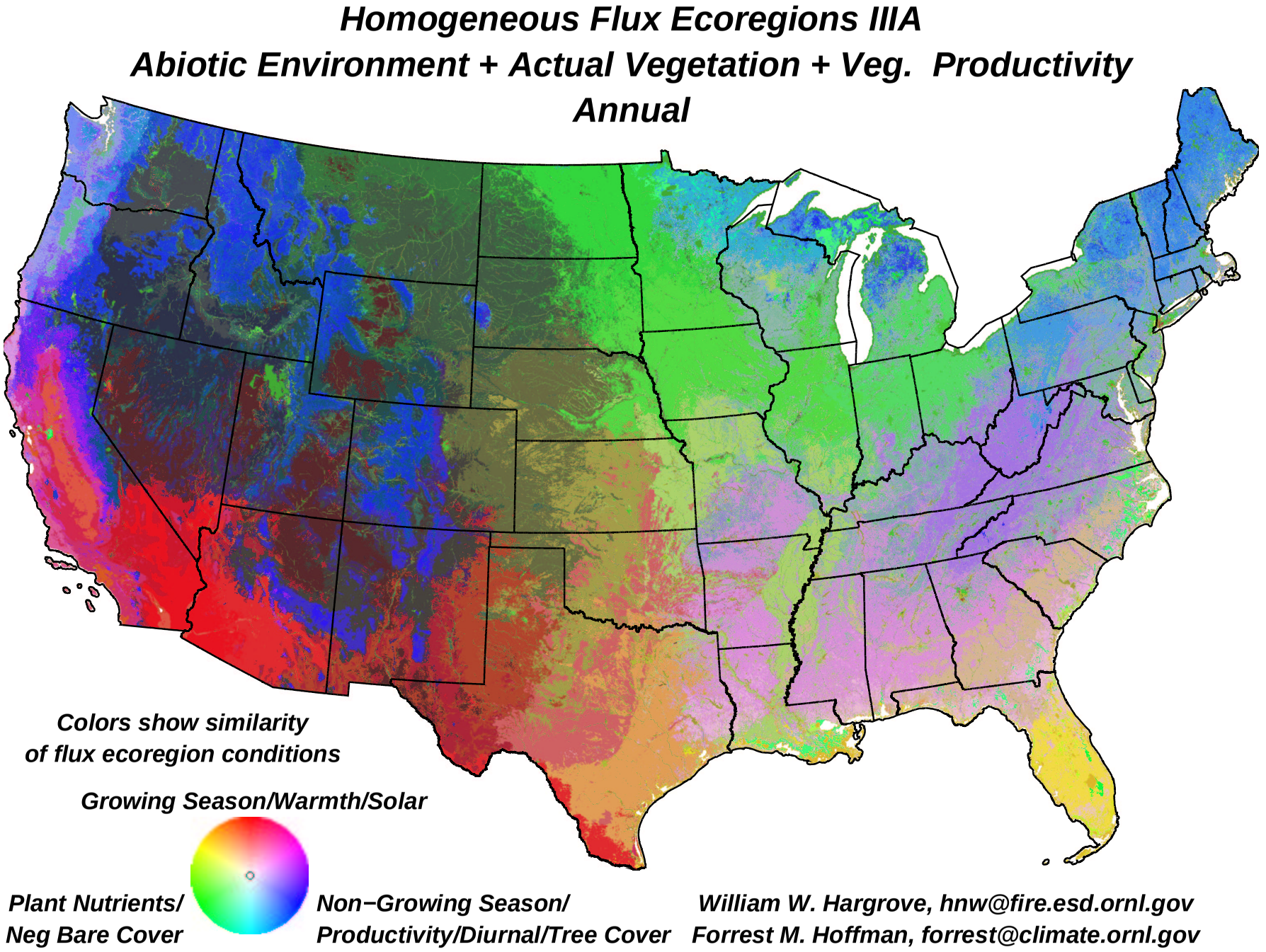

Figure 3.21: Homogeneous Flux Ecoregions IIIA Similarity Colors

Map Layer	Factor 1	Factor 2	Factor 3
Degree-days heat sum above 42°F from daytime land surface temperature during the local growing season	-0.51202	0.74590 ✓	-0.25447
Degree-days cold sum below 42°F from nighttime land surface temperature during the local non-growing season	-0.03930	-0.91969 ✓	0.03666
Number of days above 90°F during the local growing season	-0.34080	0.81534 ✓	-0.16374
Number of days below 32°F during the local non-growing season	0.01000	-0.95323 ✓	-0.09765
95th percentile of maximum diurnal surface temperature difference during the local growing season	-0.66681 ✓	-0.25865	-0.46803
95th percentile of maximum diurnal surface temperature difference during the local non-growing season	-0.55910 ✓	-0.42747	-0.37554
Precipitation sum during the local growing season	0.26967	0.66196 ✓	0.57747
Precipitation sum during the local non-growing season	0.74574 ✓	-0.15445	0.12947
Number of days with measurable precipitation during the local growing season	0.26464	0.55311	0.63357 ✓
Number of days with measurable precipitation during the local non-growing season	0.62880 ✓	-0.60227	0.10579
Depth of mineral soil	0.09290	0.17950	0.40115 ✓
Depth to water table	-0.05611	-0.12499	-0.65617 ✓
Soil Kjeldahl nitrogen to 50 cm depth	-0.02326	-0.22744	0.63907 ✓
Soil organic matter to 50 cm depth	-0.01118	-0.16369	0.57679 ✓
Soil plant-available water holding capacity to 1.5 m	0.13216	0.00632	0.54766 ✓
Compound Topographic Index (CTI)	-0.24627	0.14600	0.38739 ✓
Total solar insolation during the local growing season, including clouds, aerosols, slope and aspect physiography	-0.23852	0.93730 ✓	-0.00344
Total solar insolation during the local non-growing season, including clouds, aerosols, slope and aspect physiography	0.00388	-0.80782 ✓	-0.39059
Enhanced Vegetation Index (EVI) integrated over the local growing season	0.45202	0.61665 ✓	0.53380
Enhanced Vegetation Index (EVI) integrated over the local non-growing season	0.82542 ✓	-0.23593	0.02506
Fraction of Photosynthetically Active Radiation (FPAR) absorbed by vegetation integrated over the local growing season	0.55706	0.61823 ✓	0.40224
Fraction of Photosynthetically Active Radiation (FPAR) absorbed by vegetation integrated over the local non-growing season	0.88640 ✓	-0.27214	0.02384
Leaf Area Index (LAI) integrated over the local growing season	0.76656 ✓	0.40868	0.27481
Leaf Area Index (LAI) integrated over the local non-growing season	0.91747 ✓	-0.11818	-0.00345
Percent tree cover	0.82360 ✓	0.11114	0.13971
Percent bare cover	-0.57350	-0.06788	-0.58569 ✓
Gross Primary Production (GPP) integrated over the local growing season	0.64017 ✓	0.54125	0.39424
Gross Primary Production (GPP) integrated over the local non-growing season	0.90081 ✓	-0.12888	-0.14381
Respiration Index (RI) integrated over the local growing season	0.69959 ✓	0.49406	0.29631
Respiration Index (RI) integrated over the local non-growing season	0.91014 ✓	-0.03767	-0.07330
Factor 1: nongrowing season/productivity/diurnal/tree cover **Factor 2: growing season/temp/solar** **Factor 3: plant nutrients/negative bare cover**			

Table 3.14: Homogeneous Flux Ecoregions IIIA Rotated Factor Pattern

3.9 Homogeneous Flux Ecoregions IIIB

Table 3.15: Average Conditions Within the 90 Homogeneous Flux Ecoregions for IIIB

	Rand color	Sim color	Heat sum	Hot days	Diurnal diff grow	Precip grow	Wet days grow	Soil depth	Water table depth	Soil N	Organic matter	Soil avail water	CTI	Solar grow $\times 10^7$	EVI grow	FPAR grow	LAI grow	% tree	% bare	GPP grow	RI grow
27			22.84	2.63	15.32	28.01	14.04	132.3	5.84	4301	674	30.58	3.42	3.43	17.60	47.20	179.27	54.6	3.5	2.12	0.78
51			32.48	5.84	17.98	34.62	15.54	132.8	5.73	13162	553	53.61	3.97	4.83	25.92	65.32	270.32	44.8	4.0	3.06	1.26
20			37.10	2.82	12.26	114.64	41.53	141.6	2.82	6715	1229	49.68	5.10	5.49	63.12	101.29	577.61	68.4	0.0	6.02	2.69
8			34.02	5.75	18.85	31.50	15.56	125.9	5.83	4693	771	29.79	3.07	4.51	19.77	44.92	120.27	9.0	20.3	1.79	0.55
36			56.35	13.68	15.22	138.08	46.08	156.9	0.35	35321	18927	67.33	7.69	7.55	70.41	117.97	527.74	39.3	0.4	5.98	2.49
55			41.96	8.17	16.63	57.25	27.12	133.2	5.83	4296	673	39.66	3.43	6.19	33.96	84.86	330.80	53.0	2.6	4.02	1.50
23			39.72	4.51	12.94	110.38	39.10	149.1	4.64	6899	1279	34.11	6.38	5.71	58.65	106.43	628.62	57.7	0.1	6.85	2.82
44			54.51	19.80	14.05	147.47	46.17	158.9	1.02	24334	10954	78.31	7.57	7.51	68.62	127.07	672.17	54.3	0.3	7.84	3.39
58			47.40	6.67	13.12	137.96	47.42	145.2	3.19	5826	1050	44.02	4.78	6.73	79.29	130.33	830.99	65.9	0.0	7.36	3.33
30			31.48	5.87	10.65	119.04	44.63	0.3	0.11	12	3	0.09	10.00	6.78	4.46	1.48	2.72	2.0	1.0	0.07	0.02
75			52.73	13.35	11.21	162.68	52.49	112.0	5.50	5260	715	49.44	4.13	7.75	89.51	142.18	880.74	71.6	0.0	8.36	3.89
39			46.94	5.09	12.96	173.54	55.79	120.4	5.70	8939	1452	60.79	3.48	9.23	78.87	155.33	772.25	67.5	0.4	8.33	3.48
78			39.69	1.84	10.39	131.61	66.07	27.4	1.15	1148	234	8.70	1.88	9.95	40.15	79.66	265.09	23.1	1.9	4.12	1.23
1			58.80	21.17	13.39	168.46	47.96	162.3	0.59	9299	14715	39.95	7.74	8.00	59.24	114.01	531.63	46.9	1.3	6.92	2.69
57			63.62	17.70	29.01	21.07	12.71	67.1	5.95	4547	647	28.20	3.94	6.00	15.12	33.72	51.04	4.1	36.2	1.14	0.28
86			56.82	14.41	15.00	147.13	48.74	139.8	4.07	5415	1008	46.82	6.33	7.79	70.41	0.05	0.17	57.2	0.2	0.00	0.00
53			55.35	17.12	13.79	145.32	45.60	150.8	3.91	5772	1099	50.27	6.24	7.53	79.95	137.47	841.54	57.0	0.1	5.39	3.81
17			54.30	5.29	14.97	151.21	58.15	126.9	4.57	7013	1614	58.78	4.93	9.27	90.37	171.52	959.46	58.1	0.2	8.98	3.28
70			68.47	28.84	16.30	60.23	17.83	102.4	5.95	3769	750	36.73	3.41	9.76	53.07	132.81	584.38	41.9	2.8	4.08	3.01
69			70.65	23.21	24.67	41.43	20.91	125.8	5.84	4806	629	80.32	4.59	7.18	28.07	61.48	148.94	15.6	18.8	2.35	0.72
84			57.09	16.02	19.93	101.15	36.90	153.1	3.24	10896	1659	46.37	7.54	6.91	55.27	86.94	210.62	7.4	6.6	3.64	1.10
72			55.11	39.99	14.39	35.75	21.15	14.0	0.24	107	31	0.72	9.11	8.46	5.19	4.04	6.31	0.8	1.8	0.15	0.04
66			65.75	25.11	6.97	192.86	55.10	2.3	0.18	86	18	0.43	2.01	10.30	9.38	4.03	5.81	4.0	2.8	0.19	0.04
41			62.32	29.18	16.52	130.13	41.26	0.2	0.40	10	3	0.10	7.96	8.14	55.64	111.09	457.72	28.8	7.5	6.01	2.27
71			75.78	28.33	35.00	24.21	15.16	122.0	5.86	3908	526	39.20	6.06	6.36	16.28	31.59	46.19	3.1	34.9	1.10	0.27
90			74.98	19.83	29.40	43.86	23.99	143.5	5.93	4493	539	38.27	4.88	6.94	21.06	41.80	59.62	1.5	40.1	1.56	0.30
14			69.17	28.71	30.91	21.62	13.86	152.9	2.14	5243	815	38.48	7.99	6.40	21.80	36.05	73.44	4.0	36.6	1.35	0.38
21			62.93	32.22	14.36	159.81	47.52	0.4	0.52	15	4	0.13	7.54	8.93	52.89	0.12	0.38	18.4	2.3	0.01	0.00
76			62.86	25.93	13.17	167.97	50.11	140.2	4.88	4508	731	53.19	11.00	8.56	87.39	154.38	932.01	59.6	0.0	8.97	4.26
49			68.00	29.52	23.53	80.47	32.54	150.5	5.42	6548	1090	50.32	6.27	7.59	52.30	79.79	161.58	3.6	9.3	3.35	0.89
9			78.62	30.66	26.71	57.31	28.37	93.5	5.96	4392	630	48.45	5.16	7.34	26.86	52.88	82.37	2.4	30.9	2.12	0.41
81			69.52	29.59	19.14	103.15	38.56	143.6	4.70	5849	1021	45.11	7.07	8.48	44.47	0.19	0.25	5.2	7.8	0.01	0.00
61			68.42	21.59	21.45	147.23	44.93	155.4	3.72	8518	1856	78.27	6.51	8.28	67.20	100.90	244.99	3.4	2.0	4.28	1.40
35			84.17	43.74	14.69	229.46	60.66	182.8	0.70	5304	31381	79.13	8.01	10.70	99.00	169.92	843.00	41.7	0.1	9.13	4.37
63			66.21	21.72	15.39	159.10	48.50	152.5	4.94	5146	950	58.29	5.92	8.40	81.07	120.38	335.61	9.3	0.8	5.14	1.85
40			67.49	27.44	14.04	171.14	50.19	148.9	4.56	4411	777	52.47	5.63	8.72	87.45	157.37	962.01	18.3	0.2	8.98	4.05
22			68.92	23.03	16.62	151.50	47.88	158.8	1.88	6154	1152	65.04	6.82	8.55	74.53	113.86	284.97	8.1	1.4	4.78	1.57
68			73.80	5.70	7.87	117.51	36.53	28.6	1.28	923	112	6.85	1.32	16.60	24.91	48.77	89.36	5.9	11.9	2.39	0.42
60			74.09	45.32	12.84	196.64	50.10	166.3	5.35	3238	502	57.69	5.29	10.00	98.45	174.37	1061.70	59.6	0.0	10.07	5.17
15			72.44	35.16	14.21	181.28	50.88	156.4	4.13	4738	834	55.20	6.27	9.36	92.64	166.92	1011.80	23.6	0.1	6.46	4.75
79			83.02	38.10	24.65	83.03	32.69	150.5	5.70	4496	478	24.24	5.63	8.17	37.81	70.45	127.47	4.5	20.1	2.88	0.64
43			86.37	25.03	17.01	172.69	52.61	143.2	3.39	4808	1008	51.83	6.53	9.11	68.98	0.01	0.01	11.1	5.1	0.00	0.00
64			81.87	16.60	13.98	154.70	42.92	100.7	5.48	5705	937	43.76	3.61	14.00	101.01	214.51	930.15	49.0	0.9	13.10	3.28
19			77.02	40.78	14.40	192.87	52.56	160.4	4.56	4328	730	55.95	6.36	9.83	91.47	144.64	444.28	51.0	0.1	6.16	2.54
56			74.97	45.70	12.52	208.66	54.17	150.2	4.80	4204	673	53.81	5.56	10.20	101.08	145.36	576.50	54.0	0.1	8.56	4.20
42			102.31	40.53	27.08	65.43	29.03	59.5	5.98	4418	411	22.68	4.36	9.45	27.96	60.35	93.36	5.0	33.5	2.14	0.54
3			89.93	34.36	33.44	25.64	16.41	115.8	5.87	3120	261	27.07	6.08	7.57	12.74	21.22	23.79	0.0	85.2	0.71	0.15
65			80.67	39.14	22.71	97.72	34.05	141.8	5.20	5417	794	45.48	12.52	8.44	46.86	80.65	173.83	6.7	18.8	3.36	0.93
11			82.09	58.23	12.82	221.04	51.20	103.0	5.63	3977	485	45.93	5.39	10.80	95.52	179.22	948.86	43.1	0.1	10.35	5.22
87			83.45	44.92	9.41	259.96	65.14	0.7	0.57	22	11	0.22	5.15	12.00	53.68	152.94	493.73	25.7	2.7	9.96	2.91
74			91.51	49.46	24.29	32.09	20.01	107.9	5.15	2343	291	18.31	6.15	8.72	14.16	21.79	25.64	0.2	91.3	0.73	0.15
47			105.71	60.94	18.61	75.29	22.42	89.5	5.88	3834	549	37.70	4.10	12.80	68.77	166.79	551.22	29.2	4.3	6.71	2.13
52			90.93	55.07	17.12	188.24	45.48	142.1	4.62	6975	1010	74.63	6.01	10.30	74.52	126.55	291.04	8.2	4.2	5.63	1.64
59			87.85	45.10	14.31	329.60	69.64	153.7	4.72	5356	981	44.59	5.53	12.20	92.22	171.34	610.63	47.3	1.5	8.87	3.21
4			98.33	64.09	12.69	308.50	71.55	168.9	0.21	30941	5044	56.44	8.33	13.10	104.73	189.91	726.66	45.1	0.5	10.22	4.54
25			84.33	73.77	9.83	237.53	56.19	0.6	0.56	34	4	0.31	9.15	12.30	14.74	3.54	6.08	6.0	2.3	0.16	0.03
85			91.25	57.91	9.32	274.76	65.55	167.5	2.27	5427	1576	44.81	6.83	12.90	23.20	8.49	12.70	15.5	10.0	0.40	0.08
50			90.70	73.01	12.94	242.11	57.22	175.1	5.06	3445	483	54.29	6.06	11.90	104.84	205.09	1138.90	49.4	0.0	11.13	6.90
31			90.34	75.82	12.44	241.48	54.31	176.5	2.33	4490	564	67.00	7.02	11.90	103.38	199.91	1082.70	52.8	0.0	11.51	6.17
10			128.40	30.98	21.65	69.75	22.44	94.8	5.75	4506	512	34.39	4.42	15.30	66.71	152.33	341.63	17.4	12.1	5.82	1.55
6			97.47	64.30	5.52	354.29	76.59	4.0	0.08	129	31	0.79	2.52	14.80	1.58	2.57	3.84	3.7	5.8	0.15	0.03
32			91.91	80.55	11.91	263.10	60.65	176.5	3.36	4415	721	53.28	6.82	12.50	111.03	207.62	1127.00	64.5	0.0	11.85	7.85
5			108.78	73.27	22.94	130.32	37.83	164.3	5.83	7612	816	62.39	6.24	10.70	48.89	87.25	140.49	3.7	18.7	3.71	0.78
62			99.81	68.30	15.42	215.14	52.56	154.5	4.49	4930	722	52.96	6.72	11.80	85.93	0.02	0.06	9.2	3.4	0.00	0.00
77			105.41	70.11	7.30	380.18	81.40	185.2	0.09	27562	6141	92.60	7.88	15.00	50.81	0.46	0.69	32.3	5.0	0.03	0.01
88			93.92	74.43	12.76	268.97	64.02	152.5	3.28	4117	835	45.71	7.52	12.90	107.32	0.02	0.10	50.2	0.2	0.00	0.00
82			98.47	58.12	11.32	299.00	69.84	177.2	1.69	5269	1805	43.33	7.76	13.10	83.23	197.60	819.46	42.8	1.1	12.80	4.87
12			106.17	71.46	8.34	374.25	79.87	182.9	0.09	27133	5598	80.99	8.07	14.70	80.47	205.53	780.76	43.5	0.7	14.62	5.25
13			98.74	73.94	12.91	293.33	69.18	175.4	2.43	4774	1006	42.02	7.17	13.20	111.69	215.87	1171.30	59.5	0.1	16.43	6.46
83			101.66	71.20	15.77	243.56	54.80	171.2	2.21	5671	805	51.78	7.42	12.00	93.93	151.70	377.00	18.0	1.2	6.63	2.35
18			99.04	79.34	13.27	279.78	67.34	184.0	1.86	5114	812	37.63	7.37	13.00	107.73	218.47	1167.30	53.9	0.1	12.80	7.08
73			124.78	97.12	18.78	161.73	38.35	72.2	5.88	5844	931	33.75	5.64	12.80	68.43	125.54	252.82	12.0	13.0	5.39	1.45
54			128.67	102.75	13.52	354.91	93.78	171.2	0.01	37917	20109	164.78	8.54	16.40	128.51	216.91	818.13	43.5	0.5	11.32	5.35
80			136.96	76.41	28.76	94.53	31.85	172.5	5.95	4306	505	39.83	6.22	11.80	33.87	60.20	77.48	1.1	39.9	2.37	0.48
48			148.16	74.28	26.96	29.47	12.95	90.7	5.96	2590	178	16.85	3.94	13.70	23.76	46.43	54.97	0.3	74.9	1.09	0.38
29			138.53	80.77	30.45	65.09	28.82	121.1	5.97	3162	438	35.13	5.87	11.40	23.03	36.71	40.59	0.0	80.4	1.38	0.26
46			162.85	80.21	29.31	37.44	16.51	112.1	5.88	3775	321	39.43	5.13	14.10	42.13	87.58	140.83	4.6	22.3	3.10	0.68
16			166.84	29.98	22.54	95.05	30.22	109.4	4.68	3229	485	43.94	5.95	17.70	60.30	3.95	5.02	4.9	25.1	0.14	0.03
2			133.61	87.79	22.72	42.42	20.59	154.3	5.41	4270	450	47.12	8.06	14.90	83.07	139.01	275.41	5.6	7.9	5.27	1.25
89			148.95	93.83	17.25	376.84	100.44	192.6	0.03	40960	31444	34.39	9.27	17.70	140.79	218.54	644.38	28.8	0.1	11.42	4.81

continued on next page

continued from previous page

	Rand color	Sim color	Heat sum	Hot days	Diurnal diff grow	Precip grow	Wet days grow	Soil depth	Water table depth	Soil N	Organic matter	Soil avail water	CTI	Solar grow $\times 10^7$	EVI grow	FPAR grow	LAI grow	% tree	% bare	GPP grow	RI grow
37			122.36	101.79	17.15	206.70	48.80	179.8	5.27	4637	522	45.58	6.31	13.30	93.41	154.84	340.98	15.3	5.0	6.35	2.04
24			120.61	83.33	7.95	357.38	97.11	4.2	0.12	266	139	1.30	3.87	18.00	6.77	1.43	2.02	2.0	1.1	0.08	0.02
26			122.01	159.33	10.46	33.49	16.98	26.7	1.45	686	25	4.26	9.37	17.00	11.45	7.78	9.13	0.5	13.1	0.18	0.06
7			127.11	100.28	16.46	316.56	81.42	184.6	2.42	3815	711	33.07	7.36	15.10	115.45	197.66	505.52	30.0	1.1	8.18	3.09
45			136.74	93.45	11.72	386.96	104.50	97.5	0.59	5762	1847	31.39	8.15	18.10	117.67	265.03	1080.40	38.2	0.5	18.22	7.39
67			147.46	86.33	13.92	393.09	104.01	81.3	1.41	3056	1026	18.71	7.86	18.00	93.72	0.01	0.01	15.6	5.6	0.00	0.00
38			180.19	141.06	26.62	81.02	30.25	131.0	5.96	3255	317	31.55	5.89	15.00	42.78	77.55	104.02	2.1	39.4	2.28	0.70
34			179.19	160.40	24.45	31.30	14.90	153.5	5.63	3930	169	29.56	8.24	17.10	96.80	118.15	188.65	2.4	10.6	3.16	1.55
28			151.65	91.84	15.69	395.71	107.34	105.1	0.73	4633	1078	26.32	8.93	18.20	121.53	213.55	481.46	22.7	2.6	9.84	3.25
33			200.54	150.08	27.19	27.56	13.78	129.1	5.85	2243	134	17.45	5.54	17.00	24.70	35.31	38.53	0.0	93.5	0.73	0.29

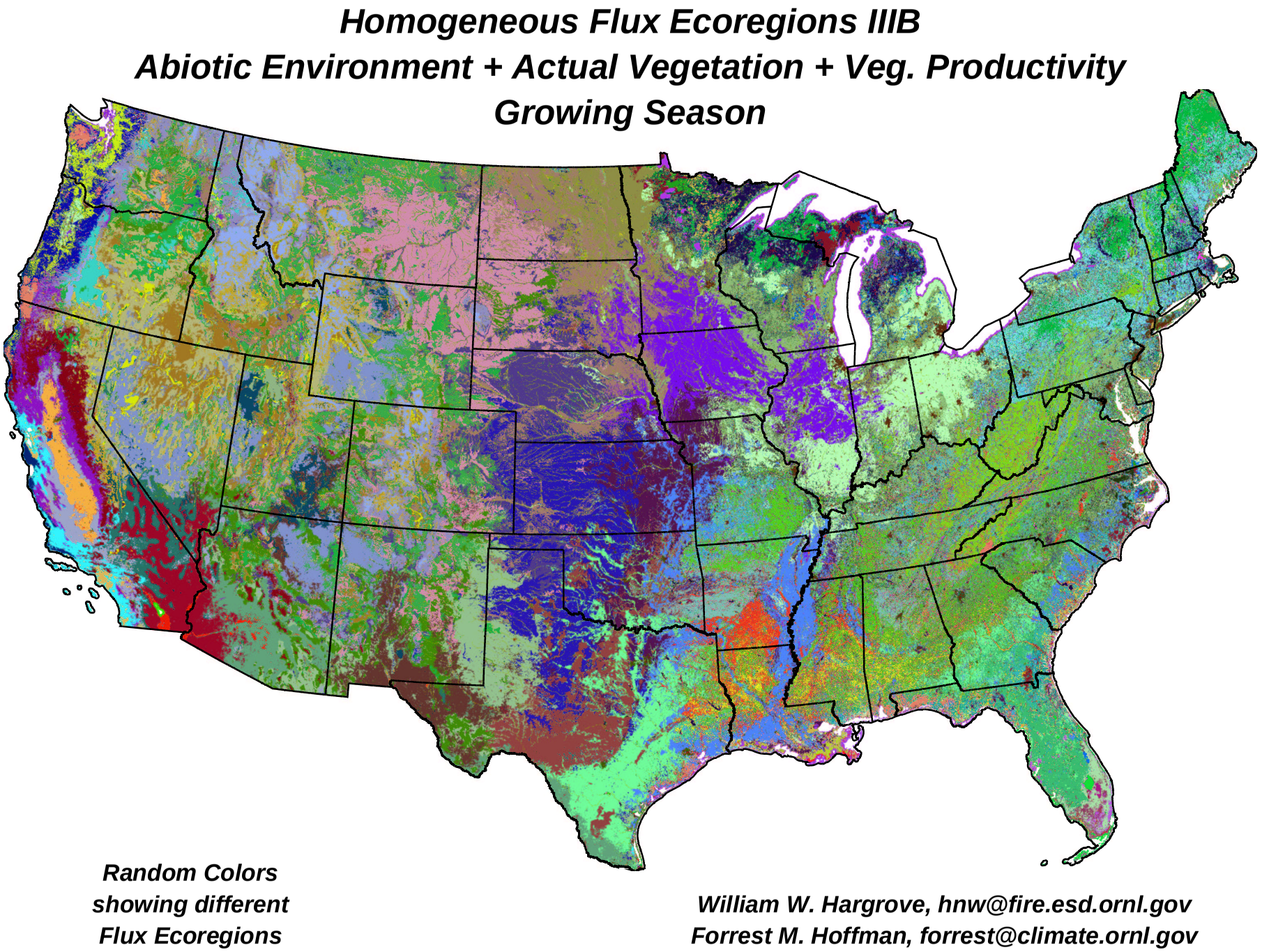

Figure 3.22: Homogeneous Flux Ecoregions IIIB Random Colors

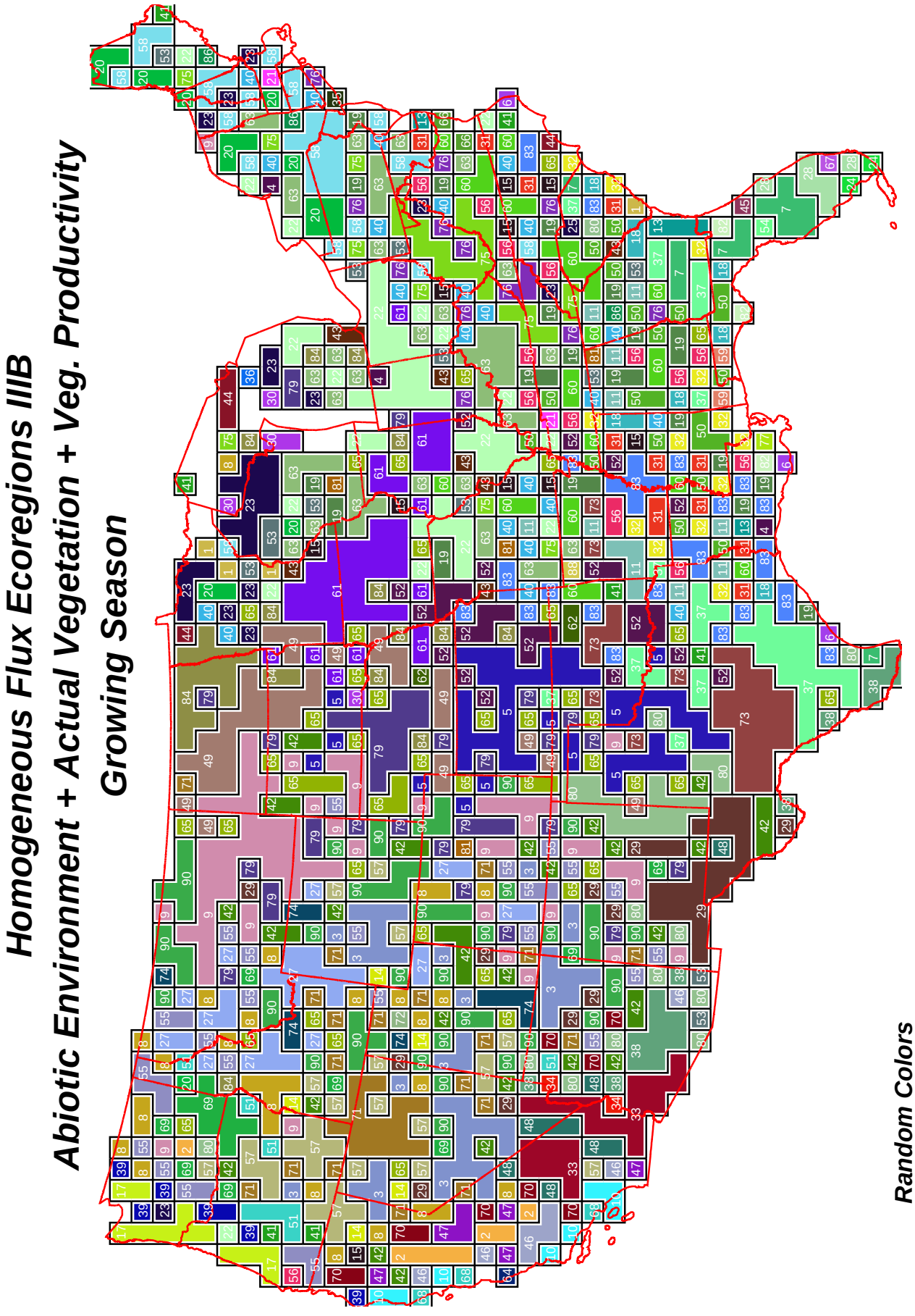

Figure 3.23: Homogeneous Flux Ecoregions IIIB Schematic

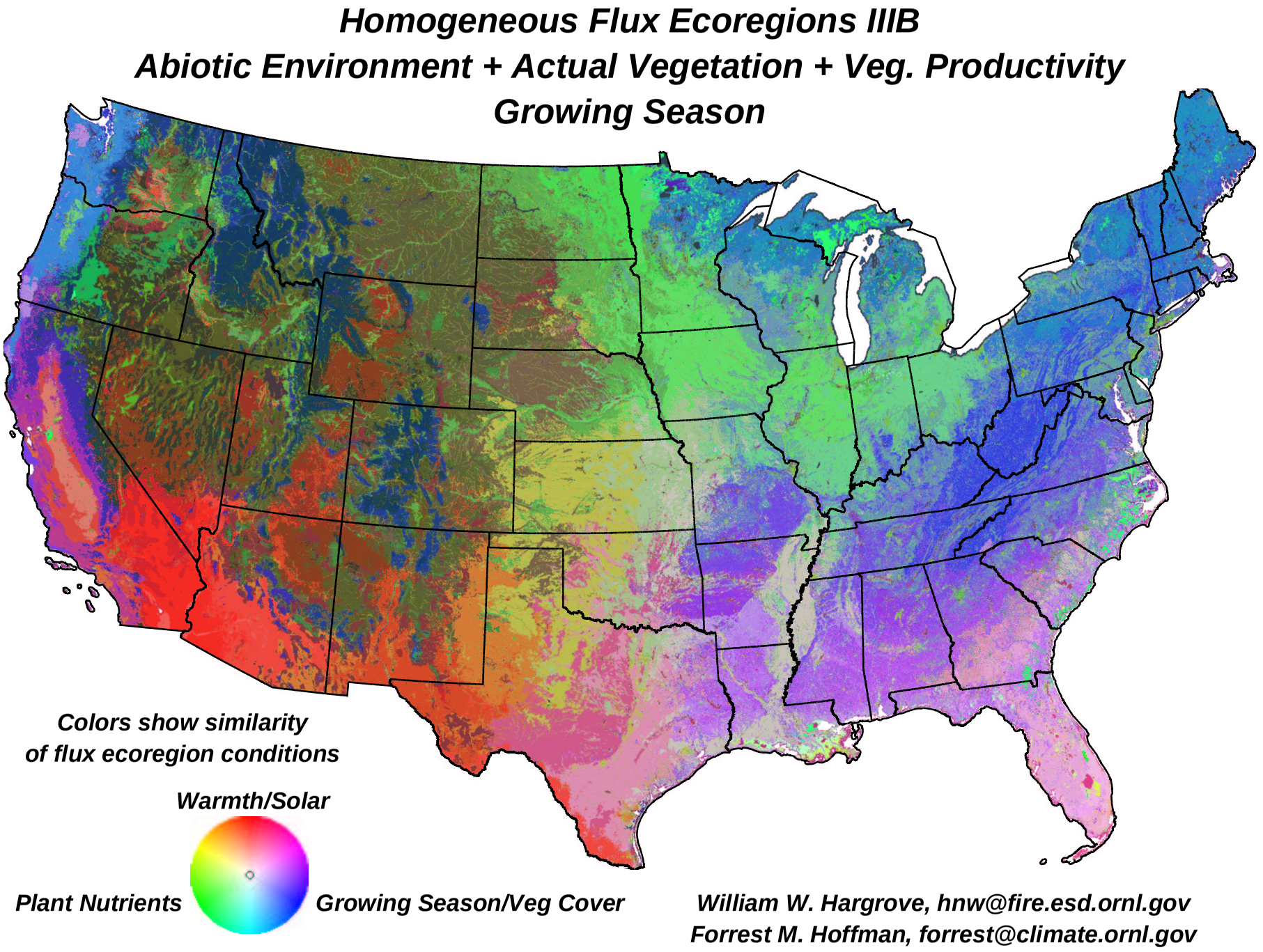

Figure 3.24: Homogeneous Flux Ecoregions IIIB Similarity Colors

Map Layer	Factor 1	Factor 2	Factor 3
Degree-days heat sum above 42°F from daytime land surface temperature during the local growing season	-0.16283	0.95227 ✓	-0.08317
Number of days above 90°F during the local growing season	0.04123	0.93323 ✓	-0.06199
95th percentile of maximum diurnal surface temperature difference during the local growing season	-0.81915 ✓	0.19597	-0.13589
Precipitation sum during the local growing season	0.77385 ✓	0.36270	0.30398
Number of days with measurable precipitation during the local growing season	0.74638 ✓	0.25746	0.34066
Depth of mineral soil	0.25988	0.18288	0.45049 ✓
Depth to water table	-0.34528	-0.00292	-0.46566 ✓
Soil Kjeldahl nitrogen to 50 cm depth	-0.01131	-0.18190	0.79940 ✓
Soil organic matter to 50 cm depth	0.00897	-0.14119	0.72162 ✓
Soil plant-available water holding capacity to 1.5 m	0.24126	-0.05623	0.59204 ✓
Compound Topographic Index (CTI)	-0.00078	0.28905	0.41462 ✓
Total solar insolation during the local growing season, including clouds, aerosols, slope and aspect physiography	0.24897	0.92292 ✓	-0.00364
Enhanced Vegetation Index (EVI) integrated over the local growing season	0.86282 ✓	0.25649	0.27701
Fraction of Photosynthetically Active Radiation (FPAR) absorbed by vegetation integrated over the local growing season	0.89537 ✓	0.22639	0.16584
Leaf Area Index (LAI) integrated over the local growing season	0.91989 ✓	-0.05572	0.01586
Percent tree cover	0.74462 ✓	-0.33492	-0.07913
Percent bare cover	-0.69252 ✓	0.30208	-0.31643
Gross Primary Production (GPP) integrated over the local growing season	0.92998 ✓	0.11396	0.13779
Respiration Index (RI) integrated over the local growing season	0.92353 ✓	0.05065	0.03980
Factor 1: growing season/veg cover **Factor 2: warmth/solar** **Factor 3: plant nutrients**			

Table 3.16: Homogeneous Flux Ecoregions IIIB Rotated Factor Pattern

3.10 Homogeneous Flux Ecoregions IIIC

Table 3.17: Average Conditions Within the 90 Homogeneous Flux Ecoregions for IIIC

	Rand color	Sim color	Cold sum	Cold days	Diurnal diff non-grow	Precip non-grow	Wet days non-grow	Soil depth	Water table depth	Soil N	Organic matter	Soil avail water	CTI	Solar non-grow $\times 10^7$	EVI non-grow	FPAR non-grow	LAI non-grow	% tree	% bare	GPP non-grow	RI non-grow
45			0.53	10.42	4.67	48.82	13.13	4.3	0.22	278	76	1.81	3.25	1.63	2.63	5.35	11.22	5.8	3.4	0.15	0.04
54			0.46	7.22	12.75	39.85	11.40	173.3	1.14	5197	1148	35.83	7.91	1.66	12.51	25.51	55.44	24.7	2.1	0.57	0.17
7			3.10	34.25	12.37	138.35	32.35	179.7	2.57	4330	703	45.16	6.96	3.84	40.24	94.38	352.53	64.6	0.0	2.83	1.20
66			4.55	42.99	13.12	145.79	35.24	181.5	1.76	5137	871	45.96	7.25	4.12	38.20	98.32	313.06	52.9	0.1	2.71	0.80
26			4.87	46.08	12.97	167.67	36.90	179.0	4.93	3536	504	51.27	6.03	4.22	39.44	102.10	323.65	58.7	0.0	2.66	0.82
61			6.33	48.41	12.71	146.22	35.75	174.7	1.71	5265	820	61.21	8.05	4.00	31.76	79.50	187.97	56.8	0.1	1.50	0.42
15			2.92	21.80	17.51	40.64	15.69	169.4	5.63	4802	559	46.11	6.59	2.92	20.73	35.85	59.80	8.3	12.9	0.62	0.15
42			4.94	24.44	19.52	14.86	7.49	121.4	5.83	2219	146	17.85	5.19	3.13	7.22	10.96	12.12	0.1	90.8	0.18	0.03
14			7.47	54.69	15.72	117.11	31.54	181.0	4.73	4176	522	39.70	6.12	4.48	34.86	68.19	121.50	17.2	5.0	1.04	0.28
51			19.32	90.17	14.65	167.77	54.41	2.5	0.23	82	19	0.55	3.24	4.66	6.27	7.82	13.94	6.0	2.5	0.16	0.04
44			10.84	68.82	15.18	161.18	40.56	158.8	5.11	3523	484	56.87	5.81	4.76	40.57	90.81	188.06	46.7	0.2	1.33	0.40
63			6.06	46.59	17.23	60.94	20.06	63.0	5.94	4933	677	27.17	4.67	4.61	28.44	56.24	102.47	12.0	17.0	1.04	0.24
72			11.82	77.06	15.23	183.89	45.78	170.0	4.98	3250	498	60.64	5.85	5.17	45.11	114.22	336.47	38.5	0.3	2.72	0.67
10			3.93	31.87	11.30	96.67	26.97	170.9	0.46	17755	9493	78.89	7.98	3.24	31.19	75.76	264.52	58.2	0.5	2.29	0.81
60			30.54	100.04	15.65	111.86	43.86	0.4	0.34	19	8	0.20	8.27	4.94	27.34	73.03	168.85	29.9	5.6	1.39	0.34
62			14.42	89.35	15.37	181.16	48.76	155.3	5.35	3482	551	57.92	5.27	5.34	42.91	109.37	296.53	69.2	0.0	2.53	0.57
70			12.87	79.53	15.47	190.11	46.63	91.4	5.69	4229	511	44.61	5.46	5.25	43.46	111.91	313.10	48.4	0.6	2.69	0.64
27			4.09	27.38	10.69	106.58	27.52	175.4	0.13	28865	5073	74.34	8.25	2.90	19.13	44.64	110.25	41.8	1.5	1.11	0.32
37			18.21	53.79	13.83	308.36	96.31	117.8	5.33	7129	1310	57.53	4.01	4.35	59.02	114.03	396.81	69.0	0.0	2.46	1.52
31			8.33	53.64	11.22	119.60	36.80	178.8	0.31	7530	13046	32.47	8.30	4.04	22.98	52.36	118.26	41.5	3.0	1.22	0.31
33			19.82	88.52	16.25	142.72	41.72	163.7	2.18	5804	846	64.03	6.92	4.85	38.07	78.29	134.26	9.9	1.1	0.93	0.26
23			21.21	56.48	15.24	467.16	104.58	122.8	5.41	7428	1512	60.09	3.97	4.49	63.41	123.79	496.13	68.5	0.0	2.58	1.43
17			22.24	67.54	14.42	477.86	114.41	117.1	5.57	7711	1434	57.20	3.66	4.49	61.71	112.75	356.24	71.0	0.0	2.98	1.81
55			38.92	121.16	15.81	137.54	55.47	3.1	0.73	80	21	0.83	8.00	5.72	24.65	0.56	2.09	19.9	3.0	0.01	0.00
40			23.89	68.29	14.69	735.76	133.80	117.4	5.52	7779	1478	53.43	3.59	4.58	66.80	124.35	449.04	69.9	0.0	2.84	1.77
57			15.50	118.06	13.96	246.62	69.25	123.1	5.75	5278	811	49.08	3.84	6.74	56.41	137.13	422.47	69.2	0.2	3.96	1.00
53			32.53	110.43	16.22	166.89	58.69	143.9	4.25	4829	847	47.38	6.33	5.59	42.46	0.42	1.10	55.8	0.4	0.01	0.00
35			24.48	58.88	17.65	269.42	100.04	132.4	4.16	6761	1546	58.20	5.93	4.56	58.07	115.67	354.12	41.9	0.6	1.75	0.72
30			15.48	69.63	28.06	34.94	18.00	147.2	5.92	3225	348	33.06	5.93	5.99	19.82	34.10	43.17	1.2	49.5	0.66	0.12
5			45.72	143.95	12.75	113.89	62.64	2.1	0.19	23	6	0.19	10.13	6.26	0.98	1.19	1.70	1.9	1.3	0.02	0.00
89			19.37	121.45	16.02	181.16	73.65	115.4	5.50	5088	695	50.07	4.74	5.96	48.31	119.97	334.93	71.9	0.1	2.80	0.66
84			20.82	109.40	13.76	335.99	71.14	107.0	5.85	3606	908	41.20	3.68	7.49	65.11	152.84	537.09	47.1	0.4	4.47	1.69
29			29.54	107.00	18.05	106.32	42.28	147.9	4.39	5170	886	46.70	6.66	5.54	21.05	0.77	3.11	9.2	9.1	0.02	0.01
8			24.13	80.46	14.68	334.48	107.49	125.2	5.44	6843	1294	57.90	4.10	5.86	77.53	156.82	721.27	64.6	0.0	2.96	1.66
19			25.13	110.42	17.18	175.05	58.65	147.6	4.95	4153	699	54.76	5.66	5.98	63.64	146.73	578.00	16.8	0.3	2.91	0.87
25			25.67	111.31	17.46	150.47	52.27	147.8	5.07	4599	730	57.74	6.03	5.60	54.45	98.16	179.03	10.7	1.9	1.27	0.36
49			28.80	114.83	18.04	146.44	58.28	148.1	3.76	5133	983	53.23	6.57	5.41	41.55	0.33	1.22	10.1	3.3	0.01	0.00
34			28.98	117.94	16.45	160.21	60.93	153.3	4.27	4713	881	54.01	5.98	5.66	51.65	136.39	430.90	22.0	0.1	1.49	0.71
12			21.08	110.71	14.21	342.66	68.70	113.8	5.92	3851	987	50.01	3.69	8.71	71.51	172.85	720.55	45.9	0.3	4.33	1.52
39			31.31	121.25	21.20	86.12	37.83	143.3	5.10	5155	718	45.77	13.21	6.21	31.20	65.56	110.49	11.1	16.6	0.95	0.22
83			24.99	113.51	21.21	65.04	25.86	149.0	5.62	7894	941	67.06	6.13	6.00	35.46	61.58	83.12	5.2	13.9	0.80	0.17
16			36.86	149.83	15.84	200.00	70.35	135.9	3.94	6416	932	36.35	4.70	5.98	53.38	138.73	415.22	67.0	0.0	2.56	0.66
80			28.16	116.94	15.27	369.54	74.23	100.8	5.88	3249	736	31.55	3.43	8.45	48.15	117.34	307.31	34.8	6.2	2.72	0.69
88			31.30	134.26	16.90	175.23	70.29	136.4	4.72	4821	866	46.70	5.35	6.34	53.80	139.23	426.16	17.7	1.1	2.97	0.76
52			31.52	85.87	16.37	541.58	129.43	121.3	5.35	8073	1402	55.44	3.66	6.15	76.20	162.99	788.23	61.2	0.4	2.52	1.24
24			42.70	144.96	16.67	141.40	64.60	147.8	4.19	5708	1024	50.01	5.89	6.21	49.40	139.55	410.07	58.4	0.0	1.35	0.63
90			37.75	136.24	19.49	140.37	68.27	155.4	2.36	6549	1381	56.85	6.90	5.54	36.07	81.76	132.26	6.8	1.6	0.87	0.23
73			32.39	156.61	13.75	265.70	93.25	119.6	5.77	4637	790	44.35	3.49	8.37	73.32	165.43	551.50	61.8	0.1	4.86	2.10
18			43.71	152.16	17.63	141.23	67.38	140.0	4.57	5500	1020	47.36	5.24	6.36	48.69	101.23	191.56	53.7	0.8	1.23	0.36
78			38.94	149.25	19.24	188.20	95.18	139.0	3.49	4923	950	55.66	4.88	6.30	57.31	142.15	447.84	64.7	0.0	2.86	0.77
87			45.49	119.38	13.64	944.12	154.92	110.7	5.73	5227	751	34.12	2.60	6.32	32.29	86.96	261.67	46.8	14.2	1.49	0.61
9			24.63	124.73	27.27	34.73	22.85	62.4	5.93	2987	284	23.37	4.94	8.08	18.67	32.37	36.17	0.0	83.2	0.56	0.09
86			42.87	145.14	20.63	96.95	43.41	154.8	4.14	8081	1621	77.26	6.36	5.85	23.94	57.51	74.44	3.7	2.3	0.57	0.12
69			46.88	118.80	15.27	611.45	141.21	118.3	5.43	6743	912	40.27	2.76	6.25	35.80	95.86	247.44	53.2	5.3	1.37	0.51
59			7.99	66.48	12.35	144.89	46.33	183.2	0.70	5305	31293	79.00	8.01	4.83	47.42	120.11	405.60	54.6	0.1	3.07	0.88
28			24.18	137.41	26.59	47.36	26.73	57.1	5.96	4129	342	23.68	4.47	8.74	26.18	53.76	67.99	2.5	41.0	1.00	0.17
50			36.76	151.66	26.15	56.65	29.55	155.0	5.75	4770	507	29.92	5.98	7.32	29.85	54.03	65.63	2.3	22.6	0.73	0.14
68			54.33	177.78	15.43	205.56	82.37	137.2	3.44	6405	954	42.92	4.93	6.92	72.82	173.12	627.37	68.6	0.0	2.84	0.94
79			29.21	134.52	30.33	32.85	24.21	151.5	5.55	2878	311	27.38	6.25	8.49	18.18	28.96	31.82	0.0	85.8	0.52	0.08
71			8.46	64.69	13.25	139.69	44.85	182.2	0.68	6598	32020	80.35	8.06	4.67	41.96	92.72	220.02	30.2	0.2	1.30	0.44
41			55.29	169.36	17.83	168.69	94.53	154.8	4.89	4370	973	31.15	5.63	7.01	53.12	148.27	435.22	50.9	0.8	2.34	0.66
6			44.15	139.35	23.58	106.63	70.42	124.5	5.63	5000	706	54.77	4.95	6.88	40.07	77.39	120.87	8.4	18.9	1.08	0.24
75			46.25	151.43	14.54	468.99	133.66	127.0	5.74	9259	835	45.62	3.10	7.11	57.66	132.72	353.82	67.3	0.2	3.31	1.16
56			29.87	144.95	29.84	41.66	26.39	154.0	5.92	4762	463	48.76	5.84	8.77	24.04	44.65	52.12	1.1	40.0	0.78	0.13
11			60.26	178.67	14.12	153.63	98.33	0.0	-0.00	-0	0	-0.00	12.04	7.43	186.36	0.00	0.00	0.0	-0.0	-0.00	-0.00
65			52.82	187.49	15.07	203.43	99.43	140.0	5.56	4569	732	38.37	3.88	8.13	72.65	165.66	526.10	61.7	0.2	3.42	1.28
3			31.14	176.72	23.08	76.89	38.85	102.2	5.97	4205	434	32.42	3.87	10.80	43.31	109.29	193.73	15.8	20.3	2.26	0.45
36			49.92	175.09	24.16	66.33	43.09	96.9	5.95	4183	599	44.28	4.82	7.46	27.55	60.08	77.42	2.1	33.2	0.75	0.15
76			60.45	185.95	16.35	191.65	96.64	138.8	3.67	6540	1423	45.25	4.96	7.52	65.47	141.06	461.43	66.6	0.1	3.03	0.87
46			65.86	186.91	17.06	125.18	68.87	141.4	3.81	7935	1339	44.31	6.42	7.42	53.69	159.63	452.23	56.2	0.4	2.48	0.61
67			57.90	178.02	16.71	227.06	99.69	138.0	4.51	5545	970	40.15	4.51	8.13	60.93	192.57	800.74	45.0	1.1	2.59	0.84
20			60.55	178.34	25.44	60.67	38.40	128.3	5.68	5522	946	46.39	5.87	7.04	24.48	58.67	73.98	3.3	19.1	0.63	0.13
64			66.11	180.08	20.76	70.00	43.19	151.5	3.85	9982	1710	47.24	7.52	6.77	22.42	57.64	76.22	6.5	7.4	0.57	0.11
32			39.37	200.47	18.03	145.95	58.85	129.7	5.92	4208	500	39.56	3.67	12.10	65.64	183.54	564.50	41.4	1.9	4.49	1.46
1			62.75	218.02	15.95	232.60	103.73	135.1	5.79	4392	642	30.49	3.18	8.31	51.15	126.30	305.06	51.5	5.0	3.18	0.78
74			29.16	94.85	14.87	107.40	52.14	165.8	0.33	35318	17567	97.59	7.88	4.71	36.51	88.29	252.10	46.3	0.5	1.65	0.50
22			60.15	189.29	28.89	49.20	36.73	115.5	5.86	3392	347	34.82	7.57	8.96	17.94	39.25	43.90	0.1	76.4	0.54	0.09
85			47.25	177.30	28.54	90.67	57.17	77.7	5.92	4390	643	33.50	4.92	10.20	29.92	72.72	100.59	3.5	36.8	1.41	0.23
81			55.62	197.74	21.07	135.91	63.27	114.3	5.93	4982	848	36.25	3.01	11.80	42.66	89.20	155.61	20.4	17.1	1.72	0.38
21			57.44	188.17	29.67	75.74	52.75	146.6	4.16	5295	753	39.17	7.90	10.10	46.67	90.64	140.20	4.1	17.9	1.68	0.35

continued on next page

continued from previous page

	Rand color	Sim color	Cold sum	Cold days	Diurnal diff non-grow	Precip non-grow	Wet days non-grow	Soil depth	Water table depth	Soil N	Organic matter	Soil avail water	CTI	Solar non-grow $\times 10^7$	EVI non-grow	FPAR non-grow	LAI non-grow	% tree	% bare	GPP non-grow	RI non-grow
43			67.39	231.84	17.42	167.30	78.89	133.2	5.87	3774	613	31.38	3.54	11.40	60.82	151.23	382.93	48.8	4.8	3.66	0.86
48			65.29	191.84	27.75	94.17	57.85	128.8	5.88	4625	664	40.25	4.75	9.72	25.95	65.04	89.64	3.2	33.9	1.04	0.19
13			49.93	195.94	20.79	173.91	86.91	126.4	5.67	9665	446	68.11	4.62	11.20	64.14	165.98	431.58	27.8	6.6	4.15	0.98
2			72.02	219.56	15.60	382.32	131.54	125.1	5.81	5384	569	28.48	2.88	10.00	32.36	86.56	177.94	34.0	12.6	1.85	0.39
4			68.64	190.46	17.19	116.82	68.21	151.2	0.79	10492	15751	45.96	7.34	7.49	54.02	162.46	460.64	50.7	0.2	2.49	0.62
58			71.79	217.66	18.18	256.48	103.48	126.5	5.81	4926	719	34.20	3.45	11.50	44.25	166.39	416.79	30.8	9.6	2.59	0.60
77			61.03	175.95	17.07	125.90	72.43	151.1	1.24	24357	10727	73.33	7.34	6.92	51.33	137.95	389.70	49.7	0.4	2.09	0.58
82			77.29	237.06	18.07	233.25	102.27	130.1	5.80	4472	732	31.50	3.42	12.10	44.25	101.83	212.59	28.4	12.4	2.49	0.52
47			34.37	113.51	18.05	98.67	52.76	162.6	0.16	38450	24702	47.56	8.21	4.64	29.99	72.16	139.02	26.4	0.4	0.84	0.24
38			82.17	243.98	17.61	275.47	95.62	125.9	5.72	3942	636	20.54	2.63	14.00	16.78	55.99	85.78	6.2	40.4	1.25	0.22

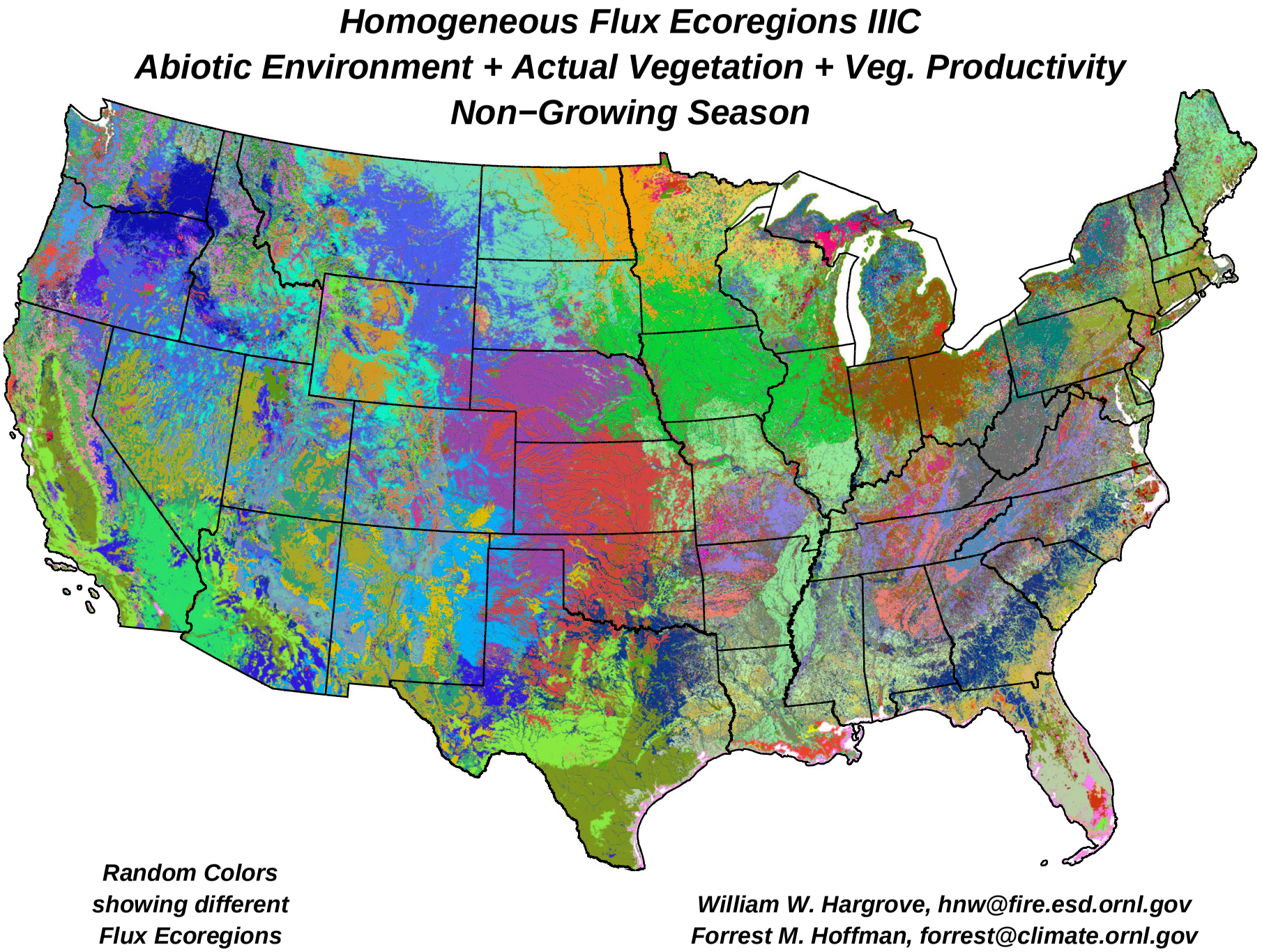

Figure 3.25: Homogeneous Flux Ecoregions IIIC Random Colors

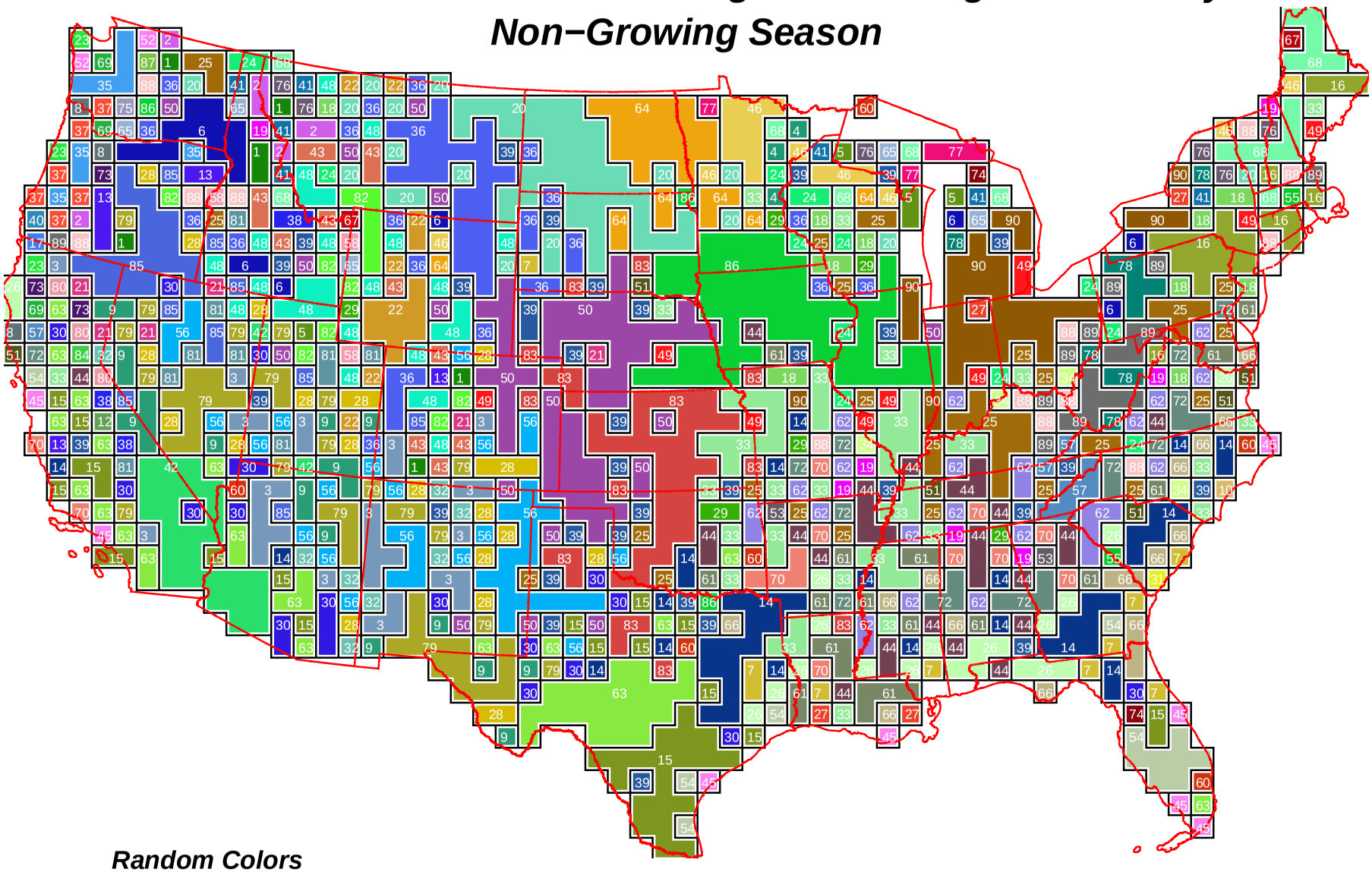

Figure 3.26: Homogeneous Flux Ecoregions IIIC Schematic

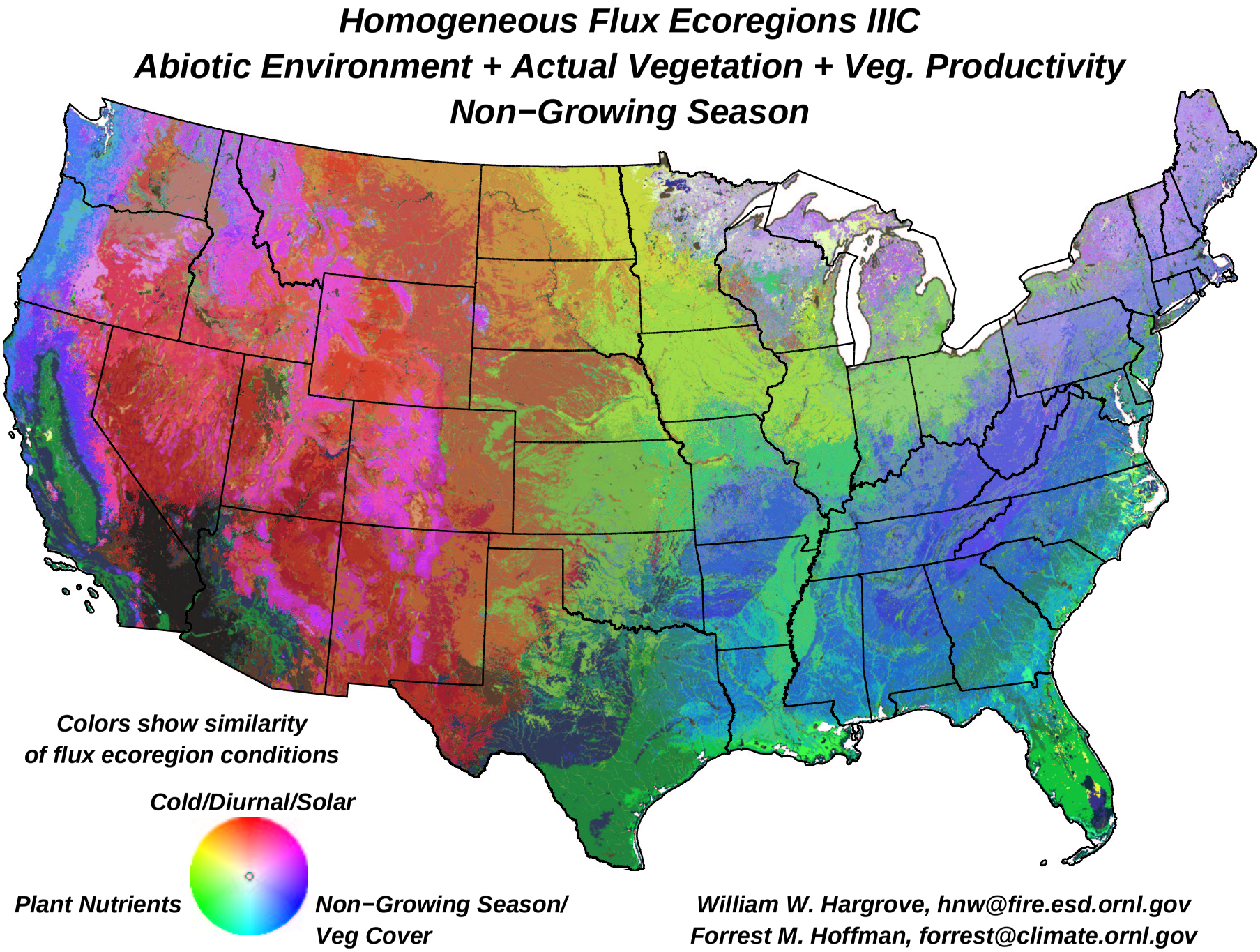

Figure 3.27: Homogeneous Flux Ecoregions IIIC Similarity Colors

Map Layer	Factor 1	Factor 2	Factor 3
Degree-days cold sum below 42°F from nighttime land surface temperature during the local non-growing season	0.06735	0.89883 ✓	0.08698
Number of days below 32°F during the local non-growing season	0.11542	0.95204 ✓	-0.03320
95th percentile of maximum diurnal surface temperature difference during the local non-growing season	-0.52003	0.62246 ✓	-0.23832
Precipitation sum during the local non-growing season	0.77912 ✓	-0.00800	0.07546
Number of days with measurable precipitation during the local non-growing season	0.72067 ✓	0.43958	0.09837
Depth of mineral soil	0.07122	-0.16943	0.47576 ✓
Depth to water table	-0.05660	0.28991	-0.53252 ✓
Soil Kjeldahl nitrogen to 50 cm depth	0.03252	0.20319	0.78955 ✓
Soil organic matter to 50 cm depth	0.03421	0.13036	0.71260 ✓
Soil plant-available water holding capacity to 1.5 m	0.13722	-0.05028	0.62228 ✓
Compound Topographic Index (CTI)	-0.26407	-0.16668	0.37981 ✓
Total solar insolation during the local non-growing season, including clouds, aerosols, slope and aspect physiography	0.09623	0.87434 ✓	-0.28031
Enhanced Vegetation Index (EVI) integrated over the local non-growing season	0.87154 ✓	0.13015	0.08251
Fraction of Photosynthetically Active Radiation (FPAR) absorbed by vegetation integrated over the local non-growing season	0.91577 ✓	0.18121	0.07936
Leaf Area Index (LAI) integrated over the local non-growing season	0.93271 ✓	0.01960	0.04369
Percent tree cover	0.79602 ✓	-0.23048	0.09790
Percent bare cover	-0.56931 ✓	0.25474	-0.46912
Gross Primary Production (GPP) integrated over the local non-growing season	0.90921 ✓	0.06404	-0.08404
Respiration Index (RI) integrated over the local non-growing season	0.92022 ✓	-0.05403	-0.02195
Factor 1: nongrowing season/veg cover **Factor 2: cold/diurnal/solar** **Factor 3: plant nutrients**			

Table 3.18: Homogeneous Flux Ecoregions IIIC Rotated Factor Pattern

Chapter 4

Discussion

Though their appearance is strikingly different, the Similarity Color maps are digitally identical to the randomly colored maps, except for the color table. The Similarity Colors are statistically derived to show the similarity of different flux ecoregions to each other. One has no control of how the variable loadings occur in PCA, yet variable loadings onto PCA factors were interpretable in every PCA used to produce Similarity Colors for alternative flux ecoregions shown here.

Most of the three-factor PCAs used to produce Similarity Colors explained only about 68% of the variance. In a sense, we worked hard to keep this number low by carefully constructing the input maps to minimize correlation and maximize uniqueness. This care, however, means that the Similarity Color maps miss 30% of the variance in the original flux environment data. This is an inescapable consequence of trying to pack all of the multivariate information into only three available colors. Still, the Similarity Color maps that result are useful for seeing regional patterns. They also make the selection of a particular number of flux ecoregions less sensitive.

We created flux regionalizations IIA and IIIA by mixing growing season- and non-growing season-divided parameters together into a single clustering pass. When we perform the three-factor PCA for Similarity Colors, the statistical process largely undoes this original mixing, and the first two principal components become growing season and non-growing season. These first two factors are nearly equal in explanatory power. This result is not surprising, and verifies that the statistical method is working. The same seasonal splitting would probably have occurred even if we had included annualized versions of these variables.

The exception to this seasonal unmixing is that growing season LAI, both seasonal GPPs and both seasonal RIs load with non-growing season variables in IIIA. These variables can be interpreted as ecosystem productivity. The start of this vegetation productivity loading can also be seen in regionalization IIA, where growing season LAI loads with non-growing season variables. Conifers have higher LAI than broadleaf trees year-round, and this may explain why growing season LAI loads with non-growing season variables and productivity. Conditions during the last non-growing season may also determine the leaf crop in the next growing season.

4.1 Patterns in Flux Ecoregions

Flux ecoregions produced by abiotic forcing factors alone (Series I) are spatially divided, and tend to follow physiographic or edaphic features. With the addition of information about existing vegetation, the flux ecoregions of Series II become more spatially cohesive and globular (Random Color maps in Sections 3.5, 3.6, and 3.7). At the same time, however, the Series II flux ecoregions become more speckled internally. This speckling is particularly noticeable in the Southeast and the Pacific Northwest, but is conspicuously absent in the desert Southwest. With the addition of ecosystem productivity information, Series III flux ecoregions (Random Color maps in Sections 3.8, 3.9, and 3.10) are similar to Series II, but show even more speckling in some regions.

Vegetation added in Series II acts as an integrator, combining flux regions that were different on the basis of abiotic factors alone. Our selected level of division into 90 flux ecoregions apparently overdivided the physical environmental differences beyond the level of specificity for most vegetation. Most plants were sufficient generalists to live in more than one of the flux ecoregions generated on the basis of abiotic factors alone. We conservatively divided the CONUS on the basis of abiotic conditions into more flux ecoregions than are discriminated by the vegetation.

We believe that the speckling is due to variations in land use, irrigation, and fertilization caused by anthropogenic management. In the Southwest, there is little anthropogenic influence. In the upper Midwest, the anthropogenic influence is homogeneously ubiquitous. But in the Pacific Northwest and in the Southeast, intensive and disparate management practices give the flux ecoregions a speckled appearance. This speckling greatly complicates the schematic maps of Series II and III flux ecoregions in these areas.

None of the alternative flux ecoregions is inherently better than any of the others. While the Series I maps are more certain, the Series III maps are more sophisticated, and come closer to approximating unmeasured NEE. Which will prove more useful for estimating flux is still unknown. Since they are empirical results, it is not necessary to make a correct interpretation of these flux ecoregion maps. Their use as a statistical foundation for estimating flux in subsequent steps does not require a complete understanding of why the homogeneous flux ecoregions look the way that they do.

Our use of color is strictly for presentation; the entire MGC process is quantitative. For example, the similarity of any two flux ecoregions can be calculated by taking the standardized coordinates of their centroids, as shown in the color table legends, and calculating the Euclidean distance between them. Once met with favorable reviews, we will use these homogeneous flux ecoregions as a basis for estimating flux values across the U.S. continent seasonally.

Chapter 5

AmeriFlux-Specific Future Products

The flux ecoregions establish a foundation and a statistical basis for several future products. All future deliverables are specific to the AmeriFlux network or to the goals of the AmeriFlux Program and NACP. Completed work described here comprises Task I, "Generating Flux-Relevant Ecoregions for the United States," from our original proposal. Four additional unfunded tasks remain: "Network Analysis of Existing AmeriFlux Towers," "Quantifying Flux Responses Along Each Environmental Axis," "Jackknifing to Estimate Flux Measurements at Withheld Towers," and "Mapping Flux Estimates for the United States." Each task sequentially utilizes the products produced in the last, starting with the flux ecoregions described here. Funding for the four remaining tasks is pending outcome of external review of this document describing the flux ecoregions.

In Task II, we will perform a separate analysis of the AmeriFlux network for each of the nine flux regionalizations produced in Task I. In Task III, we will use another statistical technique, **Metric Multi-Dimensional Scaling (MMDS)**, to estimate the changes in ecosystem flux that occur with unit changes along each axis of the data space used to create each of the regionalizations. These flux changes will provide a means for projecting existing flux measurements into new flux ecoregions that do not currently have existing flux towers by utilizing the quantitative similarity of the flux environments in those new flux ecoregions with flux ecoregions already having measurements. In Task IV, we will specifically withhold the measured flux values from certain tower locations, regenerate MMDS weights, and compare estimates of flux with the excluded flux measurements at that tower location. This task will provide an estimate of error and statistical sensitivity for the interpolated grid of flux estimates. Finally, Task V will involve the production of continuous gridded estimates of seasonal flux for each of the nine flux regionalizations produced in Task I.

5.1 Network Analysis of AmeriFlux Sites

When ecoregions are quantitatively derived, one can select a single ecoregion of interest, and then produce a sorted list of the similarity of all other ecoregions to the one selected. The chosen ecoregion establishes an origin in data space, and, using the Euclidean distance from this origin to the centroid of every other ecoregion, pairwise similarity measures can be calculated. Coding these pairwise similarity values as gray levels, a map can be made showing the degree of similarity of all ecoregions to any selected ecoregion.

If we invert the quantitative comparison concept to consider non-representativeness in the context of an existing network of sites or sample locations, we can quantify how well a particular established network is representative of a larger map which contains it. A network in this sense consists of a geographic constellation of sites or facilities. Network analysis shows how well the sampled environments represent the rest of the map, and identifies the best locations for new sites or installations. The best location for additional sites will be in places that are the least well-represented by the network of existing sites.

Instead of a one-to-one centroid comparison, we determine how different each ecoregion is from the most similar network site or sample. For each ecoregion in the map, we find the Euclidean distance in data space to the single closest ecoregion that contains a site from the network. Longer distances are coded to darker gray levels. Because this method quantifies coverage or presence of sites, sites will always sit within well-represented ecoregions, which will be colored white.

Maps showing the geographic areas represented by each individual site in the network can be generated, and uniqueness values can be calculated for each site based on the marginal representation it adds to the network. Quantifying the contribution of each site to network representation can minimize the impact of site elimination on representation. Finally, a network with a given number of sites can be designed which is theoretically optimal, having the highest possible representation of environmental conditions on a map (given that number of underlying ecoregions).

Networks of installations like AmeriFlux represent significant investments of research capital. Network analysis, as an outgrowth of the quantitative development of flux ecoregions, can provide objective guidance about the design, performance, and modification of such networks, and can improve on more idiosyncratic design approaches.

If funded for the second part of this work, we will repeat an earlier proof-of-concept network analysis of AmeriFlux tower locations (Hargrove et al., 2003) but this time using ecoregions specifically developed with regard to carbon flux. Whereas Hargrove et al. used a generalized set of ecoregions, we will now use the customized flux regionalizations produced specifically for this purpose. For each of the alternative flux regionalizations in each season, we will produce a map showing quantitatively how well the existing AmeriFlux towers represent the flux environments within the United States. These maps are based on finding, for each flux ecoregion in the map, the Euclidean distance in data space to the single closest flux ecoregion which contains a tower from the AmeriFlux network. This distance is coded to a gray level, and the map which results shows how well the existing tower network "samples" the flux environments in the map. Darker areas in these maps represent areas which are poorly represented by the existing AmeriFlux network.

Besides showing how well the AmeriFlux network represents the rest of the map, the analysis will show the best locations for new sites or installations. Adding new towers in these darker areas would dramatically improve how well the AmeriFlux observation network represents the flux conditions within the United States.

We will find the five best additional locations for AmeriFlux towers within the CONUS. These five locations will be selected such that they optimize the additional representation of the AmeriFlux network across all of the flux environments within the CONUS. Note that these five locations will be different than if only four additional locations were specified, or if five additional towers were added one by one. By calculating the addition of five towers at once, the locations will be more optimized, and more total representativeness will be added to the AmeriFlux network than if the additional sites had been added sequentially,k even if in practice they will be added over many years.

We will generate maps showing the geographic areas represented by each of the 52 individual AmeriFlux tower locations. These maps will make it easy to see what flux environments are represented by carbon flux measurements made at each tower location. We will also calculate uniqueness values for each existing tower location based on the marginal representation that tower adds to the AmeriFlux network.

5.2 Similarity Trees for AmeriFlux Tower Locations

Using conditions from our input maps describing the flux environments at each of the tower sites, we will construct a similarity tree for all AmeriFlux sites using exhaustive hierarchical clustering. There will be one tree for each of the nine regionalizations described here. These trees will show the degree of similarity of the flux environments for all AmeriFlux tower locations, *i.e.*, tower sites with similar flux environments will be located nearby on the same branch of the tree. Because this analysis is independent of the flux ecoregions described here, the similarity trees can provide independent corroboration of the uniqueness values calculated for each site from the network analysis.

5.3 Statistical Scaling of AmeriFlux Flux Measurements

We will use the quantitative similarity of the suite of flux-relevant ecosystem characteristics to extrapolate existing flux measurements to estimate fluxes within unmeasured flux ecoregions. However, a unit change in precipitation may result in a greater change in carbon flux than a unit change in temperature. The form of the flux response may be non-linear, or even non-monotonic along some axes. We will use Metric Multi-Dimensional Scaling (MMDS) to determine a transformation of data space which best corresponds to similarities in flux measurements among AmeriFlux towers. The goal of an MMDS projection is to optimize the representations so that the distances between the items in the transformed space will be as close to the original distances as possible. The degree of correspondence between the distances among points implied by MMDS map and the matrix input by the user is inversely measured by a stress function. The iterative MMDS procedure strives to maximize the preservation of similarity distances, while at the same time minimizing overall stress. MMDS will determine the nature of the multidimensional relationship of carbon flux with respect to each axis of the data space.

The optimized weight coefficients found by MMDS using all AmeriFlux towers will be used to re-estimate time-integrated flux values measured at all towers. Comparison of these estimates with the known measured values will provide a sense of the estimation error. For a select subset of towers in each of the three flux regionalizations, we will drop the measurement from a single tower, use MMDS to find a new optimum transformation, and use the new weights to predict the value at the missing tower. Repeated jackknifing will provide additional measures of estimation errors. The uniqueness of the tower to the AmeriFlux network will be indicated by the magnitude of the change in transformation weights when that tower is dropped in the jackknife exercise.

Once we receive funding we will use these flux ecoregions to quantify the similarity of flux ecoregions, analyze the representativeness of the AmeriFlux network, generate maps showing geographic areas represented by selected AmeriFlux towers, and suggest optimum locations for additional flux towers which would maximally improve the representativeness of the existing AmeriFlux sampling network. We will also use the quantified similarity of the suite of flux-relevant ecosystem characteristics to extrapolate

existing flux measurements to estimate fluxes within unmeasured flux ecoregions. Stopping short of these goals now that we have successfully created the flux ecoregions would make little scientific sense.

Acknowledgments

The authors would like to thank Craig Brandt, Environmental Sciences Division, for his assistance in writing SAS code to untransform the final flux ecoregion centroids from PCA space back into original measurement units. Dr. Maosheng Zhao provided advice and explanation of MODIS practical details. We would also like to thank Dr. Bob Cook, who provided an early review of this document. This work was sponsored as work proposal ERKP489 ($100,000) by the U.S. Department of Energy, Office of Science, Office of Biological and Environmental Research. The submitted manuscript has been authorized by a contractor of the U.S. Government under contract No. DE–AC05–00OR22725. Accordingly, the U.S. Government retains a non-exclusive, royalty-free license to publish or reproduce the published form of this contribution, or allow others to do so, for U.S. Government purposes.

Bibliography

Hargrove, W. W. and Hoffman, F. M. (2004). Quantitative methods to extend the ecoregion concept beyond the limits of human subjectivity. *Environmental Management*. Submitted.

Hargrove, W. W., Hoffman, F. M., and Law, B. E. (2003). New analysis reveals representativeness of the AmeriFlux network. *Eos Trans. AGU*, 84(48):529, 535.

Hargrove, W. W., Hoffman, F. M., and Sterling, T. (2001). The Do-It-Yourself Supercomputer. *Scientific American*, 265(2):72–79.

Hargrove, W. W. and Luxmoore, R. J. (1998). A New High-Resolution National Map of Vegetation Ecoregions Produced Empirically Using Multivariate Spatial Clustering. In *Proceedings of the ESRI Arc/INFO User Conference*.

Hartigan, J. A. (1975). *Clustering Algorithms*. John Wiley & Sons, New York.

Hoffman, F. M. and Hargrove, W. W. (1999). Multivariate geographic clustering using a Beowulf-style parallel computer. In Arabnia, H. R., editor, *Proceedings of the International Conference on Parallel and Distributed Processing Techniques and Applications (PDPTA '99)*, volume III, pages 1292–1298, Las Vegas, Nevada. CSREA Press. ISBN 1–892512–11–4.

Prince, S. D. (1991). A model of regional primary production for use with coarse resolution satellite data. *International Journal of Remote Sensing*, 12(6):1313–1330.

Rasmussen, M. S. (1997). Operational yield forecast using AVHRR NDVI data: Reduction of environmental and inter-annual variability. *International Journal of Remote Sensing*, 18(5):1059–1077.

Index